Investigation on the general activity and uncoupling of the catalytic cycle of different Cytochrome P450 monooxygenases

I n a u g u r a l d i s s e r t a t i o n

zur

Erlangung des akademischen Grades eines

Doktors der Naturwissenschaften (Dr. rer. nat.)

der

Mathematisch-Naturwissenschaftlichen Fakultät

der

Ernst-Moritz-Arndt-Universität Greifswald

vorgelegt von
Lisa Kristin Morlock
geboren am 04.06.1988
in Pforzheim

Greifswald, 18.Juni 2018

Dekan:	Prof. Dr. Werner Weitschies
1. Gutachter:	Prof. Dr. Uwe T. Bornscheuer
2. Gutachter:	Prof. Dr. Vlada B. Urlacher
Tag der Promotion	28. September 2018

Contents

List of Abbreviations

7,4-HFC	(7-Hydroxy-4-(trifluoromethyl) coumarin
Abiraterone	17-(3-Pyridyl)androsta-5,16-dien-3β-ol
ABTS	2,2'-Azino-bis(3-ethylbenzothiazoline-6-sulfonic acid)
AdR	Adrenodoxin Reductase
Adx	Adrenodoxin
Amp	Ampicillin
Ampliflu^{TM} Red	*N*-Acetyl-3,7-dihydroxyphenoxazine
APS	Ammonium persulfate
Aq. dest.	Distilled water
B. megaterium	*Bacillus megaterium*
BLAST	Basic Local Alignment Search Tool
BMR	Reductase domain of P450 BM3
BM3	P450 3 from *Bacillus megaterium*
C. apicola	*Candida apicola*
CM-DCF-DA	5-(and 6-) Chloromethyl-2'7'-dichlorodihydrofluorescein diacetate
CO	Carbon monoxide
Cpd	Compound
CPR	Cytochrome P450 reductase from *Candida apicola*
CV	Column volume
CYP	Cytochrome P450 monooxygenase
DEAE	2-Diethylaminoethyl
DMF	Dimethylformamide
DMSO	Dimethyl sulfoxide
DNA	Deoxyribonucleic acid
DTT	1,4-Dithiothreitol
dNTP	Deoxyribonucleoside triphosphate
E. coli	*Escherichia coli*
e.g.	*exempli gratia*
EDTA	Ethylenediaminetetraacetic acid
ee	Enantiomeric excess
epPCR	Error-prone PCR
FAD	Flavin adenine dinucleotide
FADS	Fluorescence-activated droplet sorting
FMN	Flavin mononucleotide
FPLC	Fast protein liquid chromatography
GC	Gas chromatography
GC-MS	Gas chromatography-mass spectrometry
H_2DCF-DA	2',7'-Dichlorodihydrofluorescein diacetate

HPLC	High performance liquid chromatography
HRP	Horseradish peroxidase
HS	High-spin
HSD	Hydroxysteroid dehydrogenase
IMAC	Immobilized metal affinity chromatography
IPTG	Isopropyl β-D-1-thiogalactopyranoside
Kan	Kanamycin
kb	Kilobases
LB	Lysogeny broth
LS	Low-spin
kDa	Kilodalton
mA	Milliampere
NAD(P)H	Nicotinamide adenine dinucleotide (phosphate)
$NAD(P)^+$	Oxidized NAD(P)H
NMR	Nuclear magnetic resonance
OD_{600}	Optical density at λ = 600nm
ORF	Open reading frame
orteronel	6-(7-Hydroxy-6,7-dihydro-5*H*-pyrrolo[1,2-c]imidazole-7-yl)-*N*-Methylnaphthalene-2-carboxamide
P. putida	*Pseudomonas putida*
PAGE	Polyacrylamide gel electrophoresis
PCR	Polymerase chain reaction
PDB	Protein Data Bank
pH	*Pondus hydrogenii*
pI	Isoelectric point
PMSF	Phenylmethanesulfonyl fluoride
S. cerevisiae	*Saccharomyces cerevisiae*
Scopoletin	7-Hydroxy-6-methoxycoumarin
SDS	Sodium dodecyl sulfate
TAE	Tris-Acetate-EDTA
TB	Terrific broth
TEMED	*N,N,N',N'*-Tetramethylethane-1,2-diamine
Tfb I/II	Transformation buffer I/II
THF	Tetrahydrofuran
TOK-001	17-(1H-Benzimidazol-1- yl)androsta-5,16-dien-3β-ol
Tris	Tris(hydroxymethyl)aminomethane
Triton X100	*O*-[4-(1,1,3,3-Tetramethylbutyl)phenoxy]polyethoxyethanol
UV/Vis	Ultraviolet/visible
V	Volt
w/o	Without

wt	Wild-type
YASARA	Yet Another Scientific Artificial Reality Application
YNB	Yeast nitrogen base
YPD	Yeast-Extract-Peptone-Dextrose
δ-Ala	δ-Aminolevulinic acid

Additionally, SI-units and the standard one- and three-letter codes for amino acids and abbreviations for nucleotides were used.

1 Introduction

1.1 Biocatalysis

Traditionally both fine and bulk chemicals like pharmaceuticals and biofuel components, respectively, are chemically produced. However, more and more often, enzymes and microbes are replacing or being incorporated into chemical processes for manufacturing these products.[1] This application of natural catalysts in synthetic chemistry is called biocatalysis and started already over 100 years ago inter alia with the synthesis of (*R*)-mandelonitrile using a plant extract, which also marks the start in the history of biocatalysis.[2,3] So far, several distinct waves of technical innovations and research, have led to the current state of the biocatalytic field and these first applications are seen as the first of now four waves.[2,4]

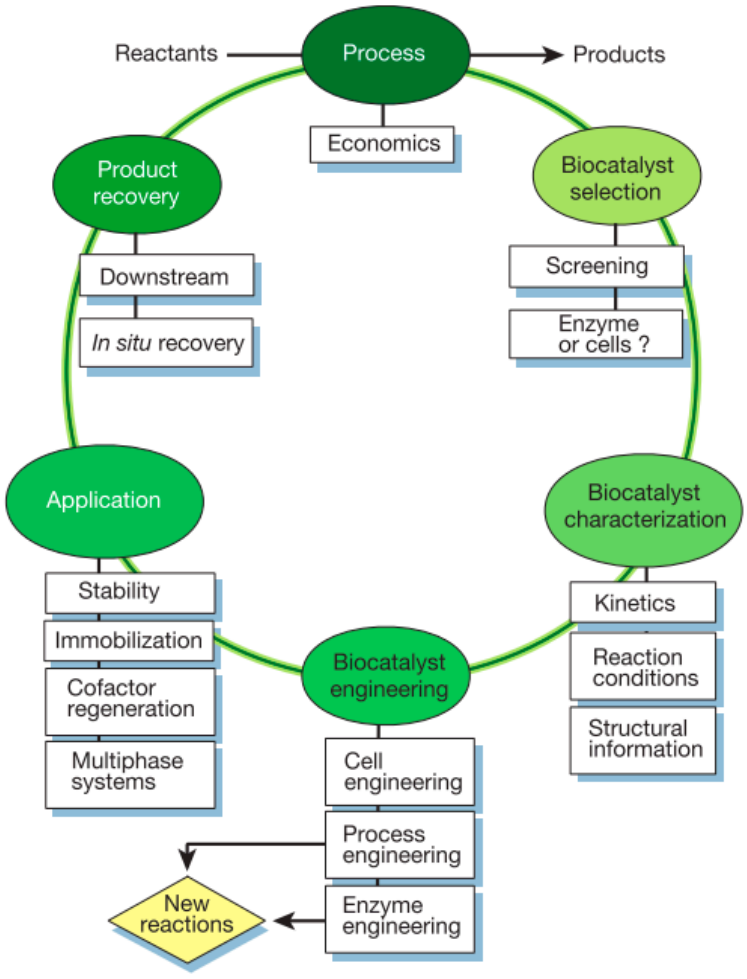

Figure 1: Scheme of the cyclic optimization process used in developing new biocatalysts. (Figure from Schmid *et al.* 2001[5])

One of the main advantages of using enzymes is that they often offer environmentally friendly alternative routes to the use of metallo- or organocatalysts.[2] Additionally, the enzymatic process usually shows high regio-, stereo- and chemoselectivity at ambient

temperatures, low pressure and they are mostly applicable in aqueous solutions. Therefore, enzymes are considered as environmentally friendly alternatives to the chemical synthesis routes they replace.[6]

As enzymes have evolved for their natural purposes under physiological conditions and natural selection pressures, they show distinct characteristics like a certain pH optimum or substrate range that need to be optimized before being capable of surpassing their chemical alternative (Figure 1). Only if the improved properties are combined with a high turnover number (>500 min^{-1}), the enzymatic process could be considered as a promising candidate to be applied in industry and be considered as economically feasible.[1,7]

The development of a biocatalytic process starts by choosing the substrate and reaction type catalyzed, followed by the identification of possible enzymatic candidates, to catalyse this reaction by screening a library consisting of microorganisms or physical enzyme variants.[5] After the identification of a proper candidate, the biocatalyst can be engineered by using protein engineering tools. After these optimizations, in addition, the general reaction conditions with the engineered biocatalyst need further investigation. For example, cofactor regeneration or the reusability of the enzyme are key features for the final applicability of the biocatalyst. Additionally, the biocatalyst is first identified, followed by optimization for small scale reactions. In order to catalyze the reaction in large industrial processes, upscaling is needed.[8–11]

Finally, at the end of every process, the product has to be separated and purified. Only if all steps in the optimization process have been conducted successfully, in the end an analysis concerning the economic feasibility decides whether the enzymatic process has surpassed the chemical alternative and will be applied on industrial scale.

For this thesis, of special interest is the optimization of the biocatalyst itself. This so-called protein engineering includes many exciting and quite diverse approaches.

1.2 Protein engineering

Protein engineering comprises numerous different techniques for the optimization of proteins, including enzymes. These techniques can be categorized into directed evolution, rational protein design, and semi-rational approaches (Figure 2).[12]

The start of using these protein engineering techniques also marks the start of the so-called second wave of biocatalysis.[2] The originally developed methods from the 1980s, were mostly structure-based. By employing those methods, it became possible to use enzymes as catalysts for the production of fine chemicals and pharmaceuticals, using substrates which were previously not converted.

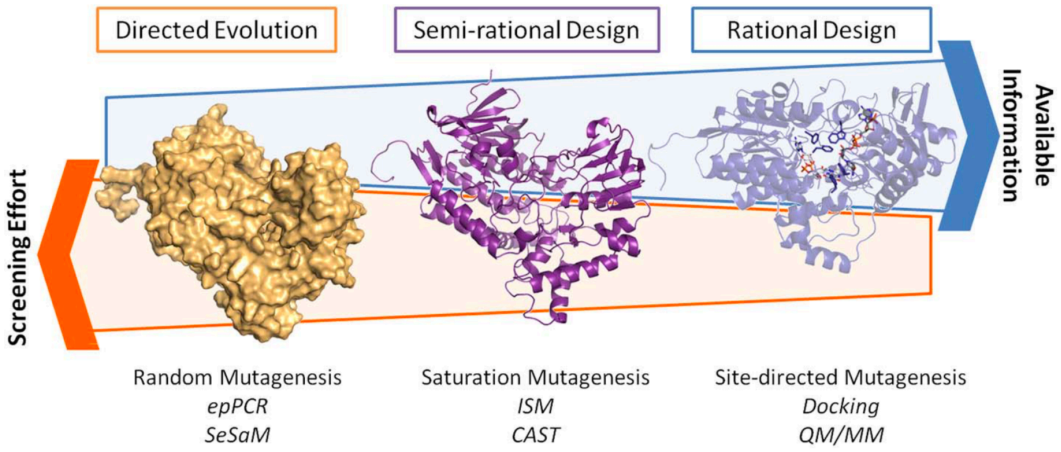

Figure 2: Scheme showing the different techniques used for protein engineering (Picture from the Protein Engineering Handbook[13]).

In the year 2000, the third wave started, by the development of directed evolution methods. With new molecular biology methods, modification of biocatalysts became much easier and faster.[4] Those methods included important protein engineering techniques: error-prone polymerase chain reaction (epPCR) and DNA shuffling. By combining those molecular biology methods with high-throughput screening assays, a rapid approach for identifying interesting mutants was developed.[4]

For the rational design of proteins, a crystal structure and ideally mechanistic information have to be available, or an accurate homology model needs to be prepared. On the basis of structural information, interesting positions for mutagenesis are identified by computational methods, resulting in the creation of small, focused libraries.[7] Although the structural approach is extremely powerful, a clear limitation is found in the difficulties in identifying combinations of mutations.

In the directed evolution approach, random mutations are introduced into the gene, for example by epPCR. Through this method, a much larger library of protein variants is generated, followed by a screening for activity.[1,7,14] The need for high-throughput screening and restraints in library design, for example through the degeneracy of the genetic code, resulting in only a fraction of possible amino acid substitutions possible through this method, hamper the effectiveness of this technique.[15]

Variants exhibiting improved activity identified from either method can be used as template for further protein engineering rounds. As both methods show certain restrains, often also combinational approaches are chosen. When combined, most limitations of the single approaches can be overcome. By focusing, resulting from rational design, on smaller regions of the protein, and inserting random mutations in the selected region, the obtained library size is strongly reduced. Furthermore, the opposite is also true. By epPCR identified interesting sites can be further investigated by more systematic characterization. This usually results in the identification of more active variants.[7,12]

1.3 Screening and selection approaches for the investigation of protein libraries

As mentioned above, for the development of an improved biocatalyst, rational protein design or directed evolution is needed. Besides choosing an appropriate candidate for optimization, having an efficient screening strategy is important, in order to identify improved variants. Each screening or selection approach has different requirements, and diverse approaches exist (Figure 3). Depending on the size of the investigated library, the different approaches are more or less suitable and have different advantages and disadvantages.

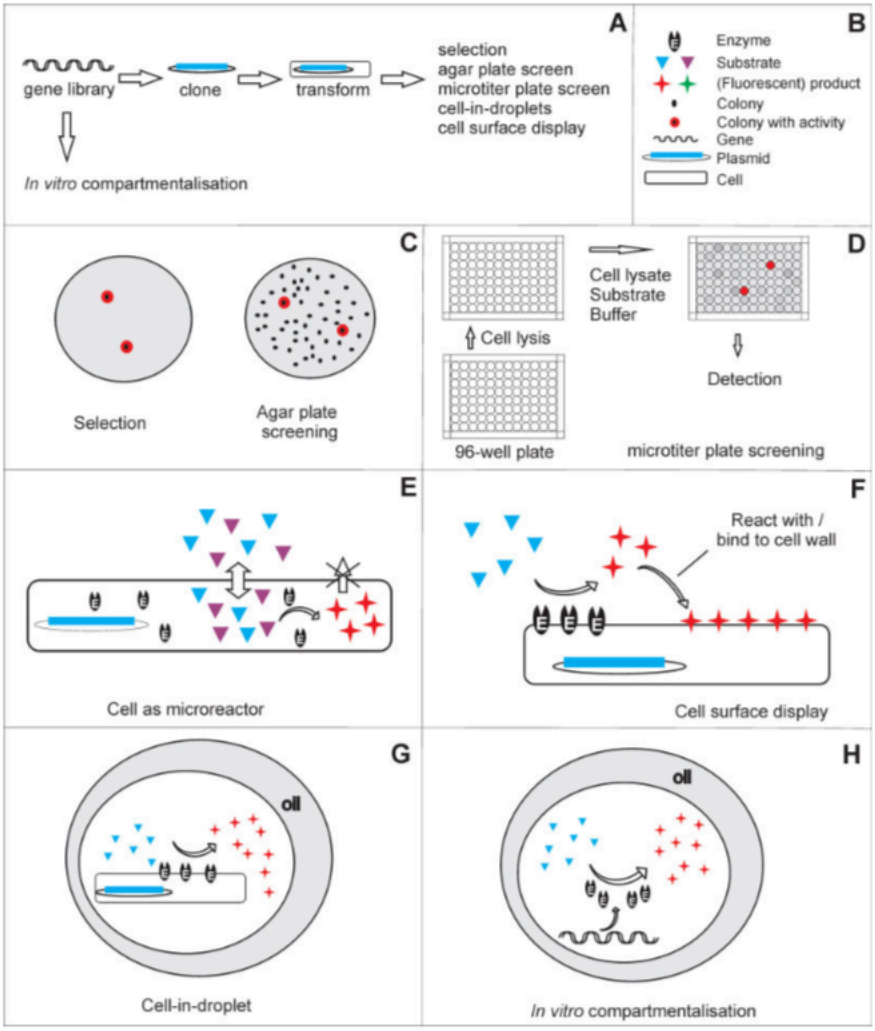

Figure 3: Overview of different screening approaches for protein libraries, further explained in section 1.3. A) Steps needed from the gene library leading to the starting point of the screen, B) legend, C) agar plate screening and selection approaches, D) microtiter plate screening approach, E) single cells as microreactors, F) surface display approach, G) droplets carrying a single cell (which can be lysed or cultured), and H) *in vitro* compartmentalization by dispersing the aqueous phase as droplets in oil (Picture from Leemhuis *et. al*., 2009[16])

By using selective agar plates not containing a molecule essential for growth (i. e. C-source, N-source or essential amino acids), which can only be produced by the investigated enzymatic activity, the library can be screened (Figure 3C).[17] With this method, large libraries can be screened and only active variants are obtained. Therefore, this method is a high throughput method (~10^9 variants). Unfortunately, this can only be employed if the screened activity leads

to a growth advantage, which is rarely the case. Additionally, through selection pressure, microbes can adapt to the applied growth conditions very fast, which also might lead to the identification of false positive colonies. Another plate-based assay is the screening of activity in colonies grown on indicator agar plates. After normal growth, the colonies are incubated with the investigated substrate. Substrate conversion finally yields in the formation of the indicator molecule in a direct way or indirectly with for example a second coupled reaction. This is a relatively simple and easy method for medium throughput (~10^5 variants), but a visual signal as activity output is needed.[16]

One of the most commonly applied methods for the screening of different protein variants is the use of microtiter plates (Figure 3D). In this format the activity can be investigated either in crude lysate or in the supernatant. Also, whole-cell biocatalysis can be performed, if the product is secreted from the cell, the product formation can be analyzed in the supernatant. Different analytical tools, but mostly absorbance or fluorometric measurements, can be used to determine the activity of the investigated protein variants. As a lot of handling is needed and the plates need to be replicated for sequencing the original clones later, this is a medium throughput method (~10^4 variants).[16]

By flow cytometry, single cells can be used for screening of fluorescent substrates (Figure 3E). After expression of the different protein variants, the investigated substrate is added and needs to diffuse over the cell membrane. After incubation, the cells can be sorted by FACS. For this approach, a substrate is needed that can easily enter the cell and remains in the cell after conversion, which is hard to accomplish. As single cells are sorted, this is a high-throughput method (~10^9 variants).[16,18]

Another concept based on single cells is the cell surface display method (Figure 3F). In this method, the enzymes are expressed in the cell and exported to the cell surface. By a linked autotransporter protein (AIDA-I), the expressed proteins (up to 10^5 per cell) are transported to the cell surface and stay attached to it. Additionally, if the cells should be sorted later, the product needs to also stay attached to the cell surface, hampering its applicability. The cells can then be analyzed by FACS or ELISA (~10^9 variants). [16,19]

The single cells expressing the enzyme variants can also be incorporated into oil droplets (Figure 3G). In these droplets the cells are separated from each other and incubated with substrate. The product formed by active enzyme variants accumulates in the droplet, linking it to the genotype and obviating the need for products that remain trapped in cells, which is in general an important issue for all screening and selection approaches, as discussed above. As all single-cell methods subjected to different sorting techniques (microfluidics or FACS), this is also a high-throughput method (~10^9 variants).[16,20] The encapsulated single cells can also be lysed in those droplets, which is called *in vitro* compartmentalization (Figure 3H). Or single genes can be encapsulated combined with *in vitro* translation systems. These droplets can be analyzed on a chip in a microfluidics system or in a FACS device, where double emulsion droplets are needed in order to work in an aqueous system, leading to additional problems in the formation of these droplets. However, this field is getting more and more attention and a

lot of progress is leading to easier applications.[21] An advantage of this technique is definitely also the high throughput (~10^9 variants).[16,22]

Besides choosing a good screening or selection assay, the choice of substrate is also important. For most approaches, a photometric detectable activity output is needed. Therefore, if neither the substrate nor the product shows the desirable properties, often surrogate substrates are used during the screening or selection process.[23,24] These surrogates consist of the original substrate, chemically linked to a reporter molecule, which is released upon enzymatic activity. Although, the usage of surrogate substrates facilitates the identification of active variants, also new problems arise from their application. These substrates are much bulkier than the actual substrate, and therefore need more space. This might lead to problems concerning substrate supply and binding. As the surrogate substrate differs from the actual substrate, an active variant found during the assay might show lower activity with the actual substrate than observed with the surrogate substrate. Therefore, all identified possible hits have to be reevaluated in a second round to circumvent false positive results.[25]

Especially, the protein engineering and screening of cytochrome P450 monooxygenases, was the main focus of this thesis, therefore, this enzymatic family will be described further in the following paragraphs.

1.4 Cytochrome P450 monooxygenases

In general enzymes can be categorized in six different classes depending on their catalyzed reaction type: oxidoreductases, transferases, hydrolases, lyases, isomerases, and ligases. In each class, different enzyme families are found. One of these families in the class of oxidoreductases, are cytochrome P450 monooxygenases.

The term “cytochrome P450” was introduced by Omura *et. al*. [26] in 1962 to designate the investigated liver microsomal membrane-bound “pigment”. This name has been used ever since to describe a large family of heme-thiolate proteins that can be found throughout all domains of life and that catalyze the insertion of single oxygen atoms from molecular oxygen into their substrate at a non-activated carbon atom in a stereo- and regioselective manner, which is a highly challenging task.[27–30] Characteristically, this enzyme class presents a distinctive absorption band at 450 nm due to the binding of a carbon monoxide molecule to the reduced heme-center. That these proteins function as oxygenases was finally elucidated in 1963 and led to growing interest in and extensive research on these enzymes.[31] One year later, Omura *et al.* showed that the enzyme contains a heme-group.[32]

Nowadays a large variety of P450 monooxygenases have been discovered. In the CYPED database (biocatnet, v6.0) approximately 52.700 sequences can be found.[33] Through the extensive research on P450 enzymes, not only their broad spectrum of substrates has been investigated, but also the different reaction types they catalyze have been discovered. In this sense, their substrates range from fatty acids, prostaglandins and steroids to several different compounds like anesthetics, carcinogens, ethanol, drugs, organic solvents and pesticides.[34]

With these substrates they catalyze not only hydroxylation reactions, but also *N*-, *O*- and *S*-dealkylation, epoxidation, deamination, peroxidation, sulfoxidation reactions, and *N*-oxide reductions.[34,35]

Due to the wide spectrum of converted substrates and the different reaction types catalyzed by the enzymes, cytochrome P450 monooxygenases show a great potential for biotechnical application. However, some drawbacks must be taken into consideration prior to their application, such as their instability, complexity and often low catalytic activity.[34,36]

1.4.1 Catalytic cycle of cytochrome P450 enzymes

The reaction mechanism of the cytochrome P450 enzymes' hydroxylation reaction was elucidated by Estabrook *et. al.* in 1971, proposing the idea of a cyclic reaction mechanism that is, with slight modifications, still valid today.[37]

This rather complex catalytic cycle (Figure 4) consists of several steps:[38,39] (1) The cycle starts with substrate binding in the active site, which leads to the dissociation of the water molecule previously bound during the resting state of the enzyme; (2) Subsequently, the iron moves from an almost planar position in the heme molecule, to a new position below the heme group, simultaneously becoming the high-spin form. This species is a better electron acceptor than the water-bound configuration and receives one electron from NAD(P)H from its electron transferring system; (3) This electron reduces the ferric ion (Fe^{3+}) to the ferrous (Fe^{2+}) form. This high-spin ferrous complex binds molecular oxygen, yielding the formation of the ferrous dioxygen complex. (4) The singlet spin state of this complex is again a good electron acceptor. Therefore, another electron is accepted resulting in the formation of the ferric-peroxo anion;[34] (5) This compound acts as a good Lewis base and subsequently accepts a proton, leading to the formation of the ferric-hydroperoxide complex, which is also often called Compound 0 (Cpd 0). (6) Afterwards, another proton is accepted by Cpd 0, which leads to cleavage of the O-O bond and the reduction of one oxygen atom to water. This newly formed water molecule is released from the active site, leaving the heme group in its ferryl state (Fe^{4+}), which is also referred to as Compound I. (7) The activated single oxygen of Cpd I is then inserted into the substrate.[40] Afterwards the product dissociates from the active site, a new water molecule is bound in the active site and the cycle can start again.

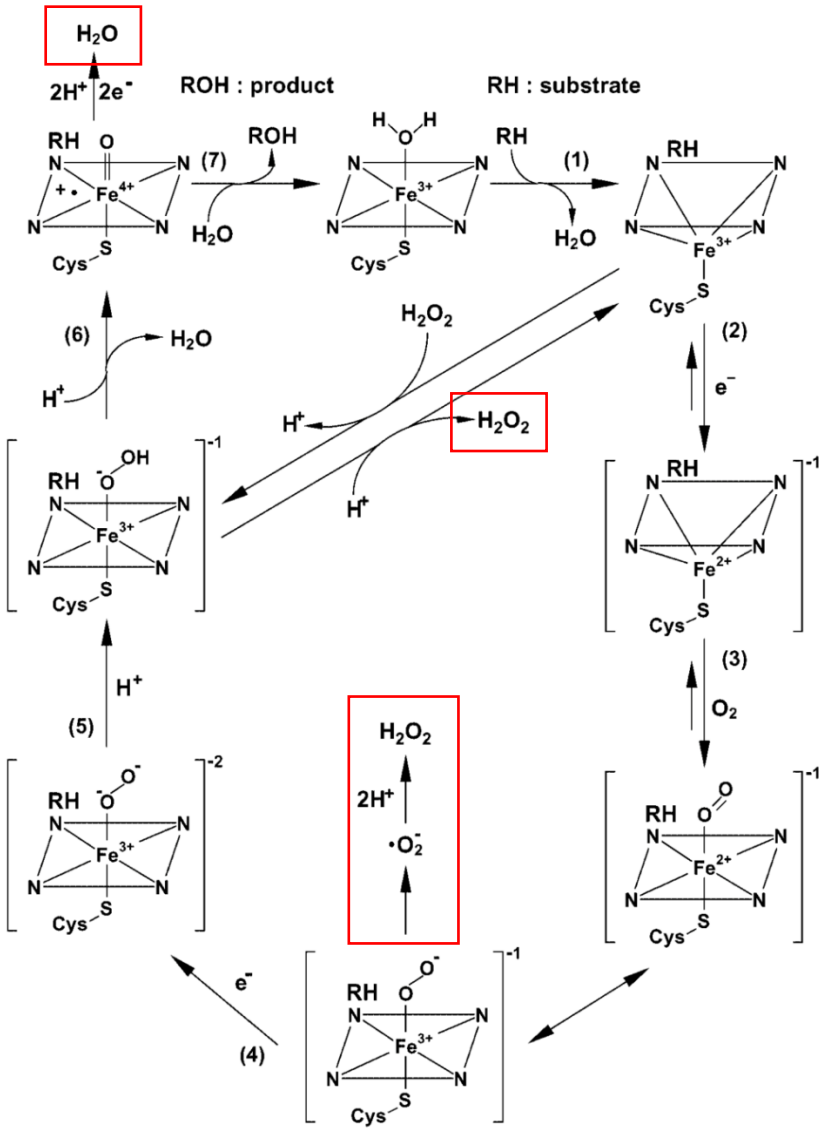

Figure 4: Scheme of the catalytic cycle of cytochrome P450 enzymes, as described in section 1.4.1. Indicated with the red boxes, is the uncoupling of the catalytic cycle. The term uncoupling, refers to the unproductive decay of the highly active iron-oxygen complex at different stages, yielding in the formation of superoxide, hydrogen peroxide, or water. The porphyrin ring is depicted by a parallelogram with nitrogen atoms at the corners and iron in the center. (Figure from Yasui *et. al.* 2005[41])

This description of the catalytic cycle is of course simplified. The binding and electron transfer steps seem to be associated with conformational changes, as shown by X-Ray crystallography.[42,43] Additionally, it was shown for the human P450 2A6, that the substrate can dissociate from and reassociate with the enzyme.[43,44] Also the linear order of all steps is not mandatory, as the enzyme can be reduced with or without substrate bound to the active site.[45] As indicated in Figure 4, the reaction catalyzed by cytochrome P450 enzymes does not necessarily result in product formation. At two different points during the catalytic cycle, uncoupling can occur, yielding hydrogen peroxide or superoxide anion.

1.4.2 Spectral properties of cytochrome P450 monooxygenases

Interestingly, upon substrate binding, the spectral properties of cytochrome P450 enzymes change. As described above, this is due to a spin shift from low-spin (LS) to high-spin (HS) induced by the substrate binding, which is detectable in a shift of the Soret band from 415-417 nm (LS) to 390-394 nm (HS).[46] Therefore, correct binding of the substrate can be investigated photometrically by a difference spectrum (type-I spectrum). This spectrum shows a minimum at 420 nm and a maximum at 390 nm and is characteristically observed if the substrate replaces the water molecules in the active site. Depending on the amplitude of the spectrum, the total amount of cytochrome P450 converted from LS to HS can be estimated. Therefore, this allows an estimation whether the investigated substrate is a good substrate for the enzyme under investigation.

Additionally, a reversed type I spectrum can be observed if a part of the enzyme population is already present in the HS state and titration of the substrate leads to a shift to LS. Observing this kind of difference spectrum indicates the presence of a weakly bound substrate, being replaced by the investigated substrate.[47]

A third type of difference spectrum observed for substrate binding studies with cytochrome P450 enzymes is the type II spectrum. This spectrum shows a maximum at 425-440 nm and a minimum at 415 nm, indicating that a six-coordinated complex with a tightly bound ligand has been formed.[46] Usually, if an investigated compound leads to the formation of this spectrum, an inhibitory effect is presumed. Although often this kind of spectrum is formed by nitrogen-containing ligands, which are indeed often inhibitors, some type-II ligands are also substrates.[48]

Another important spectral property of cytochrome P450 monooxygenases is their typical absorption maximum at 450 nm upon reduction and incubation with CO, as mentioned before. If the enzyme in not properly folded, a characteristic absorption maximum at 420 nm can be observed. This distinctive difference spectrum builds the basis for concentration determination of cytochrome P450 samples. Hence, not only the concentration of the enzyme sample can be determined, but also the percentage of correctly folded enzyme can be estimated.[27,32]

1.4.3 Uncoupling of the catalytic cycle of cytochrome P450 enzymes

Additionally, the formation and release of reactive oxygen species (ROS) is a major concern for cytochrome P450 enzymes. In this case, instead of completing the reactive cycle, the generated iron-oxygen decays, resulting in the generation of different ROS. The type of ROS formed depends on the current stage of the iron-oxygen complex. At the different branch points (indicated with red boxes in Figure 4), either superoxide anion or hydrogen peroxide, which can be further reduced to water, can be formed.[49–51] This release of ROS from the active site is called “uncoupling” and is an unfavorable side reaction as it drains electrons from the system leading to a lower catalytic efficiency. [39] Moreover, the released ROS could then lead to protein oxidation by reacting with amino acids of the enzyme itself. This latter process

also influences the reaction efficiency by denaturing and thereby inactivating the enzyme. Interestingly, it has been shown that for some cytochrome P450 enzymes, also the reversed reaction can take place. Instead of releasing hydrogen peroxide, it can be used to catalyze reactions.[52,53]

Uncoupling is influenced by different factors. These have to be investigated on a case by case basis. In several studies, different factors were identified for the cytochrome P450 enzyme investigated in this study. Concerning the substrate, there seems to be a strong reverse correlation between proper substrate binding and uncoupling. Only if the substrate is bound correctly, the heme-spin shift can take place, leading to a coupled reaction.[54] In addition, substrate accessibility plays an important role, as well as the sufficient supply of oxygen and electrons.[55,56] Furthermore, the hydration of the active site is essential.[55] For microsomal cytochrome P450 enzymes, cytochrome b_5 can alter the activity and act as an alternate electron donor.[56] Additionally, in artificial systems, lipid nature, salt composition, and the presence of detergents and additive agents have been reported to display an influence on both activity and uncoupling of the cytochrome P450 system under investigation.[56] The NADPH concentration also seems to influence the uncoupling rate. A study suggested that an optimal concentration exists. Below this concentration, productivity decreases and above it, the productivity stays the same while only uncoupling is enhanced.[49] Structurally, the size of the active site can be essential. In a study from Sibbesen *et al.* with the P450 camphor (P450cam), they demonstrated that adjusting the active site to the substrate size and shape could enhance the coupling efficiency.[57] Although it was found that the introduction of mutations yielded variants with increased uncoupling,[58] there are examples of protein engineering leading to a decreased uncoupling rate or even a fully coupled system. For instance, in another study with P450cam, the introduction of an unnatural amino acid led to a fully coupled system. It was suggested that the newly introduced methoxythreonine prevents solvent from entering the active site and, thereby, leads to an enhanced coupling efficiency.[59] Alternatively, by creating a fusion enzyme between the human P4502E1 and BMR (the reductive domain of BM3 from *Bacillus megaterium*: amino acids 473-1049) a higher conversion and a lower uncoupling rate were observed. In addition, the membrane anchor of the enzyme could be cleaved off and the expression of the enzyme was enhanced.[60] However, although the uncoupling of cytochrome P450 enzymes has been extensively investigated, it remains difficult to tell exactly which factors are the most crucial.

1.4.4 Hydrogen peroxide detection methods

In order to determine hydrogen peroxide concentrations, different methods have been described. Depending on intra- or extracellular usage, different methods have to be applied, especially due to the reductive intracellular environment. Additionally, continuous methods exist for the observation of the changes in hydrogen peroxide concentrations over time or methods only able to determine the concentration at a certain endpoint.

A classic hydrogen peroxide detection method is the use of horseradish peroxidase (HRP). This enzyme can be combined with different probes to yield different fluorescent or absorbent

products, detectable at different wavelengths. The HRP reduces hydrogen peroxide to water and oxidizes the added probe with two electrons gained per hydrogen peroxide molecule. This usually results in a 1:1 stoichiometry between the hydrogen peroxide and the oxidized, photometrically detectable probe. Examples of probes used in combination with HRP are *N*-acetyl-3,7- dihydroxyphenoxazine (Amplex® Red/Ampliflu™ Red)[61], 2,2'-azino-bis(3-ethylbenzothiazoline-6-sulfonic acid) (ABTS)[62], homovanillic acid[63] or 7-hydroxy-6-methoxycoumarin (scopoletin)[64].

For the determination of the uncoupling level of Cytochrome P450 enzymes also often applied is the Nash reagent.[65] For this method, the reaction is stopped with hydrochloric acid, followed by addition of the NASH reagent (consisting of ammonium acetate, acetylacetone and acetic acid). The hydrogen peroxide concentration can be photometrically determined after incubation.

Another endpoint measurement method applied for the detection of hydrogen peroxide formation in the reaction of cytochrome P450 enzymes is the addition of ammonium sulfate and ammonium thiocyanate to the acidified sample.[66] Also resulting in a photometrical detection of hydrogen peroxide concentration.

For intracellular measurements, the HyPer-3 protein could be used.[67] In *E. coli* a natural hydrogen peroxide sensing protein exists, the so-called OxyR protein, which undergoes conformational changes upon oxidation, resulting in the formation of a disulfide bridge. In HyPer-3, the circularly permuted yellow fluorescent protein (cpYFP) is integrated into the regulatory domain of the OxyR protein. The conformational changes in the OxyR protein also lead to conformational changes in the inserted cpYFP protein, which shows a change in the fluorescence excitation spectrum. Hydrogen peroxide levels can therefore be observed in a ratiometric fashion, observing the changes in fluorescence intensities at 500 nm and 420 nm.[67]

Additionally, 5-(and 6-)chloromethyl-2'7'-dichlorodihydrofluorescein diacetate (CM-DCFH-DA) is used for the detection of intracellular hydrogen peroxide levels. Through covalent binding of the chloromethyl group of this probe with intracellular thiols, the probe is retained inside the cell. The diacetate diffuses passively into the cell, where intracellular esterases cleave the two acetate groups, resulting in the non cell membrane-permeable CM-DCFH. Upon oxidation, the highly fluorescent product CM-DCF is produced.[68]

These methods only represent a few approaches used for hydrogen peroxide detection that are on the one hand used in the detection of uncoupling levels of cytochrome P450 enzymes, and on the other hand are relevant for this thesis.

1.5 Classification of cytochrome P450 enzymes

As previously described, the activity of cytochrome P450 enzymes relies on an adequate transfer of electrons, which are provided by either, (i) a reductase domain within the protein, (ii) a separate reductase, or (iii) a separate reductase and an additional protein acting as an electron shuttle between the reductase and the cytochrome P450 enzyme.

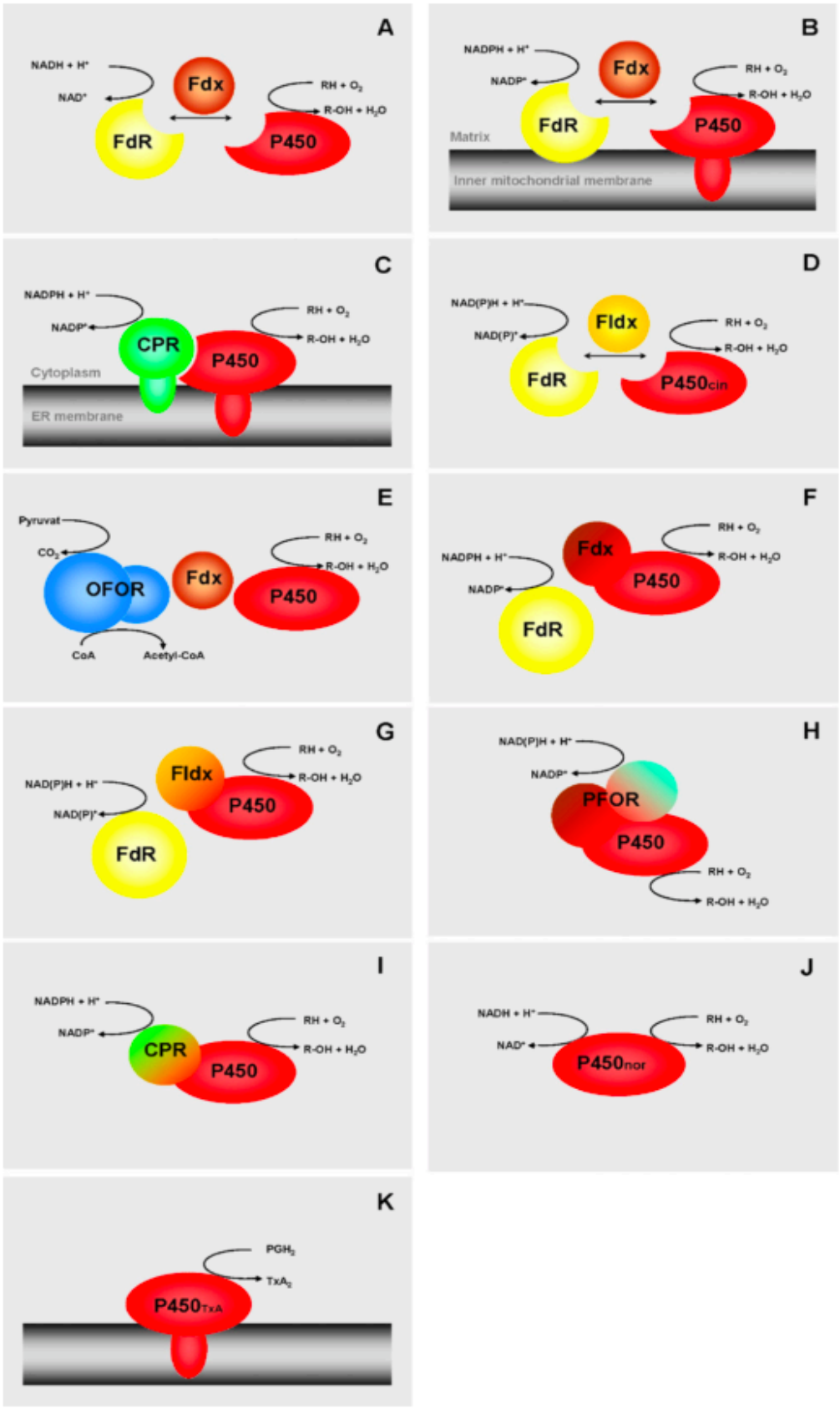

Figure 5: Scheme showing the different cytochrome P450 classes, further described in section 1.5. (Figure from Hannemann *et al*. 2007[69])

According to Hannemann *et al.,* depending on the reductase, cytochrome P450 systems can be divided into at least 10 different classes (Figure 5).[69]

Class I consists of most bacterial cytochrome P450 systems and the eukaryotic mitochondrial P450 systems. All these systems comprise three separate proteins: the ferredoxin reductase (FdR), the ferredoxin and the P450 enzyme. The first one is a FAD-dependent enzyme whose role is to transfer the reducing equivalents from NAD(P)H to the ferredoxin (Fdx). Fdx contains an iron-sulfur cluster and shuttles electrons between the FdR and the cytochrome P450 enzyme, reducing the P450 enzyme and thus allowing catalysis. Depending on the origin of the system, the components are either all three soluble proteins (bacterial, Figure 5A), or only the shuttling Fdx is soluble, being FdR membrane-associated and the cytochrome P450 enzyme is membrane-bound to the inner mitochondrial membrane (eukaryotic, Figure 5B).[34,69]

Class II contains mainly eukaryotic P450 systems, especially P450 systems from plants. These systems involve two separate integral membrane proteins (Figure 5C). In this class, the cytochrome P450 reductase (CPR) contains two prosthetic groups, FAD and FMN. This reductase is able to transfer the reducing equivalents from NADPH to different isoforms of cytochrome P450 enzymes.[69,70]

Class III was reported for the first time by Hawkes *et al* in 2002.[71] This class is similar to the bacterial members of Class I (Figure 5D), yet it shows a difference: the shuttling protein is a flavodoxin (Fldx), containing a FMN as prosthetic group, instead of the iron-sulfur cluster mentioned above.[69,71]

Class IV was identified by investigating the first thermophilic CYP119 from *Sulfolobus solfataricus*. This P450 system was the first system not using a pyridine nucleotide to obtain its electrons (Figure 5E).[69,72]

Class V systems include two components, a pyridine nucleotide-dependent reductase and a fusion enzyme of an iron-sulfur cluster containing the ferredoxin domain linked via a flexible hinge to the cytochrome P450 enzyme (Figure 5F). A member of this class was for the first time described by Jackson *et al*. in 2002.[69,73]

Class VI is similar to class V. The difference between these classes is that the fusion enzyme consists of a Fldx and the cytochrome P450 enzyme instead of a Fdx and the cytochrome P450 enzyme (Figure 5G). The first member of this class was described by Rylott *et al.* in 2006.[69,74]

Class VII comprises bacterial fusion systems with a rare structural organization (Figure 5H). Here, the P450 enzyme is fused to a special reductase domain, a phthalate dioxygenase reductase domain. Typically, this domain is not connected to the cytochrome P450. Here, the first member was described by Roberts *et al*. in 2002.[69,75] This unique domain has again three distinct domains: (i) a NADH-binding domain, (ii) a FMN-binding domain and (iii) a Fdx domain, containing an iron-sulfur cluster.[76]

Class VIII members are self-sufficient monooxygenases. This means that the cytochrome P450 enzymes of this class are fused to their CPR like (class II) reductase (Figure 5I). Here, the

probably best-known and intensively studied P450, BM3 from *Bacillus megaterium* (*B. megaterium*), was first described by Fulco *et al*. in 1974.[69,77]

Class IX is characterized by also being self-sufficient, but in contrast to class VIII, there is no CPR domain (Figure 5J). The first member, the nitric oxide reductase, is also the first soluble eukaryotic P450 to be described by Kizama *et al.* in 1991.[69,78] The enzyme is especially interesting for its function, as it converts nitric oxide to nitrous oxide, which resembles a unique process for P450 enzymes.[79]

Class X consists of cytochrome P450 enzymes which use an intramolecular transfer system (Figure 5K). Therefore, they require neither O_2 nor NAD(P)H. These enzymes use an acyl hydroperoxide as oxygen donor, to form a new carbon-oxygen bond.[69,80]

As all classes can be distinguished on the basis of their reductase system, an obvious question arises. Why did so many different systems evolve? The answer to this question remains unclear, although it might be explained by the different redox potentials of the different systems.[69]

1.6 Steroidogenesis

As mentioned previously, cytochrome P450 monooxygenases have important physiological roles. One of these roles is their crucial function in steroidogenesis, the biosynthesis of steroid hormones (Figure 6). Along with the cytochrome P450 monooxygenases, hydroxysteroid dehydrogenases are also involved (HSD).[81]

Regarding to the compounds formed, there are five different classes of steroid hormones, which are structurally similar and formed during this metabolic process. The differentiation between the groups of steroid hormones is based on their different physiological functions.[82] 1) Mineralocorticoids were named for their ability to command the renal tubes to preserve sodium and 2) glucocorticoids for their involvement in mobilizing carbohydrates.[82] 3) Estrogens induce female secondary sexual characteristics and exert immunoenhancing activities.[82–84] 4) Progestins all show the progestogenic effect, leading to a characteristic change in the estrogen-primed endometrium.[85] 5) Androgens induce male secondary characteristics and exert suppressive effects on the immune response.[82–84]

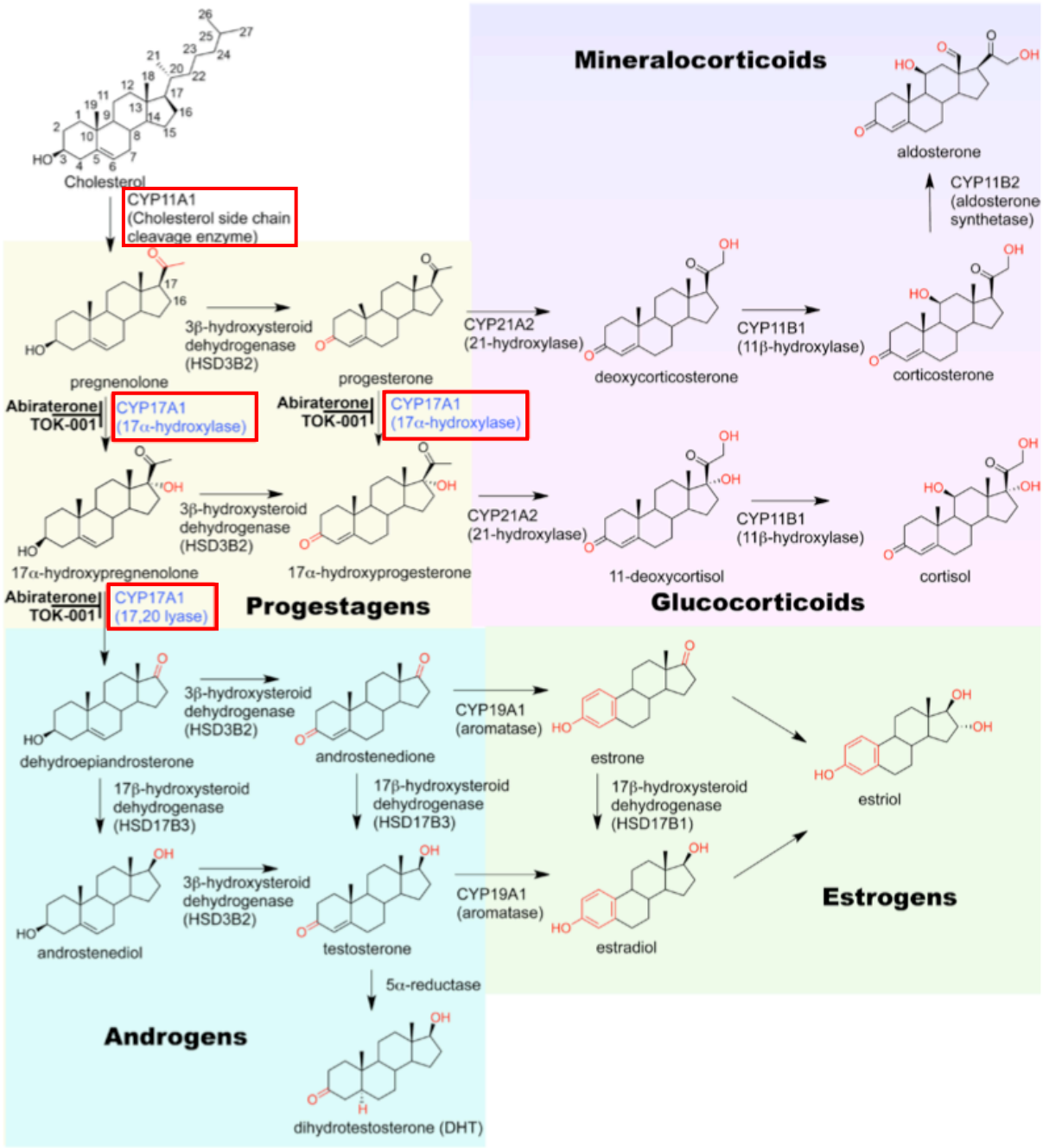

Figure 6: Overview of the biosynthesis of steroids, the so-called steroidogenesis. In this pathway, cytochrome P450s (CYPs) and hydroxysteroid dehydrogenases (HSDs) are involved, catalyzing the different steps throughout the pathways, yielding different groups of steroid hormones: Mineralcorticoids, Glucocorticoids, Estrogens, Progestagens, and Androgens. These groups as well as the biosynthesis pathways are further described in section 1.6 (Figure from supplementary information of DeVore *et al.* from 2012[86])

This pathway starts in the gonads and the adrenal cortex with cholesterol being converted by the CYP11A enzyme, yielding pregnenolone. This first step is rate-limiting and forms the basis for all following pathways.[87] Pregnenolone can then be further converted by the 3βHSD to progesterone. Both progesterone and pregnenolone are substrates for the CYP17 enzyme. This enzyme plays a key role in providing the precursors for the biosynthesis of cortisol and estradiol and all androgens.[88] All further modifications take place in different tissues. For instance, the production of androgens takes place in the gonads. In this pathway, the three

enzymes 17HSD3, CYP19, and 17HSD1 convert androstenedione to the final products testosterone and estradiol.[81] In the adrenal zona fasciculata and reticularis, progesterone and 17α-hydroxyprogesterone are further converted by CYP21 and CYP11B1 to corticosterone and cortisol, respectively. Corticosterone is then further converted by CYP11B2 to aldosterone in the adrenal zona glomerulosa.[81]

1.7 CYP11A1

One of the enzymes involved in steroidogenesis was investigated during this PhD thesis. The CYP11A1 is a mitochondrial membrane-bound P450 enzyme, which belongs to class I (Figure 5B). Therefore, it is dependent on adrenodoxin (Adx), a soluble ferredoxin containing an iron-sulfur cluster, and the membrane associated protein adrenodoxin reductase (AdR), a NADPH-dependent flavin reductase (Figure 7).[89] The enzyme is expressed in steroidogenic tissue and in the brain, where it is exclusively found at the mitochondrial membrane.[90] If the activity of CYP11A1 is impaired or completely lost, cholesterol accumulates in all steroidogenic tissues. As a consequence, the synthesis of all adrenal and gonadal steroids is affected.[91] The complete loss of the enzyme function is believed to be incompatible with human term gestation.[92] In mice, a knock-out of the gene leads to death shortly after birth. If steroids are injected, the mice can survive but show deficiencies in development of sex organs and external genitalia.[93]

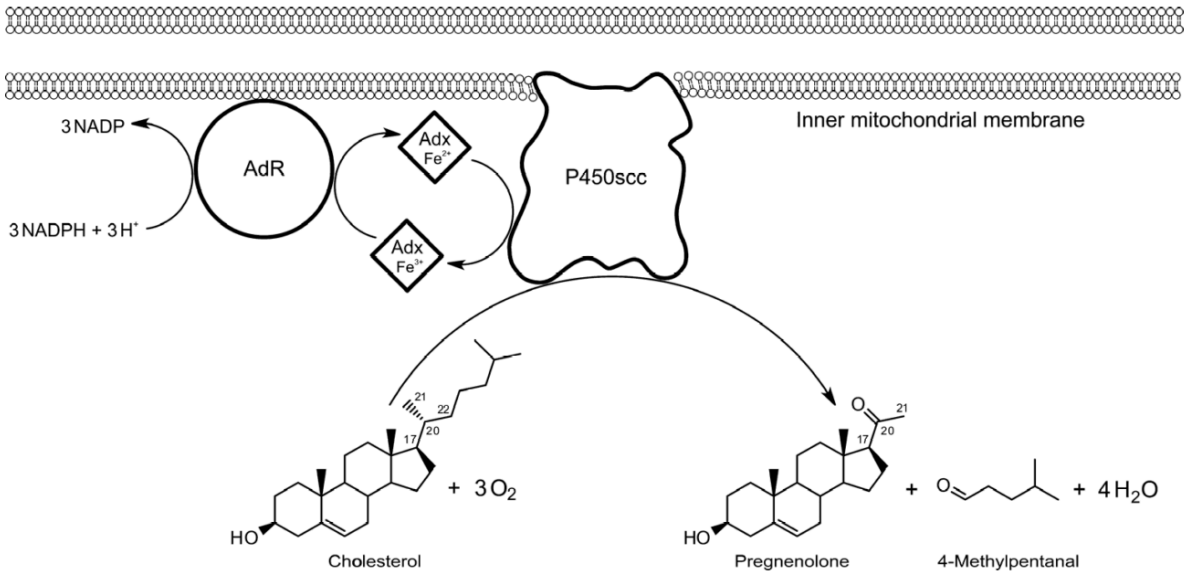

Figure 7: Scheme of the reaction of the three-component system CYP11A1 (P450scc), adrenodoxin (Adx) and adrenodoxin reductase (AdR) with cholesterol as substrate. Shown is the electron flow from AdR to Adx to P450scc, which finally catalyzes the three consecutive monooxygenation steps, converting cholesterol to pregnenolone under the consumption of three molecules of molecular oxygen. Reducing equivalents are supplied by the oxidation of three molecules of NADPH. (Figure from Makeeva *et al.* 2013[89])

Cholesterol side-chain cleavage, mediated by CYP11A1, results in pregnenolone by following three consecutive monooxygenation steps. First, the carbon atom C22 is

hydroxylated, yielding 22*R*-hydroxycholesterol, which is further hydroxylated at carbon atom C20 to produce 20α, 22*R*-dihydroxycholesterol. Subsequently, the side chain is cleaved, forming the final product pregnenolone.

Besides this important reaction, CYP11A1 is also involved in the conversion of vitamin D3. This substrate is hydroxylated at carbons 17, 20, 22 and 23, yielding in the production of at least 10 different vitamin D metabolites. This discovery points to the assumption, that the CYP11A1 enzyme also initiates vitamin D metabolism pathways. The products might have important physiological roles. Especially in the skin, it could be a new target for the treatment of skin disorders and skin cancer.[94,95] It was also found that desmosterol and the plant sterols campesterol and β-sitosterol can be converted to pregnenolone. Additionally, 7-dehydrocholesterol, ergosterol, lumisterol 3 and vitamin D2 are substrates for CYP11A1.[96] With ergosterol, the vitamin D2 precursor, CYP11A1 can form epoxy, hydroxy, and keto derivatives, without catalyzing side chain cleavage.[97]

Besides their activity, the structure of these proteins has also been studied. In this sense, the structure of the bovine P450scc enzyme was determined by Mast *et al.* in 2011[98] and the structure of the human P450scc enzyme in complex with Adx was determined by Mackenzie *et al*., also in 2011 (Figure 8).[99] For the bovine enzyme, 12 amino acids were identified within 4 Å to the bound 22-hydroxy-cholesterol (22-HC). Amino acids M202, F203, T291 and I351 form van der Waals interactions with residues of the aliphatic tail, whereas I85, L460 and W88 interact with the sterol α-face and Q356, T354, V353 and S352 interact with the sterol β-face. The edge of sterol ring A is held in place by F458. Additionally, the residues S33, H40, E53, Y62, Y83, L210, N211 and Q377 form hydrogen bonds with water molecules in the active site.

The crystal structure of the human enzyme in complex with Adx (PDB code: 3N9Y) allows conclusions concerning the interactions between the two proteins to be reached (Figure 8). Judging from the structure, first an initial electrostatic force-driven protein-protein association occurs. Subsequently, a conformational change in both proteins takes place, which leads to an optimal geometry and a close distance between the redox centers of both proteins. As the surface which is oriented towards the redox partner appears to be a conserved region of class I cytochrome P450 enzymes, it is very likely that the same applies for all members of that class.[99] The interactions of these proteins are accomplished by distinct structural features. The F-helix of Adx binds to the K-helix of the CYP11A1 enzyme at the proximal surface. Through its core domain, the loop region around the iron-sulfur cluster, Adx interacts with two helices of CYP11A1, C and L, which are also known as the heme-binding loops. At the interface between the enzymes, two salt bridges are established ($K339_{CYP11A1}$-$D72_{Adx}$ and $K343_{CYP11A1}$-$D76_{Adx}$).[99] This observation in the crystal structure is in accordance to earlier studies where the modification of those positions also affected the protein-protein interaction.[100–103] It is likely that the same region of the surface of Adx is responsible for interaction with AdR, making it impossible for a complex of all three proteins to form.[104]

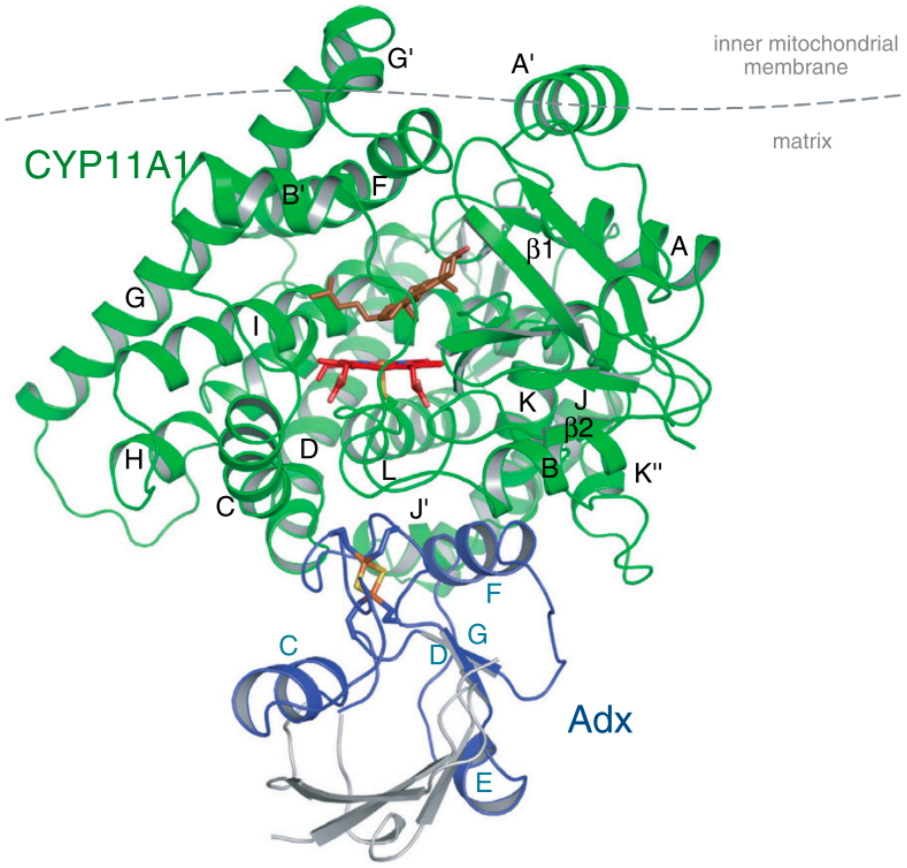

Figure 8: Crystal structure of the human CYP11A1 (green) with co-crystallized human Adx (blue) (PDB code: 3N9Y). The grey part of Adx was not well defined in this crystal structure and was therefore modeled on the basis of the bovine crystal structure (PDB code: 1AYF). The iron-sulfur cluster of Adx (orange and yellow), the heme-group of CYP11A1 (red) and the bound cholesterol (brown) in the active site of CYP11A1 are shown as sticks. (Figure from Mackenzie *et al.* 2011[99])

The residues responsible for the interaction with the inner mitochondrial membrane are found in the F-G loop, the G'-helix and the A'-helix.[99,105] Another factor that must be taken into account is that the composition of the membrane, that the CYP11A1 is embedded in, has an influence on its overall activity. Interestingly, the acyl-chain structure is important and cardiolipin was found to have an activity-enhancing effect on the enzyme.[106] Especially, the substrate binding, membrane integration and protein exchange in the membrane was discovered to be positively influenced by branched phosphatidylcholines.[107]

1.8 CYP17A1

The next step in the metabolic pathway is performed by CYP17A1 (CYP17A / P450 17A1 / P450 17α). This cytochrome P450 monooxygenase catalyzes a key step in the steroidogenesis of mammals, where pregnenolone and progesterone are accepted as substrates to be subjected to 17α-hydroxylation, followed by the C17-20 bond cleavage reaction. As a result, dehydroepiandrosterone (DHEA) and androstenedione are formed, respectively.[108,109] The 17α-hydroxylated products are further converted to glucocorticoids, whereas the C17–20 bond-cleavage reaction products lead to the formation of androgens and estrogens.[88,110]

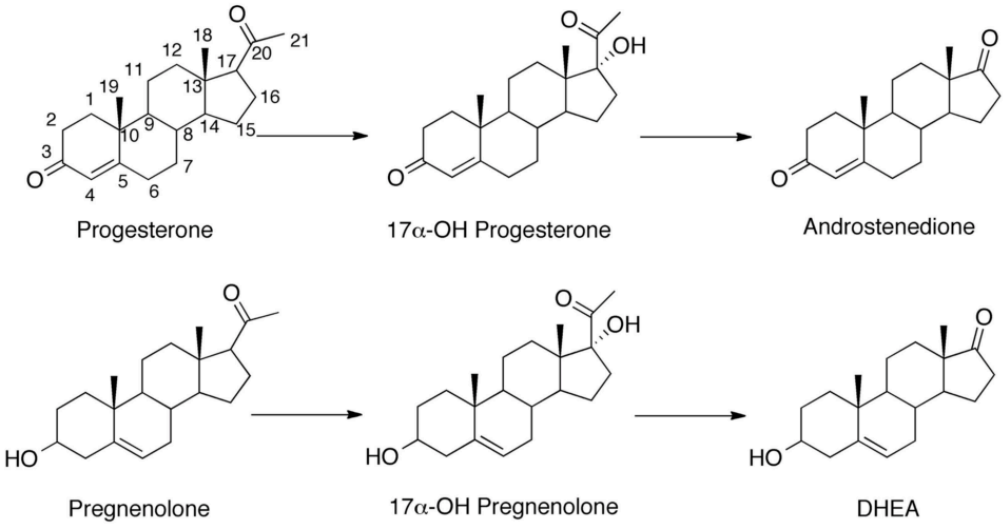

Figure 9: Scheme of the reactions catalyzed by P450 17α. The enzyme accepts both progesterone (upper reaction) and pregnenolone (lower reaction) as substrates and catalyzes first a hydroxylation reaction at C17. Subsequently, the C17-20 bond is cleaved, yielding in androstenedione and dehydroepiandrosterone (DHEA) respectively. (Figure from Pallan *et al*. 2015[111])

Interestingly, the human CYP17A1 enzyme has a side activity, the 16α-hydroxylation of progesterone.[108,112–114] However, the physiological role of 16α-hydroxyprogesterone remains unclear. No further conversion of this molecule has been reported for any enzyme. A possible role would be the inhibition of the C17-20 bond cleavage reaction, regulating the formation of the different precursors formed by the CYP17A1 enzyme, resulting in the formation of different products.[108]

The enzyme is predominantly expressed in the gonads and adrenals of mammals and, to a lesser extent, also in the heart, brain, and placenta.[112,115] As it is dependent on the flavoprotein, cytochrome P450 oxidoreductase (POR), the system can be categorized as a class II system.[116] CYP17A1 also accepts electrons from other partners for the 17-hydroxylation reaction.[117] This seems not to be the case for the C17-20 bond cleavage reaction.[118] Furthermore, cytochrome b_5 is of great relevance for the cleavage reaction[109,113,119–121], along with a serine phosphorylation of the enzyme itself, probably by facilitating the interaction between the enzyme and its reductase.[109]

The structures of the human CYP17A1, in the presence of two inhibitors, TOK-001 (PDB code: 3SWZ) and abiraterone (PDB code: 3RUK), was elucidated by DeVore *et al.* in 2012.[86] Two years later, Petrunak *et al.* determined the crystal structure of the enzyme with its natural substrates pregnenolone (PDB code: 4NKW), progesterone (PDB code: 4NKX), and 17α-hydroxyprogesterone (PDB code: 4NKY) bound in the active site.[110] Afterwards, in 2017, the crystal structure of the enzyme with the inhibitors (*R*)- and (*S*)-orteronel (PDB code: 5IRQ) and the inhibitor VT-464 (PDB code:5IRV) was determined.[122] Additionally, the structure of the CYP17A1 from *Danio rerio* with abiraterone (PDB code: 4R1Z) was elucidated by Pallan *et al.*

in 2015.[111] More recently, in 2018, a structure of the CYP17A2 from *Danio rerio* in complex with abiraterone was also solved (PDB code: 6B82).[123]

Judging from the knowledge derived from the crystal structures solved to date, different amino acids in the active site seem to play important roles in the catalytic activity of the CYP17A1 enzyme. Those residues form an extensive network of hydrogen bonds, involving the substrate and several water molecules.[124] In the literature, the residues identified forming this network were Y201, N202, R239, G297 and E305.[108,110,112,124] In this sense, the amino acid N202 forms a hydrogen bond with the 3β-OH hydrogen of pregnenolone and is thus important for correct substrate positioning and binding.[86] Similarly, residue E305 forms a hydrogen bond with N202 and might also be important for substrate positioning. Through several water molecules, also R239 and the carbonyl backbone of G297 are involved in the hydrogen bond network. In some crystal structures, Y201 was also located within hydrogen-bonding distance.[86]

A study from Swart *et al.* in 2010, focused on the production of 16α-hydroxyprogesterone as side-product formed upon conversion of progesterone by the human and chimpanzee CYP17A1.[108] Hence, they compared the active site residues of the human and chimpanzee enzymes with enzymes from pig, goat and baboon. In this comparison, they discovered that especially in position 105, human and chimpanzee enzymes differed from all other enzymes investigated. Human and chimpanzee enzymes harbor an alanine in this position, which corresponds to a leucine in the enzymes from the other species. Consequently, they exchanged A105 in the human enzyme with leucine and they exchanged the corresponding leucine in the pig, baboon and goat enzymes with alanine. Characterization of these variants revealed that this position did in fact have the foreseen influence on the side-activity of these enzymes. For the human enzyme, side-product formation was lowered from approximately 30% for the wild-type to 9% for the A105L mutant. Regarding the other investigated enzymes, they could introduce the side-activity. Therefore, they concluded that the exchange of leucine to alanine leads to more flexibility in the substrate movement, thus allowing the substrate to also present the C16 atom to the iron-oxy complex, leading to 16α-hydroxyprogesterone production.[108]

As already stated, androgens and estrogens are the final products of the steroid hormone synthesis pathways, where CYP17A1 is one of the participating enzymes. These metabolites are involved in the development of prostate cancer and hormone-responsive breast cancer. Therefore, understanding the reaction mechanism and finding possible inhibitors is especially interesting. This enzyme has already been studied as a possible drug target in both types of cancer.[110,125–127] In addition, approximately 100 mutations of CYP17A1 have been investigated due to their clinical relevance. These mutations are known to result in metabolic deficiencies in patients where either one or both functions of the enzyme are impaired.[116,128,129] As a result, patients suffer from hypokalemia, hypertension, sexual infantilism and primary amenorrhea.[116] Additionally, the fertility in both male and female patients is impaired/reduced.

1.9 Cytochrome P450 BM3

Probably the most investigated cytochrome P450 is the P450 BM3 (CYP102A1) from *Bacillus megaterium*.[130] This P450 is a self-sufficient monooxygenase and belongs to class VIII.[77] The 119.5 kDa protein consists of two domains: a 55 kDa heme-containing P450 domain (BMP) and a 65 kDa reductase domain (BMR), containing both FAD and FMN.[131,132] The physiological role of this enzyme remains unclear, as it accepts many different substrates. It is thought that the enzyme might naturally convert branched-chain saturated fatty acids and therefore be involved in the regulation of membrane fluidity.[133,134]

With known rates of over 5000 min^{-1}, which are reached in the conversion of arachidonic acid, P450 BM3 is the fastest P450 enzyme described so far.[135] In general, it hydroxylates a broad range of saturated and unsaturated fatty acids (C_{12} – C_{20}). During the years of extensive research on the P450 BM3 enzyme, a large list of substrates was added to the known converted substrates, ranging from aliphatic hydrocarbons, aromatics or fragrance and pheromone precursors to pharmaceuticals and other biomolecules.[130]

The crystal structure of the heme-domain of P450 BM3 (PDB code: 2HPD) was solved by Ravichandran *et al*. in 1993.[136] It revealed that the enzyme has a long, hydrophobic access channel, which is built out of mostly non-aromatic amino acids.[130] Based on the crystal structures and on different mutational studies, several catalytically relevant residues of P450 BM3 were identified. In this sense, R47 and Y51 may regulate the admission of substrate, co-solvent and water to the active site.[130,137] F87 seems to play an important role in displacing the axial water ligand for substrate binding and may also be involved in active site reorganization upon substrate binding.[138,139] In the substrate-free structure, the side chain of F87 is oriented perpendicular to the porphyrin system and is rotated in the substrate bound form. There it resides in a position between substrate tail and the iron-center.[140] In addition, position F87 influences the specificity and the activity of the enzyme. As for all cytochrome P450 enzymes and enzymatic variants, for some activity is enhanced,[141] for others especially the peroxide uncoupling rate is raised significantly.[142] As mutating this position creates more space in the active site, it is often mutated in protein engineering approaches, for the conversion of bulky substrates. Another noteworthy residue is E267 since its side chain forms a hydrogen bond with a water molecule in the substrate-free structure. Mutating this position leads to higher uncoupling rates and lower activity. On the basis of the results of different studies, it was concluded that this residue is involved in the proton delivery pathway and in correct substrate positioning.[58,143] Residue T268 might also position a water molecule in the active site, which is important for the catalytic activity of the enzyme.[144] Altering this residue results in the impairment of both NADPH consumption and uncoupling rates for a number of substrates.[62,144]

Additionally, several other positions are significant for the catalytic activity of the P450 BM3 enzyme. Depending on the reaction catalyzed, different residues are crucial and have to be considered on a case by case basis. A good overview of investigated mutations and substrates can be found in a review from Whitehouse *et al*. from 2012.[130]

1.10 Redox partner systems

Cytochrome P450 enzymes need reductases, or a redox partner system, for electron supply and catalytic activity. Besides their natural reductases, reductases from other cytochrome P450 systems can also be used to drive catalysis. For example, in *in vitro* biocatalysis, if the natural redox partner system has not been identified or is not available, different redox partner systems can be investigated and can replace the natural system for studies of the activity of the cytochrome P450 monooxygenase.

One of these reductases, described by Girhard *et al*. in 2013, is the reductase CPR from *Candida apicola*.[145] As cofactor, CPR harbors FAD and FMN in its active site. The optimized membrane-anchor truncated protein, shows a reducing activity towards cytochrome *c* with a K_M of 13.8 µM and a k_{cat} of 1.915 min^{-1}. In the same study, Girhard *et al.* could also demonstrate activity of CYP109B1 and CYP145E1 in the presence of this reductase. They compared different reductases in combination with the two enzymes and demonstrated that CPR displayed the highest coupling rates and conversion rates with CYP109B1. Concerning CYP154E1, biocatalysis with CPR as reductase also displayed good conversion, although the putidaredoxin (Pdx)/ putidaredoxin reductase (PdR) system from *Pseudomonas putida* showed even higher conversion.

The Pdx/PdR system is the natural redox partner system for the camphor hydroxylating cytochrome $P450_{cam}$ enzyme. Pdx is an iron-sulfur cluster containing ferredoxin and PdR, a FMN containing ferredoxin reductase.[146] The system was discovered in 1968 by growing *P. putida* on camphor as carbon source.[147] The whole system has been studied extensively ever since. As this redox partner system was one of the first to be described, it was very often employed for other enzymes, where the natural redox partner system was not yet identified.

In another approach, the reductive domain of cytochrome P450 BM3 (BMR) was separated from the rest of the protein by cloning experiments and applied as a reductase for other cytochrome P450 enzymes.[49,60,130,145,148–152] The advantage of using this reductase is that only one protein needs to be expressed and purified, as is the case for CPR. Additionally, it is a soluble protein, therefore it has some major advantages in application, compared to membrane-bound reductases.

1.11 Challenges in applying cytochrome P450 enzymes

In general, P450 enzymes catalyze challenging reactions and are therefore very interesting enzymes for industrial applications. However, the use of these enzymes in chemical synthesis is hampered by many factors. The major drawbacks lie in their functional complexity, low activity and limited stability, which therefore need to be optimized.[153,154]

The main focus of most studies to make cytochrome P450 enzymes more attractive candidates for industrial application lies in understanding how structural aspects are related to the catalytic mechanism; development of alternative electron-transfer systems; discovery of new sensitive high-throughput screening methods; and of course, in the generation of new

mutants that selectively convert certain substrates to products of interest.[154] The volumetric productivity needs to be optimized, not only by protein engineering, but also by optimizing the process concerning reaction media and different bacterial strains used for expression.[146]

1.11.1 Structure-function relationships in P450 enzymes

Thanks to the growing number of crystal structures of different cytochrome P450 enzymes, with different substrates and inhibitors bound to the active site, investigating structure-function relationships is becoming the topic of more and more studies. When combining this data with dynamic information gained by NMR and MS, some key features are considered to be important for substrate recognition and binding.[155] Residues in the I helix, β3 and β5 strands and for larger substrates also amino acids from the A helix, appear to be important for the determination of substrates binding in the active site. The B-C loop, the B'-helix and the F-G loop were described to determine the orientation of the bound substrate. These regions are reorganized in order to reach a catalytically active final conformation.[155]

1.11.2 Engineering of cytochrome P450 enzymes by rational design and directed evolution

Based on the information available on structure-function relationships, rational protein design of cytochrome P450 enzymes becomes possible.[28] For instance, P450 BM3 was the focus of many studies, along with $P450_{cam}$. The examples here, which only represent a very small number of published examples, will focus on the engineering of P450 BM3. Ost *et al.* could enhance the affinity of P450 BM3 for alkanoic acids and fatty acids shorter than C_{12} by a rational approach.[156] In other studies, new activities could be achieved. Graham-Lorence *et al.* turned the P450 BM3 into a stereo- and regioselective (14*S*,15*R*)-arachidonic acid epoxygenase[157] and Li *et al.* turned it into 3-chlorostyrene epoxygenase, which showed high enantioselectivity.[158] Whitehouse *et al*. engineered the P450 BM3 to show higher coupling, NADPH consumption rates, and product formation rates for (+)-α-pinene, fluorene, 3-methylpentane and propylbenzene. The first two substrates mentioned were not converted by the wild-type and the conversion of the last two was strongly enhanced.[159] A very relevant issue is the bioremediation of water, which contains a lot of chemical contaminants. Therefore, cytochrome P450 BM3 has been engineered for the conversion of naphthalene, fluorene and acenaphthene.[160]

In other studies, cytochrome P450 BM3 variants were created by directed evolution with enhanced peroxide-driven hydroxylation activity.[53,161] Additionally, it was also shown that general characteristics like thermostability could be improved by (up to) 18°C.[162] Another example of the directed evolution approach is the use of error-prone PCR to improve the tolerance of P450 BM3 against solvents like DMSO and THF.[163]

Both strategies can be combined for the identification of new interesting mutants. For example, cytochrome P450 BM3 has been engineered by combining directed evolution with site-directed mutagenesis. The purpose was altering the regio- and enantioselectivity of alkane hydroxylation. In the end, good mutants with 40% ee for the *S*-2-octanol and 55% ee for *R*-2-alcohols could be identified, achieving high activities with rates up to 400 min^{-1}.[164]

A good summary of reactions catalyzed by wild-type and different engineered cytochrome P450 BM3 variants can be found in recent reviews by Whitehouse *et al.* and Fasan *et al*.[130,165]

1.11.3 Screening methods for Cytochrome P450 enzymes

After understanding the reaction mechanism and finding hotspots for the introduction of mutations, high-throughput screening methods are needed. Traditionally, assays used to investigate P450 activities were radiolabeling[166], the use of fluorogenic substrates,[167–169] and HPLC or GC/GC-MS[148,158] analysis.[153] Not all of these assays can be scaled up to a medium- or high-throughput level. Therefore, usually an NAD(P)H consumption assay is the method of choice.[170] The advantage of this assay is its applicability, which is independent of the substrates investigated. On the other hand, the drawback is that the activity itself is not measured by product formation and might therefore lead to erroneous results, as side-reactions or for cytochrome P450 enzymes uncoupling can occur. An alternative approach is the measurement of activity by using surrogate substrates. Here, the substrate is chemically linked to a chromophore. If the reaction is catalyzed, the chromophore is released and this can be followed photometrically.[23] This approach can also be combined with flow cytometry and is therefore compatible with high-throughput assays.[171] Generally, this type of assay measures activity directly, but only of a surrogate substrate, which may be very different from the actual substrate. Although active variants can be identified with this method, it remains unclear whether more active variants could be found by using the cognate substrate.

1.11.4 Challenges in applying membrane bound cytochrome P450 enzymes

Additionally, new problems may arise if membrane-bound cytochrome P450s are studied. It is now commonly accepted that membrane proteins can not only be considered as such, but more as protein-lipid complexes. Therefore, some proteins might need specific lipid molecules acting as cofactors or that are needed for stability and correct folding.[172] Hence, heterologous expression of membrane proteins is not only dependent on the use of the right promoter, terminator, targeting signals and posttranslational processing, but also might be influenced by the lipid environment present in the host organism.[172] For CYP11A1, for example, reconstitution in vesicles with different compositions of phospholipids, had a strong influence on enzymatic activity.[106,173–175]

1.11.5 Challenges in using cytochrome P450 systems requiring a separate reductase system

In addition, the use of cytochrome P450 enzymes requiring a separate reductase system, increases the challenges of applying them in large scale processes. Due to the need for more than one protein, several factors from parallel expression of two or three proteins in one host cell might lead to new challenges, like the balance of the enzyme ratio and impairment of the growth of the cells. Additionally, the stability of more than one protein becomes an issue, independent of the *in vivo* or *in vitro* systems used. These problems have been addressed before by fusion of the cytochrome P450 2E1 to BMR. This did not only increase the soluble expression level, but also the stability of the fused cytochrome P450 enzyme without the need

for lipids or detergents.[176] In another study the chimeras of CYP2C9, CYP2C19 and CYP3A4, displayed the same enhanced solubility and similar activities to wild-type enzymes in reconstituted systems with their natural partners.[151] Additionally, electron supply can be provided by an electrode, if both the protein and the electron surface have been engineered.[149]

2 Scope of this PhD thesis

The scope of this thesis was to investigate different characteristics of cytochrome P450 monooxygenases. One major topic concerning the activity of cytochrome P450 monooxygenases is the uncoupling of the catalytic cycle, resulting in the formation of reactive oxygen species. This not only reduces the overall activity, by draining electrons from the catalytic cycle, but also might lead to the inactivation of the enzyme itself, as reactive oxygen species can react with amino acids of the protein, leading to protein (per-)oxidation and finally to the denaturation of the protein. Therefore, reducing the extent of uncoupling of the catalytic cycle is a major topic in enhancing the overall activity of cytochrome P450 monooxygenases.

2.1 Development of an assay for the investigation of the uncoupling:

In order to find variants with enhanced activity and reduced uncoupling, one main focus of the thesis was to find a reliable screening assay. With the assay, generated variants can be investigated, concerning their activity and uncoupling level. Furthermore, a high-throughput assay would enable the screening of large variant libraries. As the uncoupling process is to date not completely understood, rational protein design to influence the uncoupling level remains difficult. Therefore, random mutagenesis might be the method of choice to tackle the problems of enzyme inactivation resulting from uncoupling.

2.2 Investigation of stability and activity of membrane-bound cytochrome P450 enzymes:

Additionally, the overall stability and activity of membrane-bound cytochrome P450 monooxygenases was a major topic of this thesis. Especially for the use of membrane bound proteins, the expression in artificial host systems is difficult. These proteins are often unstable if separated from their hydrophobic surrounding and might need special detergents or even lipid vesicles to remain in their active form. Furthermore, as for all proteins, optimal pH and temperature are important factors for the overall stability and activity of enzymes. Hence, the monooxygenases were investigated concerning pH and temperature stability.

2.3 Alanine scanning for further investigation of the catalytic activity:

As already mentioned, another focus lay on studying the overall activity of the investigated cytochrome P450 monooxygenases. Here, the active site was further investigated. An alanine scanning was the method of choice, followed by investigation of the activity of the variants obtained. With these results, the goal was to possibly identify important residues for catalytic activity. Although it is known that the reaction itself is catalyzed by the inherent prosthetic heme-group, other factors like substrate supply and especially substrate binding influence not only the activity but are also thought to influence the uncoupling rate. Especially substrate binding can be investigated by the alanine scanning as most likely positions in the active site are responsible not only for substrate binding, but also for correct substrate positioning, influencing also the regioselectivity of the enzyme.

3 Results

As described in the *Scope of this PhD thesis* section, one objective was the investigation of the uncoupling of cytochrome P450 enzymes. Therefore, a suitable assay for the detection of hydrogen peroxide production was needed. As most methods described in literature were endpoint measurements, these methods were not suitable for determining the hydrogen peroxide concentrations during the reaction, without taking time samples.[177] Additionally, initial high-throughput screening is often undertaken by only measuring NAD(P)H consumption rates. This measurement does not take the often-occurring uncoupling of cytochrome P450 enzymes into account and might, therefore, result in misleading results. Consequently, a method for simultaneously assaying NAD(P)H consumption and hydrogen peroxide production was established.

3.1 Development of a hydrogen peroxide detection assay

3.1.1 Expression of the enzyme cytochrome P450 BM3

For the development of the assay, cytochrome P450 BM3 was used as model enzyme.[130] First, the expression and purification of the cytochrome P450 BM3 enzyme was investigated. Since the expression of this enzyme is well-established, the expression protocol was only slightly modified by using different inducer concentrations and different OD_{600} at time of induction (section 7.2.1.5.1). Finally, the enzyme was successfully expressed in soluble form in *E. coli* BL21 (DE3) harboring the pET22b_BM3 plasmid.

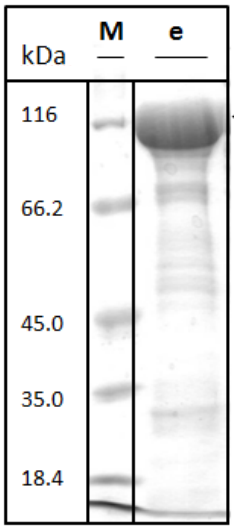

Figure 10: SDS-PAGE showing the elution fraction of the purification of P450 BM3 with a cobalt column. The elution (e) was accomplished with 50 mM imidazole.

For the purification, IMAC was used. Here, after optimizing the imidazole concentration in the washing buffer, in order to wash off other proteins and still obtain high concentrations of the investigated enzyme (section 7.1.8.5.1), a concentrated solution of cytochrome P450 BM3

could be obtained (Figure 10). The concentration of the 119 kDa protein was determined by a CO difference spectrum.[37] According to it, approximately 3 mg of cytochrome P450 BM3 were obtained after purification from a 200 mL culture.

3.1.2 Investigating HyPer-3 as a potential hydrogen peroxide reporter protein

As first attempt, the Hy-Per3 protein was tested for suitability as hydrogen peroxide detector for the uncoupling assay. As described in the introduction, this protein can be used to investigate hydrogen peroxide concentrations by monitoring the emission ratio from 500 nm to 420 nm.[67]

To investigate the suitability and sensitivity of this hydrogen peroxide sensor, the protein was expressed and purified. With slight modifications, this was accomplished as described by Bilan *et al*. in 2013.[67] With this protocol, expression of the soluble recombinant protein could be accomplished (Figure 11). Although the flow-through (ft) also contained HyPer-3 protein, a high protein concentration of relatively pure HyPer-3 solution could be obtained after elution (e; Figure 11).

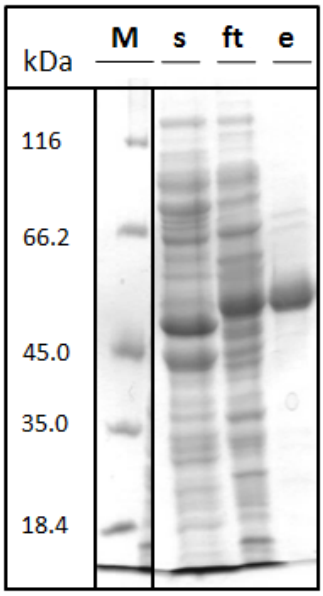

Figure 11: SDS-PAGE of the purification of HyPer-3 on a cobalt column. A molecular weight marker (m), the supernatant (s) after lysate clarification, the flow-through (ft) fraction, and the elution (e) fraction were loaded on the gel.

After obtaining the hydrogen peroxide sensing HyPer-3 protein in an enriched form, the protein was incubated with different concentrations of hydrogen peroxide and the fluorescence emission at 530 nm after ratiometric excitation at 420 nm and 500 nm monitored (

Figure 12). Judging from these results, the HyPer-3 protein was not sensitive enough for detection of hydrogen peroxide concentrations in the desired 100 nM to 50 µM range. Hence, other systems for the detection of hydrogen peroxide were investigated.

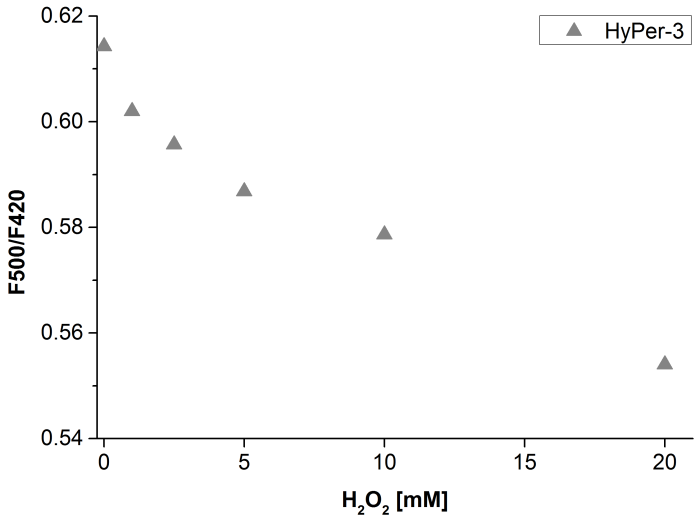

Figure 12: Response of purified HyPer-3 (in 40 mM Tris-HCl buffer (pH 7.5) containing 150 mM KCl, 10 mM $MgSO_4$ and 5 mM 2-mercaptoethanol) in the presence of 20, 10, 5, 2.5, 1 and 0 mM of hydrogen peroxide. The ratio of fluorescence emission at 530 nm after ratiometric excitation at 420 nm and 500 nm is plotted. Duplicates were measured; therefore, no standard deviation was calculated.

3.1.3 Comparison between Ampliflu™ Red and ABTS

A widely used system for the hydrogen peroxide detection is ABTS in combination with horseradish peroxidase (HRP).[178] Additionally, Ampliflu™ Red can also be applied in the same fashion. Both molecules differ in their absorption spectra when in their oxidized and reduced forms. Therefore, from both molecules, absorption spectra of their oxidized and reduced forms were determined and compared to the spectrum of NADPH (Figure 13). As both concentrations need to be determined at the same time, it was essential that none of them interfered with each other.

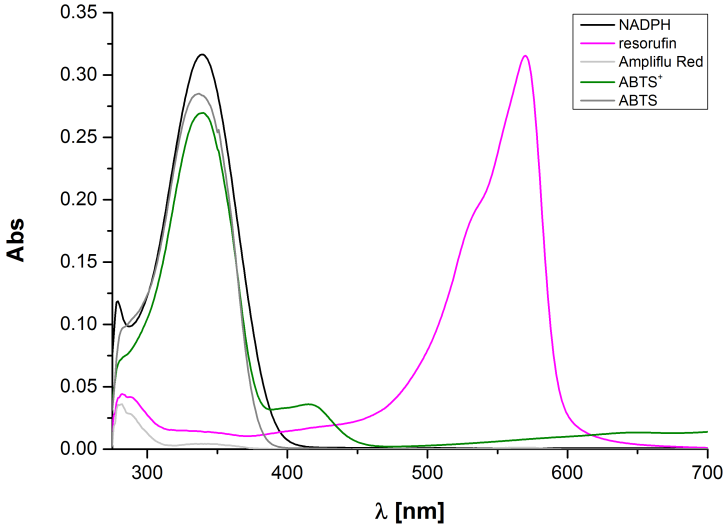

Figure 13: Overlay of the spectra of Ampliflu™ Red (light grey), resorufin (magenta), ABTS (dark grey), ABTS* (green), and NADPH (black) between 275 nm and 700 nm. As buffer, 50 mM sodium phosphate buffer (pH 7.4) was used. Final concentrations of Ampliflu™ Red and ABTS were 10 µM and 50 µM for NADPH. (Figure adapted from first publication: Morlock *et al*. 2018[179])

From the comparison of the spectra, it became obvious that only by using Ampliflu™ Red it was possible to investigate the NADPH concentration at the same time. As ABTS clearly has an absorption maximum at approximately 340 nm, which is the same wavelength as the absorption maximum of NADPH, they are incompatible with each other. Due to this finding, only the hydrogen peroxide detection with Ampliflu™ Red was further investigated.

3.1.4 Investigating the detection limits of Ampliflu™ Red

First, basic parameters of the system itself were examined. An important issue was the sensitivity of the assay. Therefore, the detection limits of the assay were determined. As the resorufin produced is a fluorophore, both absorbance and fluorescence measurements were performed. After incubating the Ampliflu™ Red assay solution with different hydrogen peroxide concentrations, the lower and upper detection limits were found to be 0.5 µM and 50 µM, respectively. For fluorescence measurements, an excitation wavelength of 550 nm and an emission wavelength of 590 nm were chosen. The upper limit was also found to be 0.5 µM, whereas the lower limit, at 50 nM, was significantly lower. Although fluorescent measurement was found to be more sensitive, absorbance measurement was used due to faster measuring time.

3.1.5 Investigating the pH range, the signal stability and optimal enzyme concentration for the Ampliflu™ Red assay

Additionally, the pH range was investigated by incubating solutions with different hydrogen peroxide concentrations (0.5–50 µM) at different pH values; the Ampliflu™ Red assay solution was adjusted to the same pH value. In general, a linear correlation between the absorbance of resorufin and hydrogen peroxide concentration was found for all pH values investigated (pH 6.0–9.0). The results were approximately the same for pH 7.0, 7.4, 8.0, 8.5, and 9.0. Only at lower pH (pH 6.0 and 6.5), the slope (and thus the extinction coefficient) of the observed linear regression decreased (Figure 14a). As most enzymes are usually naturally exposed to physiological pH values, pH 7.4 was chosen for all further investigations.

Besides investigating the detection limits and the pH range, the stability of the signal was also examined. For this purpose, the experimental set-up stayed the same, but absorbance was observed over a time span of 20 min (Figure 14b). For the incubated samples, the signal stayed relatively stable over time. The deviation over the whole time of measurement for hydrogen peroxide concentrations ranging from 5 µM to 100 µM, was found to be around 4% when the final values were compared to the initial values. For lower concentrations, the deviation was found to be higher (approximately 15%).

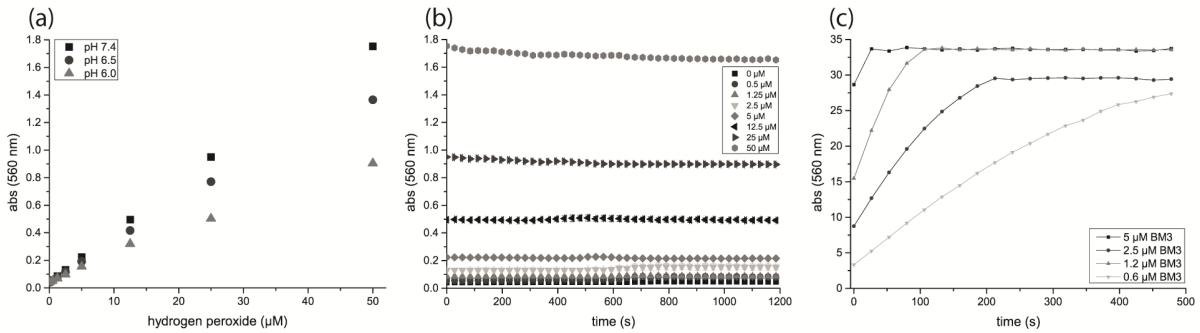

Figure 14: Determination of signal stability, optimal pH, and enzyme concentration for the Ampliflu™ Red assay. The assay solution consisted of 100 µM Ampliflu™ Red, 0.2 U·mL^{-1} in 50 mM sodium phosphate buffer (pH 7.4). (a) For the investigation of the pH range, 100 µL assay solution adjusted to the investigated pH were incubated with 100 µL hydrogen peroxide solution (100, 50, 25, 10, 5, 2.5, and 1 µM) prepared with the same buffer. Only the results for pH 6.0, pH 6.5, and 7.4 are depicted since pH 8.0, 8.5, and 9.0 gave results not distinguishable from pH 7.4. (b) At pH 7.4, the signal stability was determined with the same concentrations of hydrogen peroxide as in (a). (c) The optimal Cytochrome P450 BM3 concentration was determined by incubation of 50 µL containing different enzyme concentrations (5, 2.5, 1.2, and 0.6 µM) with the Ampliflu™ Red assay solution supplemented with 75 µM NADPH. Absorbance was measured at λ = 560 nm. All experiments were performed in triplicates. (Figure from first publication: Morlock *et al.* 2018[179])

Different cytochrome P450 BM3 concentrations were incubated with NADPH in the absence of substrate. Both NADPH consumption (340 nm) and hydrogen peroxide production (560 nm) were followed simultaneously. The NADPH concentration was adjusted to the upper detection limit, which was found to be 50 µM as described above. Without substrate present, it must be presumed, that only uncoupling instead of product formation can result from NADPH consumption. Enzyme stock solutions with 0.6 µM, 1.2 µM, 2.5 µM, and 5 µM were prepared. In the final reaction, these stock solutions were diluted 1:4. The reactions were observed for 500 s (Figure 14c). At higher enzyme concentrations, the reaction went to completion faster; at the lowest concentration, the reaction did not go to completion within the measured time interval. To shorten measuring times, but still be able to follow the course of the reaction, the stock solutions with 1.2 µM cytochrome P450 BM3 (*i.e.*, 0.3 µM final concentration) were used for further experiments.

3.1.6 Investigation of the hydrogen peroxide formation by cytochrome P450 BM3 and five mutants in the reaction with different substrates

Next, the established reaction conditions were tested in the reaction of different enzymes with different substrates. As enzymes, cytochrome P450 BM3 and five mutants found in literature (F87Y[141], R47L[180], Y51F[135], A82L[164] and T268A[181]), were used. These mutants were chosen for different reasons. Cytochrome P450 BM3 F87Y was described before, as an unproductive but correctly folded enzyme, which showed high uncoupling rates.[141] All other mutants have been reported to show different activities and different uncoupling rates in the reaction with different substrates. Therefore, this selection of cytochrome P450 enzyme variants allows the investigation of the reliability of the developed Ampliflu™ Red assay.

Standard substrates for cytochrome P450 BM3 were used as follows: lauric acid (LA), palmitic acid (PA), pentadecanoic acid (PDA), 1-octanol (1-O), and oleic acid (OA).[130] Additionally the reaction without substrate (woS) was investigated.

The results demonstrated that all variants showed preferences for different substrates. The total NADPH consumption, as well as the hydrogen peroxide production, varies for each variant-substrate combination (Table 1).

Table 1: Consumed NADPH and produced hydrogen peroxide (H_2O_2) in the reaction of 0.3 µM purified enzyme with 50 µM NADPH and 100 µM substrate.

	BM3 wt		**BM3 F87Y**		**BM3 R47L**		**BM3 Y51F**		**BM3 A82L**		**BM3 T268A**	
	NADPH	H_2O_2	NADPH	H_2O_2	NADPH	H_2O_2	NADPH	H_2O_2	NADPH	H_2O_2	NADPH	H_2O_2
LA	48.2±1.7	0.3±1.0	20.8±0.8	7.0±1.5	30.0±6.1	3.3±4.2	21.6±1.5	0.3±0.2	24.5±2.0	1.0±0.7	34.2±3.0	0.4±0.7
PA	40.7±0.9	1.6±0.8	11.3±1.6	7.9±1.4	30.7±1.3	6.2±0.6	13.0±1.4	2.2±1.3	32.7±3.5	2.4±0.8	28.3±2.8	1.4±0.2
PDA	38.7±2.9	1.5±0.5	16.7±1.5	7.2±0.8	34.3±0.9	5.9±0.5	14.8±0.7	1.2±1.5	31.1±9.9	1.8±1.7	35.0±1.0	1.5±0.7
1-O	30.1±0.9	1.0±0.8	21.6±0.3	6.6±1.1	38.5±1.0	5.5±0.8	20.8±1.2	0.6±1.2	24.1±0.8	1.4±1.5	20.8±0.9	1.5±2.1
OA	38.4±3.3	1.6±0.5	21.3±0.9	6.4±0.1	36.6±4.2	4.0±0.2	19.2±1.7	0.8±0.4	38.9±1.6	1.1±0.9	26.9±9.6	1.7±1.4
woS	32.1±3.7	12.0±2.3	5.1±1.5	8.0±0.9	23.6±0.8	8.1±0.2	12.5±2.5	4.2±2.3	22.4±0.7	7.4±0.8	22.5±0.1	9.9±6.6
bg	1.5±1.2	0.2±0.3	0.0±2.1	0.7±0.0	0.0±2.1	0.9±0.2	1.6±0.4	0.2±0.3	1.6±0.4	0.2±0.3	1.5±1.2	0.2±0.3

LA: lauric acid, PA: palmitic acid, PDA: pentadecanoic acid, 1-O: 1-octanol, woS: without substrate, bg: background/no enzyme and no substrate) in 50 mM sodium phosphate buffer (pH 7.4) at room temperature for 10 min reaction time.

Assuming that the difference between hydrogen peroxide formation and NADPH consumption equals to some extent product formation (Table 2), the preferred substrate for each variant can be identified based on the data. For cytochrome P450 BM3 wild-type, as well as for the Y51F and T268A mutants, lauric acid is the best substrate. 1-octanol appears to be the best substrate for F87Y and R47L, and oleic acid the best substrate for A82L. On the other hand, lowest conversion seems to appear in the reaction of cytochrome P450 BM3 wild-type with 1-octanol as substrate. For A82L and T268A, 1-octanol also gives the lowest conversion among the tested substrates. For variants F87Y, R47L, and Y51F, the lowest conversion was observed using palmitic acid as substrate.

Table 2: Subtraction of the produced H_2O_2 (µM) from the consumed NADPH (µM) in the reaction of 0.3 µM purified enzyme with 50 µM NADPH and 100 µM substrate.

	BM3 wt	**BM3 F87Y**	**BM3 R47L**	**BM3 Y51F**	**BM3 A82L**	**BM3 T268A**
LA	47.9	13.8	26.7	21.3	23.5	33.9
PA	39.1	3.4	24.5	10.8	30.3	26.9
PDA	37.2	9.5	28.4	13.6	29.2	33.5
1-O	29.2	15.0	33.0	20.3	22.8	19.3
OA	36.8	14.9	32.6	18.4	37.7	25.2
woS	20.2	-2.9	15.5	8.3	14.9	12.6
bg	1.3	0.3	-0.7	1.6	1.6	1.3

LA: lauric acid, PA: palmitic acid, PDA: pentadecanoic acid, 1-O: 1-octanol, woS: without substrate, bg: background/no enzyme and no substrate) in 50 mM sodium phosphate buffer (pH 7.4) at room temperature for 10 min reaction time.

In general, cytochrome P450 BM3 wild-type is known as a well-coupled enzyme;[170] this was also confirmed by the results obtained applying the Ampliflu™ Red assay. Variant F87Y showed almost no conversion and higher uncoupling than the wild-type for all tested substrates, which is in accordance to the literature.[141] This variant was described to show high uncoupling rates, resulting in the formation of water. Herein, the presented data however suggest that the variant F87Y also shows high hydrogen peroxide formation. The difference between consumed NADPH and produced hydrogen peroxide might in addition account for water formation, yielding no to very little product.

Furthermore, positions R47 and Y51 are involved in correct substrate positioning and substrate binding and, therefore, influence efficient catalysis.[135] When exchanging these residues, the resulting variants will show different uncoupling rates, as the substrate positioning will be influenced. For the investigated substrates, there is no literature data available for variant R47L. Only variants with other amino acid exchanges in this position have been investigated with lauric acid as substrate. With alanine or glycine in position 47, k_{cat} K_m^{-1} drops in the conversion of lauric acid, from 17.8 ± 1.4 μM^{-1} min^{-1} for cytochrome P450 BM3 wild-type to 4.6 ± 0.7 μM^{-1} min^{-1} and 4.2 ± 0.6 μM^{-1} min^{-1}, respectively. The k_{cat} K_m^{-1} for the conversion of laurate was less influenced for variant Y51F, which was found to be 14.2 ± 1.0 μM^{-1} min^{-1}.[135] Additionally, cytochrome P450 BM3 Y51F was described as a well-coupled enzyme for the oxidation of laurate, which is also in accordance with the results for this variant presented in this thesis.

Variant T268A showed good conversion for pentadecanoic acid with approximately 90% of the wild-type conversion. With only 70% and 68% of wild-type product formation, lauric acid and palmitic acid, respectively, were found to be worse substrates for this variant. These findings are supported by data found in the literature, where similar coupling efficiencies to wild-type were described for pentadecanoic acid, although lower conversions could be achieved for lauric and palmitic acid.[181] Only higher uncoupling rates, which were reported by Cryle *et al.* in 2008, could not be verified with the assay. However, it is possible that the variant might show uncoupling, forming water, which would not be detected with the hydrogen peroxide assay.

For variant A82L, no data is available in the literature for the conversion of the substrates investigated. For all substrates tested, this variant was found to show average to high conversion and low uncoupling rates when compared to wild-type enzyme.

Since all variants showed a clear difference between consumed NADPH and produced H_2O_2 in reactions performed without substrate, it is likely that water formation accounts for a high percentage of uncoupling products.

In addition to investigating the conversion of the six enzyme variants with different substrates, the uncoupling of cytochrome P450 BM3 wild-type without substrate was investigated. Here, the focus was on the other possible uncoupling products, superoxide anion and water. When subtracting hydrogen peroxide formation from NADPH consumption in the absence of substrate, the difference accounts for the other two uncoupling products. In

general, the aim of this experiment was to see which uncoupling product was the most prominent one in catalysis of cytochrome P450 BM3. However, it must also be noted that these results might differ from substrate to substrate. In addition, without substrate present, uncoupling is usually more prominent. Judging from the results obtained, hydrogen peroxide is the most pronounced uncoupling product for cytochrome P450 BM3 wild-type (Figure 15). The addition of superoxide dismutase did not result in a big difference, when compared to the same reaction without the superoxide dismutase, indicating that the formation of the superoxide anion as uncoupling product is less significant.

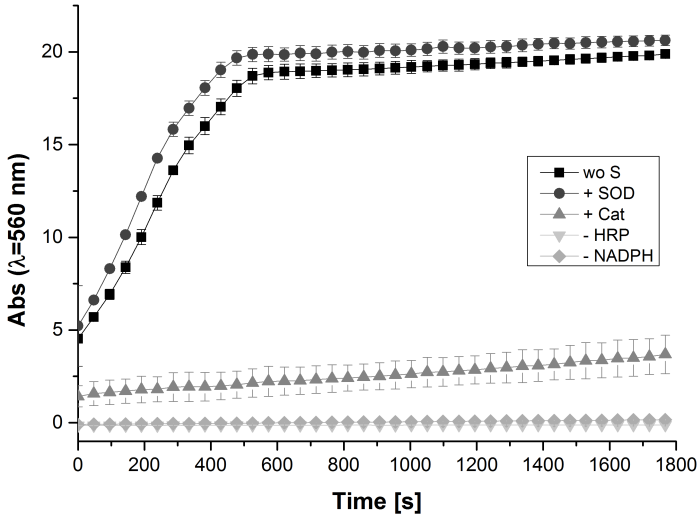

Figure 15: Control reactions with the Ampliflu™ Red assay. With cytochrome P450 BM3 wild-type (0.3 µM final concentration in 50 mM sodium phosphate buffer; pH 7.4) without NADPH (- NADPH), without substrate and horseradish peroxidase (- HRP), without substrate and with 20 U·mL^{-1} catalase (+ Cat), without substrate and with 2 U·mL^{-1} superoxide dismutase (+ SOD) and without substrate (woS). (Figure adapted from first publication: Morlock *et al.* 2018[179])

To confirm that only hydrogen peroxide was detected by the Ampliflu™ Red assay, several negative controls were included (Figure 15). If only NADPH was incubated with the Ampliflu™ Red assay solution, no signal was detected. Without NADPH and only enzyme, substrate, and the assay solution present, again, no signal was detected. The same could be observed if no horseradish peroxide was added to the reaction. This indicated that the signal must be mediated by HRP. When adding catalase to the reaction mixture, the signal was lowered significantly, leading to the assumption that predominantly hydrogen peroxide is detected by the assay.

3.1.7 Investigating the hydrogen peroxide formation by CPR from *C. apicola* with the Ampliflu™ Red assay

Another test of the reliability of the Ampliflu™ Red assay was performed by investigating the uncoupling reaction of the reductase CPR from *C. apicola*.[145] As reductases are thought to produce only hydrogen peroxide and superoxide anion as uncoupling products, the difficulty of investigating water formation was abolished.[182] When adding superoxide dismutase, which converts the superoxide anion to hydrogen peroxide, all uncoupling

products produced can be detected using the same assay. The reductase CPR consumed 14.7 ± 0.6 µM, 7.1 ± 0.9 µM, and 2.5 ± 1.3 µM of the initially applied 22 µM, 12 µM, and 6 µM NADPH, while producing 14.4 ± 0.4 µM, 6.7 ± 0.1 µM, and 3.1 ± 0.2 µM hydrogen peroxide, respectively (Table 3). As the differences between these values were as little as 0.3 µM, 0.4 µM and 0.6 µM, respectively, it can be assumed that the assay gives reliable results.

Table 3: Consumed NADPH, produced H_2O_2, and the difference between both values in the reaction of CPR incubated with different NADPH concentrations.

Initial NADPH concentration [µM]	NADPH [µM]	H_2O_2 [µM]	NADPH-H_2O_2 [µM]
22 µM	14.7 ± 0.6	14.4 ± 0.4	0.3
12 µM	7.1 ± 0.9	6.7 ± 0.1	0.4
6 µM	2.5 ± 1.3	3.1 ± 0.2	-0.6

For each sample, 0.2 µM CPR was incubated with 22 µM, 12 µM, or 6 µM NADPH in 50 mM sodium phosphate buffer (pH 7.4) at room temperature for 30 min. All samples were investigated as triplicates.

The negative controls showed that the reductase cannot directly interact with Ampliflu™ Red. By adding catalase, the signal was significantly lowered, but not completely abolished, with 20% residual signal. As the horseradish peroxidase and catalase activities competed, the signal could not be completely suppressed but only strongly reduced. If the reductase would have interacted directly with Ampliflu™ Red, the addition of catalase would have had less influence on the result of the experiment.

3.1.8 Applicability of the Ampliflu™ Red assay in cell lysate

Although purified enzyme was used in the first tests mentioned above, for high-throughput measurements cell lysate is usually used. Therefore, the signal stability and the results of cytochrome P450 BM3 also needed to be investigated in crude cell lysate.

First, the signal stability was examined. With 50 µL *E. coli* TOP10 cell lysate (1 mg wet cell pellet per 5 mL buffer), the Ampliflu™ Red assay solution and different concentrations of hydrogen peroxide were incubated in a total volume of 200 µL (Figure 16). The solutions were incubated at room temperature for 3 h. Here, it could be shown that the signals were stable over the investigated time span as was observed for samples incubated in buffer. Only for lower concentrations the signal increased over time. This deviation might be explained by the sensitivity of Ampliflu™ Red towards oxygen and light.[183] If small amounts of the probe are oxidized, this would have a greater influence at lower concentrations of hydrogen peroxide.

After finding that the signal was also stable when incubated with cell lysate, the reaction of cytochrome P450 BM3 wild-type and variant T268A in cell lysate was investigated to compare the results to those obtained using purified enzymes.

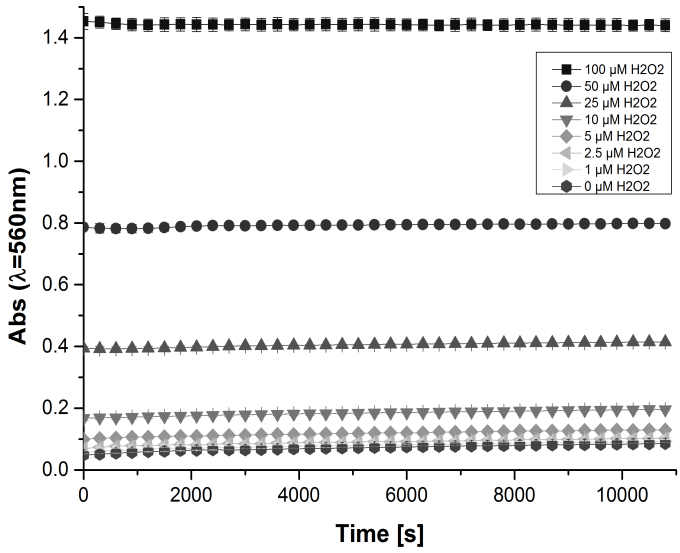

Figure 16: Determination of the signal stability of the Ampliflu™ Red assay when incubated with cell lysate. Assay solution (100 µL) consisting of 100 µM Ampliflu™ Red, 0.2 U·mL^{-1} in 50 mM sodium phosphate buffer (pH 7.4) were incubated with 50 µL hydrogen peroxide solutions prepared with the same buffer (400, 200, 100, 40, 20, 10, and 4 µM) and 50 µL *E. coli* Top10 cell lysate. The stability of the signal was observed at room temperature over 3 h. (Figure adapted from first publication: Morlock *et al.* 2018[179])

The assay was performed under the same conditions as used for the purified enzymes (Table 4). Although the absolute values for the measurements with purified and crude enzyme preparations differed, the tendency for the substrate conversion profiles of both enzymes stayed the same. In both experiments, lauric acid was identified as the best substrate for both enzymes; 1-octanol was least accepted by both enzymes. Noteworthy, all values were higher when investigating the reaction in cell lysate. Upon the addition of NADPH, there might be some other reactions occurring in the unpurified samples. In the cell lysate there are many proteins and molecules present, making it hard to judge which factor exactly is interfering with the measured reaction. However, apparently these influences were small enough to still detect the hydrogen peroxide formation and NADPH consumption during the investigated catalysed reactions.

Table 4: Consumed NADPH, produced hydrogen peroxide (H_2O_2), and difference between the values for the investigated reaction of Cytochrome P450 BM3 wild-type and T268 with different substrates.

	BM3 wild-type			BM3 T268A		
	NADPH [µM]	H_2O_2 [µM]	subtraction	NADPH [µM]	H_2O_2 [µM]	subtraction
LA	50.8±0.3	1.3±0.3	49.5	56.2±1.1	3.1±3.4	53.1
PA	53.3±0.8	4.5±0.8	48.8	54.5±0.6	5.8±0.6	48.7
PDA	49.9±0.2	4.8±0.2	45.1	56.0±0.9	5.4±3.5	50.6
1-O	45.0±1.2	5.2±2.5	39.9	54.7±0.1	11.9±3.0	42.8
OA	54.4±0.7	4.9±0.3	49.5	55.1±0.4	3.6±3.7	51.6
woS	54.8±0.6	23.0±0.3	31.8	55.2±1.5	35.4±7.4	19.8
bg	0.5±0.6	2.8±0.0	-2.2	0.0±0.7	0.3±0.1	-0.3

0.3 µM enzyme in cell lysate was incubated with 50 µM NADPH and 100 µM substrate (LA: lauric acid, PA: palmitic acid, PDA: pentadecanoic acid, 1-O: 1-octanol, woS: without substrate, bg: background/no enzyme and no substrate) in 50 mM sodium phosphate buffer (pH 7.4) at room temperature within 10 min.

3.2 Investigating the bovine CYP11A1 system

For the investigation of the CYP11A1 system, all three proteins, CYP11A1, Adx, and AdR, needed to be expressed and purified. For each protein, different approaches for expression and purification were necessary. In general, expression optimization can be achieved by changing different parameters including the expression host, temperature, expression vector, inducer concentration, cell density at the time of induction, and the co-expression of chaperones. Especially, the co-expression of chaperones can help to enhance the amount of soluble protein obtained, as chaperones facilitate proper protein folding.[184,185] They are also known to resolubilize aggregates.[186] There are various kinds of chaperones, some of which are essential for the correct folding of many proteins and are constitutively expressed in the cell (*e.g.*, GroEL and GroES), whereas others are only expressed in cellular stress responses (*e.g.*, heat-shock proteins).[187]

Additionally, adding precursors for co-factors might be important. For example, during the expression of cytochrome P450 enzymes, the addition of the heme-precursor δ-aminolevulinic acid is well-established to be important for achieving high expression levels.

3.2.1 Expression optimization of bovine CYP11A1

For the expression of the bovine CYP11A1 enzyme, different *E. coli* strains harboring the pTrc99A_P450scc plasmid were initially investigated. *E. coli* TOP10 (DE3), BL21 (DE3), C41 (DE3), C43 (DE3), and *E. coli* Shuffle T7 were used as hosts. Expression was performed at 30°C overnight. With the obtained samples, CO difference spectra were recorded (Table 5) and expression analyzed by SDS-PAGE (Figure 17).

The results of the CO difference spectra indicated that no soluble expression of bovine CYP11A1 occurred. This was confirmed by SDS-PAGE. The results show that all protein was obtained in the insoluble fraction. Next, the expression temperature was lowered to 17°C and

the cultivation time increased to two days. Unfortunately, still no properly folded protein was detected by the CO difference spectra (Table 5).

Table 5: Results of the CO difference spectrum measurement of the obtained cultivation samples. at 30°C (overnight) and 17°C (two days) for bovine CYP11A1 production in the *E. coli* strains TOP10 (DE3), BL21 (DE3), C41 (DE3), C43(DE3), and SHuffle (DE3). After expression, cells were lysed in 50 mM sodium phosphate buffer (pH 7.4) containing 0.2% Triton X-100 and 1 mM EDTA.

	30°C		**17°C**	
***E. coli* strain**	**P450 [nmol L^{-1}]**	**P450 [µg L^{-1}]**	**P450 [nmol L^{-1}]**	**P450 [µg L^{-1}]**
TOP10 (DE3)	0.05	3.0	0.01	0.6
BL21 (DE3)	0.19	11.5	0.05	3.3
C41 (DE3)	0.12	7.3	0.03	1.8
C43 (DE3)	0.10	6.0	0.02	1.3
SHuffle T7	-	-	-	-

Expression of bovine CYP11A1was performed in the *E. coli* strains TOP10 (DE3), BL21 (DE3), C41 (DE3), C43(DE3), and SHuffle (T7)at 30°C (overnight) and 17°C (two days) for production. After expression, cells were lysed in 50 mM sodium phosphate buffer (pH 7.4) containing 0.2% Triton X-100 and 1 mM EDTA.

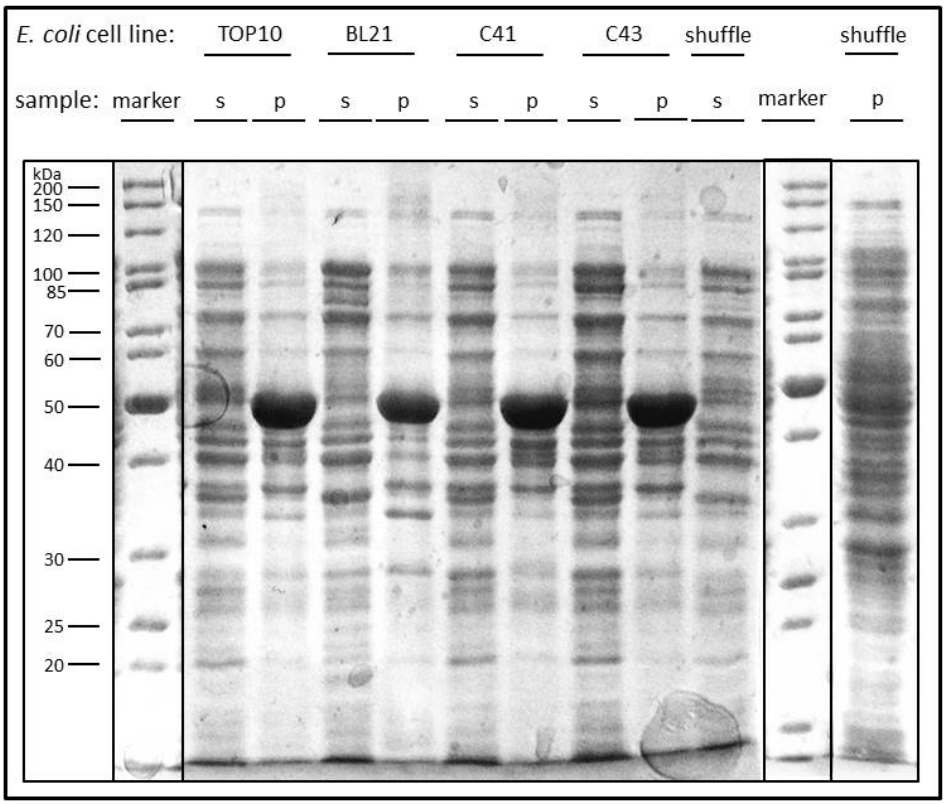

Figure 17: SDS-PAGE of the cultivation samples of the *E. coli* strains TOP10 (DE3), BL21 (DE3), C41 (DE3), C43 (DE3) and, Shuffle T7 harboring the pTrc99A_P450scc plasmid. All samples were taken after overnight expression and normalized to 7/OD_{600}. After cell lysis by sonication in 50 mM sodium phosphate buffer (pH 7.4) containing 0.2% Triton-X-100 and 1 mM EDTA, the soluble fraction (s) was separated from the insoluble fraction (p) by centrifugation for 30 min at 4.000*g*.

Subsequently, the established protocols for the expression of the bovine CYP11A1 in *E. coli* described in literature were tested. Similar to the protocol published by Janocha *et al.* in 2011,

E. coli JM109 (DE3) cells were transformed with pTrc99A_P450scc, cultured and harvested.[188] Since there was no soluble expression visible according to SDS-PAGE analysis, a new protocol with a solubilization step of the membrane bound P450scc was tested.[189] Neither a clear band after SDS-PAGE, nor a positive result from the CO-assay could be observed. Therefore, the protocol of Lepesheva *et al.* from 1998 was investigated.[190] Different cultivations were carried out with *E. coli* JM109 (DE3) transformants containing pTrc99A_P450scc, *E. coli* JM109 (DE3) co-transformants containing pTrc99A_P450scc and pGro7, and *E. coli* JM109 (DE3) transformed with pTrc99A_P450scc and the addition of 3% (v/v) ethanol, which introduces the production of heat-shock proteins, to the culture medium.

Table 6: Results of the expression optimization of CYP11A1 using the protocol of Lepesheva *et al*. from 1998.[190]

Expression vectors	**incorrectly folded P450 [mg mL^{-1}]**	**correctly folded P450 [mg mL^{-1}]**	**total volume [mL]**	**correctly folded P450 (in 75 mL) [mg]**
pTrc99A_P450scc	0,022	0,007	5	0,035
pTrc99A_P450scc, pGro7	0,005	0,012	5	0,060
pTrc99A_P450scc + 3 % EtOH	0,003	0,014	3	0,042

E. coli *was transformed with pTrc99A_P450scc or in combination with pGro7. Further, the effect of the addition of 3% ethanol to the culture was investigated. The differences in total volume are achieved by harvesting cells and resuspending in different volumina, depending on wet cell weight*

The approach with the added ethanol showed the best ratio between correctly and incorrectly folded CYP11A1. The highest total amount of correctly folded enzyme was obtained by co-expression of the chaperones GroEL and GroES from pGro7.

As the co-expression of GroEL and GroES was successful, the co-expression of other chaperones was also investigated, using the same expression protocol as before. Here, four different chaperone plasmids from the Takara Chaperone Plasmid Set (Section 7.1.6) were investigated (Table 7). Additionally, two different *E. coli* JM109 (DE3) strains were compared, one with and one without T1 phage resistance. The resistance is achieved by a knockout of an outer membrane protein receptor for ferrichrome, involved in the transport of the ferrichrome-iron over the outer membrane.[191] Time samples of the cultivation were taken after two and three days and the concentration of correctly folded and incorrectly folded P450 determined by CO difference spectra.

Table 7: Result of the CO-spectrum measurement.

Chaperone plasmid	*E. coli* (DE3)	JM109	Time [h]	P450 [nmol L^{-1}]	P420 [nmol L^{-1}]	P450 [mg L^{-1}]
pGro7		+	48	128.9	0	7.8
			72	4.1	41.9	0.2
pGro7		-	48	189.5	0	11.4
			72	238.5	0	14.4
pKJE7		-	48	0	4.0	0
			72	8.7	6.5	0.5
pGTf2		-	48	0.8	4.1	0.1
			72	5.4	10.0	0.3
pTf16		-	48	0	12.4	0
			72	89.2	32.1	5.4

The + indicates that CYP11A1 was expressed in E. coli *JM109 (DE3) with phage resistance. The - indicates that P450scc was expressed in* E. coli *JM109 (DE3) without phage resistance. The plasmid pTrc99A_P450scc encoding the CYP11A1 gene was used in all approaches. The plasmid pKJE7 harbors the genes* dnaK*,* dnaJ*, and* grpE*; the plasmid pGTf2 harbors the genes* groEL*,* groES*, and* tig*; the plasmid pGro7 harbors the genes* groEL *and* groES*; the plasmid pTf16 harbors the* tig *gene*.

As shown above, the co-expression of GroEL and GroES enhanced the P450scc expression level. By using cells without phage resistance, the expression was improved further. After three days cultivation of an *E. coli* JM109 (DE3) cell culture without phage resistance harboring the plasmids pTrc99A_P450scc and pGro7, expression levels of approximately 14 mg l^{-1} correctly folded CYP11A1 were achieved, which equals a concentration of 240 nmol LL^{-1}. Besides pGro7, co-expression of chaperones from pKJE7 (*dnaK*, *dnaJ* and *grpE*), pGTf2 (*groEL*, *groES* and *tig*) and pTf16 (*tig*) was tested, but did not result in further improvement of the soluble expression level.

As described in the work of Janocha *et al.* in 2011, the exchange of one amino acid of CYP11A1 (K193E) leads to a 4-fold increased expression rate and a 3-fold increased solubility of the enzyme, while having no effect on enzymatic activity.[188]

Therefore, this mutation was introduced by site-directed mutagenesis. Both, the variant and wild-type were expressed under the best conditions identified before. The results of the CO difference spectra showed that the expression of the CYP11A1 K193E variant is only enhanced after two days, whereas after three days the expression of wild-type P450scc was the best, with approximately 14 mg per liter culture compared to 2.1 mg per liter for the variant (Table 8).

Table 8: Results of the CO difference spectrum measurement of the expression comparison of CYP11A1 and CYP11A1 K193E.

CYP11A1	*E. coli* JM109 (DE3)	Time [days]	P450 [nmol L^{-1}]	P420 [nmol L^{-1}]	P450 [mg L^{-1}]
wild-type	-	2	11.1	39.5	0.7
		3	233.5	0	14.1
K193E	-	2	100.3	0	6.1
		3	34.4	0	2.1

The + indicates that P450scc was expressed in E. coli *JM109 (DE3) with phage resistance. The - indicates that CYP11A1 was expressed in* E. coli *JM109 (DE3) without T1 phage resistance. In all four expression approaches GroEL and GroES were co-expressed.*

To determine the best time to harvest the cells during cultivation, the expression of CYP11A1 was monitored over time. Besides determining the CYP11A1 content of the cell cultures, the OD_{600} was determined (Table 9). For this experiment, two separate cultivation flasks under the established standard conditions were monitored and time samples were taken alternating from each flask. As for the CO assay 50 mL sample volume was needed, two flasks had to be used for the amount of time samples investigated. The resulting differences in the OD_{600} of both cultures might result from better oxygen supply after sampling.

Table 9: Over a cultivation time of 72 hours the optical density (OD_{600}) and the CYP11A1 content was monitored.

	OD_{600}		
Time [h]	**flask 1**	**flask 2**	**CYP11A1 [mg L^{-1}]**
0	0.7	0.7	-
16	3.8	3.4	6.9
20	4.3	3.9	9.5
24	5.0	4.2	7.8
40	9.9	5.6	11.9
44	10.5	6.3	10.3
48	12.7	7.0	12.0
64	12.0	8.8	10.9
68	16.7	8.8	13.8
72	16.5	14.7	20.1

For each day three samples of 50 mL each were taken from the two different flasks in a sequential order. For the sample time point of each flask, the OD_{600} is shown with a light gray background. The initial volume in each flask was 500 mL of TB medium.

Both the concentration of CYP11A1 and the OD_{600} increased over time. The highest concentration of CYP11A1 was achieved after 72 h cultivation time with a final concentration of 20.1 mg L^{-1}.

Additionally, a substrate binding spectrum of the last sample was recorded with cholesterol in order to investigate whether the obtained CYP11A1 enzyme was capable of binding the substrate (Figure 18). The substrate was added from a 10 mM stock solution in 45% (ω/v) aqueous 2-hydroxypropyl-β-cyclodextrin, resulting in a final concentration of 0.2 mM. As

baseline, the spectrum of the same CYP11A1 solution was measured, before adding the substrate solution. The resulting difference spectrum is a type-I spectrum, which is typical for substrates correctly bound in the active site of cytochrome P450 enzymes.[46]

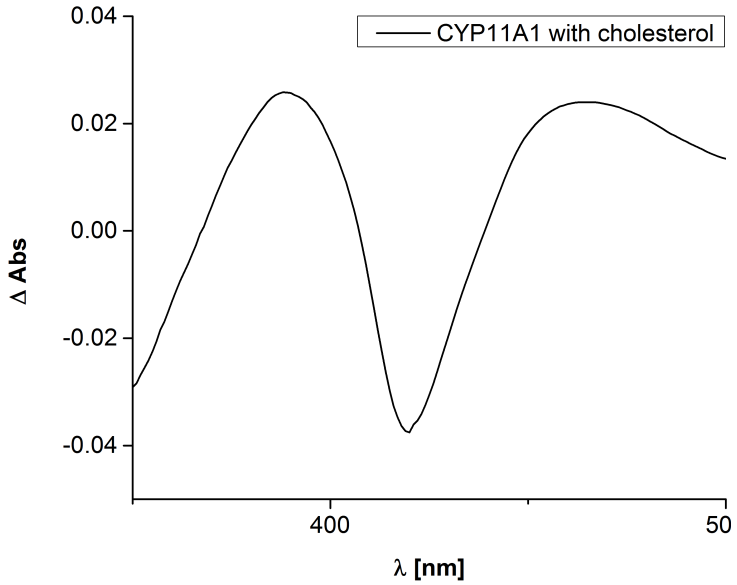

Figure 18: Substrate binding spectrum of CYP11A1 incubated with 0.2 mM cholesterol, added from a 10 mM stock solution in 45% (w/v) aqueous 2-hydroxypropyl-β-cyclodextrin. As blank, the same CYP11A1 solution, without substrate present was measured first. The spectrum was recorded over a wavelength range from 350 nm to 500 nm.

3.2.2 Purification of bovine CYP11A1

To obtain pure enzyme, a C-terminal His-tag was introduced into the P450scc coding sequence on the pTrc99A plasmid.

In a study by Mosa *et al*. from 2015, the purification of the His-tagged CYP11A1 was described.[192] By following this protocol, with slight modifications, CYP11A1 was found in the elution fraction (Figure 19). The eluted enzyme solution had a concentration of 4 µmol L^{-1}, which equals a concentration of 242 mg L^{-1}. Unfortunately, high amounts of CYP11A1 are found in the flow-through and in the washing fraction. This result indicates a problem with binding to the Ni-NTA column used, which might have been due to the additives (sodium cholate, sodium acetate and TWEEN 20) in the buffers used for purification. As the washing buffer did not contain imidazole, the problems with binding did not occur due to a too high imidazole concentration. Some of the additives might interfere with the availability of the His-tag, by shielding it, for example.

Therefore, the purification in 50 mM sodium phosphate buffer (pH 7.4) without additives was also investigated. Although the purity of CYP11A1 was further enhanced, the protein stability was decreased and most protein was found to be incorrectly folded.

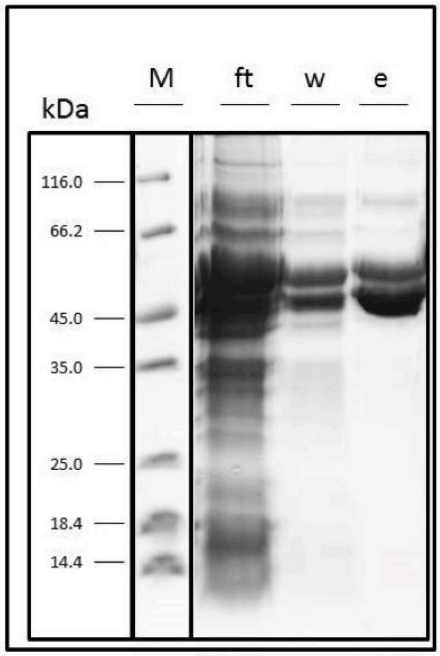

Figure 19: SDS-PAGE analysis of bovine P450scc purification by IMAC. After after cell lysis, the His-tagged enzyme was purified from the supernatant on a Ni-NTA column. A molecular marker (M), the flow-through (ft), the washing (w) fraction, and the eluate (e) from the purification were loaded onto the gel.

Alternatively, purification with SP Sepharose resin was examined. As the enzyme was only stable in the buffer used in the study of Mosa *et al.*, this buffer was also used for this purification approach. Unfortunately, the CYP11A1 protein did not bind to the column under the investigated conditions and was exclusively found in the flow-through (data not shown).

3.2.3 Expression of bovine Adx

For the investigation of the CYP11A1, Adx is needed as electron shuttle between AdR and CYP11A1. Therefore, the expression and purification of this protein were also investigated. Adx is a soluble, iron-sulfur containing protein with a molecular weight of 14 kDa.[193]

First, the expression was tested for the two different plasmids pBad_Adx and pKKHc_Adx in *E. coli* BL21 (DE3) and *E. coli* JM109 (DE3). This first test indicated a higher expression level with the pKKHc_Adx plasmid, judging from SDS-PAGE analysis (Figure 20). Hence, *E. coli* BL21 (DE3) cells harboring the pKKHc_Adx plasmid were used for further investigations.

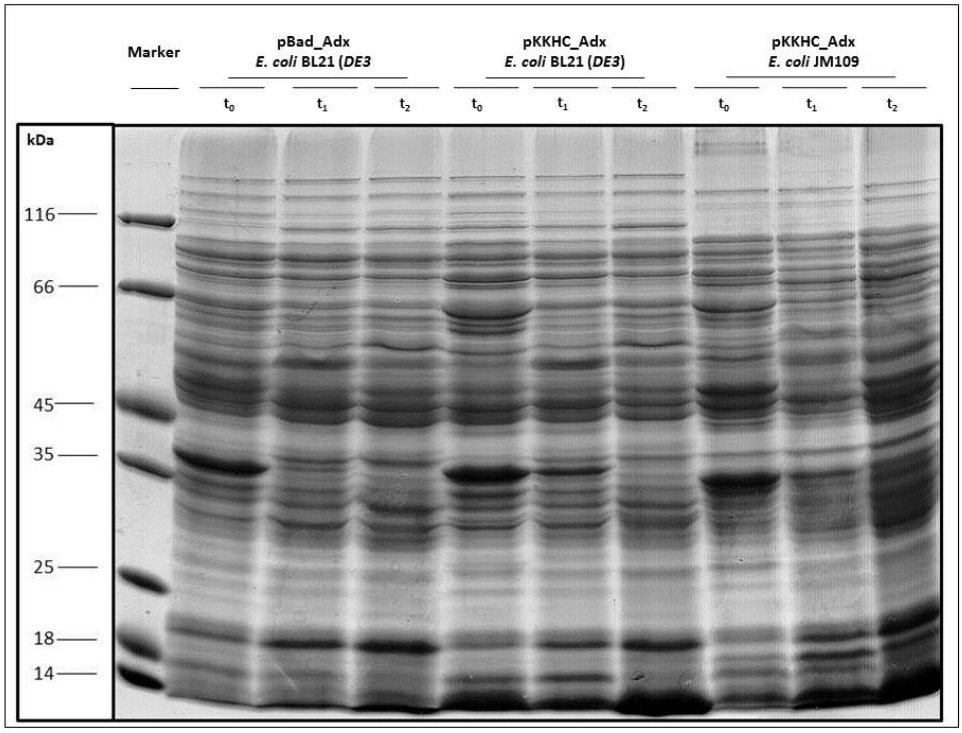

Figure 20: SDS-PAGE analysis of the expression of Adx from pBad_Adx in *E. coli* BL21 (DE3) and pKKHC_Adx in *E. coli* BL21 (DE3) and JM109 (DE3). Besides the marker, samples at the time point of induction (t_0) and a sample after one day (t_1) and two days (t_2) of cultivation were loaded on the gel.

3.2.4 Purification of bovine Adx

After finding cultivation conditions for successful expression of soluble bovine Adx, the purification of the protein was investigated. A study from Suhara *et al.* from 1972 suggested that purification of the protein could be accomplished by using anion-exchange chromatography with DEAE-cellulose as column material.[194] In that study, however, the protein was purified from bovine adrenal cortex tissue samples.

As buffer, 10 mM potassium phosphate (pH 7.4) was used. For elution, different gradients were tested. A 0–1 M KCl gradient over 10 CVs showed the best results (Figure 21). For the elution fraction, a spectrum of wavelengths ranging from $\lambda = 500$ nm to $\lambda = 280$ nm was recorded (Figure 22A). This spectrum shows the three typical absorption maxima of the iron-sulfur cluster of Adx and is in accordance to the published spectrum (Figure 22B).[194]

Since adding another purification step might enhance the purity of the obtained protein solution, a gel filtration step was included after the purification on DEAE-cellulose.

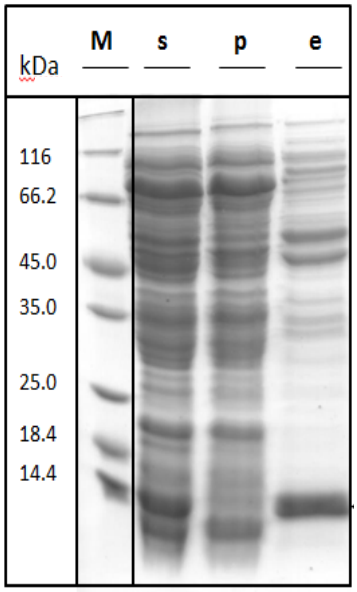

Figure 21: SDS-PAGE analysis of bovine adrenodoxin (Adx). The enzyme was purified from the supernatent after cell lysis on a DEAE-cellulose column. A molecular marker (M), the supernatant (s), the pellet (p) after cell lysis, and the eluate (e) of the purification were loaded onto the gel.

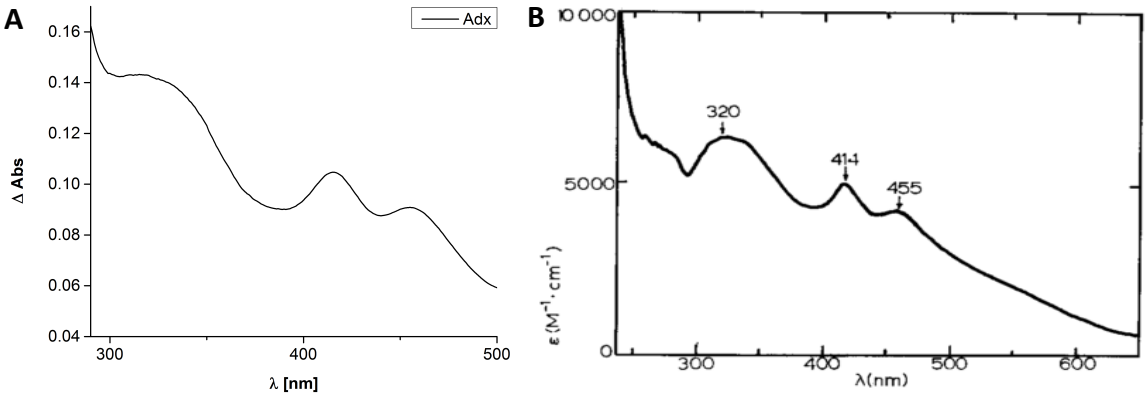

Figure 22: A) Absorption spectrum of the elution fraction from a purification of bovine Adx on a DEAE-cellulose column. B) Characterisic absorption spectrum of bovine Adx. The iron-sulfur clustur in the active site causes these characteristic peaks. (Figure from Suhara et al. 1972 [194])

After gel filtration on a Superdex 200 column, using 10 mM potassium phosphate buffer (pH 7.4), the purity of the bovine Adx was further enhanced (Figure 23). Unfortunately, the protein fraction had completely lost the typical brown color. This might indicate that the iron-sulfur cluster was lost during gel filtration. Therefore, a spectrum was recorded for this elution fraction and none of the typical three peaks were detected anymore, supporting the assumption that the iron-sulfur cluster was lost.

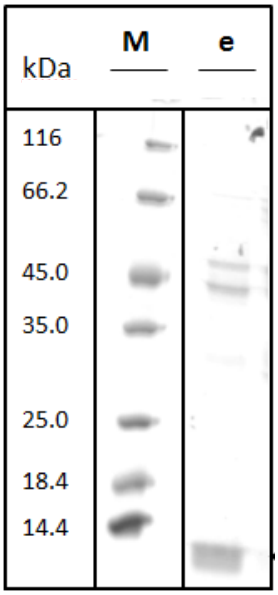

Figure 23: SDS-PAGE analysis of a bovine Adx sample. The enzyme was purified from the supernatent after cell lysis on a DEAE-cellulose column and further purified on a Superdex 200 column. A molecular marker (M) and the elution (e) fraction of this purification were loaded on the gel.

As a last approach, hydrophobic interaction chromatography was tested for the purification of bovine Adx. As the calculated pI of the protein is 4.72, Adx in 10 mM potassium phosphate buffer (pH 7.4) was used on a Phenyl Sepharose column. Unfortunately, the protein did not bind to the column material under these conditions. As changing the pH of the used buffer might help with protein binding. If the protein would be unstable at a different pH, this would however not be advantageous. Therefore, the pH stability of the enzyme was of interest for the optimization of the purification procedure using anion exchange chromatography.

3.2.5 Expression of bovine AdR

In addition to the soluble Adx, the membrane-bound protein AdR with a size of 51 kDa is needed for the electron supply of CYP11A1.[195]

As before, expression was investigated using *E. coli* JM109 (DE3) and *E. coli* BL21 (DE3) as host organisms with the plasmids pBar1607_AdR and pET28_AdR. Additionally, the co-expression of groEL and groES was investigated.

From all cultivations, SDS-PAGE analysis was performed for samples taken at different time points. The best result was obtained for *E. coli* BL21 (DE3) harboring the plasmids pET28_AdR and pGro7 (Figure 24). Purification of the expressed protein was subsequently investigated.

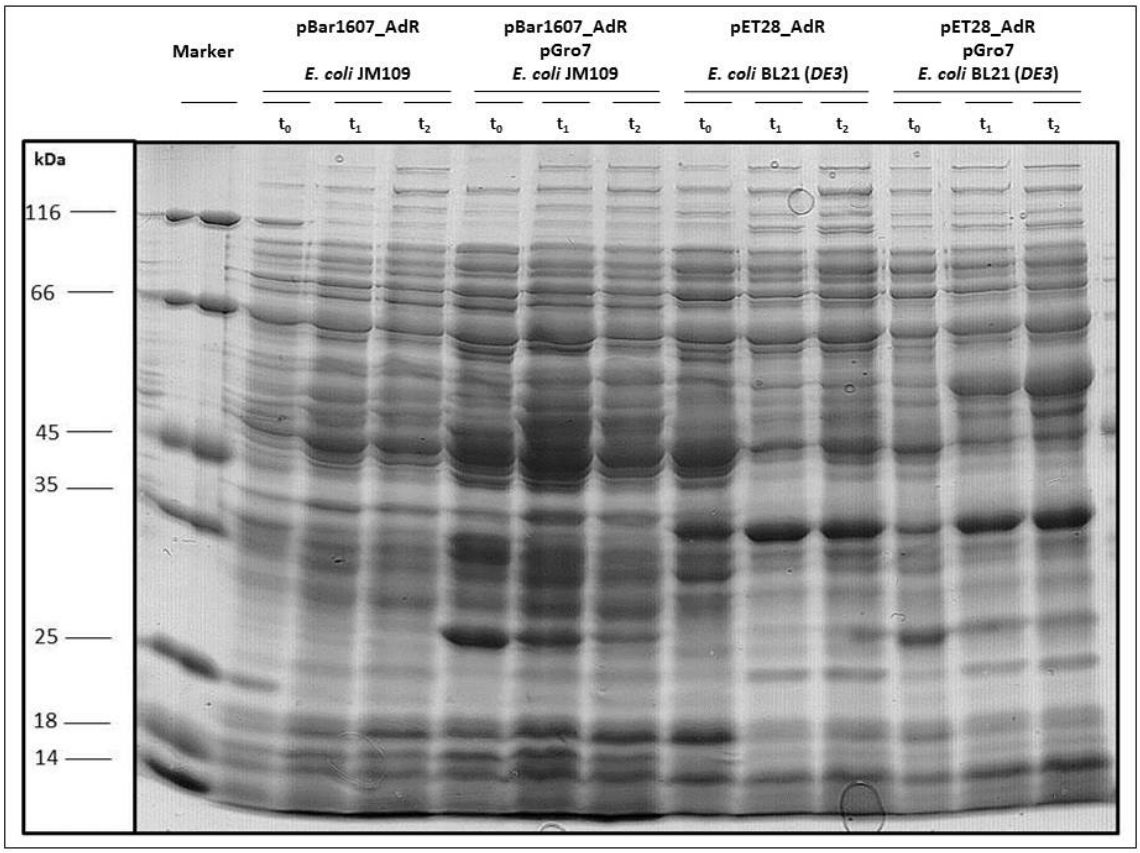

Figure 24: SDS-PAGE analysis of the expression of AdR from pBar1607_AdR in *E. coli* JM109 with and without chaperone co-expression (groEL and groES from pGro7) and pET28_AdR in *E. coli* BL21 (DE3) with and without chaperone co-expression. Besides the marker, samples at the time point of induction (t_0) and a sample after one day (t_1) and two days (t_2) of cultivation were loaded on the gel for all four cultivations.

3.2.6 Purification of bovine AdR

For purification of the bovine AdR protein, a similar approach as used for Adx was chosen. First, an anion-exchange chromatography was tested on a DEAE Sepharose resin. As buffer, sodium phosphate (pH 8.5) was used and elution accomplished by a linear gradient over 10 CVs from 0 to 1 M KCl. The eluate was collected in 2 mL and analyzed by SDS-PAGE. Afterwards, the most concentrated fractions were pooled and again analyzed by SDS-PAGE (Figure 25). As the elution fraction obtained was not sufficiently pure, further purification strategies were investigated.

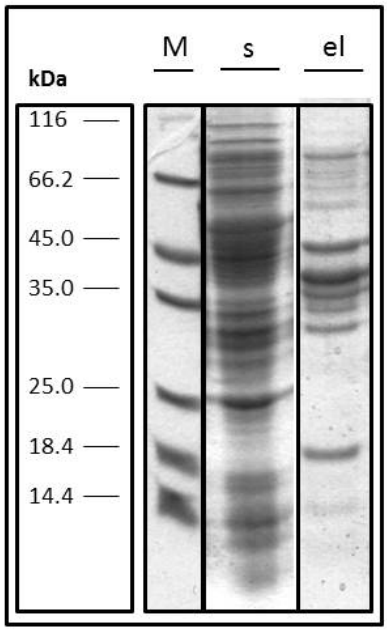

Figure 25: SDS-PAGE analysis of bovine adrenodoxin reductase (AdR) expression. after cell lysis the enzyme was purified from the supernatant on a DEAE column. A molecular marker (M), the supernatant (s), and the pooled eluates (el) of the purification were loaded onto the gel.

As the pI of the bovine AdR protein was calculated as 6.79, another anion-exchange chromatography approach was tested. As proteins interact differently with different column materials, a Source Q resin was used with 10 mM potassium phosphate buffer (pH 8.0) supplemented with 1 mM EDTA. Here, no binding was observed, and no good elution fraction obtained.

Next, purification on a 2'5' ADP Sepharose column was investigated. This resin has a structural NADP analog immobilized on Sepharose and is, therefore, used for the purification of NADPH dependent enzymes. Here, again, a potassium phosphate buffer (pH 8.5) was used and elution performed with a linear gradient from 0 to 500 mM KCl over 5 CVs. Unfortunately, no protein bound to the column.

3.2.7 Biocatalysis transformation with the bovine CYP11A1

As the purification and expression of bovine AdR remained difficult, different redox partner systems were investigated with the purified recombinant bovine CYP11A1 enzyme. Therefore, the Pdx/PdR system from *P. putida* and CPR from *C. apicola* were expressed and purified (Figure 26). Additionally, Adx was combined with PdR as alternative redoxin. Furthermore, glucose-dehydrogenase (GDH) was added to regenerate NAD(P)H.

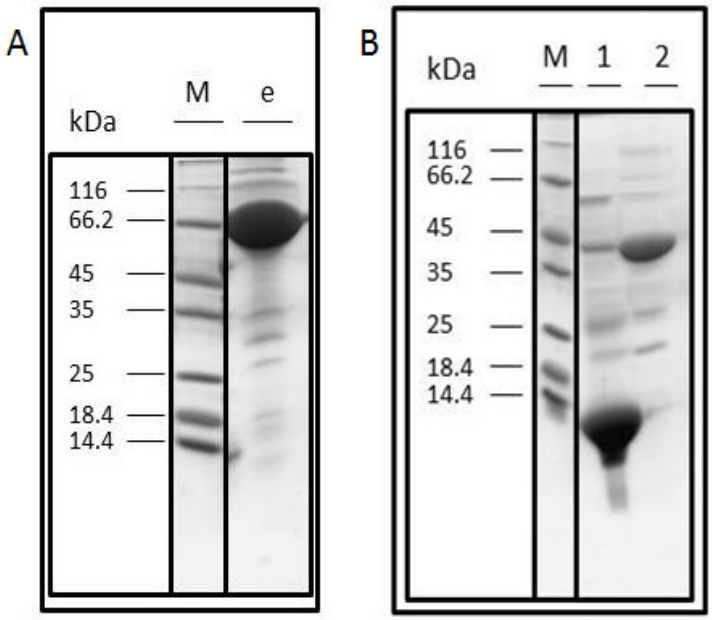

Figure 26: SDS-PAGE analysis of different redox partners. The His-tagged enzymes were purified from the supernatant after cell lysis via IMAC (Ni-NTA). (A) CPR from *C. apicola*: molecular marker (M) and the eluate (e) were loaded on this gel. (B) Pdx and PdR from *P. putida*. A molecular marker (M) and the eluates containing Pdx (1) and PdR (2) were loaded on this gel.

Biocatalysis was performed overnight at 37°C, 300 rpm for 16 h. After extraction and derivatization with MSTFA, the samples were analyzed by GC-MS (Table 2).

Table 10: Results of the first biocatalytic approach for the conversion of cholesterol with purified, recombinant bovine CYP11A1 enzyme in combination with different redox partner systems.

Sample description	ret. time	Cholesterol [mM]
CYP11A1 + Pdx/PdR + GDH	10.302	0,38
CYP11A1 + CPR + GDH	10.296	0,60
CYP11A1 + Adx/PdR + GDH	10.292	0,45
CYP11A1 w/o redox partner system	10.390	1,53
w/o P450 + Pdx/PdR + GDH	10.381	1,44
w/o P450 + CPR + GDH	10.401	1,69
w/o P450 + Adx/PdR + GDH	10.377	1,60
CYP11A1 + Pdx/PdR	10.299	0,53
CYP11A1 + CPR	10.304	0,66
CYP11A1 + Adx/PdR	10.303	0,53
Substrate only	10.387	1,86
CYP11A1 + Pdx/PdR + GDH (t=0 h)	10.383	1,80

1.75 mM cholesterol were incubated with 0.4 µM of the purified bovine CYP11A1 enzyme in combination with different redox partner systems (5 µM Pdx/0.5 µM PdR from P. putida, 0.4 µM CPR from C. apicola, or 0.5 µM bovine Adx combined with 0.5 µM PdR from P. putida) in 20 mM HEPES-HCl buffer (pH 7.3) containing 50 mM KCl and 0.1 mM DTT at 37°C, 300 rpm for 16 h. For some samples, GDH 0.1 mM glucose were added for co-factor recycling. As co-factor 1.5 mM NADH was added for PdR and 1.5 mM NADPH for CPR.

The GC-MS results showed decreased cholesterol concentrations for all samples containing a redox partner system and the cytochrome P450 enzyme with the substrate and necessary co-factor. The negative controls without cytochrome P450 enzyme showed only slight decrease in cholesterol concentration, presumably resulting from extraction problems. Additionally, the negative control containing the bovine CYP11A1 but no redox partner system also showed no substrate consumption.

Unfortunately, no pregnenolone was detected, although the analytical method used was thoroughly investigated regarding the extraction procedure and the simultaneous detection of substrate and product by GC-MS analysis. Hence, analytical problems could be excluded. Due to the negative controls, impurities in the concentrated protein fractions could be excluded, since only applying the redox partner system or the cytochrome P450 enzyme did not result in a decrease of cholesterol concentration. Another possibility could be that cholesterol is trapped in the active site of the enzyme, but since the concentration of P450scc was only 0.4 µM and the concentration of cholesterol was 1.75 mM this seems unlikely.

As no product formation was detected, neither an additional product peak was found, nor an explanation was found, the experiment was repeated with CYP11A1 and Pdx/PdR as redox partner system. Different time samples were taken to investigate whether the decrease in cholesterol concentration occurs over time. This time, no decrease in cholesterol concentration was observed in the samples containing CYP11A1 and the redox partners. Negative controls showed no decrease in cholesterol concentrations, as expected. These results indicate, that the first observed reduced cholesterol concentrations might have been erroneous.

3.2.8 Fusion protein of CYP11A1 and the reductive domain of BM3 (BMR)

In literature, fusion proteins of type-I cytochrome P450 enzymes with the reductive domain of BM3 (BMR) have been described to not only enhance the activity, but also the soluble expression levels of these enzymes.[49,60,151,152]

Therefore, a plasmid for the expression of the fusion construct consisting of CYP11A1 and BMR was constructed by FastCloning.[196] As template, the pET28a_BMR plasmid was used and amplified with primers containing 30 bp long overhangs coding for the terminal nucleotides on both sides of the CYP11A1 gene. From the pTrc99A_P450scc plasmid, the CYP11A1 gene without stop codon was amplified with 30 bp long overhangs coding for the 5'-nucleotides of BMR and a portion of the pET28a plasmid backbone. After obtaining both fragments, FastCloning was performed and the plasmid sequenced. The newly assembled plasmid contained the correct fusion sequence (Figure 27). Subsequently, expression experiments were performed in *E. coli* BL21 (DE3) using different expression temperatures and inducer concentrations. CO difference spectra were recorded to investigate the final concentration of the CYP11A1_BMR fusion protein. Unfortunately, in none of the investigated samples, soluble protein could be detected.

Figure 27: Plasmid map of the pET28a(+)_P450scc_BMR plasmid constructed by FastCloning.

In parallel, *in vitro* biocatalysis was performed with both separate proteins the purified CYP11A1 and the BMR present. The activity of BMR was investigated before by adding NADPH and DCPIP. Here, a fast NADPH depletion was observed along with the conversion of dark blue DCPIP to its colorless reduced form. The conversion of 1.2 mM cholesterol was investigated at 20°C and 30°C with the GDH system for NADPH recycling. Unfortunately, for none of the samples a decrease in cholesterol was detected; new product peaks could not be detected either.

Therefore, no further investigations on the expression of the CYP11A1_BMR fusion protein were conducted. The focus was shifted to the CYP11A1 system regarding the pH and thermal stability of all three proteins.

3.2.9 Stability experiments with the CYP11A1 system

Christopher Grimm (Master thesis student under my co-supervision) performed investigations on the stability of all three proteins of the CYP11A1 system during his master thesis. Briefly, the cell pellets of the individually expressed proteins were lysed in various buffers at different pH and incubated at different temperatures.

For the CYP11A1 enzyme in crude lysate, the above described buffers of Mosa *et al.* (50 mM potassium phosphate buffer with 20% (w/v) glycerol, 1.5% (w/v) sodium cholate, 500 mM sodium acetate, 1.5% (w/v) TWEEN 20, 0.1 mM EDTA, and 0.1 mM DTT as additives)[192] and a HEPES-HCl buffer (pH 7.4) without additives were used. Incubation was performed at 20°C to 60°C for 1 h. At 20°C, the highest concentration of correctly folded CYP11A1 was found in the described buffer with additives. Therefore, further investigations were exclusively performed

in this buffer. Next, the pH optimum was determined by adjusting the potassium buffer to pH 7, 8, 9 and 10. Here, the highest stability with 91.4 ± 1.1% at pH 7was determined by CO-assay after 1 h incubation time. Further, the stability over 6 h was investigated under the same conditions with shaking (800 rpm). After 6 h, approximately 63.2 ± 3% of the initial concentration of CYP11A1 were still found to be correctly folded as determined by CO-assay.

For Adx, the purification was further optimized by using a more distinct elution gradient between 400 mM and 600 mM KCl (instead of 0 mM to 1 M). Thereby, a high purity of Adx with 0.51 mg total protein from 100 mL culture volume were obtained. Afterwards, stability experiments were performed with purified Adx and crude lysate as described for the CYP11A1 enzyme. First, the pH stability was investigated in 100 mM Davies buffer ranging from pH 2 to pH 12. Interestingly, the purified protein was found to be stable at a very broad range from pH 6 to 12 with over 96% protein stability after 1 h incubation. As the CYP11A1 enzyme showed the highest stability at physiological pH, further investigations were performed at pH 7.4. The Adx protein remained stable at temperatures up to 40°C, with 91.3 ± 0.5% after 1 h incubation time in HEPES-HCl buffer pH 7.4. At 50°C and 60°C, the stability decreased, with only 57.0 ± 0.5% and 29.0 ± 0.3% remaining after 1 h incubation, respectively.

For AdR, further expression experiments were performed. The expression in different *E. coli* strains from two AdR-coding plasmids – pET28a_AdR and pBar1607_AdR – was investigated. Most protein was found in the insoluble fractions. Although only visible as a minor band after SDS-PAGE analysis, AdR was best expressed in TOP10 cells harboring the pBar1607_AdR plasmid. With these cultivation conditions, purification was investigated on DEAE Sepharose using 50 mM potassium phosphate buffer (pH 9.0). Elution was accomplished by a 100–200 mM KCl gradient. No further improvement to the above described purification strategy was achieved (Section 3.2.6). It remains unclear if the protein was obtained, as the recorded spectra hardly differed from the recorded spectra of the empty vector *E. coli* cell lysate. Usually, an absorption peak at 425 nm can be observed for AdR. Also, an assay investigating the reductivity of the protein hardly differed between *E. coli* cell lysate and the AdR sample.

Therefore, further experiments with different unnatural redox partner systems were performed. With the cytochrome c assay, different redox partner systems can be compared. If cytochrome c is incubated with the redox partner system only, the reduction can be monitored over time. When adding CYP11A1 to the same sample, the difference in cytochrome c reduction equals the amount of reduced CYP11A1 by the investigated redox partner system. This assay showed that apparently none of the investigated redox partner systems (CPR, BMR, Pdx/PdR, and Adx/PdR) were suitable for transferring electrons to the CYP11A1 enzyme.

Therefore, *in vivo* biocatalysis was investigated using the pBar_Triple plasmid, kindly provided by Dr. Ludmila Novikova (Lomonosov Moscow State University, Russia).[89]

3.2.10 Whole-cell catalysis with the CYP11A1 system

With *E. coli* TOP10 (DE3) cells harboring the pBar_Triple plasmid, encoding all three proteins, whole cell biocatalysis was performed as described by Mekeeva *et al.* in 2013.[89] The 0.27% conversion of the substrate cholesterol observed after 24 h was comparable to the 0.22% conversion reported in the literature.[89]

Christopher Grimm investigated the whole-cell biocatalysis approach further by investigating a different detergent to enhance the possibly enhance the solubility of cholesterol. Makeeva *et al*. could already demonstrate, that the employed solubilization agent influences the conversion, by comparing two different detergents: Tween 80 and methyl-β-cyclodextrin (MCD).[89] As the employment of 33% (w/v) MCD showed a 3-fold increased conversion the whole-cell approach, additionally the conversion of cholesterol solved in 45% (w/v) 2-(hydroxypropyl)-β-cyclodextrin (HPCD) was investigated. By employing HPCD the substrate supply could be further optimized. This increased substrate conversion 10-fold to 2.2 ± 0.6%.

Concluding from all experiments performed with the CYP11A1 system, the CYP11A1 enzyme seems to be unstable. Additionally, the activity determined for whole-cell transformations was low. The aim of this work was to introduce different mutations and study their influence on both the overall activity and the uncoupling of the catalytic cycle. However, enzyme variants are likely to have reduced activity, compared to the wild-type, suggesting that the whole-cell biocatalysis assay would not be sensitive enough to detect the activity of important mutants. Taking in consideration that the expression and purification of AdR remained difficult, *in vitro* biocatalysis could not be performed, and the focus was shifted to another cytochrome P450 enzyme, the human CYP17A1. Work on this enzyme described in the following section.

3.3 Investigating the CYP17A1 enzyme

Next, the activity of the CYP17A1 enzyme, catalysing the next step in steroidogenesis was investigated. For the human enzyme, the crystal structure was solved.[124] Additionally, the bovine enzyme showed in a whole-cell approach, described in literature using 100 µM substrate, full conversion after 24 h.[197] Therefore, this enzyme seemed to be better suited for the investigation of the influence of different active site variants.

For the CYP17A1 enzyme, the natural redox partner system was not available. Consequently, for *in vitro* activity tests, a suitable reductase or redox partner system for efficient electron transfer to the active site of CYP17A1 had to be identified. It has been shown that a reductase present in *S. cerevisiae* are suitable partners for this enzyme.[197] Hence, whole-cell biocatalysis using *S. cerevisiae* cells was attempted.

3.3.1 Expression and purification of the human CYP17A1 enzyme

Expression of the human CYP17A1 was accomplished by cultivating *E. coli* JM109 (DE3) cells harboring the pCW17A1Δ19H plasmid. Following the cultivation protocol by Petrunak *et al*. from 2014, human CYP17A1 was expressed successfully, yielding approximately 4 mg of soluble protein per 100 mL culture.[110] Although purification of the protein was investigated, no optimal purification conditions could be identified. For all purification conditions investigated, the protein did either not bind to the column and was found in the flow-through, or the protein did in fact bind to the resin, it was unstable in the buffer used and therefore no longer correctly folded after purification. Hence, further investigations were carried out using crude lysate.

3.3.2 Comparison between Pdx/PdR and CPR as potential redox partner systems for human CYP17A1

Biotransformations were performed using the expressed recombinant human CYP17A1. *In vitro* transformations using this enzyme have not been described in literature. As mentioned above, the natural redox partner was not available. Thus, the often-applied system Pdx/PdR from *P. putida* and CPR from *C. apicola* were tested.

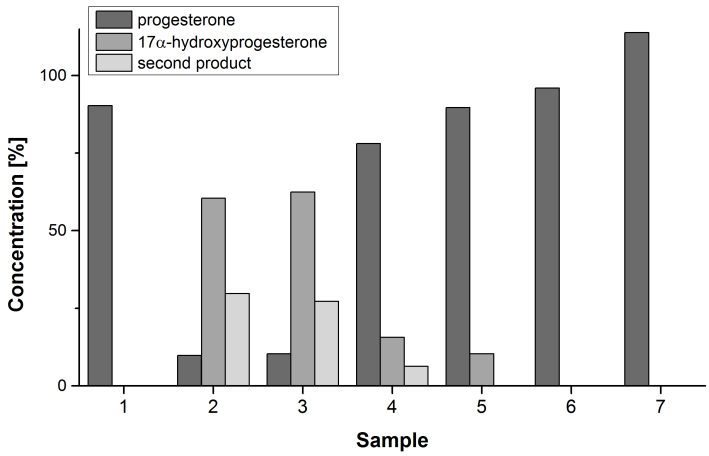

Figure 28: Results of the *in vitro* biocatalysis approach using lysate from *E. coli* JM109 (DE3) expressing human CYP17A1. For each sample, 100 µM progesterone was incubated with 4 µM CYP17A1, 0.5 µM PdR, 2.5 µM Pdx or 2.5 µM CPR, and 25 µM NAD(P)H. For the Pdx/PdR system and CPR, NADH and NADPH were used, respectively. All samples were incubated at 30°C, 600 rpm for 24 h. Samples: **1**: 0 h (no incubation); **2**: Pdx/PdR; **3**: Pdx/PdR without (w/o) NADH; **4**: CPR; **5**: CPR w/o NADPH; **6**: no redox partner system; **7**: no CYP17A1. All samples were extracted with ethyl acetate and analyzed by HPLC. All samples were measured as duplicates, from two separat biocatalytic approaches. Therefore, standard deviation was not calculated.

In vitro biocatalysis using the Pdx/PdR system resulted in 90.2% conversion of the substrate with 9.8% progesterone remaining after 24 h (Figure 28, sample **2**). In contrast, the samples containing CPR had 78.1% progesterone remaining in the sample after 24 h incubation (Figure 28, sample **4**). The negative controls without CYP17A1 (Figure 28, sample **7**) or without redox partner system added (Figure 28, sample **6**) showed no conversion. No product formation observed in the sample (**1**) immediately after addition of NAD(P)H, i.e. without incubation.

Only the negative controls without addition of NAD(P)H showed conversion. In case of the Pdx/PdR system (Figure 28, sample **3**), same conversion was achieved for both samples, whereas for CPR the conversion was lower without addition of NADPH (Figure 28, sample **5**). For the sample containing CPR without addition of NADPH, 89.7% progesterone remained after 24 h incubation time, which is 11.6% more than the CPR sample with addition of NADPH.

As the conversion of progesterone by human CYP17A1 with the Pdx/PdR system was much higher compared to the conversion with CPR as redox partner system, the Pdx/PdR system was chosen for further experiments.

3.3.3 *In vitro* biocatalysis using the human CYP17A1 enzyme

As a next step, more negative controls were added to investigate the conversion of progesterone using CYP17A1 in combination with the Pdx/PdR system. As the samples without adding NADH showed conversion in previous experiments, the uncoupling variant T306A was investigated as a potential additional negative control. The T306A variant was described by Khatri *et al.* in 2014.[198] As the CYP17A1 T306A variant is also applied in crude cell lysate, possible side reactions in the cell lysate can be investigated. Additionally, in this approach ultrafiltration using a centrifugal filter with a 30 kDa cutoff was used in an attempt to reduce the NADH/NAD^+ concentration present in the cell lysate.

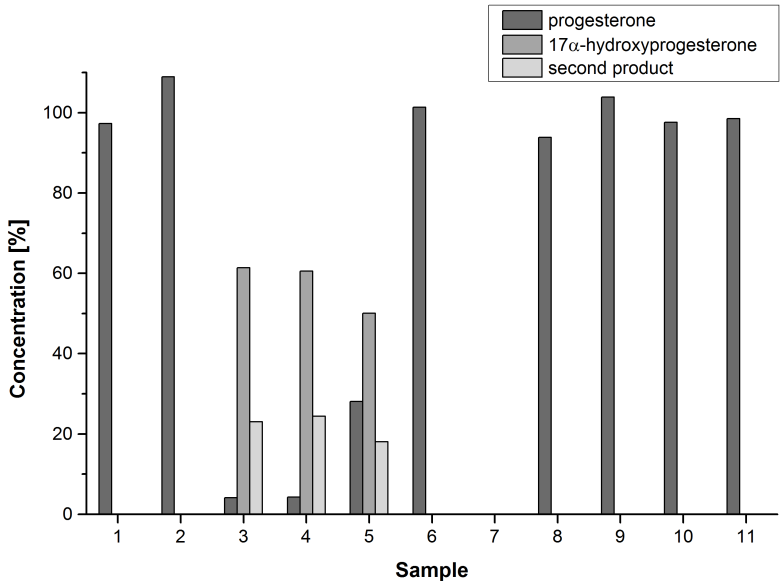

Figure 29: Results of the *in vitro* biocatalysis approach with *E. coli* JM109 (DE3) cell lysate containing human CYP17A1 wild-type (wt) or variant T306A. For each sample, 100 µM progesterone was incubated with 4 µM CYP17A1, 0.5 µM PdR, 2.5 µM Pdx, and 25 µM NADH. All samples were incubated at 30°C, 600 rpm for 24 h. Samples: **1**: no enzyme, 0 h (no incubation); **2**: no enzyme; **3**: wt; **4**: wt with 50 µM NADH concentration; **5**: wt without (w/o) NADH; **6**: wt w/o Pdx/PdR; **7**: wt w/o substrate; **8**: T306A; **9**: T306A with 50 µM NADH; **10**: T306A w/o Pdx/PdR; **11**: T306A w/o NADH. All samples were extracted with ethyl acetate and analyzed by HPLC. All samples were measured as duplicates, from two separat biocatalytic approaches. Therefore, standard deviations were not calculated.

The samples containing NADH and wild-type CYP17A1 showed almost full conversion with only 4.2% progesterone remaining after 24 h (samples **3–4**, Figure 29). The sample of CYP17A1 wild-type without added NADH showed lower conversion with 28.1% progesterone remaining

after 24 h incubation. The negative control without added substrate also showed no product formation. Without enzyme present and for all samples containing the variant CYP17A1 T306A, no product formation was observed (samples **8–11**, Figure 29).

Judging from these results, the CYP17A1 T306A variant could be used as a suitable negative control for subsequent experiments.

3.3.4 Alanine scanning of the active site of recombinant human CYP17A1

For an alanine scanning of the active site of human CYP17A1, all residues within 4 Å of the bound substrate progesterone were identified using PyMol (PDB code: 4NKX) and exchanged with alanine by site-directed mutagenesis (Table 11). After confirming the correct sequence of all mutated pCW17A1Δ19H plasmids, the alanine variants were expressed in *E. coli* JM109 (DE3). Concentrations were determined by the measurement of CO difference spectra (Table 11) and biocatalysis was performed using the previously established conditions. As electron transfer can be impaired for the mutants, both CPR and Pdx/PdR were investigated as redox partner systems.

Table 11: Results of the CO difference spectra measurements of the investigated human CYP17A1 wild-type and variants.

CYP17A1 variant	**P450 [µmol L^{-1}]**	**P450 [mg L^{-1}]**	**P420 [µmol L^{-1}]**
Wild-type	3.7	203.5	1.7
F114A	-	-	1.4
Y201A	0.4	23	1.1
N202A	-	-	0.6
I205A	-	-	1.2
I206A	-	-	1.4
L209A	-	-	0.7
R239A	-	-	1.2
G297A	0.2	11	1.1
G301A	0.04	2.2	0.9
E305A*	n.a.	n.a.	n.a.
V336A	-	-	2.0
I371A*	n.a.	n.a.	n.a.
V482A	-	-	1.9
V483A	-	-	0.9

*the correct plasmid was not obtained, therefore no experiments with this mutant were performed

All enzymes were expressed in *E. coli* JM109 (DE3) from the pCW17A1Δ19H plasmid under the conditions described by Petrunak et al. with slight modifications.[110] For each sample, 100 mL culture were centrifuged and the cell pellets resuspended in 2 mL of 50 mM sodium phosphate buffer (pH 7.4) containing 20% (w/v) glycerol.

Biocatalysis was performed with CYP17A1 wild-type and each variant, 0.5 µM PdR, 2.5 µM Pdx or 2.5 µM CPR, and 25 µM NAD(P)H. All samples were incubated at 30°C at 600 rpm

shaking velocity for 24 h. As negative controls, samples lacking the redox partner system were prepared. An additional sample was incubated without adding substrate.

Unfortunately, none of the variants showed product formation. Only the wild-type showed results comparable to those obtained before. As most variants showed only incorrectly folded protein (P420; Table 11) as determined by CO difference spectra, a stability test using different buffers was conducted.

3.3.5 Investigating the stability of the human CYP17A1 wild-type and alanine variants

To investigate whether exchanging the buffer influences the stability of the human CYP17A1 wild-type and alanine variants, different tests were performed. After cultivation, using the old glycerol stocks and freshly bought *E. coli* JM109 (DE3) transformed with the plasmids, the cell pellets were lysed in different buffers and the concentrations were determined by CO difference spectra. Additionally, melting curves were recorded and substrate binding was investigated.

As before, sodium phosphate buffer (50mM sodium phosphate, 20% (w/v) glycerol, pH 7.4; buffer **1**), Tris-HCl (50mM Tris-HCl, 1 mM EDTA, 20% (w/v) glycerol, pH 8; buffer **2**), the buffer best suitable for CYP11A1 (50 mM potassium phosphate, 20% (w/v) glycerol, 1.5% (w/v) sodium cholate, 500 mM sodium acetate, 1.5% (v/v) TWEEN 20, 0.1 mM EDTA, 0.1 mM DTT, 0.1 mM PMSF, pH 7.4 ; buffer **3**),[192] another Tris-HCl buffer (50mM Tris-HCl, 1 mM EDTA, 600 mM sorbitol, pH 8.0; buffer **4**),[199] potassium phosphate buffered saline (100 mM potassium phosphate, 50 mM NaCl, pH 7.4 ; buffer **5**),[198] and a MOPS buffer (50 mM MOPS, pH 7.4; buffer **6**)[200] were used. For all variants and for the wild-type enzyme, expressed from the old glycerol stocks (see page x), the highest concentrations of correctly folded P450 were found in buffer **2**, in the cultivation inoculated from glycerol stocks (old). Therefore, only the results for buffer **2** are shown in Figure 30.

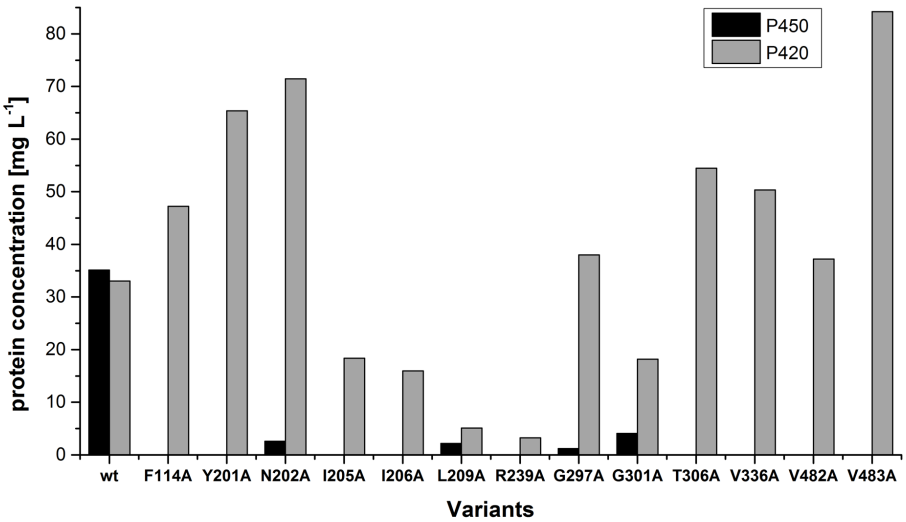

Figure 30: Protein concentrations of human CYP17A1 wild-type (wt) and 12 alanine variants expressed in *E. coli* JM109 (DE3) cells. After harvesting the cells, cell lysis was performed in buffer 2 (50mM Tris-HCl, 1 mM EDTA, 20% (w/v) glycerol, pH 8), followed by determination of protein concentration by CO difference spectra. Based on the recorded spectra, the amounts of correctly folded (black, P450) and incorrectly folded (grey, P420) protein were calculated and expressed in mg·L^{-1}.

The obtained concentrations of the different CYP11A1 variants could not be improved. Additionally, approximately 48% of the wild-type enzyme was incorrectly folded. This might be due to the cleaved membrane anchor of the plasmid construct used. This plasmid was originally used for expression and crystallization of the enzyme.[86] Therefore, it was assumed that the cleavage of the membrane anchor did not influence the protein stability. The long-term stability in fact was not investigated in the publication of the crystal structure.

The same samples were analyzed using the NanoTemper Prometheus NT.48 to see whether the melting temperatures of the different CYP17A1 variants were influenced by the different buffers. In this experiment, no significant differences were found between the variants and the wild-type. Importantly, the buffers did not seem to have a strong influence on the melting temperatures. As these meassurements were performed in cell lysate, it remains unclear, whether the protein concentrations were high enough to detect the melting temperatures or the observed melting events are observed for cell lysate in general.

Additionally, substrate binding of progesterone was investigated by recording difference spectra after adding progesterone to samples prepared in buffer **2**. For all variants except L209A and R239A, type I binding spectra were observed, which indicated that the substrate was still correctly bound in the active site of these enzyme variants. The type II spectra observed for the L209A and R239A variants indicated that the substrate might interact like an inhibitor.

3.3.6 Whole-cell biocatalysis using the bovine CYP17A1 enzyme

As the alanine mutants of the human enzyme showed only little to no stability, and consequently no conversion *in vitro*, a whole-cell approach was chosen to study the activity of CYP17A1. Whole-cell biocatalysis using bovine CYP17A1 expressed in yeast had previously been reported in the literature.[197] Therefore, this pre-established system, kindly provided by Dr. Stephan Mauersberger (TU Dresden, Germany), was used for further investigations. This system consists of the *S. cerevisiae* GRF18 strain harboring the YEp5117α plasmid.[197]

The wild-type bovine CYP17A1 activity of this system was investigated by incubating 100 µM progesterone with the whole-cell cultivation for 24 h. Samples were taken at several timepoints and analyzed by HPLC (Figure 31). After 4 h reaction time, the first product 17α-hydroxyprogesterone was detected. The second product is most likely 17α,20α-dihydroxyprogesterone and appeared after 10 h of incubation. The formation of the second product has been reported in the literature to not be caused by the heterologously expressed bovine CYP17A1 enzyme.[197,201] After 24 h, in total 95.6% of the substrate was consumed.

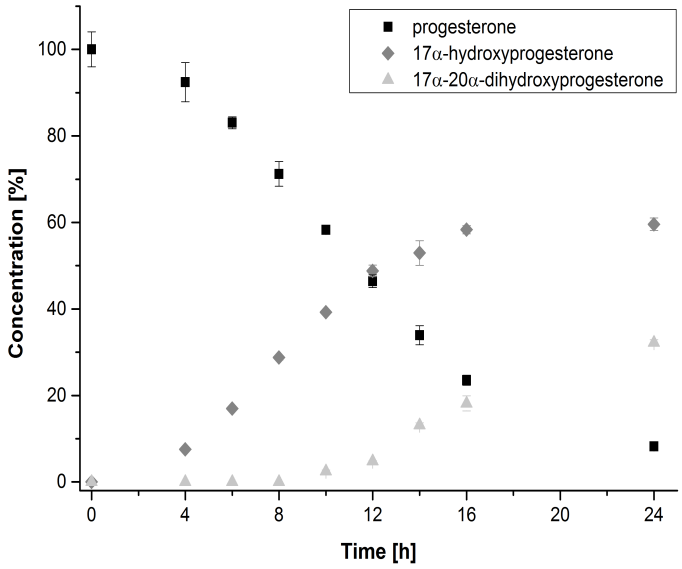

Figure 31: Whole-cell biocatalysis using the bovine CYP17A1 expressed in *S. cerevisiae* GRF18. The conversion of 100 µM progesterone was followed over 24 h. The sample composition is displayed in concentration (%) with the substrate progesterone (black squares), the product 17α-hydroxyprogesterone (dark grey diamonds), and the 17α,20α-dihydroxyprogesterone by-product (light grey triangles). All samples were analyzed as triplicates by HPLC. (Figure from second publication[202])

In negative controls performed using *S. cerevisiae* GRF18 (not transformed with the bovine CYP17A1 expression vector), no conversion of progesterone could be observed. This was also found in other studies.[197,203,204] The natural second product androstenedione (Figure 43)was not found in the whole-cell biocatalysis approach employing *S. cerevisiae*.

3.3.7 Homology model of the bovine CYP17A1 enzyme

The activity of the bovine CYP17A1 enzyme was further investigated by alanine scanning of the active site. However, since the structure of the bovine CYP17A1 had not been determined yet, a homology model needed to be created.

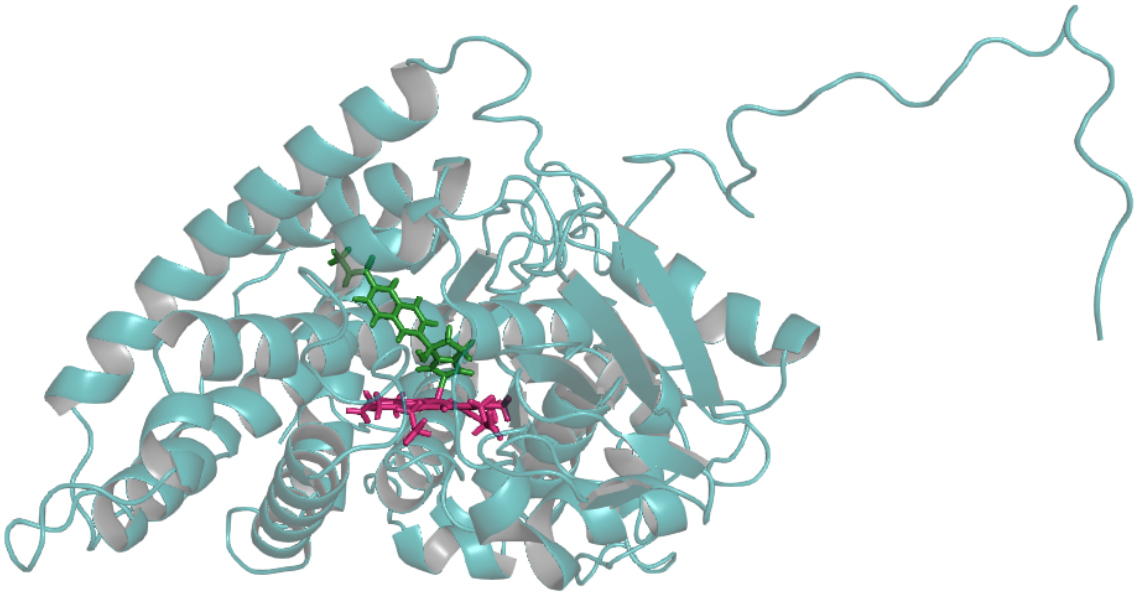

Figure 32: Homology model of bovine CYP17A1. The homology model was generated using YASARA and was based on the template structures with PDB codes 4NKW,[110] 4NKY,[110] 5IRQ,[122] 4R1Z,[111] and 4R20.[111] The image was prepared using PyMol. The heme-group is shown as sticks in magenta and the bound inhibitor (*R*)-orteronel is shown as sticks in green.

A model was created with the homology modeling function of YASARA[205] (Figure 32). The BLAST search performed by the program chose the crystal structures on which the homology model is calculated. For the homology model of the bovine CYP17A1, the human CYP17A1 (71% sequence identity compared to bovine CYP17A1) with its substrate pregnenolone (PDB code: 4NKW[110]), the first product 17α-hydroxyprogesterone (PDB code: 4NKY[110]), and the inhibitor orteronel bound in the active site (PDB code: 5IRQ[122]) were included. Additionally, the crystal structures of the CYP17A1 (46% sequence identity compared to bovine CYP17A1; PDB code: 4R1Z[111]) and CYP17A2 (43% sequence identity compared to bovine CYP17A1; PDB code: 4R20[111]) of zebrafish were chosen; both had the inhibitor abiraterone bound in the active site. The program created several different possible homology models. Ultimately, a model constructed from the best parts, of all homology models generated, was used. After a refinement conducted with YASARA, the final construct was evaluated with MolProbity with a score of 1.23 (Table 12).[206] Although the homology model evaluation reveals, that some parameters are not optimal, it was assumed that especially the sequence identity to the human enzyme with 71% was high, therefore making it more likely for the homology model to be accurate. It also needs to be taken in consideration, that for all of the crystallized proteins, the membrane anchor was cleaved off. This membrane anchor however is in the homology model, leading to problems in the creation of the homology model.

Table 12: Result summary of the MolProbity[206] analysis for the homology model of bovine CYP17A1. The color code is added by the software and indicates that the values were evaluated as good (green), okay (yellow) or bad (red).

All-Atom Contacts	**Clashscore, all atoms:**	**0.38**		**100th percentile* (N=456, 2.20 Å ± 0.25 Å)**
	Clashscore is the number of serious steric overlaps (> 0.4 Å) per 1000 atoms.			
Protein Geometry	Poor rotamers	13	3.03%	Goal: <0.3%
	Favored rotamers	398	92.77%	Goal: >98%
	Ramachandran outliers	2	0.41%	Goal: <0.05%
	Ramachandran favored	470	96.51%	Goal: >98%
	MolProbity score^		1.23	100th percentile* (N=10167, 2.20 Å ± 0.25 Å)
	Cβ deviations >0.25Å	1	0.22%	Goal: 0
	Bad bonds:	12 / 4000	0.30%	Goal: 0%
	Bad angles:	13 / 5428	0.24%	Goal: <0.1%
Peptide Omegas	Cis Prolines:	0 / 27	0.00%	Expected: ≤1 per chain, or ≤5%
	Twisted Peptides:	1 / 488	0.20%	Goal: 0

In the two column results, the left column gives the raw count, right column gives the percentage. * 100th percentile is the best among structures of comparable resolution; 0th percentile is the worst. For clashscore the comparative set of structures was selected in 2004, for MolProbity score in 2006. ^ MolProbity score combines the clashscore, rotamer, and Ramachandran evaluations into a single score, normalized to be on the same scale as X-ray resolution.

3.3.8 Alanine screening of the active site of bovine CYP17A1

Based on the bovine CYP17A1 homology model, residues in the active site, within 4 Å from the bound substrate progesterone, were identified as: L105, F114, V201, N202, I205, L206, R239, G297, D298, G301, E305, T306, V366, I371, L482, and V483. Additionally, the active site residues are conserved throughout the different CYP17A1 enzymes, also shown in a sequence alignment of the amino acid sequences of the proteins used as basis for the creation of the homology model (Figure A 1).

By site-directed mutagenesis, these residues were exchanged with alanine in the enzyme-coding ORF in the YEp5117α plasmid. After sequencing all plasmids, whole-cell biocatalysis in *S. cerevisiae* was performed, as described for the wild-type enzyme.

The different alanine variants showed different activities with the substrate progesterone (Figure 33). For variants V201A, D298A, V366A, and L482A, the overall activities were hardly influenced. The activities of the variants N202A, I205A, E305A, T306A, and I371A were completely or almost completely lost. As described in the literature for the human CYP17A1, position N202 is thought to be involved in correct substrate positioning, as it forms a hydrogen bond with the C3-OH of progesterone in the crystal structure.[110] As substrate positioning is

very important for enzymatic activity, the finding that the N202A variant of bovine CYP17A1 was inactive was not surprising. Also based on the crystal structure, E305 was described to be involved in an extensive H-bond network in the active site.[124] Position T306 is thought to be important for efficient proton delivery and, therefore, important for efficient catalysis. Furthermore, variant T306A was discovered as almost complete uncoupling variant with only 0.7% coupling efficiency.[198] This is in agreement with the whole-cell biocatalysis results, in which the T306A bovine CYP17A1 showed only 0.6% of wild-type activity. As the hydrogen peroxide formation in whole-cells is difficult to investigate, no information on uncoupling activity was obtained.

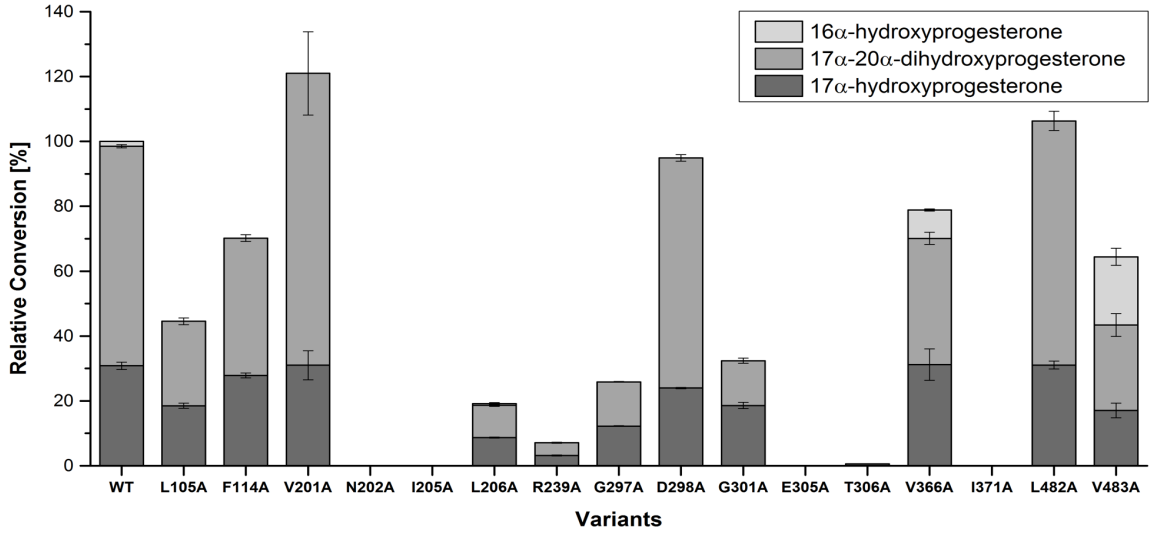

Figure 33: Comparison of the whole-cell biocatalysis of wild-type (WT) bovine CYP17A1 and 16 variants in *S. cerevisiae* GRF18. Progesterone was used as substrate. The resulting products are displayed relative to the wild-type conversion (16α-hydroxyprogesterone in light grey, 17α,20α-dihydroxyprogesterone in grey, and 17α-hydroxyprogesterone in dark grey). All samples were investigated as triplicates of separate biocatalytic approaches. (Figure from second publication[202])

The variants L206A, R239A, and G297A had only 19.5%, 7.2%, and 26.3%, respectively, of the wild-type activity. Of these residues, two were mentioned in the study of DeVore *et al*. from 2012, which elucidated the crystal structure of the human CYP17A1 with the inhibitors abiraterone and TOK-001 bound in the active site.[86] In the structure with TOK-001, the guanidino group of Arg239 was found to be oriented towards the C6 atom of the inhibitor. Additionally, they also observed an extensive hydrogen bond network. In this network, residues N202, E305, and R239 are involved besides several water molecules and the carbonyl-backbone of residue G297.[86] As mutating these positions clearly affected the activity of the bovine CYP17A1 towards progesterone, it might be that these residues also form a hydrogen bond network when progesterone is bound to the active site. Furthermore, this network might also play a role in correct substrate positioning and/or substrate binding in general.

The variants F114A, L105A, and G301A also showed decreased activities, with 71.3%, 45.2%, and 32.9%, respectively, of wild-type activity. Only residue Leu105 had been

investigated before.[108] In 2010, Swart *et al*. analyzed the influence of residue 105 on the side-product formation by human CYP17A1 in the conversion of progesterone, yielding 16α-hydroxyprogesterone. Generally, the human wild-type enzyme catalyzes side-product formation of up to 30% and harbors an alanine at position 105. They compared the CYP17A1 enzymes of different species and found that only enzymes harboring alanine at this position showed significant side-product formation, whereas enzymes with leucine at position 105 showed very little to negligible side-product formation. Therefore, they exchanged A105 in the human CYP17A1 enzyme with leucine and could demonstrate that the wild-type side-product formation dropped drastically to non-significant values. For enzymes of other species, they could introduce the side-activity by introducing L105A, as described in the Introduction. This finding, however, does not seem to apply to the bovine CYP17A1 investigated here. The wild-type enzyme with a leucine at position 105 shows little (1.3%) side-product formation. Contrary, the L105A mutant does not produce measurable side-product levels anymore.

More interestingly, variants L206A, V366A, and V483A showed an increased side-product formation compared to wild-type bovine CYP17A1. The overall activity of variant L206A was decreased to 19.5% of wild-type activity and showed with 2.6% of total product formation the least side-product formation. Variants V366A and V483A showed good substrate conversion and variant V483A was found to produce the highest amount of 16α-hydroxyprogesterone with 32.6% of total product formation in this first approach.

As this was a very interesting result, preparative biocatalysis with variant V483A was performed to characterize the side-product by NMR.

3.3.9 Preparative biocatalysis with bovine CYP17A1 V483A

In the preparative biocatalysis approach, 100 mg progesterone were converted in a 1 L culture of *S. cerevisiae* harboring the plasmid YEp5117α_V483A. After 72 h of incubation, 2 mL of the supernatant was extracted with ethyl acetate and analyzed by HPLC (the HPLC analysis can be found in the Appendix: Figure A 2). The chromatogram showed that the substrate was fully consumed and the final ratio of 17α:16α product was 1:0.67. In the preparative biocatalysis approach, the 16α-hydroxyprogesterone formation was even higher than observed before, at approximately 40% of total product formation.

With the remaining supernatant, preparative HPLC was used to separate the presumed 16α-hydroxyprogesterone from the other steroid products. Here, the final yield of isolated side-product was 30%. With the separated compound, NMR analysis was performed by Sascha Grobe, confirming that the side-product was 16α-hydroxyprogesterone. The NMR results can be found in the Appendix: ^{1}H NMR: Figure A 4; ^{13}C NMR: Figure A 5.

Furthermore, to investigate whether the yield of obtained 16α-hydroxyprogesterone could be enhanced further, all three possible double mutants were created by site-directed mutagenesis. Whole-cell biocatalysis, using plasmids encoding the three double mutants, was performed by Sascha Grobe. Unfortunately, all double mutants showed very low activities and the ratio of 17α:16α product could only be enhanced by the L206A/V483A double mutant.

This double mutant, however, had only 1% residual activity, compared to the wild-type enzyme.

3.3.10 Molecular docking using the wild-type and V483A bovine CYP17A1 homology models

To investigate possible structural reasons for the enhanced 16α-hydroxyprogesterone formation of variant CYP17A1 V483A, molecular docking experiments were performed with Dr. Kathleen Balke. Therefore, the V483 in the homology model of the wild-type was exchanged with alanine, followed by another energy minimization and refinement. For the wild-type enzyme and the V483A variant, progesterone was docked into the active site (Figure 34). As different orientations of the substrate were observed, only those resembling approximately the same positioning as observed in the crystal structures (with bound substrates) were used (PDB code: 4NKW and 4NKX).[110]

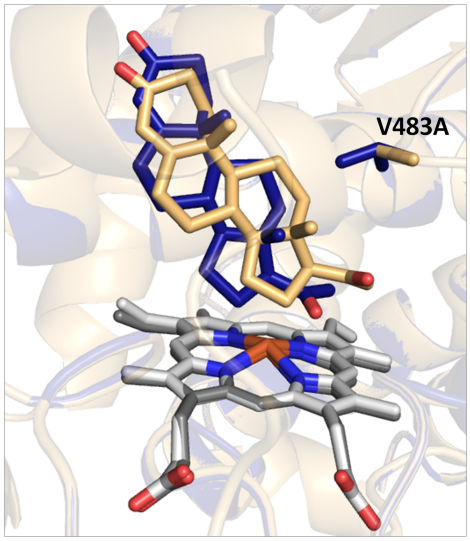

Figure 34: Overlay of the docking results of the homology model of bovine CYP17A1 wild-type and V483A mutant with the substrate progesterone. The active sites of both models are overlaid. The heme-group is shown in light grey, wild-type is shown in yellow and V483A in dark blue. The image was created using YASARA. (Image from second publication[202])

For the docking, different orientations of the substrate were observed, therefore, the distances of the closest C-atoms to the heme-iron were measured, using YASARA (Table 13). Of the in total 14 docking results, in 8 the substrate was found in the active site above the heme-group. Of these 8 docking results, in 3 C15, C16 and C17 were found closest to the heme-group as also observed in all crystal structures of CYP17A1 enzymes with bound substrate elucidated (1,3 and 5; Table 13). Therefore, only these docking result with the substrate being orientated with the C15, C16 and C17 atoms close to the heme group were taken in consideration. In two of these three docking results, the C16 atom was found closest to the heme-iron with 4.1 Å and 4.0 Å. Only in one docking, the C15 atom was found to reside the closest to the heme-iron, a bit further away with 4.9 Å. Also, for this result, the C16 atom was the second closest with 5.1 Å. For the wild-type enzyme, the C17 atom (3.8 Å) was found to be closer to the iron atom than the C16 atom (4.1 Å).

Therefore, it seems as if the slightly smaller alanine at position 483 instead of valine allows the bound substrate to rotate a bit in the active site, facilitating the hydroxylation of position C16 of progesterone by this variant.

Table 13: Docking results of progesterone in the active site of the CYP17A1 V483A prepared and evaluated with YASARA. A scheme of the progesterone molecule with the numbering of the C-atoms can be found in Figure 9.

Docking result	Distances of closest C-atoms to the heme-iron
1	C16: 4.0 Å; C17: 4.3 Å; C15: 4.7 Å
2	C3: 5 Å; C2: 5.4 Å
3	C15: 4.9 Å; C16: 5.1 Å; C17: 6.7 Å;
4	C2: 2.9 Å; C1: 4.0 Å; C3: 4.1 Å
5	C16: 4.1 Å; C17: 5.1 Å; C15: 4.5 Å
6	C4: 5.6 Å; C6: 5.2 Å
7	C2: 7.6 Å
8	C20: 3.9 Å; C21 4.7 Å
9	-*
10	-*
11	-*
12	-*
13	-*
14	-*

*the substrate molecule was not found in the active site, but somewhere else in the structure of the homology model

3.4 First investigations on a dual screening assay

In addition to investigating the structural background for P450 activity, as demonstrated with the alanine scanning of CYP17A1, another goal of this thesis was to develop suitable screening assays for application in high-throughput screening. The Ampliflu™ Red assay simultaneously measured NADPH consumption and hydrogen peroxide formation. Absorbance measurement was used for the detection of NADPH consumption, which is not applicable to fluorescence-based sorting methods in the attempted droplet-based final application. Therefore, another assay was investigated, applying a substrate coupled to the fluorophore 7-hydroxy-4-trifluoromethylcoumarin. Upon hydroxylation by the cytochrome P450 enzyme, a hydroxylated fatty acid is formed and the fluorophore released. This reaction can be followed by excitation at 400 nm and detection of fluorescence emission at 500 nm. In combination with the Ampliflu™ Red probe or another fluorescent probe for hydrogen peroxide detection, both hydrogen peroxide and product formation can be measured at different wavelengths.

3.4.1 Substrate synthesis and verification by NMR spectroscopy

As the substrate for this approach was not commercially available, it needed to be synthesized. Substrate synthesis was accomplished following the protocol by Neufeld *et al*. from 2014.[24] The first methylation step was omitted by using the commercially available methyl ester of 11-bromoundecanoic acid. Furthermore, the final product differed from the product synthesized by Neufeld *et al*. since the fatty acid used was undecanoic acid instead of dodecanoic acid (Figure 35).

After substrate synthesis, the final product was purified by silica gel chromatography. In total, 120.9 mg, which equals 0.29 mmol of product was obtained (22.0% based on the used amount of 1.32 mmol free methyl 11-bromo undecanoate). Using 10 mg of the product, NMR analysis was performed. The NMR result can be found in the Appendix: Figure A 6. When compared to the ^{1}H-NMR for 12-(4-trifluoromethylcoumarin-7-yloxy)undecanoic acid, the spectra were very similar. Differences resulted from the one missing CH_2-group in the product synthesized in this thesis.

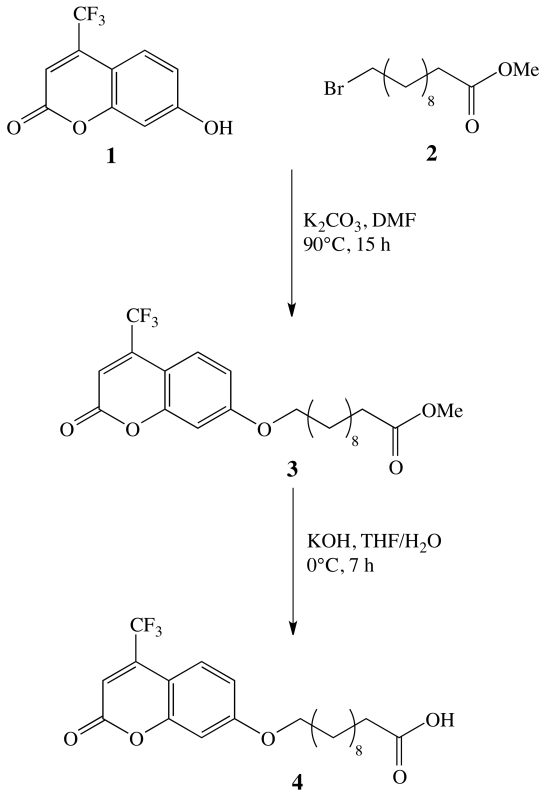

Figure 35: Substrate synthesis of 11-(4-trifluoromethylcoumarin-7-yloxy)undecanoic acid (**4**). The synthesis was performed similar to the synthesis of 12-(4-trifluoromethylcoumarin-7-yloxy)undecanoic acid, described by Neufeld *et al.* in 2014.[24] (**1**: 7-hydroxy-4-trifluoromethylcoumarin; **2**: methyl 11-bromoundecanoate; **3**: 11-(4-trifluoromethylcoumarin-7-yloxy)undecanoate)

The goal was to use this substrate to develop a dual screening for simultaneous product formation and hydrogen peroxide formation catalysed by cytochrome P450 enzymes. An assay compatible with microfluidically generated droplets was envisaged (sorting by

fluorescence-activated droplet sorting (FADS)).[207] Therefore, a probe to report the hydrogen peroxide concentration was needed.

3.4.2 Investigation of a suitable hydrogen peroxide detection probe

Next, potential hydrogen peroxide detection probes were investigated. It is essential that such probes are compatible with the substrate in terms of the wavelengths used for their detection. The sensitivity towards hydrogen peroxide was is equally important.

Therefore, the hydrogen peroxide-sensitive probe HDCF-DA was investigated, a probe used for the detection of oxidative stress in whole cells. It diffuses into the cell, where the chloromethyl group reacts with glutathione and other thiols. After oxidation, highly fluorescent DCF probe remains inside the cells.

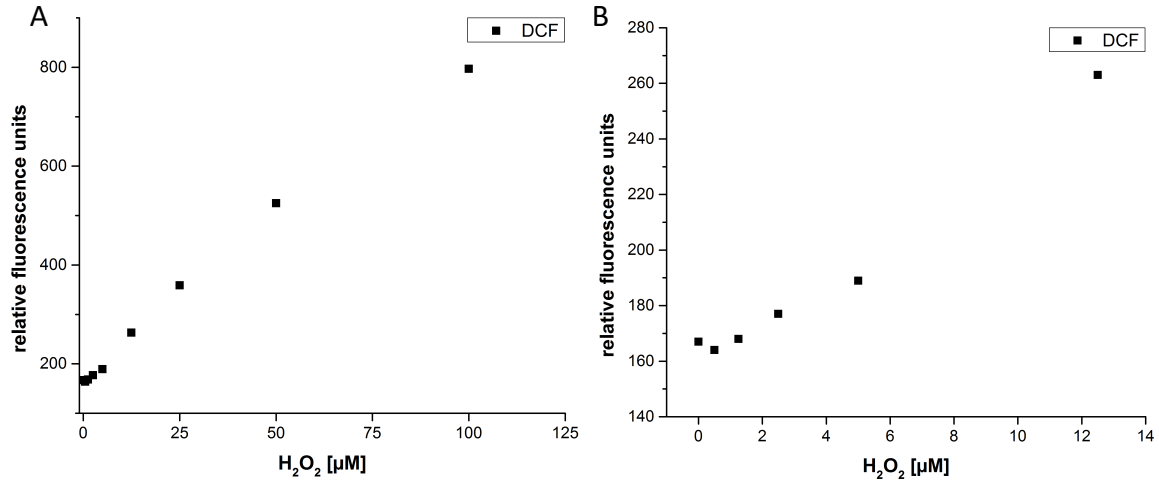

Figure 36: Investigation of the detection limit of HDCF-DA when incubated with (A) 0.5, 1.25, 2.5, 5, 12.5, 25, 50, and100 µM H_2O_2. Fluorescence values were obtained at $\lambda_{excitation}$ = 490 nm and $\lambda_{emission}$ = 520 nm (gain: 50%) in 96-well plates at the Tecan device using the i-control™ software. (B) Display of the results of 0, 0.5, 1.25, 2.5, 5 and 12.5 µM.

A linear relationship between the hydrogen peroxide concentration and fluorescence was clearly observed (Figure 36A). Unfortunately, the detection limit was 2.5 µM (Figure 36B), whereas the detection limit using Ampliflu™ Red was significantly lower, at 50 nM. Additionally, the excitation and emission wavelengths of Ampliflu™ Red are further separated from the wavelengths used for the detection of the 7,4-HFC. Hence, further investigations were performed with the Ampliflu™ Red probe (section 3.1.4).

3.4.3 Signal stability test of (7-hydroxy-4-(trifluoromethyl)coumarin and resorufin in the HFE 7500 oil

Since the goal was to develop an assay compatible with droplet microfluidics, the question arose whether the two fluorescent products (7-hydroxy-4-(trifluoromethyl) coumarin, resulting from P450 activity, and resorufin, resulting from Ampliflu™ Red oxidation) would stay in the droplets or diffuse into the HFE-7500 oil used for encapsulation. If the probes tended to partition into the oil phase, the fluorescent signals would be lowered, especially if this diffusion was fast. This is a general problem in microfluidics, commonly solved by working

on model reactions with suitably water-soluble substrates. However, due to limited flexibility in fluorophore selection in this study, the compatibility of (7-hydroxy-4-(trifluoromethyl)coumarin and resorufin with water-in-oil emulsions had to be investigated. The fluorescence of many dyes is influenced by the pH dependent ionisation of one or more functional groups. For example, both 7,4-HFC and resorufin have ionisable OH groups, with the deprotonated forms being more fluorescent. Since this ionisation also influences hydrophobicity (and thus the likelihood of these molecules escaping into the oil phase), the retention of 7,4-HFC (pKa 7.26) and resorufin (pKa 6.0) in the aqueous phase was investigated at several pH values, above and below their respective pKa values.

The HFE-7500 oil was overlaid with sodium phosphate buffers (50 mM with pH ranging from 6.0 to 9.0), containing 50 µM resorufin or 7,4-HFC in a ratio of 10:1 in screw cap tubes. Afterwards, these tubes were incubated in a shaker at 30°C and 1,200 rpm for 24 h. Time samples were taken, and dye concentrations were determined by fluorescence measurements.

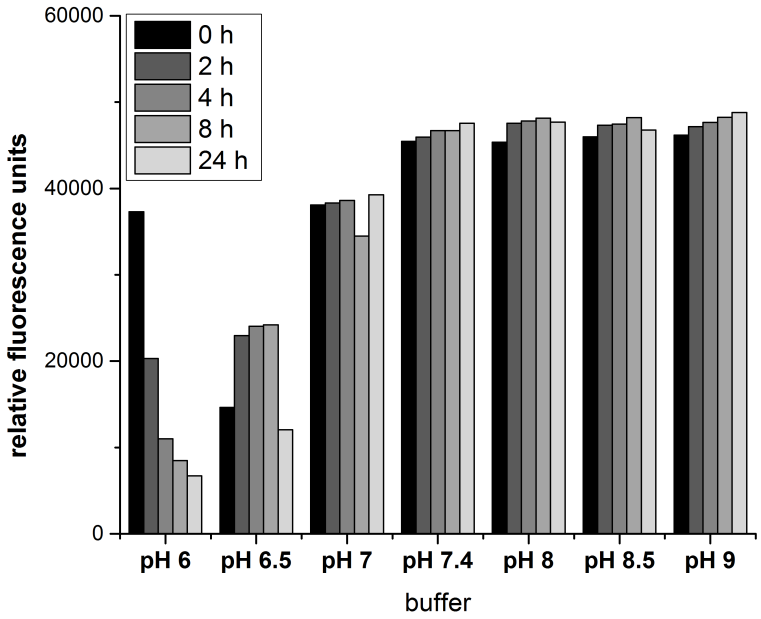

Figure 37: Incubation of 50 µM resorufin in 50 mM sodium phosphate buffer adjusted to different pH values. A volume of 100 µL buffer was pipetted on top of 1000 µL HFE-7500 (oil used for droplet formation for FADS). The two-phase system was incubated at 25°C at 14,000 rpm shaking velocity for 24 h. At different timepoints, samples were taken and fluorescence was measured at $\lambda_{excitation}$ = 560 nm and $\lambda_{emission}$ = 590 nm (gain: 84%) in 96-well plates at the Tecan device using the i-control™ software.

For resorufin (Figure 37), the buffers adjusted to different pH values had a big influence on the probes diffusion tendency from the water into the oil phase. For buffer pH >7.0, 100% of the probe was found in the aqueous phase after 24 h; in systems employing buffers adjusted to pH <6.5, partial diffusion of the probe into the oil phase was observed. For the buffer with pH 6.0, only 18% of the probe was still found in the water phase after the 24 h incubation. Therefore, for the application of this probe, pH >7.0 should be used.

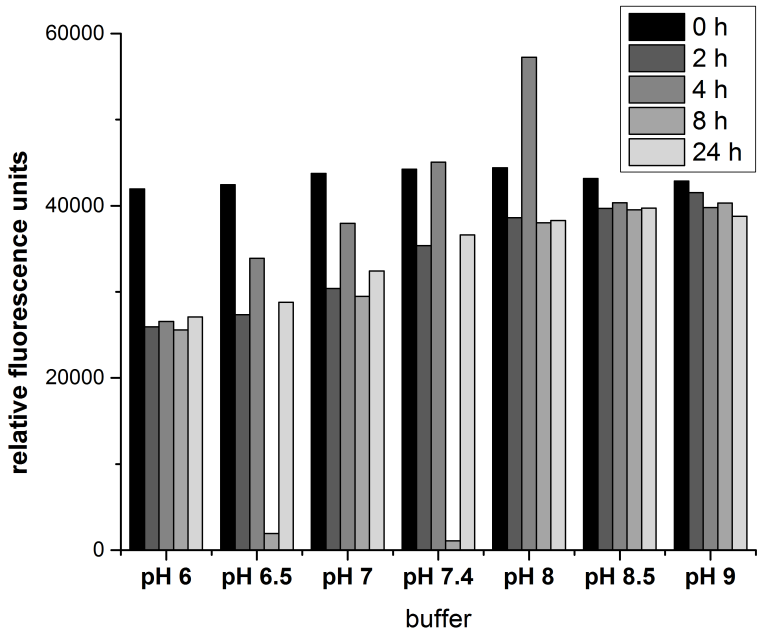

Figure 38: Incubation of 50 µM 7-hydroxy-4-(trifluoromethyl)coumarin in 50 mM sodium phosphate buffer adjusted to different pH values. A volume of 100 µL buffer was pipetted on top of 1000 µL HFE-7500 (oil used for droplet formation for FADS). The two-phase system was incubated at 25°C at 14,000 rpm shaking velocity for 24 h. At different timepoints, samples were taken and fluorescence was measured at $\lambda_{excitation}$ = 400 nm and $\lambda_{emission}$ = 500 nm (gain: 100%) in 96-well plates at the Tecan device using the i-control™ software.

For 7,4-HFC (Figure 38), the results were not as consistent as those for resorufin. For samples taken at 8 h incubation time, apparently a mistake occurred. As only 10 µL samples were taken, pipetting mistakes most likely account for it. Nevertheless, also for this probe differences were detectable corresponding to the different pH values. As seen for resorufin, also for the 7,4-HFC, buffers adjusted to lower pH values led to a decrease in fluorescence of the probe during incubation in the aqueous phase. For pH ≥7.4, the concentrations remained stable with ≥83% fluorescence intensity after 24 h incubation time. For buffers with lower pH, fluorescence decreased over time, indicating that only 74% (pH 7.0), 68% (pH 6.5), and 65% (pH 6.0) of the dye remained in the aqueous phase after 24 hours.

The diffusion into the oil, depends on the ionization of the molecules and is therefore dependent on the pK_a values of both probes. The pK_a value of resorufin is 6.0 and for the 7,4-HFC, 7.26. At lower pH, the probes become less hydrophilic through loss of charge, making it more likely the probes will diffuse into the oil. Definitely a pH above the pK_a values above both probes should be used.

In the assay, the droplets might be incubated for reaction times most likely shorter than 24 h. Thus, pH of 7.4 was chosen for subsequent experiments. For resorufin, pH 7.4 is optimal; for 7,4-HFC, 83% were still found in the water phase after 24 h. In addition, cytochrome P450 BM3 activity assay, as well as the Ampliflu™ Red assay, were previously shown to work at pH 7.4 (section 3.1.5).

3.4.4 Investigation of the optimal substrate to NADPH ratio

For optimal screening, reaction parameters need to be optimized initially. Therefore, the conversion of the substrate was investigated with cytochrome P450 BM3 wild-type and two variants in microtiter-plates. In the publication, showing the substrate synthesis of 12-(4-trifluoromethylcoumarin-7-yloxy)undecanoic acid, the variant A74G/F87V exhibited strongly enhanced substrate conversion compared to the wild-type.[24] Hence, it was used as positive control for the investigation of the substrate to NADPH ratio. The variant F87Y was used as negative control. This variant was already investigated with the Ampliflu^{TM} Red assay (section 3.1.6) and showed high uncoupling and very low product formation, which was also described in the literature.[130]

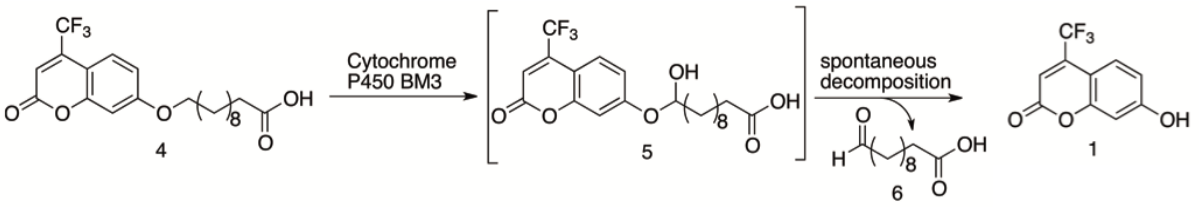

Figure 39: Conversion of 11-(4-trifluoromethylcoumarin-7-yloxy)undecanoic acid (**4**) by cytochrome P450 BM3, resulting in the formation of the unstable hemiacetal intermediate (**5**), which spontaneously decomposes, resulting in the formation of an aldehyde (**6**) and the free fluorophore 7-hydroxy-4-(trifluoromethyl)coumarin (**1**).

First, NADPH was used in excess, as cytochrome P450 BM3 is known to perform multiple hydroxylations of some fatty acids. If the substrate gets hydroxylated, the unstable hemiacetal is formed, which spontaneously decomposes to yield the free product and the fluorescent 7,4-HFC (Figure 39). If the free aldehyde gets hydroxylated, no further fluorophore is released, which will not be detected by the assay. Hence, the ratio of consumed NADPH per substrate molecule could be higher than 1:1.

First, the conversion of 10 µM substrate with 150 µM NADPH present was investigated (Figure 40). The investigated cytochrome P450 BM3 A74G/F87V produced the highest amount of fluorophore (Figure 40(A)). Additionally, when compared to wild-type, the reaction rate was higher, with a especially fast, initial rate. The highest 7,4-HFC concentration was reached after approximately 200 s and 400 s for cytochrome P450 BM3 A74G/F87V and the wild-type, respectively. For the wild-type, substrate conversion was detected, whereas no product formation was observed with the uncoupling mutant (F87Y). The production of hydrogen peroxide was the highest for the wild-type without substrate, followed by the uncoupling variant with substrate, and the wild-type with substrate(Figure 40(B)). The double mutant showed in the reaction with substrate the lowest hydrogen peroxide formation. Both the uncoupling variant F87Y and the A74G/F87V variant rapidly produced hydrogen peroxide. The highest hydrogen peroxide concentration was reached after 100 s. For wild-type, again, 400 s were needed to reach the final concentration.

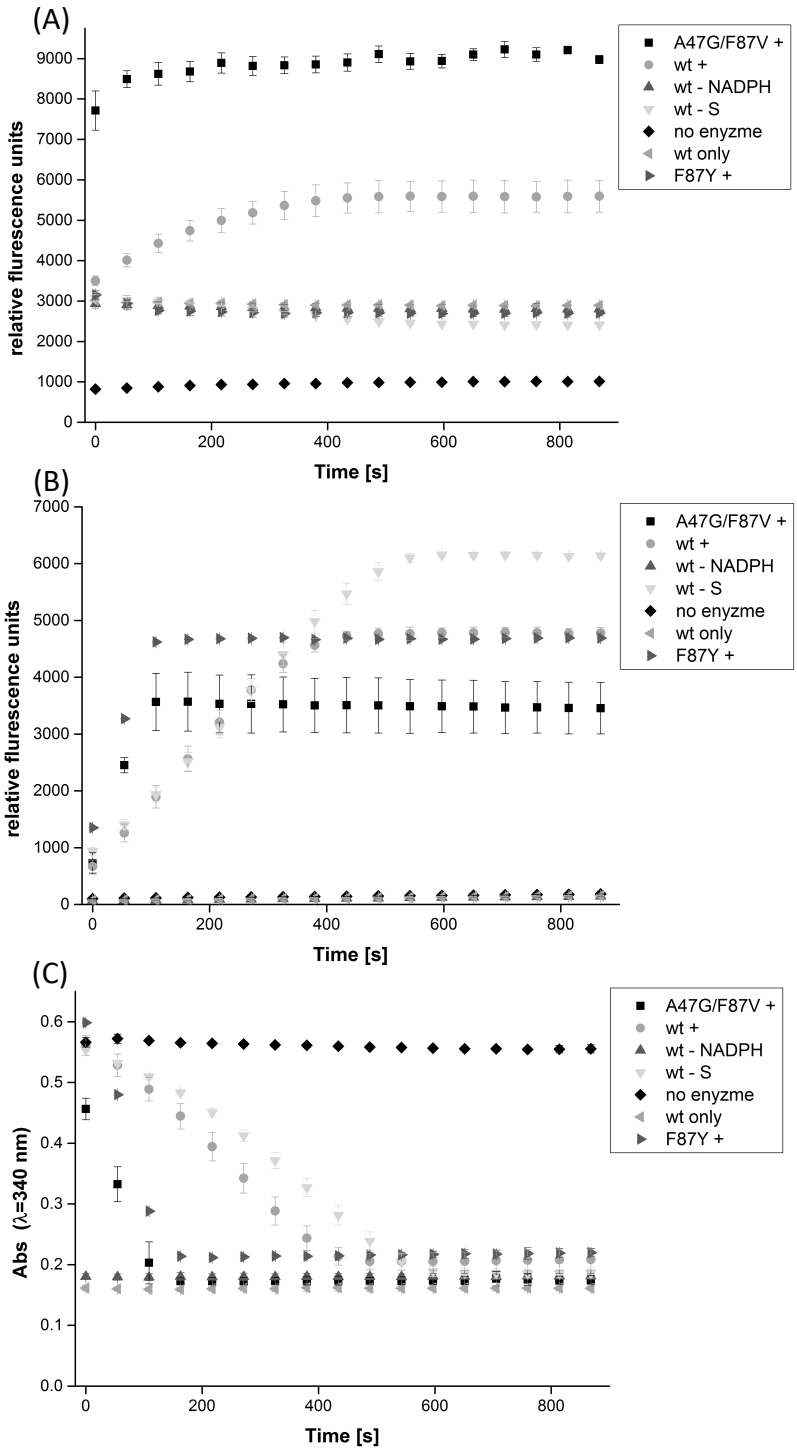

Figure 40: Conversion of 10 µM 11-(4-trifluoromethylcoumarin-7-yloxy)undecanoic acid with 0.5 µM cytochrome P450 BM3 wild-type (wt) and the variants A47G/F87V and F87Y with substrate (+). For BM3 wt, two negative controls were added (without NADPH (wt - NADPH), without substrate (wt - S)), as well as one sample without enzyme (no enzyme). If added, a concentration of 150 µM NADPH was used. The following parameters were determined: (A) The formation of free 7,4-HFC ($\lambda_{excitation}$ = 420 nm and $\lambda_{emission}$ = 500 nm (gain: 100%)), (B) the formation of hydrogen peroxide with the Ampliflu™ Red assay ($\lambda_{excitation}$ = 550 nm and $\lambda_{emission}$ = 590 nm (gain: 50%)), and (C) the depletion of NADPH (absorption measured at λ = 340 nm).

NADPH was consumed over time in all samples containing enzymes (Figure 40(C)). Fast depletion of NADPH was observed for the samples containing the variants F87Y and A74G/F87V; the wild-type enzyme consumed NADPH more slowly. In the study of Neufeld *et al.* from 2014, the A74G/F87V was described to show the highest catalytic efficiency with

0.458 min^{-1} μM^{-1} for the substrate 12-(4-trifluoromethylcoumarin-7-yloxy)dodecanoic acid investigated in their study.[24] Unfortunately, Neufeld *et al.* did not identify kinetic parameters for the wild-type. They only demonstrated that, in crude lysate, the activity of the wild-type cytochrome P450 BM3 is 8-fold lower than that of the most active mutant, A74G/F87V.

Next, lower NADPH concentrations in combination with the substrate were tested, as the ratio of NADPH to the substrate was most likely too high. In case of limited substrate access and high NADPH excess, also the presumable good variants will show uncoupling, as no substrate is bound in the active site.[130]

Therefore, the ratio of substrate to NADPH was optimized. Additionally, the enzyme concentration was decreased. Furthermore, the total amount of cells was calculated by measuring OD_{600} at the end of the cultivation. With the total cell count, the concentration of all samples was adjusted to 1 cell per 4 pL, which equals approximately the concentration obtained when a single cell is lysed in a 20 µm diameter droplet.

The best results were obtained by using 100 µM substrate in combination with 25 µM NADPH (Figure 41). For the best variant, cytochrome P450 BM3 A74G/F87V, equimolar concentrations of hydrogen peroxide and 7,4-HFC were detected. The variant F87V was also described by Neufeld *et al*. to catalyze good conversion of the substrate investigated in their study and showed approximately a 7-fold increased conversion compared to the wild-type.

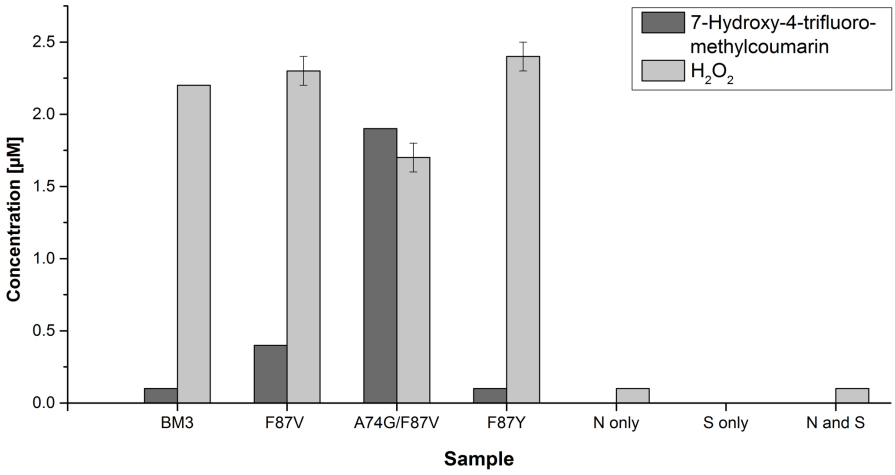

Figure 41: Dual detection of the substrate (100 µM 11-(4-trifluoromethylcoumarin-7-yloxy)undecanoic acid) conversion and hydrogen peroxide formation by cytochrome P450 BM3 wild-type and variants F87V and A74G/F87V in 50 mM sodium phosphate buffer (pH 7.4) supplemented with 25 µM NADPH. As negative controls, only NADPH (N only), only substrate (S only) and substrate with NADPH were incubated. For the detection of hydrogen peroxide Ampliflu™ Red was used (Assay solution: 100 µM Ampliflu™ Red, 0.2 U mL^{-1} in 50 mM sodium phosphate buffer (pH 7.4); detection: $\lambda_{excitation}$ = 560 nm and $\lambda_{emission}$ = 590 nm) and substrate conversion was measured by detection of 7,4-HFC (detection: $\lambda_{excitation}$ = 400 nm and $\lambda_{emission}$ = 500 nm).

Here, 25 µM NADPH was used, the product and hydrogen peroxide concentrations were much lower. It is possible that a part of the NADPH was used to hydroxylate the free fatty acid at different positions, not leading to a detectable signal. Another possibility might be that the cytochrome P450 BM3 and the variants are able to perform side reactions with other molecules in the cell lysate. To determine which NADPH-dependent reaction is catalyzed,

further analysis would be necessary including reaction scale-up to analyze the resulting products by GC-MS or NMR, for example. Additionally, controls for each experiment without substrate present would have had to be performed. Unfortunately, these measurements could not be performed due to time constraints.

3.4.5 Application of the dual screening to investigate five Cytochrome P450 BM3 variants

After finding good conditions for investigating the three cytochrome P450 BM3 variants (A74G/F87V, F87V, and F87Y), six other variants were created and investigated: R47L, Y51F, A82L, T268A, and I401P. The first five variants are the enzymes used to test the suitability of the Ampliflu™ Red assay, described in Section 3.1.6. They show uncoupling, depending on the substrate used. I401P was added as a variant with increased coupling efficiency in the oxidation of non-natural substrates[28] and showing a higher rate of NADPH consumption in the absence of substrate (referred to as leak rate).[130]

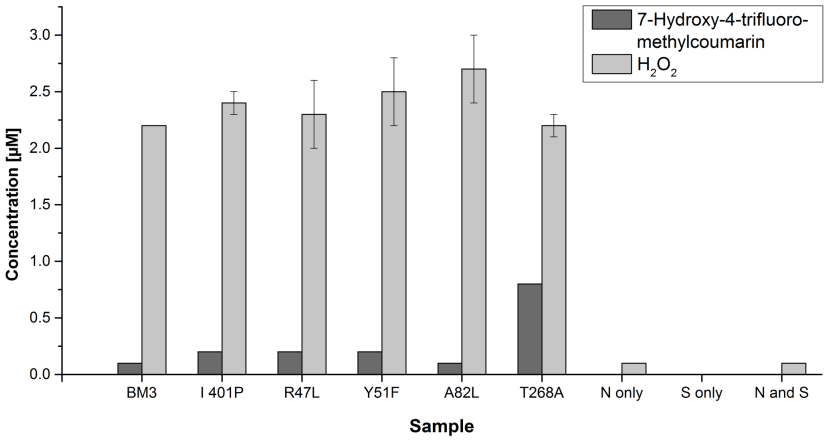

Figure 42: Dual detection of the substrate conversion (100 µM 11-(4-trifluoromethylcoumarin-7-yloxy)undecanoic acid) and hydrogen peroxide formation by cytochrome P450 BM3 wild-type and variants I401P, F87Y, R47L, Y51F, A82L, and T268A in 50 mM sodium phosphate buffer (pH 7.4) containing 25 µM NADPH. As negative controls, only NADPH (N only), only substrate (S only), and substrate with NADPH were incubated. For the detection of hydrogen peroxide, Ampliflu™ Red was used (Assay solution: 100 µM Ampliflu™ Red, 0.2 U mL^{-1} in 50 mM sodium phosphate buffer (pH 7.4); detection: $\lambda_{excitation}$ = 560 nm and $\lambda_{emission}$ = 590 nm) and substrate conversion was measured with detection of 7,4-HFC (detection: $\lambda_{excitation}$ = 400 nm and $\lambda_{emission}$ = 500 nm).

Interestingly, of the five variants investigated, cytochrome P450 BM3 T268A showed enhanced product formation (600% compared to wild-type and 210% compared to the F87V variant). In comparison to the best variant A74G/F87V, the product formation was lower (28%, Figure 41).

4 Discussion

4.1 Development of the Ampliflu™ Red assay

In the first part of this PhD thesis, the aim was developing an assay for the characterization of cytochrome P450 monooxygenases, in terms of their activities and uncoupling rates.

First, the HyPer-3 protein was examined as a possible reporter for the detection of hydrogen peroxide formed during cytochrome P450-catalyzed reactions. After successful expression and purification, the protein was investigated in terms of its sensitivity towards hydrogen peroxide. It became clear that the signals obtained using this protein would not be sensitive enough for *in vitro* detection of hydrogen peroxide at µM concentrations. Furthermore, the signal is based on a ratiometric measurement, at two wavelengths, which would lead to additional complications in the application of this assay for high-throughput screening. Additionally, Bilan *et al*. reported that, upon contact with hydrogen peroxide, the signal is only stable for approximately 2 min.[67] Hence, the protein is not suitable for the determination of the total hydrogen peroxide formed during reactions that need longer incubation times.

Therefore, two other probes were investigated that are suitable hydrogen peroxide reporters when used in combination with the HRP enzyme. Both probes have been described for the determination of uncoupling levels during the reaction of cytochrome P450 enzymes.[61,178] In order to determine whether the two probes are compatible with a parallel measurement of the NADPH consumption at λ=340 nm, which has not been reported before, a spectrum of each probe and its reduced form was recorded. Unfortunately, it was found that the ABTS probe absorbs light at λ=340 nm (Figure 13). Therefore, if this probe were used, the NADPH consumption could only be monitored if the reaction were stopped at a certain point and the ABTS/HRP system necessary for hydrogen peroxide detection were added afterwards. As this was not the goal and the spectrum of Ampliflu™ Red and the oxidized form resorufin showed no absorption at λ=340 nm, this probe was chosen for further characterisation concerning its suitability in the parallel screening approach.

After finding that the Ampliflu™ Red assay can be performed at physiological pH of 7.4, the signal stability was investigated. Although the signal remained stable for concentrations above 5 µM, the deviation of the signal obtained for 0.5 µM hydrogen peroxide increased to 15% over the 20 min incubation period. This deviation results most likely from the sensitivity of the Ampliflu™ Red probe towards light.[183] It is logical, that small signals are influenced more significantly by the photooxidation of small amounts of Ampliflu™ Red, as the same amount of Ampliflu™ Red molecules influenced lead to the same change of signal in each sample, resulting in a higher percentage for the lower signals. Therefore, the reaction should be performed in a dark environment. Additionally, if a high-throughput assay is performed, with the usage of good positive controls the threshold for the sorting can be adjusted to a good valu, in order to find all variants matching the screening criteria.

Moreover, the assay was further investigated with cytochrome P450 BM3 as model enzyme. The clear advantage of using this enzyme is that it is a self-sufficient enzyme, not needing additional proteins for its catalytic activity. The cytochrome P450 BM3 is also one of the most studied cytochrome P450 enzymes and shows a high overall activity.[130] After successful expression and purification, first tests were performed to find a good working concentration of the enzyme for the assay. A cytochrome P450 concentration of 0.4 µM in the assay was found to be optimal in order to provide a fast reaction, but also provide the chance to monitor the hydrogen peroxide formation over time.

To further evaluate the assay, the reaction of cytochrome P450 BM3 wild-type and five variants, in combination with different substrates, were investigated. The results were in agreement with data found in literature. [135,141,170,181]

One of the goals was to investigate the uncoupling process and thereby possibly contribute to the understanding of the uncoupling process. In this context, the results of variants R47L and Y51F were especially interesting. Both residues (R47 and Y51) are known to be responsible for substrate binding and substrate access, due to the close localization to the substrate-access channel.[137] Additionally, one theory concerning uncoupling is that too loose binding of substrates leads to uncoupling, as well as to difficulties in substrate accessibility.[54] Therefore, it was very interesting to find that both variants catalyzed the formation of hydrogen peroxide more rapidly than the wild-type, for all substrates investigated.

By assaying different negative controls in the reaction of cytochrome P450 BM3 wild-type without substrate, it was demonstrated that the observed change in absorbance is clearly mediated by hydrogen peroxide formation and its reaction with HRP. After reduction of hydrogen peroxide, resulting in the formation of water, the HRP oxidizes Ampliflu™ Red, leading to the formation of one molecule of resorufin per molecule of hydrogen peroxide. The formation of resorufin is then detected by a change in absorbance.[208] By adding catalase and obtaining a strong reduction of the signal, it was demonstrated that it is indeed hydrogen peroxide that is detected. As both the catalase and HRP compete for the same hydrogen peroxide, the signal is only reduced rather than completely eradicated. By performing a measurement without HRP and obtaining no signal, possible side reactions, that might directly convert the Ampliflu™ Red to resorufin, were ruled out. Additionally, in contrast to NADH, which was described to interfere with the measurement by interacting with the probe,[183] this was not observed for NADPH, as negative controls with only NADPH, HRP and the probe showed no resorufin formation.

As most high-throughput assays are performed on crude cell lysate, it was also necessary to determine the signal stability in crude cell lysate. The signal showed was as stable in crude cell lysate as in buffer (Figure 14, Figure 16). Additionally, similar results, concerning hydrogen peroxide formation and NADPH consumption, were obtained when either crude cell lysate or purified enzymes were used in enzyme assays. Despite differences between the absolute values measured (using crude or purified enzyme), the relationships between variants, in terms of P450 activity and uncoupling rate, were the same using both assay strategies.

By investigating the uncoupling of the reductase CPR of *C. apicola*, it was shown that the Ampliflu™ Red assay produced reliable results. As uncoupling by reductases do not result in the formation of water,[182] the addition of superoxide dismutase (which converts superoxide to hydrogen peroxide) enables the detection of all possible uncoupling products with the Ampliflu™ Red assay. In this approach, the NADPH consumed equaled the detected formation of hydrogen peroxide.

Concluding from all data, the suitability of the Ampliflu™ Red assay could be demonstrated, not only for the detection of hydrogen peroxide formation, but also for the parallel detection of NADPH consumption (compatible absorbance maxima). Although several methods of studying the extent of uncoupling of cytochrome P450 monooxygenase-catalyzed reactions have been developed,[56,63,66,209] none of these methods were so far suitable for investigating hydrogen peroxide formation in parallel (i.e. in the same well of a microtiter plate) with NAD(P)H consumption.

Measurement of NAD(P)H consumption is a general and often-applied strategy for the indirect determination of enzymatic activity.[210] Although this might be a useful approach for other enzymes, this can lead to erroneous results, especially for cytochrome P450 enzymes, as the NAD(P)H consumption due to uncoupling cannot be distinguished from NAD(P)H consumption due to enzyme activity. Therefore, only by monitoring NAD(P)H consumption *and* hydrogen peroxide formation simultaneously, can the activities of a cytochrome P450 enzyme towards different substrates be estimated, without the need for quantification of the unique products of each reaction. The major advantage of the method developed during this thesis, over other assays described so far, is that it enables, for the first time, reliable detection of uncoupling.[179]

A minor limitation of the assay is that water as possible uncoupling product cannot be detected. Superoxide anion formation, however, can be detected indirectly, by the addition of superoxide dismutase, which converts the superoxide anion to hydrogen peroxide. The assay thereby also enables the determination of the amount of uncoupling resulting in water formation. If the product is quantified, in addition to measuring NAD(P)H consumption, hydrogen peroxide formation, and superoxide formation, the formation of water could be calculated (H_2O = [NAD(P)H] - [product + H_2O_2 + O_2^-]). As this however was not the aim of this thesis, this aspect was not further investigated.

4.2 Investigating the CYP11A1 system

In this part of the thesis, the stability and activity of the bovine CYP11A1 monooxygenase system was investigated. As the CYP11A1 monooxygenase is a class I cytochrome P450 enzyme, a redox partner system is needed for its activity. Therefore, also the stability of the natural redox partner system, consisting of Adx and AdR, was investigated.

Although already described in literature, the heterologous expression and purification of the membrane-bound bovine CYP11A1 proved to be challenging. First, expression experiments were performed, comparing the expression in different *E. coli* (DE3) strains at

30°C. Almost no cytochrome P450 was obtained in the soluble fraction, but rather in the insoluble fraction, presumably as inclusion bodies. Aggregation is a common problem in heterologous expression, especially for membrane proteins.[211] The insoluble aggregates formed consist of misfolded or partially folded proteins. If proteins are not (yet) properly folded, hydrophobic motifs are exposed, resulting in intermolecular interactions between the partially folded molecules, finally leading to aggregation.[212] In order to recover correctly folded protein from inclusion bodies, solubilization and refolding needs to be performed. As this approach can be quite time consuming and differs for each protein, expression optimization was investigated instead.[213] Therefore, lowering the expression temperature from 30°C to 17°C was investigated, which might help obtain correctly folded protein. Lowering the expression temperature is thought to slow down protein expression, giving the recombinant protein more time for correct folding and thus improving the yield of soluble protein. As this did not result in a higher level of soluble protein expression, different protocols found in the literature were investigated.

These protocols differ especially with respect to the composition of the buffer in which the protein was solubilized. This step of solubilization is crucial in the investigation of membrane proteins, and necessary in order to separate the protein from the membrane fraction. The solubilization components help to cope with the hydrophobic membrane anchor but need to enable the hydrophilic parts of the protein to be exposed to the aqueous phase.[211] Hence, optimization not only of the expression conditions, but also of the buffer and detergent compositions, was crucial.

After unsuccessfully trying to reproduce the expression and solubilization protocols described by Janocha *et al*.[188] and Woods *et al*.,[189] the protocol of Lepesheva *et al*. from 1998 was investigated.[190] In parallel with investigating the third protocol, the use of chaperones was studied, as well as the natural induction of expression of heat shock proteins by the addition of ethanol.[214] Although the addition of ethanol resulted in an increase in the amount of correctly folded protein, chaperone co-expression from a second plasmid was more effective in improving the yield of correctly folded protein. Additionally, the growth of the culture with added ethanol was strongly impaired. Hence, although the maintenance of a second plasmid results in an additional metabolic burden on the cell, this approach was chosen for further investigations. The plasmid used encodes the chaperones GroEL and GroES.[185] Next, the influence of using other chaperones was studied in order to further increase the obtained yield of correctly folded protein. Additionally, the expression in T1 phage-resistant *E. coli* JM109 (DE3) cells as used in this thesis before, was compared to the expression in non-T1 phage resistant *E. coli* JM109 (DE3) cells. T1 phage resistance is accomplished by the knockout of the gene encoding FhuA, an outer membrane protein receptor for ferrichrome, involved in the transport of ferrichrome-iron over the outer membrane.[191] It was hypothesized that the knockout of this gene might also influence the transport of the heme-precursor δ-aminolevulinic acid over the cell membrane. Although the use of different chaperones resulted in a decrease of obtained correctly folded protein, when

compared to the co-expression of GroEL and GroES, the use of a non-T1 phage resistant *E. coli* JM109 strain almost doubled the yield of soluble, properly folded cytochrome P450, from 7.8 mg L^{-1} to 14.4 mg L^{-1}. The aspect whether the T1 phage resistance itself is influencing the accessibility of the heme-precursor or if other factors in the cell influence the expression rate cannot be answered by the conducted experiments.

As the K193E variant of CYP11A1 was described in literature to show a fourfold increased expression rate and threefold increased yield of soluble protein, this mutation was introduced by site-directed mutagenesis and the expression compared to the expression of the wild-type enzyme.[188] The during this thesis obtained results contradicted these findings, where only after two days the expression of the variant was higher compared to wild-type with 6.1 mg L^{-1} and 0.7 mg L^{-1}. After three days of expression the wild-type yielded 14.1 mg L^{-1}, whereas the expression level for the variant was decreasing already, yielding only 2.1 mg L^{-1}. Although reducing the expression time would be advantageous, the goal of obtaining more correctly folded, wild-type protein was prioritized.

For the expression, the best time to harvest the cells, containing the highest amount of correct folded CYP11A1, was investigated. By taking time samples during cultivation this was achieved. On the basis of this cultivation experiment, it seemed as if longer cultivation time resulted in higher yields of correctly folded protein (up to three days investigated, Table 9). Although for some proteins, protein degradation exceeded expression after a certain time, resulting in a decrease in soluble protein yield if cultivated too long, this was not found for the conducted cultivation. Furthermore, the substrate binding was investigated with the last time sample, obtained after three days of cultivation, resulting in obtaining a type-I spectrum upon addition of cholesterol to the enzyme. A type-I spectrum is only observed when the heme-group of the enzyme is transformed from its low-spin form to the high-spin form upon substrate binding. After observing a high amount of presumably correctly folded protein, indicated by the CO-difference spectrum, purification was investigated.

For purification of the CYP11A1 enzyme, a C-terminal His_4-tag, as used by Mosa *et al*., was successfully introduced into the pTrc99A_P450scc plasmid. As the expression and IMAC purification of a His-tagged variant of the CYP11A1 protein was described by Mosa *et al*. in 2015, their protocol was followed.[192] After purification, the obtained CYP11A1 eluate showed a concentration of 242 mg L^{-1}. The protein was obtained in a relatively pure form, since only one other major band was observed after the SDS-PAGE analysis, as reported by Mosa *et al.* (Figure 19).[192] As a high amount of CYP11A1 was found in the elution fraction and the buffer used contained glycerol, sodium cholate, sodium acetate, and TWEEN 20, the observed problems with protein binding to the column, might arise from interference of the detergence, by for example shielding the His-tag. There was no imidazole in the washing buffer. Next, the purification in a buffer without additives was investigated. Although the purity of the protein was strongly enhanced, as well as the binding of the protein to the column, the protein was found to be incorrectly folded after purification, indicating the importance of these additives in the originally used buffer. Additionally, these results might indicate, that the His-tag of the

correctly folded protein might also not be freely accessible. As a last approach for purification optimization, cation exchange chromatography on a SP Sepharose column was investigated, using a similar buffer to the above-mentioned buffer (20 mM potassium phosphate, pH 7.4, 20% (w/v) glycerol, 0.1 mM DTT, 0.1 mM EDTA, 10 mM imidazole, 1% sodium cholate, and 0.1% Tween-20). This approach was chosen, based on the calculated pI of 8.82 for the His-tagged protein. Hence, it was assumed that the protein might be positively charged in the buffer at pH 7.4. Unfortunately, CYP11A1 could not bind to the SP Sepharose column under the applied conditions. Although the calculated pI of the protein might be accurate, the actual pI of all amino acids on the protein surface might differ from the calculated value. By changing the pH of the buffer, the purification method might be optimized. As the CYP11A1 proved in general to be sensitive to buffer conditions, first investigations on the pH stability had to be performed, before optimizing the purification.

In parallel, the expression and purification of Adx (14 kDa, solubly expressed) was investigated. The expression was successfully established. The addition of $FeSO_4$ to the cultivation medium at timepoint of induction is important to supply the *E. coli* cells with high amounts of iron and sulfur in order to build the iron-sulfur cluster of the Adx protein.

For purification a protocol of Suhara *et al*. from 1972 was followed, resulting in an approximately 50% pure protein solution. The elution fraction showed all characteristic absorption peaks necessary for clear identification of the iron-sulfur protein. Afterwards, a size exclusion chromatography approach was investigated, resulting in a relatively pure protein fraction, which had lost the typical brown color of the protein. This color loss most likely indicated the loss of the iron-sulfur cluster, which was confirmed by investigation of the absorption spectrum, which did not show the characteristic peaks anymore. Also, a hydrophobic interaction chromatography approach remained unsuccessful. Hence, also for the Adx protein the investigation of the pH stability might help to optimize the purification strategy by being able to adjust the pH of the buffer and investigating anion and cation exchange chromatography steps further.

The expression and purification of the third protein, the membrane-bound AdR, was also studied. The expression with two different plasmids (pBar1607_AdR and pET28_AdR) in combination with two different *E. coli* host strains (*E. coli* JM109 (DE3) and *E. coli* BL21 (DE3)) was investigated. Additionally, as the co-expression of chaperones increased the amount of correctly folded protein for the other membrane-bound protein investigated, the influence of co-expression of groEL and groES was investigated. Judging from SDS-PAGE analysis and the spectral properties of the proteins obtained, the best result was obtained for *E. coli* BL21 (DE3) harboring plasmids pET28_AdR and pGro7.

With the protein solution obtained, purification experiments were performed. As the pI of the AdR molecule was calculated to be 6.79, two different anion exchange chromatography approaches at pH 8 and pH 8.5 as well as an affinity chromatography approach using a 2'5' ADP Sepharose column was tested. Only by anion exchange chromatography at pH 8.5, AdR was obtained in the final elution fraction, along with other proteins. Also, the investigation of

the typical spectrum of the FAD-containing protein, indicated that only very small amounts of AdR were obtained by these purification methods, therefore also the pH stability of this protein needed to be investigated first to optimize the purification strategy further.

As the main goal was to investigate the overall activity of the CYP11A1, *in vitro* biocatalysis was performed with purified CYP11A1. As the expression and purification of AdR remained difficult, other redox partner systems were investigated. Although the first biocatalytic approach showed a clear substrate decrease for samples containing the P450 enzyme along with a redox partner system, no product or side-product formation was detected. Additionally, background activity was ruled out by different negative controls. The substrate or product also cannot be still attached to the enzyme, as only 0.4 µM enzyme was used in the conversion of 1.2 mM substrate. As a consequence of not identifying the problem, the experiment was repeated, and the scanning method of the GC-MS broadened, in order to find possible side-products. Unfortunately, the first positive results were not reproducible.

Therefore, a different redox partner system, the reductase domain of cytochrome P450 BM3 (BMR) was investigated. On the one hand as a fusion protein consisting of CYP11A1 and BMR and on the other hand in *in vitro* biocatalysis with purified enzymes. The idea, of using a fusion construct, arose from other studies indicating that the soluble expression level of membrane bound cytochrome P450 enzymes can be increased by fusion to the BMR domain, along with an increase in activity of the created self-sufficient fusion protein.[49,60,151,152] Hence, the plasmid for the expression of the fusion protein was created by FastCloning[196] and first expression experiments performed, which resulted in no expression of the fusion construct. As no spacer was used to link the two proteins, the construct might have been too rigid, resulting in incorrectly folded or insoluble fusion protein.[215–217] In parallel, *in vitro* biocatalysis was performed, which showed no product formation. Hence, it seemed most likely that the BMR domain was not able to transfer electrons to the cytochrome P450 monooxygenase. As not all redox partner systems are compatible with all cytochrome P450 enzymes, the focus was switched back to the investigation of the natural redox partner system.

As the pH stability is important for the optimization of ion-exchange purification strategies and the temperature stability is a key factor for successful biocatalytic approaches, both properties were investigated for all three proteins in the Master thesis of Christopher Grimm. Although the investigated CYP11A1 system originated from mammals, it was surprising to see that its temperature optimum was found to be at 20°C. On the other hand, the pH optimum for long-term stability was found to be around physiological pH. As the purification was already performed at pH7.4, no further optimization concerning ion exchange chromatography could be achieved. The small, soluble Adx protein remained remarkably stable over a broad pH spectrum, but purification optimization was rather achieved by improving the salt gradient in the already established purification method. The previously used gradient was quite broad, and the optimal elution concentration could be estimated from the previous purification. Therefore, the use of a washing step with a salt concentration

below the elution concentration, followed by an elution step with a narrow salt concentration range succeeded in obtaining a relatively pure protein solution. The temperature stability of the Adx protein was found to be higher when compared to CYP11A1, which will therefore most likely not lead to problems in biocatalytic approaches. These problems would more likely result from the stability issues of the CYP11A1 enzyme. Additionally, further expression optimization and purification approaches with the AdR protein did not result in any improvement. As a consequence, further activity investigations were conducted using a whole-cell system approach, with an already published plasmid encoding all three proteins.[89] The published conversion level was reproduced in a first approach and a 10-fold increase was achieved by the use of a different solubilization detergent for the cholesterol substrate. This increase might be associated with an improved substrate supply over the cell membrane caused by the new detergent. In total, the conversion was still very low (2.2% optimization).

Concluding, from the data obtained, the CYP11A1 monooxygenase is a membrane-bound enzyme with low activity and stability, even in whole-cell biocatalysis experiments. By using an approach with growing cells, the observed activity compared to *in vitro* biocatalysis should be improved for unstable proteins, by continuous production of fresh protein. As the creation of alanine variants most likely results in obtaining variants with reduced activity, the very low activity of the CYP11A1 proved to be a problem. Although described in literature, the use of radioactive labeled substrates was not an option. As additionally no high concentrations of AdR could be obtained, the focus was shifted to a different membrane-bound cytochrome P450 monooxygenase, the CYP17A1.

4.3 Investigating the CYP17A1 enzyme

As the goal was to investigate the general activity of the CYP17A1 enzyme, the expression of the human wild-type enzyme was first investigated. By following the protocol of Petrunak *et al.* the human CYP17A1 was successfully expressed in *E. coli* JM109 cells transformed with the pCW17A1Δ19H plasmid.[110] This plasmid encodes the human CYP17A1 with a 19-residue *N*-terminal truncation and *C*-terminal His-tagged version of the enzyme, also used for the crystallization of the protein. Although different conditions for purification of the His-tagged protein were investigated, no proper binding to the column was achieved. For His-tag based purification, the His-tag has to be freely accessible for binding to the column material. For some proteins, the His-tag can be incorporated into the tertiary structure and therefore, no interaction with the column material is possible. Additionally, the used buffer contained Emulgen 913, a detergent used for the solubilization of membrane-bound proteins along with glycerol. As both detergents were also present in the buffer used for purification of the CYP11A1 protein, also showing difficulties to bind to the column, it is possible, that the detergent somehow interfere with the binding ability of the His-tag to the column.

Hence, the general activity was investigated in crude cell lysate. For the CYP17A1 enzyme, the natural redox partner system is not known, therefore, other redox partner systems were investigated. Here, the CYP17A1 in combination with the Pdx/PdR system from *P. putida*

showed the highest activity. Interestingly, the negative control without addition of NADH showed the same conversion as the sample with added NADH. In general, *E. coli* lysate contains NADH, therefore observing activity without adding NADH can occur. It was however not expected to see the same extent of conversion in both samples. In an approach of Zhou *et al*. from 2013, the intracellular NADH levels of different *E. coli* strains were investigated and found to range between approximately 0.5 mM and 0.75 mM.[218] As approximately 400 µL cell lysate in a total volume of 1 mL were used for the biocatalytic approach, this might result in a final NADH concentration of 0.2 mM when calculating with the lowest measured concentration. Therefore, the conversion of 0.1 mM substrate would also be possible without external addition of NADH. The reason for obtaining only 90.2% conversion instead of full conversion in both samples although applying enough NADH might indicate an activity loss over time or a high uncoupling level, also resulting in activity loss.

In order to investigate the NADH problems observed with the negative control further, for the next biocatalysis, the CYP17A1 protein from the cell lysate was washed with the used buffer, using centrifugal filters with a cutoff value of 30 kDa. By this washing step, the NADH concentration in cell lysate should at least be reduced. Additionally, as possible negative control for further investigations, the T306A variant was created by site directed mutagenesis and successfully expressed. This mutant was described in literature as an uncoupling variant, showing only 0.9% coupling in the reaction with progesterone.[198] The results confirmed that the NADH concentration in cell lysate might have been responsible for the high activity in the sample without addition of NADH, as the cell lysate treated with the centrifugal filters showed a decreased activity without addition of NADH. Additionally, the sample with the 200 µM NADH added showed the exact same conversion as the sample with 100 µM of added NADH. Although the observed conversion was a little higher with 95.8%, full conversion could not be achieved independent of the NADH concentration used. This further strengthens the theory of problems with protein stability of uncoupling resulting in protein instability might be an issue. Furthermore, the biocatalysis performed with the T306A resulted in no product formation, resembling a good negative control. Here all components of the biocatalysis are present, even cytochrome P450 enzyme. Therefore, biocatalysis performed with T306A could be regarded as good control to observe any background reaction.

Next, the importance of all active site residues in 4 Å proximity to the bound substrate were identified with PyMol and exchanged with alanine by site-directed mutagenesis, followed by expression. Although expression of soluble protein was achieved, the recorded CO difference spectra showed that all expressed variants were mostly or completely incorrectly folded. Although introducing mutations in proteins in general can lead to misfolding of the proteins, observing this for all variants was unexpected. The folding of proteins is a complex process and therefore, small differences can result in significant effects.[219,220] In addition, the His-tag of the protein, might also negatively influence the stability of the protein.[221] Even the wild-type protein was observed to be 31.5% incorrectly folded from the very start, indicating stability problems with the construct used.

Next, all variants were again expressed, and different buffers were used for the resuspension of the pellets followed by cell lysis. In total six different buffers were used with different detergents. In none of the used buffers an increase of obtained correctly folded protein concentration was achieved. Therefore, a whole-cell system, expressing the bovine CYP17A1 in its native form, with its membrane anchor and without His-tag, of the protein was investigated.

The first whole-cell biocatalysis approach, using the *S. cerevisiae* strain GRF18 transformed with the YEp5117α plasmid following the protocol of Shkumatov *et al*.[197] showed almost full conversion of progesterone over 24 h. The first product 17α-hydroxyprogesterone was detected along with a second product, not resembling the natural occurring second product androstendione, but rather 17α, 20α -dihydroxyprogesterone. The formation of this product is most likely performed by an endogenous enzyme of *S. cerevisiae* (Figure 43b). The search of an analogue to mammalian 20α-hydroxysteroid-dehydrogenase (20α-HSD), an enzyme being capable of performing the observed reaction, revealed two possible candidates.[222] Szczebara *et al*. found in their study the proteins Gcy1p, the yeast galactose-inducible crystalline-like protein and Ypr1p, which resembles a yeast aldo-keto reductase.

This was also found in other studies.[197,203,204] Therefore, the formation of 20-hydroxyprogesterone does not occur and only 17α-hydroxyprogesterone is converted to 17α-,20α-dihydroxyprogesterone. If the activity of the CYP17A1 enzyme is investigated, both products need to be considered, as the double-hydroxylated product is only formed if the single-hydroxylated product is present.

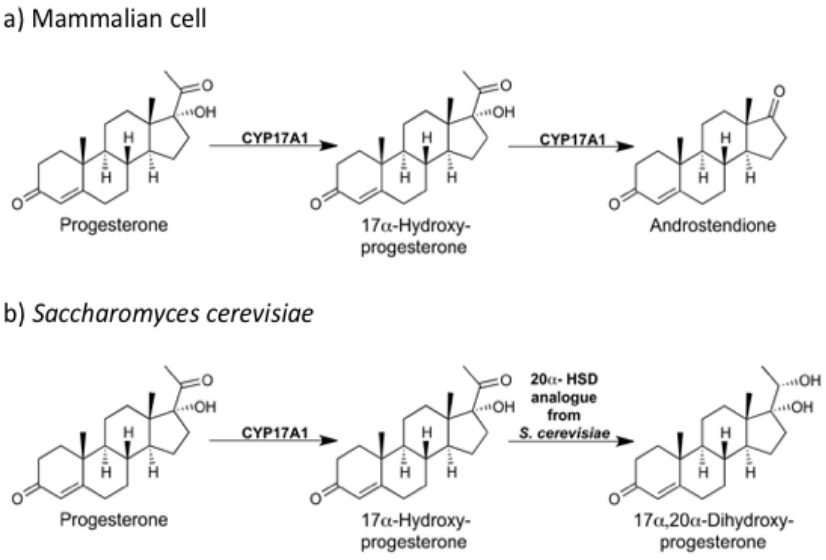

Figure 43: Comparison between conversion of progesterone in mammalian cells (a) and whole-cell biocatalysis in *S. cerevisiae*. a) Under physiological conditions, the CYP17A1 enzyme catalyzes a 17α-hydroxylation followed by a C17-20 bond cleavage reaction, resulting in conversion of progesterone to androstendione. b) In *S. cerevisiae* however, progesterone is converted to 17α-hydroxyprogesterone by the bovine CYP17A1, which is a substrate for the 20α-hydroxysteroid dehydrogenase (20α-HSD) analogue from *S. cerevisiae*. This enzyme converts 17α-hydroxyprogesterone to 17α-20α-hydroxyprogesterone. (Figure from second publication[202])

The natural second product androstendione (Figure 43a) was not found in the whole-cell biocatalysis approach employing *S. cerevisiae*. On the one hand, a study by Estrada *et al*. from 2013 showed that interaction with cytochrome b5 seems to facilitate the C17-C20 bond cleavage reaction through an allosteric interaction with the enzyme.[223] On the other hand, post-translational phosphorylation was also found to influence the formation of androstenedione to a certain extent.[109]

Hence, the missing post-translational phosphorylation might influence the absent C17-C20 bond cleavage reaction in *S. cerevisiae*. Additionally, it is possible that the affinity of the 20α-HSD analogue towards 17α-hydroxyprogesterone is higher and, therefore, also the favored reaction over the catalyzed C17-C20 bond cleavage reaction by the investigated bovine CYP17A1 enzyme.

Next, the influence of different active site residues on the overall activity of CYP17A1 was investigated. After obtaining a homology model with YASARA, all residues in 4 Å proximity to the bound substrate were identified and exchanged with alanine by site-directed mutagenesis. The activities of all variants were investigated by whole-cell biocatalysis. The obtained results seem to confirm the importance of positions N202, R239, G297, E305, and T306A, which were described in literature.[86] Although the position L105 seems to influence the side product formation of 16α-hydroxyprogesterone for the human CYP17A1 enzyme, this was not found to be the case for the bovine CYP17A1 enzyme.[108] For the bovine enzyme, the exact opposite of the findings of Swart *et al*. were observed. Here the wild-type showed side-product formation, whereas the alanine mutant showed no formation of 16α-hydroxyprogesterone. Even more interesting was the identification of three other positions (L206, V366 and V483) that seem to largely influence the 16α-hydroxyprogesterone formation by the bovine enzyme. After performing a preparative biocatalysis with the V483A variant, the side-product was isolated and analyzed by NMR, confirming that 16α-hydroxyprogesterone was obtained. Afterwards, molecular docking was performed with the homology model of wild-type and the V483A variant. Although 14 different docking results were obtained, only the docking results resembling the same substrate orientation as observed in the crystal structure with bound substrate were taken in consideration. Of these 14 results, only three resembled a similar orientation as found in the elucidated crystal structures of CYP17A1 enzymes with bound substrate of different species. Here, in two the C16 atom was found to be oriented the closest to the heme-group with 4.0 Å and 4.1 Å. Therefore, the one result resembling the closest distance to the heme iron was further analyzed by an alignment of CYP17A1 wild-type. When comparing both structures, the orientation of the bound progesterone was slightly shifted in variant V483A. Therefore, the C17 atom was closer to the heme-iron, than observed for the wild-type enzyme. Hence, the V483A position might be important for correct substrate positioning. With alanine at position 483, the substrate has a little more freedom and therefore, might be able to move more freely in the active site, resulting in 17α-hydroxylation. As also the 16α-hydroxylation is still catalyzed by this variant, the idea of the substrate not being bound rigidly, seems to be likely.

Although these results are very compelling, unfortunately the expression level could not be determined, as the samples of lysed cells showed too high turbidity and SDS-PAGE analysis of the yeast samples showed no clear band for over-expression of the protein. Therefore, it remains unclear whether the different levels of activity are just linked to activity loss out of structural reasons, or if there were also differences in expression level. Additionally, the loss of function can also be a result of incorrect folding of the expressed proteins as observed for the human CYP17A1 variants.

However, concluding from the results obtained, it seems likely that not only incorrect folding and expression levels are the main reason for the observed results. As the obtained data seems to resemble the findings and suggestions in literature, it seems more likely that the observed activities resemble the influence on activity through the alanine scanning. Additionally, the expression levels are a current topic of further investigation.

4.4 First investigations on a dual screening assay

The last section of the PhD thesis also describes the development of a screening assay. The focus was on the development of a dual screening system for substrate conversion and hydrogen peroxide formation in parallel in a high-throughput format. The goal was to find conditions to perform the final assay in water-in-oil droplets for obtaining a screening platform for a large enzyme library.

Therefore, a fatty acid linked to (7-hydroxy-4-(trifluoromethyl)coumarin was used as substrate. Hence, the investigation of this assay started with the chemical synthesis of the substrate, followed by purification and NMR spectroscopy analysis. As the correct substrate was obtained, according to NMR spectroscopy analysis, the next step was to find a suitable hydrogen peroxide detection assay.

First, The DCFH-DA probe was investigated. This probe is usually used in the detection of intracellular hydrogen peroxide levels. After oxidation, the highly fluorescent probe DCF stays in the cells. The idea for using this probe was that if the probe is usually used intracellular and is known to stay in the cells after oxidation, hopefully, the probe would also stay in the droplets. Although a linear relation between hydrogen peroxide concentration and fluorescent signal was observed, the sensitivity of the probe was not high enough with a detection limit of 2.5 µM. As the sensitivity of the previously established Ampliflu^{TM} Red assay was much higher (50 nM), this probe was further investigated on suitability for the dual screening approach.

Therefore, with the first experiment the continuance of resorufin and in parallel of the 7,4-HFC in the aqueous phase, when incubated with the HFE-7500 oil under vigorous shaking was investigated. For both probes, the tendency of diffusion into the oil phase at lower pH was observed. This is most likely explainable by the protonation degree of the probes at the different pH values. The pK_a value of resorufin is 6.0 and for the 7,4-HFC, 7.26. At lower pH, the probes become less hydrophilic through loss of charge, making it more likely the probes will diffuse into the oil. Definitely a pH above the pK_a values above both probes should be

used. For both probes, using pH 7.4 seemed to be a good compromise for also having a good working pH for enzymatic activity and still having the main part of both probes residing in the aqueous phase, necessary for detection.

Next, assay conditions were investigated with cytochrome P450 BM3 wild-type and different variants, found in the literature.[24] An uncoupling variant (F87Y) was used as negative control, the A74G/F87V variant was used as positive control. With the same conditions used in the Ampliflu™ Red assay, different substrate to NADPH ratios were investigated. By Degregorio *et al*. it was found, that the NADPH : substrate ratio is crucial for low uncoupling in general.[49] In their investigation, product formation increased with increased NADPH concentration, but reached a plateau at a certain point. Hydrogen peroxide formation also increased linearly but showed no plateau. Therefore, after obtaining high uncoupling levels for all investigated variants, the idea was to reduce the NADPH concentration. By doing so, the uncoupling extent of all variants was lowered and the ratio between product formation and hydrogen peroxide formation improved. However, it remains unclear where the difference in added NADPH and formed products arises from. It might be explained by the cytochrome P450 BM3 enzyme performing multiple hydroxylations of the substrate. As only one hydroxylation yields the 7,4-HFC, multiple hydroxylation is not detectable with the assay. The cytochrome P450 BM3 is in general known for its multiple hydroxylation of several substrates.[224] To further investigate this idea, GC-MS analysis of the obtained products should be performed in order to see if this was the problem. If the multiple hydroxylation accounts for the difference, this is not a major issue for the assay, as it still detects product formation and hydrogen peroxide formation. Only if the difference accounts for a background reaction not related with the enzymatic function, this would be a problem. Negative controls with NADPH and the substrate in combination with the Ampliflu™ Red probe did not show any reaction. This at least indicates no direct interaction of substrate and NADPH with the Ampliflu™ Red probe.

Afterwards, the assay was further investigated by performing the assay with the variants created for the Ampliflu™ Red assay. Judging from the obtained results, it seems as if the assay might be suitable in identifying new variants in a high-throughput screening, as the investigated enzyme concentration equals the final enzyme concentration and still the signal was detectable. Additionally, already one variant was found showing the same uncoupling extent as wild-type and F87V, but higher product formation. By investigating a library, probably new variants can be identified showing lower uncoupling and higher product formation. It will be interesting to analyze which residues lead to this result and even more interesting to perform molecular docking experiments with these variants and compare them to each other. Hopefully, this will increase the understanding of the occurrence of uncoupling.

A point for further optimization might be the use of the GDH system for NADPH recycling in combination with very low concentrations of NADPH, as this may circumvent problems with the leak rate. As described above, especially too high NADPH concentrations can result in high

uncoupling. By keeping the NADPH level at a low concentration over a longer time, product formation might be improved and the extent of uncoupling reduced.

5 Summary

In the 1940s cytochrome P450 monooxygenases have been discovered and have been the focus of many studies ever since. Although they catalyze very interesting reactions that might find applications in the production of fine chemicals or pharmaceuticals, their low activity and stability often reduces their economic value.[153,225–228] Both properties, the activity and the stability, are influenced by the uncoupling of the catalytic cycle.[165,229]

In this PhD thesis, an assay for the screening of activity and uncoupling of cytochrome P450 enzymes was successfully developed.[179] After finding optimal conditions for the assay, concerning pH and enzyme concentration, the uncoupling of cytochrome P450 BM3 and five mutants (F87Y, R47L, Y51F, A82L and T268A) was investigated. With the results obtained, a comparison of data from literature was possible and revealed similarities. Additionally, through negative controls, the reliability of the assay could be further demonstrated. Although other methods have been described for the detection of hydrogen peroxide formation, the combination of NADPH consumption measurement and hydrogen peroxide formation in parallel was new and represents a very good basis for a pre-screening of large mutant libraries, followed by closer investigation of selected variants.

For the investigation of the activity of the CYP11A1 system, consisting of CYP11A1 and Adx and AdR as redox partner system, the expression and purification for all three proteins was investigated first. For the protein CYP11A1 and Adx, good expression levels were achieved, whereas for AdR the protein concentration obtained was very low. The purification of all three proteins was partially accomplished but left room for improvement. Therefore, in the Master thesis of Christopher Grimm, the pH and temperature stability of all three proteins was further investigated in order to improve conditions used for ion exchange chromatography and to investigate possible conditions for *in vitro* biocatalysis. As unfortunately even with further investigation of the expression of AdR, no improvement was achieved, a whole-cell system was further investigated. Here, the product formation could be increased 8-fold in comparison to the published data, from 0.27% conversion to 2.2% conversion over 24 h by using a different detergent for substrate solubilization, which might have led to a better substrate supply to the enzyme.

Due to the low activity and stability, a different P450 system, the CYP17A1 enzyme, was subsequently investigated, first by *in vitro* biocatalysis with the human CYP17A1 expressed in *E. coli*. Therefore, a suitable redox partner system needed to be found for efficient electron supply of the enzyme. In *in vitro* biocatalysis, in combination with the Pdx/PdR system of *P. putida* the CYP17A1 enzyme showed the highest conversion with 91% after 24 h. To investigate the activity of the enzyme further, all active site residues in 4 Å proximity to the bound substrate were exchanged with alanine. After expression of the variants, almost no correctly folded protein was obtained for the variants. Also, after investigating different buffers to possibly enhance the stability, no improvements were achieved. Therefore, a whole-cell approach with the bovine enzyme was chosen in order to investigate the activity

of the alanine variants. Here the importance of positions N202, R239, G297, E305, and T306A, described in literature to be important for catalytic activity, was confirmed. Most importantly, three positions that alter the regioselectivity of the enzyme were identified. The reaction of the V483A mutant was therefore also further investigated by preparative biocatalysis. Afterwards the new product was separated by preparative HPLC and identified as 16α-hydroxyprogesterone as confirmed by NMR spectroscopy analysis.

In the last part of the thesis, another screening approach for possible high-throughput screening was investigated. In contrast to the other screening approach, here the investigation of the substrate conversion and the hydrogen peroxide formation were optimized for application in droplets. After finding that DCFH-DA was not sensitive enough towards hydrogen peroxide, the Ampliflu™ Red probe was used. As both fluorescent products were found to stay in the aqueous phase above pH 7.4, the conditions investigated for the Ampliflu™ Red assay were applied and only NADPH to substrate ratio was investigated by using an uncoupling variant, an active variant from literature and the cytochrome P450 BM3 wild-type enzyme. After finding a good ratio, the five variants used for the investigation of the Ampliflu™ Red assay were investigated in the same concentration later on found in the droplets (1 cell per 4 pL), and one variant showed improved product formation compared to wild-type. This finding clearly shows the applicability of the assay for high-throughput screening in droplets.

6 Zusammenfassung

Cytochrom P450 Monooxygenasen wurden in den 1940er Jahren entdeckt und wurden seither intensiv erforscht. Obwohl sie sehr interessante Reaktionen katalysieren, die Anwendung in der Produktion von Feinchemikalien und Pharmazeutika finden könnten, wird ihre Wirtschaftlichkeit meist durch ihre Aktivität und Stabilität negativ beeinflusst.[153,225–228] Beide Eigenschaften, die Aktivität und die Stabilität, werden durch die Entkopplung des katalytischen Zyklus beeinflusst.[165,229]

Im Rahmen dieser Doktorarbeit, wurde ein Assay für das „screening“ auf Aktivität und Entkopplung erfolgreich entwickelt.[179] Nachdem optimale Reaktionsbedingungen für das Assay identifiziert waren, wurde die Entkopplung von Cytochrom P450 BM3 und fünf Mutanten (F87Y, R47L, Y51F, A82L and T268A) mit verschiedenen Substraten untersucht. Obwohl bereits viele andere Wasserstoffperoxid Detektionsmethoden beschrieben wurden, war die Kombination einer parallelen Bestimmung der NADPH Abnahme und der Wasserstoffperoxid Bildung neu. Dieser parallele Ansatz stellt eine gute Basis für ein „pre-screening“ großer Mutantenbibliotheken dar, worauf eine detaillierte Untersuchung von ausgewählten Varianten folgt.

Um die Aktivität des CYP11A1 Systems, bestehend aus CYP11A1, Adx und AdR als Redox Partner System, untersuchen zu können, wurde zunächst die Expression und Aufreinigung aller drei Proteine untersucht. Für die Proteine CYP11A1 und Adx, wurden gute Expression Levels erreicht, wohingegen die Konzentration für AdR sehr gering war. Für alle drei Proteine wurde nach Aufreinigungsversuchen eine konzentrierte Lösung erhalten, die jedoch noch andere Proteine enthielt. Daher wurde in der Masterarbeit von Christopher Grimm, die pH und Temperaturstabilität aller drei Proteine untersucht, um die Bedingungen während der Ionenaustauschchromatographie als Aufreinigungsmethode optimieren zu können und optimale Bedingungen für *in vitro* Biokatalysen zu finden. Leider wurde trotz weiterer Expressionsversuche mit AdR keine Verbesserung erzielt, wodurch ein Ganzzellsystem als nächstes untersucht wurde. Für dieses System konnte die Produktbildung auf 2.2%, achtfach erhöht werden, im Vergleich zu den publizierten 0.27% Umsatz nach 24 h durch die Verwendung eines anderen Detergenz zur Lösung des Substrates Cholesterol, wodurch vermutlich die Bereitstellung des Substrates für das Enzym erleichtert wurde.

Auf Grund der beobachteten geringen Aktivität und Stabilität, wurde anschließend ein weiteres P450 System untersucht, das CYP17A1 Enzym. Zunächst wurden *in vitro* Biokatalysen mit dem humanen CYP17A1 durchgeführt, welches in *E. coli* exprimiert wurde. Nachdem verschiedene Redox-Partner Systeme getestet wurden, erzielte das Pdx/PdR System von *P. putida* in Kombination mit dem CYP17A1 Enzym den höchsten Umsatz, mit 91% nach 24 h. Um die Aktivität des Enzyms näher zu untersuchen, wurden alle Aminosäuren in einem Abstand von 4 Å zum gebundenen Substrat durch Alanine ersetzt. Alle Varianten wurden exprimiert, jedoch konnte kaum richtig gefaltetes Protein erhalten werden. Auch nachdem verschiedene Puffer untersucht wurden, zur eventuellen Stabilitätserhöhung, konnte keine

Verbesserung festgestellt werden. Deshalb wurde auch hier auf einen Ganzzellansatz zurückgegriffen. Dieser bestand aus dem Enzym aus Rind welches in *S. cerevisiae* exprimiert wurde. Mit diesem System, wurde die Bedeutung der Positionen N202, R239, G297, E305 und T306A bestätigt, die in der Literatur als wichtig für die katalytische Aktivität beschrieben werden. Am wichtigsten waren drei Positionen, die die Regioselektivität des Enzyms verändern. Die Reaktion der V483A-Mutante wurde daher auch durch präparative Biokatalyse weiter untersucht. Danach wurde das neue Produkt durch präparative HPLC getrennt und als 16α-Hydroxyprogesteron identifiziert, was mittels NMR-Spektroskopie bestätigt werden konnte.

Im letzten Teil der Arbeit wurde ein weiterer Screening-Ansatz für ein mögliches Hochdurchsatz-Screening untersucht. Im Gegensatz zum bereits beschriebenen Screening-Ansatz wurde hier die Untersuchung der Substratumwandlung und der Wasserstoffperoxidbildung für den Einsatz in „droplets“ optimiert. Nachdem festgestellt wurde, dass DCFH-DA gegenüber Wasserstoffperoxid nicht empfindlich genug war, wurde das Ampliflu™ Red / HRP System verwendet. Da beide fluoreszierenden Produkte oberhalb von pH 7,4 in der wässrigen Phase blieben, wurden die für den Ampliflu™ Red Assay untersuchten Bedingungen angewendet. Das NADPH-Substrat-Verhältnis wurde mit einer Entkopplungsvariante, einer aktiven Variante aus der Literatur und dem Cytochrom P450 BM3 Wildtyp-Enzym untersucht. Nach Ermittlung eines guten Verhältnisses wurden die fünf für die Untersuchung des Ampliflu™ Red Assays verwendeten Varianten in der gleichen Konzentration untersucht, die später in den „droplets“ gefunden wird (1 Zelle pro 4 pL). Hier zeigte eine Variante eine verbesserte Produktbildung im Vergleich zum Wildtyp. Dieser Befund zeigt deutlich die Anwendbarkeit des Assays für Hochdurchsatzscreening in „droplets“.

7 Material and Methods

7.1 Materials

7.1.1 Strains

For recombinant expression of proteins and cloning experiments different *Escherichia coli* (*E. coli*) strains and one *Saccharomyces cerevisiae* (*S. cerevisiae*) strain were used (Table 14).

Table 14: List of used strains for cloning and protein expression experiments.

species	strain	genotype	company
E. coli	BL21 (DE3)	*fhuA2 [lon] ompT gal (λ DE3) [dcm] ΔhsdS λ DE3 = λ sBamHIo ΔEcoRI-B int::(lacI::PlacUV5::T7 gene1) i21 Δnin5*	New England Biolabs (Frankfurt am Main, Germany)
E. coli	TOP10 (DE3)	F- *mcrA* Δ(*mrr-hsd*RMS-*mcr*BC) Φ80*lac*ZΔM15 Δ *lac*X74 *rec*A1 *ara*D139 Δ(*araleu*)7697 *gal*U *gal*K *rps*L (StrR) *end*A1 *nup*G	Thermo Fisher Scientific (Waltham, USA)
E. coli	JM109 (DE3)	endA1, recA1, gyrA96, thi, hsdR17 (rk–, mk+), relA1, supE44, Δ(lac-proAB), [F´ traD36, proAB, laqIqZΔM15]	New England Biolabs (Frankfurt am Main, Germany)
E. coli	C43 (DE3)	F^- ompT galdcmhsdS(r^- m^- BBB)(DE3)	Sigma-Aldrich (Steinheim, Germany)
E. coli	SHuffle®Express	*fhuA2 lacZ::T7 gene1 [lon] ompT ahpC gal λatt::pNEB3-r1-pNEB3-cDsbC (Spec^R,lacI^q) ΔtrxB sulA11 R(mcr-73::miniTn10*--Tet^S)2 [dcm] *R(zgb-210::Tn10 -- Tet^S) endA1 Δgor Δ(mcrC-mrr)114::IS10*	New England Biolabs (Frankfurt am Main, Germany)
S. cerevisiae	GRF18	Matα his3-11 his3-15 leu2-3 leu2-112 can^R cir$^+$	Prof. Stefan Mauersberger, Technical University Dresden (Germany)

7.1.2 Plasmids

Table 15: List of used plasmids.

Plasmid	description	Received from / company
pET22_BM3	Harbors the gene for Cytochrome P450 BM3 from *B. megaterium*	Constructed by Jan Muschiol, former PhD student of Prof. Dr. Uwe T. Bornscheuer, Greifswald University (Germany)
pET28a_BMR	Harbors the gene for the reductase-domain of Cytochrome P450 BM3 from *B. megaterium*	Constructed by Jan Muschiol, former PhD student of Prof. Dr. Uwe T. Bornscheuer, Greifswald University (Germany)
pTrc99A_P450scc	Harbors the gene for bovine CYP17A1[188]	Prof. Dr. Rita Bernhardt, University of Saarland (Germany)
pET28a_P450scc_BMR	Harbors a construct for the expression of a chimera protein of P450scc and BMR	Constructed during this work
pBad_Adx,	Harbors the gene for the bovine Adx	Prof. Dr. D. B. Janssen, University of Groningen (The Netherlands)
pKKHC_Adx	Harbors the gene for the bovine Adx[230]	Prof. Dr. Rita Bernhardt, University of Saarland (Germany)
pBar1607_AdR	Harbors the gene for the bovine AdR[231]	Prof. Dr. Rita Bernhardt, University of Saarland (Germany)
pET28_AdR	Harbors the gene for the bovine AdR[231]	Prof. Dr. D. B. Janssen, University of Groningen (The Netherlands)
pBar_Triple	Harbors the genes for bovine CYP11A1, Adx and AdR with three ribosom binding sites[89]	Dr. Ludmila Novikova, Lomonosov Moscow State University (Russia)
pET28a_Pdx	Harbors the gene of Pdx from *P. putida*[232]	Prof. Dr. Vlada B. Urlacher, Heinrich- Heine- University Düsseldorf (Germany)
pET28a_PdR	Harbors the gene of PdR from *P. putida*[232]	Prof. Dr. Vlada B. Urlacher, Heinrich- Heine- University Düsseldorf (Germany)

pET28a_CPR	Harbors gene for CPR from *C. apicola* with N-terminal 22 amino acids deletion and N-terminal His-tag[145]	Prof. Dr. Vlada B. Urlacher, Heinrich- Heine- University Düsseldorf (Germany)
pQE-30-HyPer3	Harbors gene for HyPer-3 expression, natural H_2O_2 sensor-protein from E. coli (OxyR) which was genetically modified[67]	Addgene, Cambridge (United Kingdom)
pCW17A1Δ19H	Harbors gene for N-terminal truncated human CYP17A1 (19 residues), C-terminal His_4-tag[86,110]	Prof. Dr. Emily E. Scott, University of Michigan (United States)
YEp5117α	Harbors gene for bovine CYP17A1, shuttle vector for amplification in *E. coli* and expression of the protein in *S. cerevisiae*[197]	Dr. Stefan Mauersberger, Technical University Dresden (Germany)

7.1.3 Enzymes

Table 16: List of used enzymes.

Enzyme	**Company**
Catalase from bovine liver	Sigma-Aldrich (Steinheim, Germany)
Cholesterol oxidase from *Streptomyces* spec.	Sigma-Aldrich (Steinheim, Germany)
DpnI	New England BioLabs® Inc. (Ipswich, USA)
GDH 105	Codexis (Redwood, USA)
Horseradish peroxidase	Sigma-Aldrich (Steinheim, Germany)
Superoxide dismutase	Sigma-Aldrich (Steinheim, Germany)
Opti*Taq*	Roboklon (Berlin, Germany)
Taq	Roboklon (Berlin, Germany)

7.1.4 Oligo nucleotides

All used oligonucleotides were synthesized by Thermo Fisher Scientific (Waltham, USA).

Table 17: List of primer used for sequencing (fw – forward, rev – reverse).

Primer	**Sequence (from 5' to 3')**	**Purpose**
eLMO Seq1	GAGGTTAAGCCAGCCATTGTCAC	Sequencing primers for pTrc99A_P450scc plasmid
eLMO Seq2	GCCAATATTACGGAGATGCTGGC	
eLMO Seq 3	GATCCCTCGAACTTGAAGAGATG	
eLMO Seq 4	TGTAAAACGACGGCCAGT	
eLMO Seq 5	CAGGAAACAGCTATGACC	

pBAD fw	ATGCCATAGCATTTTTATCC	Sequencing primer for pBad_Adx plasmid
T7 fw mod T7 term	CCCGCGAAATTAATACGACTCAC CTAGTTATTGCTCAGCGGT	Sequencing primer for all pET plasmids
LMO020_Amp-fw LMO021_Amp-rv	GGCTGGCTGGTTTATTGCTG CGAGACCCACGCTCACC	Sequencing primers binding to the β-lactamase gene
LMO032_CYP17a_mid_fw LMO033_CYP17a_mid_rev LMO034_CYP17a_beg_rev LMO035_CYP17a_end_fw LMO036_CYP17a_Vend_fw	CTGTTAGACATATTCCCTGTGCTGAAG CTTCAGCACAGGGAATATGTCTAACAG GCCACTTTGGGACGCCCAGAG CACAAGGCTGTCATTGACTCCAG CAGGCTGAGGGTAGCACC	Sequencing primers for the YEp5117α (encoding bovine CYP17A1)
LMO049 pCW17A1 Seq 1 LMO050 pCW17A1 Seq2 LMO051 pCW17A1 Seq3 LMO052 pCW17A1 Seq4 LMO053 pCW17A1 Seq5 LMO054 pCW17A1 Seq6	CGAAGAAAACCGGTGCAAAATACC CTTTCAAAAGATTCACTCGTTGACC GAAGTCATTATTAATCTTTGGGCAC GAGGCTCAGGCGGAAGGTTCAAC GTATTTTGCACCGGTTTTCTTCGC CGGTTGTTGCTCGCAATATCGAG	Sequencing primers for the pCW17A1Δ19H (encoding human CYP17A1)
LMO089_BM3_Seq1 LMO090_BM3_Seq2 LMO091_BM3_Seq3	GCCAACTGCTCCTGCGTTTTCC GGATGCGGCGATAAAAACTGGG CTCGATTTCTTCATCACCTCGTGTC	Sequencing primers for the Cytochrome P450 BM3 gene

Table 18: List of used primerd for site directed mutagenesis (QC - QuikChange™, fw – forward, rev – reverse)

Primer	**Sequence (from 5' to 3')**	**Purpose**
pET22b_BM3_R47L_fw	GCCTGGTCTGGTAACGCGCTAC	QuikChange™ primers used for introduction of different mutations into the Cytochrome P450 BM3 gene
pET22b_BM3_R47L_rev	CGTTACCAGACCAGGCGCCTCG	
pET22b_BM3_Y51F_fw	CGCGCTTCTTATCAAGTCAGCGTC	
pET22b_BM3_Y51F_rev	CTTGATAAGAAGCGCGTTACACG ACC	
pET22b_BM3_A82L_fw	CGTGATTTTCTGGGAGACGGGTT ATTTAC	
pET22b_BM3_A82L_rev	CCCGTCTCCCAGAAAATCACGTA CAAATTTAAG	
LMO030 QC BM3 F87Y fw	GTTATATACAAGCTGGACGCATG	
LMO031 QC BM3 F87Y rev	GCTTGTATATAACCCGTCTCCTGC	

pET22b_BM3_T268A_fw	GATTTATTAGCGCATATGCTAAACGGAAAAGATCC	
pET22b_BM3_T268A_rev	GTTTAGCATATGCGCTAATAAATCATCGCTTTGTTC	
LMO045 QC BM3 F87V fw	GTTAGTTACAAGCTGGACGCATG	QuikChange™ primers used for introduction of different mutations into the Cytochrome P450 BM3 gene
LMO046 QC BM3 F87V rev	GCTTGTAACTAACCCGTCTCCTGC	
LMO047 QC BM3 A74G	GTCAAGGGCTTAAATTTGTACGTG	
LMO048 QC BM3 A74G	CAAATTTAAGCCCTTGACTTAAGTTTTTATC	
LMO087_BM3_QC_I401P_fw	GTGCGTGTCCCGGTCAGCAGTTC	
LMO088_BM3_QC_I401P_rev	CTGACCGGGACACGCACGCTGAC	
LMO018_CypH6-fw	AGGACCCGCCCCAGGCGCATCATCACCATCACCACTGACCGGAGAGGGCGG	Primer used for introduction of a His_6-tag into the pTrc99A_P450scc plasmid
LMO019_CypH6-rv	CCCGCCCTCTCCGGTCAGTGGTGATGGTGATGATGCGCCTGGGGCGGGTC	
LMO055 pCW17A1 QC T306A fw	GTTGAAGCCACTACTTCCGTCG	
LMO056 pCW17A1 QC T306A rev	GAAGTAGTGGCTTCAACTCCTGCG	
LMO057_QC_pCW_ F114A_fw	CATCGCTGCCGCTGACTCAGG	
LMO058_QC_pCW_F114A_rev	GTCAGCGGCAGCGATGCCTTTAC	
LMO059_QC_pCW_Y201A_fw	CAGAACGCTAACGAAGGTATTATTGAC	
LMO060_QC_pCW_Y201A_rev	CTTCGTTAGCGTTCTGAATCACG	QuikChange™ primers used for introduction of different mutations into the human CYP17A1 gene encoded by the pCW17A1Δ19H plasmid
LMO061_QC_pCW_N202A_fw	GAACTATGCCGAAGGTATTATTGACAATC	
LMO062_QC_pCW_N202A_rev	CAATAATACCTTCGGCATAGTTCTGAATC	
LMO063_QC_pCW_I205A_fw	CGAAGGTGCTATTGACAATCTTTCAAAAG	
LMO064_QC_pCW_I205A_rev	GTCAATAGCACCTTCGTTATAGTTCTG	
LMO065_QC_pCW_I206A_fw	GAAGGTATTGCTGACAATCTTTCAAAAGATTC	
LMO066_QC_pCW_I206A_rev	GATTGTCAGCAATACCTTCGTTATAGTTC	

LMO067_QC_pCW_L209A_fw	GACAATGCTTCAAAAGATTCACT CGTTG	
LMO068_QC_pCW_L209A_rev	CTTTTGAAGCATTGTCAATAATAC CTTCG	
LMO069_QC_pCW_R239A_fw	GTAAAAATCGCTAACGATTTGCT GAAC	
LMO070_QC_pCW_R239A_rev	CAAATCGTTAGCGATTTTTACATG AC	
LMO071_QC_pCW_G297A_fw	CCACCATCGCTGACATCTTCG	
LMO072_QC_pCW_G297A_rev	GATGTCAGCGATGGTGGTCAG	QuikChange™ primers used for introduction of different mutations into the human CYP17A1 gene encoded by the pCW17A1Δ19H plasmid
LMO073_QC_pCW_G301A_fw	CATCTTCGCCGCAGGAGTTG	
LMO074_QC_pCW_G301A_rev	CTCCTGCGGCGAAGATGTCAC	
LMO075_QC_pCW_E305A_fw	CAGGAGTTGCAACCACTACTTCC	
LMO076_QC_pCW_E305A_rev	GTAGTGGTTGCAACTCCTGCG	
LMO077_QC_pCW_V366A_fw	CGTCCTGCTGCGCCTATGC	
LMO078_QC_pCW_V366A_rev	CATAGGCGCAGCAGGACGTAAA C	
LMO079_QC_pCW_I371A_fw	CTATGCTTGCTCCACACAAAGCC	
LMO080_QC_pCW_I371A_rev	GTGTGGAGCAAGCATAGGCGC	
LMO081_QC_pCW_V482A_fw	CCCAAAAGCTGTTTTTCTTATTGA CTC	
LMO082_QC_pCW_V482A_rev	GAAAAACAGCTTTTGGGATGCCT TC	
LMO083_QC_pCW_V483A_fw	CAAAAGTTGCTTTTCTTATTGACT CATTTAAAG	
LMO084_QC_pCW_V483A_rev	CAATAAGAAAAGCAACTTTTGGG ATGCC	
LMO095_YEp_F114A_fw	CATTGCCGCCGCCGACCATGGTG	
LMO096_YEp_F114A_rev	GTCGGCGGCGGCAATGCCCTTTT G	QuikChange™ primers used for introduction of different mutations into the bovine CYP17A1 gene encoded by the YEp5117α plasmid
LMO097_YEp_V201A_fw	CAAAATGCCAATGATGGCATCCT GGAGG	
LMO098_YEp_V201A_rev	CATCATTGGCATTTTGTATGGCCT TCAGGG	
LMO099_YEp_N202A_fw	CAAAATGTCGCCGATGGCATCCT GGAGG	
LMO100_YEp_N202A_rev	GCCATCGGCGACATTTTGTATGG CCTTC	

LMO101_YEp_I205A_fw	CAATGATGGCGCCCTGGAGGTTC TG	
LMO102_YEp_I205A_rev	CCTCCAGGGCGCCATCATTGACA TTTTG	
LMO103_YEp_L206A_fw	GGCATCGCCGAGGTTCTGAGCAA G	
LMO104_YEp_L206A_rev	GAACCTCGGCGATGCCATCATTG AC	
LMO105_YEp_L105A_fw	GACATCGCGTCAGACAACCAAAA GGG	
LMO106_YEp_L105A_rev	GTCTGACGCGATGTCTAGAGTGG C	
LMO107_YEp_R239A_fw	CAAACGGCCAATGAATTGCTGAA TGAAATCC	
LMO108_YEp_R239A_rev	CAATTCATTGGCCGTTTGAACAC AACCC	QuikChange™ primers used for introduction of different mutations into the bovine CYP17A1 gene encoded by the YEp5117α plasmid
LMO109_YEp_G297A_fw	CTACTATAGCGGACATCTTCGGG G	
LMO110_YEp_G297A_rev	GATGTCCGCTATAGTAGCGAGCA TG	
LMO111_YEp_G301A_fw	CATCTTCGCGGCTGGTGTGGAG	
LMO112_YEp_G301A_rev	CACCAGCCGCGAAGATGTCCC	
LMO113_YEp_E305A_fw	GGTGTGGCGACCACCACGTCTG	
LMO114_YEp_E305A_rev	GGTGGTCGCCACACCAGCCC	
LMO115_YEp_V366A_fw	CGGCCTGCGGCCCCTACG	
LMO116_YEp_V366A_rev	GTAGGGGCCGCAGGCCGG	
LMO117_YEp_I371A_fw	CTACGCTGGCCCCCCACAAGG	
LMO118_YEp_I371A_rev	GTGGGGGGCCAGCGTAGGGG	
LMO119_YEp_L482A_fw	CCAGTGCCGTCTTGCAGATCAAA C	
LMO120_YEp_L482A_rev	CAAGACGGCACTGGCATGGC	
LMO121_YEp_V483A_fw	CAGTCTCGCCTTGCAGATCAAAC C	
LMO122_YEp_V483A_rev	CTGCAAGGCGAGACTGGCATG	
LMO123_YEp_T306A_fw	GTGGAGGCCACCACGTCTGTGAT AAAG	
LMO124_YEp_T306A_rev	CGTGGTGGCCTCCACACCAGC	
LMO125_YEp_D298A_fw	CTATAGCGACATCTTCGGGGCTG	
LMO126_YEp_D298A_rev	GATGTCCGCTATAGTAGCGAGCA TG	

Table 19: All used oligonucleotides for fast cloning (fw – forward, rv/rev – reverse).

Primer	Sequence (from 5' to 3')	
LMO024_P450scc_BMR_fw	CTTTAAGAAGGAGGATCCTAATATGGTCTCCACAAAGACCCCTC	Primer used for the fast cloning approach to construct the pET28a_P450scc_BMR plasmid
LMO025_P450scc_BMR_rev	GTATAGCACAAGCAGCGGCATCGCCTGGGGCGGGTCCTG	
LMO026_pET28BMR_fw	CAACCAGGACCCGCCCCAGGCGATGCCGCTGCTTGTGCTATAC	
LMO027_pET28BMR_rev	GAGGGGTCTTTGTGGAGACCATATTAGGATCCTCCTTCTTAAAGTTAAAC	

7.1.5 Chemicals and consumables

All chemicals and reagents used were purchased from Sigma Aldrich (Munich, Germany) if not stated otherwise.

7.1.6 Kits

Table 20: List of used Kits.

Kit	Producer
innuPrep Plasmid Kit	Analytik Jena AG (Jena, Germany)
Pierce™ BCA Protein Assay Kit	Thermo Fisher Scientific (Waltham, USA)
Chaperon Plasmid Set	TaKaRa Bio Inc (Kusatu, Japan)

Table 21: Plasmid List of the "Chaperone Plasmid Sets" Kit from TaKaRa Bio Inc.

Plasmid	Chaperone	Protein Size	Inductor
pKJE7	DnaK	70	L-arabinose
	DnaJ	40	
	GrpE	22	
pG-KJE8	DnaK	70	L-arabinose
	DnaJ	40	
	GrpE	22	
	GroEL	60	Tetracycline
	GroES	10	
pTf16	Tf	56	L-arabinose
pGro7	GroEL	60	L-arabinose
	GroES	10	
pG-Tf2	GroEL	60	Tetracycline
	GroES	10	
	Tf	56	

7.1.7 Media, additives and inductors

Table 22: Media recipes used for liquid cultures.

Medium, buffer or solution	Components and preparation
10x SOC	10 mmol•L^{-1} NaCl, 2.5 mmol•L^{-1} KCl, 10 mmol•L^{-1} $MgCl_2$, 20 mmol•L^{-1} $MgSO_4$, 20 mmol•L^{-1} glucose, solved in aq. dest., filter sterile
10x TB salts	164.4 g K2HPO4 • 3 H2O, 23.2 g KH2PO4 in 1 L aq. dest.
Glycerol solution	60 % (w/v) in aq. dest., autoclave
LB medium	1% (w/v) peptone/tryptone, 1% (w/v) NaCl and 0.5% (w/v) yeast extract in aq. dest., autoclave
LB-SOC	10x SOC added 1:10 to sterile LB-medium
TB medium	8 g glycerol, 12 g peptone/tryptone, 24 g yeast extract in 900 mL aq. dest., autoclave, add 100 mL 10x TB-salts
YNB medium	13.4g yeast nitrogen base in 1000 mL aq. dest., autoclave
YPD medium	1% (w/v) yeast extract, 2% (w/v) peptone in aq. dest., autoclave, adding sterile filtered 10% (w/v) D-glucose in aq. dest. in 1:10 ratio

In order to create agar plates the above mentioned liquid media recipes were used and 12% (w/v) agar-agar was added to the solution before autoclaving.

Table 23: Recipes for concentrated used antibiotic and inductor stock solutions.

Antibiotic / inductor / Additives	Components and preparation
1000x ampicillin	100 mg mL^{-1} in aq. dest., filter sterile
1000x chloramphenicol	50 mg mL^{-1} in ethanol, filter sterile
1000x kanamycin	100 mg mL^{-1} in aq. dest., filter sterile
1000x IPTG	1 mol L^{-1} in aq. dest., filter sterile
200x D-galactose	400 g L^{-1} in aq. dest., keep at 60°C until dissolved, filter sterile
1000x δ-aminolevulinic acid	0.5 M in aq. dest, filter sterile

7.1.8 Buffers and solutions

7.1.8.1 Chemical Competent E. coli cells

Table 24: Buffers and solution recipes needed for the preparation of chemical competent *E. coli* cells.

Buffer / solution	Components and preparation
Tfb I buffer	100 mM RbCl, 50 mM $MnCl_2$, 30 mM KOAc, 10 mM CaCl2 and 15% glycerol in aq. dest., adjust pH to 5.8, filter sterile

Tfb II buffer	100 mM RbCl, 75 mM $CaCl_2$, 10 mM MOPS and 15% glycerol in aq. dest., adjust pH to 7.0, filter sterile
$MgCl_2$ solution	1 M in aq. dest., filter sterile

7.1.8.2 Electrocompetent E. coli cells

Buffer / solution	Components and preparation
10% glycerin solution	100 mL glycerine, adjust volume with aq. dest to 1 L, autoclave

7.1.8.3 Chemical Competent S. cerevisiae cells

Table 25: Buffers and solution recipes needed for the preparation of chemical competent *S. cerevisiae* cells.

Buffer / solution	Components and preparation
TE buffer (pH 7.5)	10 mM TRIS, 1 mM EDTA in aq. dest., adjust pH to 7.5 with HCl, filter sterile
LP-Mix	40% polyethylene glycol 4000, 0.1 M lithium acetate in TE buffer, filter sterile
Sheared Salmon sperm DNA	Ready-to-use; 10 mg mL^{-1}; catalog number: 15632-011; Thermo Fisher Scientific (Waltham, USA)

7.1.8.4 Agarosegel electrophorese

Table 26: Buffers and solution recipes needed for agarose gel electrophorese.

Buffer / solution	Components and preparation
50x TAE buffer (pH 8.5)	242 g TRIS, 57.1 mL glacial acetic acid, 18.6 g EDTA in 1000 mL aq. dest
agarose gel (1%)	1 g agarose in 100 mL 1x TAE buffer, dissolved by heating in microwave oven, per 50 mL gel 3 µL RotiStain (Carl Roth, Karlsruhe) were added for visualization under UV light
Loading buffer	For all PCR approaches buffer C was used, already containing a loading buffer (Roboklon, Berlin)

7.1.8.5 Protein purification

7.1.8.5.1 CYP102A1

Table 27: Buffers used for purification and storage of Cytochrome P450 BM3.

Buffer	Components and preparation
BM3 equilibration buffer	50 mM sodium phosphate in aq. dest., adjust pH to 7.4
BM3 wash buffer	20 mM imidazole in 50 mM sodium phosphate buffer, adjust pH to 7.4

BM3 elution buffer	100 mM imidazole in 50 mM sodium phosphate buffer, adjust pH to 7.4
BM3 storage buffer	50 mM sodium phosphate, 20% (v/v) glycerol in aq. dest., adjust pH to 7.4

7.1.8.5.2 CYP11A1

Table 28: Buffers used for purification of CYP11A1 with IMAC using hand columns.

Buffer	Components and preparation
CYP11A1 lysis buffer	50 mM potassium phosphate buffer, 20% (v/v) glycerol, 1.5% sodium cholate, 500 mM sodium acetate, 1.5% Tween-20, 0.1 mM EDTA, 0.1 mM DTT, 0.1 mM PMSF, adjust pH to 7.4
CYP11A1 equilibration and wash buffer	50 mM potassium phosphate buffer, 20% (v/v) glycerol, 1% sodium cholate, 500 mM sodium acetate, 1% Tween-20, 0.1 mM EDTA, 0.1 mM DTT, 0.1 mM PMSF, adjust pH to 7.4
CYP11A1 elution buffer	50 mM sodium phosphate buffer 150 mM imidazole, 20% (v/v) glycerol, 1% sodium cholate, 500 mM sodium acetate, 1% Tween-20, 0.1 mM EDTA, 0.1 mM DTT, 0.1 mM PMSF, adjust pH to 7.4
CYP11A1 storage buffer	50 mM potassium phosphate, 20% (v/v) glycerol, 1% sodium cholate, 0.05% Tween-20, 0.1 mM EDTA and 0.1 mM DTT, adjust pH to 7.4

Table 29: Buffer used for purification of CYP11A1 by Ion exchange chromatography.

Buffer	Components and preparation
CYP11A1 buffer used for purification using SP-Sepharose	20 mM potassium phosphate, 20% (v/v) glycerol, 0.1 mM DTT, 0.1 mM EDTA, 10 mM imidazole, 1% sodium cholate, 0.1% Tween-20, adjust pH to 7.4

7.1.8.5.3 Adx

Table 30: Buffers used for purification of Adx using DEAE-Sepharose, Phenylsepharose or a column packed with Superdex G200.

Buffer	Components and preparation
Adx equilibration buffer	50 mM sodium phosphate; adjust pH to 7.4
Adx elution buffer	50 mM sodium phosphate, 1 M KCl; adjust pH to 7.4

7.1.8.5.4 AdR

Table 31: Buffers used for purification of AdR using columns packed with Source Q, 2-5 ADP Sepharose or DEAE-Sepharose.

Buffer	Components and preparation

AdR equilibration buffer	10 mM potassium phosphate, 1 mM EDTA, 1 mM PMSF; adjust pH to 8
AdR elution buffer (2-5 ADP Sepharose)	10 mM potassium phosphate, 1 mM EDTA, 1 mM PMSF, 400 mM NaCl; adjust pH to 8
AdR elution buffer (DEAE Sepharose)	10 mM potassium phosphate, 1 mM EDTA, 1 mM PMSF, 500 mM NaCl; adjust pH to 8

7.1.8.5.5 Pdx

Table 32: Buffers used for purification and storage of Pdx.

Buffer	Components and preparation
Pdx equilibration buffer	500 mM NaCl, 10 mM β-mercaptoethanol in 50mM sodium phosphate buffer, adjust pH to 7.4
Pdx wash buffer	500 mM NaCl, 20 mM imidazole, 10 mM β-mercaptoethanol in 50 mM sodium phosphate buffer, adjust pH to 7.4
Pdx elution buffer	500 mM NaCl, 500 mM imidazole, 10 mM β-mercaptoethanol in 50 mM sodium phosphate buffer, adjust pH to 7.4
Pdx storage buffer	50 mM TRIS, 10 mM β-mercaptoethanol, 20% (v/v) glycerol in aq. dest., adjust pH to 7.4

7.1.8.5.6 PdR

Table 33: Buffers used for purification and storage of PdR.

Buffer	Components and preparation
PdR equilibration buffer	300 mM NaCl, 5% (v/v) glycerol in 50 mM sodium phosphate buffer, adjust pH to 7.4
PdR wash buffer	300 mM NaCl, 10 mM imidazole, 5% (v/v) glycerol in 50 mM sodium phosphate buffer, adjust pH to 7.4
PdR elution buffer	300 mM NaCl, 150 mM imidazole, 5% (v/v) glycerol in 50 mM sodium phosphate buffer, adjust pH to 7.4
PdR storage buffer	12% (w/v) glycerol in 50 mM sodium phosphate buffer, adjust pH to 7.4

7.1.8.5.7 CPR

Table 34: Buffers used for purification and storage of CPR (adapted from Girhard *et al*. 2013[145]).

Buffer	Components and preparation
CPR equilibration buffer	50 mM TRIS, 500 mM NaCl in aq. dest., adjust pH to 7.5
CPR wash buffer	50 mM TRIS, 500 mM NaCl, 15 mM imidazole in aq. dest., adjust pH to 7.5
CPR elution buffer	50 mM TRIS, 500 mM NaCl, 100 mM imidazole in aq. dest., adjust pH to 7.5

CPR storage buffer	50 mM TRIS, 25 mM NaCl, 5% (v/v) glycerol in aq. dest., adjust pH to 7.5

7.1.8.5.8 Human CYP17A1

Table 35: Buffers used for purification and storage of human CYP17A1 (adapted from Petrunak *et al*. 2014[110])

Buffer	Components and preparation
CYP17A1 equilibration buffer	50 mM TRIS, 300 mM NaCl, 0.2% (v/v) Emulgen 913, 20% (v/v) glycerol in aq. dest., adjust pH to 7.4
CYP17A1 wash buffer	50 mM TRIS, 300 mM NaCl, 100 mM glycine, 0.2% (v/v) Emulgen 913, 20% (v/v) glycerol in aq. dest., adjust pH to 7.4
CYP17A1 elution buffer	50 mM TRIS, 300 mM NaCl, 100 mM glycine, 80 mM histidine, 0.2% (v/v) Emulgen 913, 20% (v/v) glycerol in aq. dest., adjust pH to 7.4
CYP17A1 storage buffer	50 mM TRIS, 50 mM NaCl, 100 mM glycine, 20% (v/v) glycerol in aq. dest., adjust pH to 7.4

7.1.8.5.9 HyPer-3

Table 36: Buffers used for purification and storage of HyPer-3 (adapted from Bilan *et al*. 2013[67]).

Buffer	Components and preparation
HyPer-3 equilibration buffer and wash buffer	40 mM TRIS, 150 mM KCl, 10 mM $MgSO_4$, 5 mM β-mercaptoethanol in aq. dest., adjust pH to 7.5
HyPer-3 elution buffer	40 mM TRIS, 150 mM KCl, 10 mM $MgSO_4$, 400 mM imidazol in aq. dest., adjust pH to 7.5
HyPer-3 storage buffer	40 mM TRIS, 150 mM KCl, 10 mM $MgSO_4$, 5 mM β-mercaptoethanol, 20% (v/v) glycerol in aq. dest., adjust pH to 7.5

7.1.8.6 SDS-PAGE

Table 37: Buffers and solution recipes needed for SDS-PAGE.

Buffer / solution	Components and preparation
Lower TRIS buffer	18.2 g TRIS, 0.1 g SDS in 100 mL aq. dest., adjust pH to 8.8
Upper TRIS buffer	6 g TRIS, 0.1 g SDS in 100 mL aq. dest., adjust pH to 6.8
APS solution	10% ammonium persulfate in aq. dest.
Separation gel (12%)	2.677 mL aq. dest., 2 mL lower TRIS buffer, 3.33 mL acrylamide solution, mix by inverting, add 40 µL APS solution and 4 µL TEMED, pour gel immediately

Stacking gel (4%)	2.47 mL aq. dest., 1 mL upper TRIS buffer, 3.33 mL acrylamide solution, mix by inverting, add 40 µL APS solution and 4 µL TEMED, pour gel immediately
Loading buffer	20% (w/v) glycine, 6% (w/v) 2-mercaptoethanol, 0.0025% bromophenol blue in Upper TRIS buffer
Protein Ladder	Roti®-Mark STANDARD (Carl Roth, Karlsruhe, Germany) PageRuler™ Unstained Protein Ladder (Thermo Fisher Scientific, Waltham, USA)
Running buffer	3.03 g TRIS, 14.4 g glycine, 1 g SDS in 1000 mL aq. dest., adjust pH to 8.4
Staining solution	1 g Coomassie-brilliant-blue G250, 100 mL glacial acidic acid, 300 mL ethanol, 600 mL aq. dest.
Destaining solution	300 mL ethanol, 100 mL glacial acidic acid, 600 mL aq. dest.

7.1.8.7 Ampliflu Red™ Assay

Table 38: Buffers and solutions used for the Ampliflu Red™ assay.

Buffer / solution	**Components and preparation**
Buffer A	50 mM sodium phosphate in aq. dest., adjust pH to 7.4
Ampliflu Red™ stock solution (100x)	10 mM Ampliflu Red™ in DMSO
HRP stock solution (100x)	20 U mL^{-1} HRP in aq. dest.
Ampliflu Red™ assay solution	1x Ampliflu Red™, 1x HRP in 50 mM sodium phosphate (pH 7.4)

7.1.8.8 Biocatalysis

Table 39: List of used buffers and solutions for biocatalytic approaches.

Biocatalytic approach	**Buffer/solution**	**Components and preparation**
In vitro biocatalysis bovine CYP11A1	HEPES buffer	20 mM HEPES, 50 mM KCl and 0.1 mM DTT, adjust pH to 7.3
	2x DOPC vesicle solution containing cholesterol	Preparation of vesicles with 3.4 mg mL^{-1} DOPC, 3.5 mM cholesterol (added with DOPC, before vesicle preparation)
	20x D-Glucose	2 mM glucose, dissolve in ddH_2O
	20x GDH solution	10 mg mL^{-1} GDH 105, dissolve in ddH_2O
	10x NAD(P)H stock	1,5 mM NAD(P)H, dissolve in ddH_2O

Whole cell biocatalysis with CYP11A1	Microelement solution I	4.07 g L^{-1} $FeCl_2 \cdot 6H2O$, 0.28 g L^{-1} $CaCl_2 \cdot 2H_2O$, 0.28 g L^{-1} $CoCl_2 \cdot 6H_2O$, 0.19 g L^{-1} $ZnCl_2 \cdot 4H_2O$, 0.26 g L^{-1} $CuSO_4 \cdot 5H_2O$, 0.07 g L^{-1} H_3BO_4, dissolve in ddH_2O
	Microelement solution II	0.28 g L^{-1} $Na_2MoO_4 \cdot 2H_2O$, dissolve in ddH_2O
	100x Cholesterol stock	50 mM cholesterol, dissolve in 250 mM (2-Hydroxypropyl)-β-cyclodextrin
In vitro biocatalysis with human CYP17A1	20x NADPH stock	2 mM NADPH, dissolve in ddH_2O
	100x progesterone stock	10 mM progesterone, dissolve in EtOH
Whole cell biocatalysis with bovine CYP17A1	10x stock D-galactose	20% (w/v) D-glucose, dissolve in ddH_2O
	100x progesterone stock	10 mM progesterone, dissolve in EtOH

7.1.8.9 Dual screening approach

Table 40: Used chemicals and buffers for the investigations on the dual screening approach.

Chemical/Buffer	**Company/Preparation**
Assay buffer	50 mM sodium phosphate, dissolve in aq. dest.; adjust pH to 7.4 (additionally, other pH values were investigated)
HFE-7500 3M™ Novotec™; Referred to as HFE-7500	Fluorochem Ltd. (Hadfield, United Kingdom)

7.1.9 Equipment

Table 41: Used equipment.

Equipment	**Name**	**Producer**
Agarose electrophoresis	Mini-Sub Cell GT	Bio-Rad (Munich, Germany)
	Compact XS/S	Biometra GmbH (Göttingen, Germany
Balances	PCB350-3	Kern & Sohn GmbH (Belingen, Germany)
	PCB2500-2	
	Explorer E14130	Ohaus (Parsippany, USA)
	MC1 Analytic AC 120S	Sartorius (Göttingen, Germany)
Centrifuges	Biofuge pico	Thermo Fisher Scientific (Waltham, USA)
	Biofuge 400R	Thermo Fisher Scientific (Waltham, USA)

	Multifuge 3S-R	Thermo Fisher Scientific (Waltham, USA)
	Fresco 17	Thermo Fisher Scientific (Waltham, USA)
	Sprout-Minizentrifuge	Biozym Scientific (Oldendorf, Germany)
Cell lysis	Sonoplus HD/UW 2070 Equipped with:	Bandelin (Berlin, Germany)
	Ultrasonic horn MS72 Ultrasonic horn KE76	Bandelin (Berlin, Germany)
Cleanbench	HeraSafe KS15	Thermo Fisher Scientific (Waltham, USA)
FPLC	ÄKTApurifier	GE Healthcare (Buckinghamshire, United Kingdom)
Gas chromatography	GC-2010(plus) incl. AOC-20i-s	Shimadzu (Duisburg, Germany
	GCMS-QP2010	Shimadzu (Duisburg, Germany
Heating-/stirring plate	RCT basic	IKA Labortechnik (Staufen, Germany)
Homogenization	FastPrep-24	MP Biomedicals, Inc. (Eschwege, Germany)
HPLC	LaChrom L7100	Merck Hitachi (Darmstadt, Germany
	Equipped with L7100 pump, L7420 UV-Detector, L7200 Autosampler, D7000 Interface	Merck Hitachi (Darmstadt, Germany)
Incubation	Incucell	MMM Medcenter Einrichtungen GmbH (Gräfelfing, Germany)
	Multitron Standard	Infors AG (Bottmingen, Switzerland)
	Minitron	Infors AG (Bottmingen, Switzerland)
pH-meter	PH211	Hanna Instruments (Vöhringen, Germany)
Photometer	Jasco V-550 with PSC-498T Temperature controller	Jasco Analytical Instruments (Easton USA)

	NanoDrop™ 1000	Peqlab (Erlangen, Germany)
	UV Mini-1240	Shimadzu (Duisburg, Germany)
Power supply for electrophoresis	EPS EV231	Consort (Turnhout, Belgium)
	Standard Power Pack 25	Biometra (Göttingen, Germany)
Protein electrophoresis	Minigel-Twin	Biometra (Göttingen, Germany)
Sterilization	V-120 autoclave	Systec (Bergheim-Glessen, Germany)
	Laboklav ECO	SHP Steriltechnik AG (Detzel, Germany)
	Dry-Line oven	VWR International (Darmstadt, Germany)
Thermocycler	FlexCycler²	Analytic Jena (Jena, Germany)
	FlexCycler	Analytic Jena (Jena, Germany)
	DNA Engine Tetrad® 2	BioRad (Hercules, USA)
Thermoshaker	Thermomixer comfort	Eppendorf (Hamburg, Germany)
UV table	Benchtop UV Transiluminator	UVP (Upland, USA)
Vortex	Vortex Genie 2	Scientific Industries (Bohemia, USA)
96-well plate reader	Infinite® M200PRO	Tecan Trading AG (Männedorf, Switzerland)

7.2 Methods

7.2.1 Microbiological and Molecular-biological Methods

7.2.1.1 Strain maintenance

For storage of transformants and strains, they were kept on agar plates (LB for *E. coli* and YPD for *S. cerevisiae*) and stored at 4°C. If a selection method could be used, the plates contained the according substances. For longer storage at 4°C, fresh plates were prepared every 6 – 8 weeks.

For long-term storage, also glycerol stocks were prepared for each strain / transformant. Here, 1 mL overnight culture was mixed 1:1 with a 60% glycerol solution. These vials were stored at -80°C.

7.2.1.2 Preparation of overnight cultures

For the preparation of overnight cultures, 5 mL medium containing appropriate selection marker(s) (LB for *E. coli* and YPD for *S. cerevisiae*) were inoculated with single colonies picked from agar plates or 10 µL glycerol stock. These cultures were grown overnight (*E. coli* at 37°C and *S. cerevisiae* at 30°C).

7.2.1.3 Preparation of competent cells

7.2.1.3.1 Preparation of chemical competent *E. coli* cells

For the preparation of chemical competent *E. coli* cells, 100 mL LB medium were inoculated from an overnight culture and grown at 37°C at 200 rpm until OD_{600} of 0.5 was reached. Next, the cells were harvested for 15 min at 4°C and 4000 *g*. The pellet was resuspended in 30 mL pre-cooled Tfb I buffer. Afterwards 3.2 mL 1 M pre-cooled $MgCl_2$ was added and the cells were kept on ice for 15 min. After another centrifugation step for 10 min at 4000 *g* and 4°C, the supernatant was discarded, and the cell pellet was resuspended in 4 mL pre-cooled Tfb II buffer. The suspension was incubated on ice for 15 min, followed by separation into 50 µL aliquots, which were shock-frozen in liquid nitrogen. The aliquots were stored at -80°C until usage.

7.2.1.3.2 Preparation of electrocompetent *E. coli* cells

Electrocompetent *E. coli* cells were prepared by inoculating 500 mL LB medium with 5 mL overnight culture. Cells were grown at 37°C and 180 rpm until OD_{600} of 0.6 was reached. Afterwards the cells were cooled on ice for 20 min and centrifuged for 30 min at 4500*g* at 4°C. The cell pellet was than washed three times but resuspended the first time in 500 mL pre-cooled 10% glycerin solution, the second time in 250 mL ice cold 10% glycerin solution, the third time in 20 mL ice cold 10% glycerin solution and finally in 1.5 mL ice cold 10% glycerin solution. All centrifugation steps were carried out for 30 min at 4°C and 4500*g*. The residual 1.5 mL were split into 50 µL aliquots and stored at -80°C until usage.

7.2.1.3.3 Preparation of chemical competent *S. cerevisiae* cells

For *S. cerevisiae*, competent cells were always freshly produced and used immediately (7.2.1.4.3).

7.2.1.4 Transformation

7.2.1.4.1 Transformation of chemical competent E. coli cells

For each transformation, one aliquot of frozen competent cells was thawed on ice for 10 min. After incubation with 50 ng μL^{-1} plasmid DNA on ice for 30 min, the cells were heat-shocked at 42°C for 45 s in a water bath. Then, the cells were incubated for 5 min on ice and 500 µL LB-SOC was added. The mixture was incubated at 37°C and 180 rpm for one hour and afterwards spread on LB agar plates containing the appropriate antibiotic(s). The plates were incubated at 37°C overnight and afterwards stored at 4°C.

7.2.1.4.2 Transformation of electrocompetent E. coli cells

One aliquot of electrocompetent E. coli cells was mixed with 25 ng plasmid DNA (in a maximal volume of 10 µL aq. dest). The cells were kept on ice for 30 min and filled into pre-cooled electroporation cuvettes. After electroporation for 5 ms at 2500V, 1 mL pre-warmed LB-medium was added. The solution was incubated for one hour at 37°C and 180 rpm and spread on selection plates. The plates were incubated at 37°C overnight and afterwards stored at 4°C.

7.2.1.4.3 Transformation of chemical competent S. cerevisiae cells

S. cerevisiae cells were grown in 5 mL YPD medium at 30 °C and 180 rpm shaking velocity until an OD_{600} of 0.8 was reached. For each transformation 1.4 mL of the culture were harvested with 10000*g* for 5 min. The supernatant was discarded, and 1 µg plasmid DNA and 100 µg shredded salmon sperm DNA were added. Afterwards 500 µL LP-Mix and 55 µL DMSO were added. After inverting the tube four times, the mixture was incubated for 15 min at room temperature. The heat shock was then performed at 42°C for 15 min. The mixture was afterwards diluted with 500 µL sterile TE buffer and the cells were harvested for 1 min at 1000*g* and washed with 1 mL TE buffer. After centrifugation for 2 min at 2000 *g*, the cell pellet was resuspended in 100 µL TE buffer and platted on YNB agar plates containing the selection marker. The plates were incubated at 30°C for three to five days and afterwards stored at 4°C.

7.2.1.5 Cultivation and Protein Expression

7.2.1.5.1 CYP102A1 (P450 BM3)

P450 BM3 was expressed in *E. coli* BL21 (DE3). For overexpression, 400 mL TB-Amp medium supplemented with ampicillin in a 2-L baffled Erlenmeyer flask were inoculated with 4 mL overnight culture. Untill OD_{600} of 0.6 was reached, the cells were grown at 37°C and 160 rpm. Then, overexpression was started by addition of 0.25 mM IPTG. The heme-precursor δ-Ala in a final concentration of 0.5 mM, was added at the same time. Afterwards, cultivation was continued for 48 h at 30°C. The cells were harvested at 4500*g* for 30 min at 4°C. If not used directly, the cell pellets were stored at -20°C until further usage.

7.2.1.5.2 CYP11A1

7.2.1.5.2.1 Investigation of Expression using different *E. coli* strains

In order to investigate the expression of CYP11A1, *E. coli* TOP10 (DE3), BL21 (DE3), C41 (DE3), C43 (DE3) and SHuffle (DE3) were transformed with the pTrc99A_P450scc plasmid. A volume of 20 mL LB-Amp medium was inoculated with a certain amount of overnight culture to obtain an OD_{600} of 0.08. Initial growth was performed at 37°C and 135 rpm shaking velocity. When the cultures had reached OD_{600} of 0.5, the temperature was lowered to 30°C or 17°C. After addition of 1 mM IPTG and 0.5 mM δ-Ala the cultivation was accomplished overnight at 30°C and over two days at 17°C. For cell lysis, the pellet was resuspended in 50 mM sodium phosphate buffer pH7.5 containing 0.2% Triton-X100 and 1 mM EDTA. Afterwards CO difference spectra were recorded.

7.2.1.5.2.2 Expression according to Janocha *et al.*

Following the protocol of Janocha *et al.*[188] 50 mL TB-Amp medium were inoculated with *E. coli* JM109 (DE3) ells harboring the pTrc99A_P450scc plasmid and grown at 37°C with 180 rpm shaking velocity. After reaching OD600 of 1.0, 0.5 mM IPTG and 1 mM δ-Ala were added and the incubation temperature lowered to 28°C. With a shaking velocity of 135 rpm, cultivation was carried on for another 24 h. After harvesting the cells at 4.000*g* for 25 min, the cell pellet was resuspended in a 50 mM sodium phosphate buffer pH7.0, containing 300 mM NaCl, 10 µM cholesterol and 0.1% (w/v) sodium cholate.

7.2.1.5.2.3 Expression according to Lepesheva *et al.*

According to the protocol of Lepesheva *et al.*[190] 50 mL TB-Amp medium were inoculated with *E. coli* JM109 (DE3) cells harboring the pTrc99A_P450scc plasmid and different chaperone plasmids. After growing the cell culture at 37°C and 180 rpm shaking velocity until OD_{600} of 0.6 was reached, the temperature was lowered to 28°C. Induction was accomplished by addition of 0.5 mM IPTG. At the same time also 0.5 mM δ-Ala were added (and 3% ethanol for one sample). Afterwards cultivation was carried on for 48 h and the cells were harvested at 4.000*g* for 20 min. The cell pellet was resuspended in 20 mM sodium phosphate buffer pH 7.4, containing 1 mM EDTA, 1 mM DTT and 20% glycerol. After cell lysis, 1% Emulgen 913 was drop wise added for 1 h on ice, followed by another centrifugation step at 17.000*g* for 45 min.

7.2.1.5.2.4 Expression experiment for determination of optimal timepoint for harvesting

With the above described conditions of Lepesheva *et al.* two flasks containing 500 mL TB-Amp-Chl medium each, *E. coli* JM109 (DE3) harboring the pTrc99A_P450scc and the pGro7 plasmid were cultivated. At each sample timepoint (0, 16, 20, 24, 40, 44, 48, 64, 68, 72 h) the OD600 of both cultivations was measured. Additionally, 50 mL sample were taken from one of the flasks in an alternating fashion.

7.2.1.5.2.5 Final cultivation conditions

E. coli C43 (DE3) cells without λ-phage resistance harboring the pTrc99A_P450scc plasmid and the pGro7 plasmid, were cultivated in 200 mL TB-Amp-Chl medium in a 2 L baffled flask. After reaching OD_{600} of 0.6, protein expression was induced by addition of 0.5 mM IPTG and 0.5% L-arabinose. At the same time, 0.5 mM δ-Ala were added. Afterwards, the cultivation temperature was lowered to 28°C and the shaking velocity reduced to 95 rpm. After 72 h, the cells were harvested and kept on ice or frozen at -20°C.

7.2.1.5.3 Adx

With *E. coli* BL21 (DE3) cells, harboring the pKKHc_Adx plasmid, the protein Adx was overexpressed. A volume of 400 mL TB medium containing ampicillin in a 2 L flask was inoculated with 4 mL overnight culture and grown at 37°C and 180 rpm until OD_{600} of 0.5 was reached. Overexpression was induced by the addition of 1 mM IPTG. 0.3 mM $FeSO_4$ were added at the same time. Cultivation continued at 30°C and 160 rpm for 48 h. Cells were harvested by centrifugation at 4500*g* at 4°C for 30 min. The cell pellet was than either kept on ice and used directly or stored at -20°C.

7.2.1.5.4 AdR

For the expression of AdR *E. coli* BL21 (DE3) were transformed with pET28_AdR and with both pET28_AdR and pGro7. *E. coli* JM109 cells without phage resistance were transformed with pBar1607_AdR and with both pBar1607_AdR and pGro7. The cells harboring the pET28_AdR plasmid were cultivated in LB-Kan medium, whereas the cells harboring the pBar1607_AdR plasmid were cultivated in TB-Amp medium. For cells harboring additionally the pGro7 plasmid chloramphenicol was added. All cells were cultivated in 100 ml at 37°C and 135 rpm until an OD_{600} of 0.6 was reached. The expression was induced with 1 mM IPTG. Afterwards the temperature was lowered to 20°C and cells were harvested after 24 h.

7.2.1.5.5 Pdx

Overexpression of the protein Pdx was achieved by cultivation of *E. coli* BL21 (DE3) harboring the pET28a_Pdx plasmid. In a 2 L flask, 400 mL TB medium containing kanamycin were inoculated with 4 mL overnight culture. Cells were grown at 37°C and 180 rpm until an OD_{600} of 0.8 was reached. Overexpression was induced by the addition of 1 mM IPTG. At the same time, 0.3 mM FeSO4 were added and the temperature was lowered to 30°C. The shaking velocity was also lowered to 140 rpm. Cells were harvested after 48 h at 4500*g* for 30 min at 4°C. If not used directly, the cell pellets were stored at -20°C until further usage.

7.2.1.5.6 PdR

For the overexpression of PdR, *E. coli* BL21 (DE3) cells were used harboring the pET28a_PdR plasmid. With 4 mL overnight culture, 400 mL TB medium containing kanamycin in a 2 L flask were inoculated and grown at 37°C and 140 rpm until OD_{600} of 0.6 was reached. After induction with 1 mM IPTG, the incubation temperature was lowered to 20°C. Overexpression was stopped after another 48 h cultivation time and the cells were harvested at 4500*g* at 4°C for 30 min. The cell pellets were either used directly and kept on ice or stored at -20°C until further usage.

7.2.1.5.7 BMR

The reductive domain of P450 BM3 was overexpressed in *E. coli* BL21 (DE3), harboring the pET28a_BMR plasmid. From an overnight culture, 400 mL TB medium containing kanamycin were inoculated in a ratio of 1:100. Cells were grown at 37°C and 180 rpm until overexpression was induced with 1 mM IPTG when an OD_{600} of 0.6 was reached. After lowering the cultivation temperature to 30°C and reducing the shaking velocity to 160 rpm, overexpression continued for 24 h. Cells were harvested by centrifugation at 4500*g* for 30 min at 4°C. The resulting cell pellet was kept on ice or stored at -20°C for later usage.

7.2.1.5.8 CPR

The protein CPR was overexpressed in *E. coli* BL21 (DE3) cells, harboring the pET28a_CPR_His plasmid (adapted from Girhard *et al*. 2013[145]). 50 mL TB medium containing kanamycin was inoculated with 500 µL overnight culture and grown until OD_{600} of 0.8 was reached at 37°C and 180 rpm. Overexpression was started by addition of 0.25 mM IPTG. The cultivation temperature was lowered to 25°C and the shaking velocity reduced to 140 rpm.

After another 24 h of cultivation, cells were harvested at 4500*g* for 30 min at 4°C. If used directly, the cell pellet was kept on ice or for later usage stored at -20°C.

7.2.1.5.9 CYP17A1

7.2.1.5.9.1 Human CYP11A1

Human CYP17A1 (adapted with slight modifications from Petrunak *et al.* 2014[110]):

For expression of a truncated version (deletion of residues 1-19) of human CYP17A1, *E. coli* JM109 was used, harboring the pCW17A1Δ19H plasmid. The overnight culture was grown at 250 rpm at 37°C. After 18 h 400 mL TB medium containing ampicillin were inoculated with 4 mL overnight culture. Until OD_{600} of 0.5 was reached, cultivation conditions were kept the same. After induction of the overexpression with 0.5 mM IPTG and the addition of 0.5 mM δ-Ala, the temperature was lowered to 28°C and the shaking velocity reduced to 140 rpm. After 72 h, the cells were harvested by centrifugation at 4500*g* at 4°C for 30 min. Cells were kept on ice for direct use or stored at -20°C.

7.2.1.5.9.2 Bovine CYP11A1

Bovine CYP17A1 (adapted with slight modifications from Shkumatov *et al.* 2002[197]):

The bovine CYP17A1 was expressed in S. cerevisiae, harboring the YEp5117α plasmid. A volume of 20 mL YPD medium was inoculated with a single colony picked from an agar plate and grown over night at 30 °C and 180 rpm. For the cultivation, 45 mL YPD in a 300 mL Erlenmeyer flask were inoculated with 5 mL overnight culture and grown at 30°C and 180 rpm. After 24h 5mL D-galactose (20% Stock in ddH_2O) and 500 µL progesterone (10 mM Stock in ethanol) were added.

7.2.1.5.10 HyPer-3

The HyPer-3 protein was expressed using *E. coli* Shuffle (DE3) cells. With 2 mL overnight culture, 200 mL fresh LB medium, supplemented with ampicillin, was inoculated. The cell culture was grown at 37°C and 180 rpm for [67]

7.2.1.6 Cell disruption

For SDS-PAGE samples, samples were normalized on the basis of their cell counts. Therefore, 7 / OD_{600} samples were taken and harvested by centrifugation at 14000*g* for 10 min at 4°C. The cell pellet was resuspended in 500 µL buffer and lysed by sonication twice on ice for 1 min (50% power, 20% cycle). The cell lysate was separated from cell debris by centrifugation at 14000*g* for 15 min at 4°C. Afterwards, the supernatant was transferred to a new reaction tube and the pellet, containing insoluble proteins was resuspended in 500 µL buffer.

In order to lyse bigger samples, the cells were harvested at 4°C and 4000*g* for 1h. The cell pellet was resuspended in three times the volume of its weight (5 mL buffer per 1 g cell pellet). Cell lyses was obtained by sonication twice, on ice for 6 min (50% power, 20% cycle).

7.2.2 Molecular Biological Methods

7.2.2.1 Plasmid isolation

Plasmids were isolated by usage of the innuPREP Plasmid Mini Kit (Analytik Jena). All steps were performed as described in the manufacturer's manual, except for the elution step. Here, 50 µL or 100 µL (for 5 mL or 10 mL culture volume) sterile aq. dest, pre-warmed to 70°C was used.

7.2.2.2 PCR methods

7.2.2.2.1 Site-directed mutagenesis

For most site-directed mutagenesis approaches, a standard PCR mixture was used (Table 42).

Table 42: Standard PCR mixture as applied for site-directed mutagenesis. Only the concentration of DMSO was variable.

component	One reaction (40 µL)
PCR buffer C (10x)	5 µL
DMSO	0.4 µL
Template DNA	25 ng
5' oligo	2 µL
3' oligo	2 µL
dNTPs	2 µL
Opti*Taq*	1 µL
ddH_2O	Adjust volume to 40 µL

After site-directed mutagenesis was performed, a DpnI digest followed for each approach to digest template DNA. Afterwards, the 5 µL were used to transform *E. coli* TOP10 cells. These were grown overnight on agar plates containing appropriate selection marker. For each variant, 2 clones were picked to inoculate overnight cultures. From these overnight cultures, plasmids were isolated and send of for sequencing to Eurofins genomics (Ebersberg, Germany).

7.2.2.2.1.1 CYP102A1

For pET22_BM3, site directed mutagenesis was carried out with a standard PCR mixture (Table 42) using pET22_BM3 as template. The temperature program was optimized for the used Opti*Taq* polymerase (Table 43).

Table 43: Temperature program used for the site-directed mutagenesis of P450 BM3.

step	Temperature [°C]	Time [s]	
Initial denaturation	95	180	
Denaturation	95	15	35*
Annealing	58	30	
Elongation	72	540	
Final elongation	72	1080	
	15	∞	

7.2.2.2.1.2 CYP11A1

In order to exchange lysine 193 with glutamic acid in the pTrc99A_P450scc plasmid, site-directed mutagenesis was performed using a slightly different Master Mix (Table 44). The temperature program was similar to the program used for site directed mutagenesis of the Cytochrome P450 BM3 gene (Table 43). Only the annealing temperature was different with 55°C, only 25 cycles were used for amplification, elongation was performed for 390 s and final elongation for 780 s.

Table 44: Composition of the Mastermix for 8x25 µL= 200 µL used for site-directed mutagenesis of the CYP11A1 gene.

Component	Volume [µl]
10x buffer C	25
dNTPs	5
primer fw	2,5
primer rev	2,5
template (62,7 ng μl^{-1})	7
DMSO	1
Opti Taq	2,5
ddH_2O	110,5

7.2.2.2.1.3 Human CYP17A1

For the alanine screening performed with the human CYP17A1, site-directed mutagenesis was used to exchange different residues to alanine, using pCW17A1Δ19H as template. To the standard PCR mixture (Table 42) 0.4 µL DMSO were added and only 0.5 µL of each primer and 0.5 µL OptiTaq were used. As temperature program, a touch-up program was applied. Standard time intervals and temperatures were the same as for the site-directed mutagenesis of P450 BM3 (Table 43). Initial denaturation and denaturation were the same. Annealing temperature for the first cycle was set to different temperatures depending on the primers annealing temperatures. For F114A, Y201A, N202A, I205A, I206A, L209A and R239A an initial annealing temperature of 52°C was used, for G297A, G301A, E305A, V482A and V483A 51°C and for V336A and I371A 53°C. This temperature was increased for the first 5 cycles by one degree each cycle and kept for another 30 cycles afterwards at initial annealing temperature

plus 5°C (equals actual annealing temperature. Elongation time was set to 420 s. And final elongation to 840 s.

7.2.2.2.1.4 Bovine CYP17A1

For the generation of different variants of the bovine CYP17A1, site directed mutagenesis was performed, using Yep5117a as template. The standard PCR mixture (Table 42Table 42) was changed, by using 0.5 µL of each primer, 100 ng template DNA and only 0.5 µL polymerase. The temperature program was similar to the program used for the creation of P450 BM3 variants (Table 43). Only, the annealing temperatures were different variants (annealing temperatures: 58°C for L482A & V483A; 59°C for G297A & D298A; 60°C for L105A, R239A & G301A; 61°C for V201A & L206A; 62°C for N202A, I205A, E305A, T306A, V366A & I371A; 64°C for F114A) and a touch-up PCR was performed. Therefore, for the first 5 cycles the annealing temperature was lowered 5 degrees from the actual annealing temperature and increased with each cycle by one degree. Afterwards, 20 cycles with the actual annealing temperature followed.

7.2.2.2.2 Colony PCR

In general colony PCR was applied to identify clones harboring the freshly introduced plasmid.

7.2.2.2.2.1 *E. coli*

Each clone was picked and streaked out on a master agar plate. The remaining cells were suspended in 10 µL colony PCR master mix (Table 45). After amplification (Table 46), all samples were analyzed by agarose gel electrophorese.

Table 45: Master Mix *E. coli* colony PCR.

component	5 samples [µL]
PCR buffer C (10x)	5
DMSO	2.5
5’ oligo	1
3’ oligo	1
dNTPs	1.5
Taq-polymerase	3
ddH_2O	36

Table 46: Temperature program fort the colony PCR of *E. coli*.

step	Temperature [°C]	Time [s]	
Initial denaturation	98	300	
Denaturation	95	30	40*
Annealing	Primer dependent	30	
Elongation	72	60 kbp^{-1}	
Final elongation	72	120 kbp^{-1}	
	15	∞	

7.2.2.2.2.2 *S. cerevisiae*

Each picked colony was first put on a new agar plate. The remaining cells were lysed by incubation in 20 µL 20 mM NaOH at 95°C for 10 min. A volume of 2 µL was used as template DNA in the colony PCR master mix (Table 47). After amplification (Table 48) all samples were analyzed by agarose gel electrophoresis.

Table 47: Master Mix *S. cerevisiae* colony PCR.

component	1 reaction [µL]
ddH_2O	14.55
PCR buffer C (10x)	2
dNTPs	0.4
5’ oligo	0.4
3’ oligo	0.4
Taq-polymerase	0.25
Template DNA	2
Total	20

Table 48: Temperature program *S. cerevisiae* colony PCR.

step	Temperature [°C]	Time [s]	
Initial denaturation	95	300	
Denaturation	95	30	30*
Annealing	Primer dependant	30	
Elongation	72	60 kbp^{-1}	
Final elongation	72	120 kbp^{-1}	
	15	∞	

7.2.2.2.3 Fast cloning

As backbone pET28a(+)_BMR was chosen and amplified with primers binding directly in front of the BMR gene. Those primer had 30bp overhangs coding for the start and end sequence of P450scc. As insert the P450scc gene was amplified from the pTrc99a_scc plasmid.

The whole gene without the stop codon was amplified adding also 30bp fitting overhangs to both ends. After dpnI digest a PCR clean-up was performed. After determining the concentrations by nano drop of both fragments, their molar concentrations were calculated (Equation 1).

$$pmols = \frac{(weight\ in\ ng) * 1000}{(base\ pairs * 650\ daltons)}$$

Equation 1: Equation for calculating concentration of correctly folded Cytochrome P450 enzyme, from values determined by the recorded difference spectrum.

For the fast cloning approach a molar ratio of backbone to insert of one to three was chosen.

7.2.2.2.4 *DpnI* digestion

After each performed PCR, *DpnI* (New England BioLabs® Inc., Ipswich, USA) digest of the template PCR needs to be performed. A volume of 0.5 µL enzyme solution was added to 10 µL of sample volume. The digestion was performed at 37°C for 2 h, followed by a heat inactivation of the enzyme at 80°C for 20 min.

7.2.2.3 Quantification of DNA

7.2.2.3.1 NanoDrop

Determination of DNA concentrations was achieved by usage of the UV-Vis photometer NanoDrop. The device measures absorbance at a wavelength of λ=260 nm. Additionally, other important wavelengths are measured to assure the purity of the DNA sample.

7.2.2.3.2 Agarose gel electrophoresis

For separation of DNA fragments or plasmids by size, agarose gel electrophoresis was applied. The agarose gel was prepared with TAE buffer, which was heated until boiling in the microwave oven to solve the appropriate amount of agarose. 5 µL of Roti®-GelStain (Carl Roth) were added per 100 mL agarose solution for later visualization of DNA. The gel was casted and left for cooling. Samples were prepared by mixing with 6x loading dye (1:6). After applying 6 µL of each sample and 5 µL DNA ladder (1kbp DNA ladder, Carl Roth), the gel was run at 110 V for 25 min. The final result was investigated after illumination on a UV table.

7.2.3 Biochemical Methods

7.2.3.1 Protein purification

7.2.3.1.1 Hand columns

In general, approximately the same protocol was used for all proteins if hand columns were used for purification (CYP102A1, CYP11A1, Pdx, PdR, CPR, BMR, human CYP17A1 and HyPer-3). When the cell pellet was stored at -20°C, it was thawed slowly on ice and washed two times with equilibration buffer. After cell lyses in equilibration buffer, by sonication, the crude cell lysate was separated by centrifugation at 10000*g* for 1 h at 4°C. After filtering the supernatant with a 0.45 µm filter, the His-tagged enzyme was purified on a Ni-NTA hand column (Roti®garose-His/Ni Beads, Carl Roth GmbH & Co. KG, Germany). First, the column was washed

and preequilibrated with five column volumes (5 CV) of equilibration buffer, followed by loading of the filtered supernatant. After washing the column with 2 CV of wash buffer, the protein was eluted. Elution was obtained with 2 CV of elution buffer. Only eluate with strong color (for P450: red-brownish, for Adx & Pdx dark brown and for AdR, PdR, CPR, BMR and Hyper-3 yellow-greenish) was collected. Afterwards, the eluted protein sample was desalted and stored in storage buffer or used immediately.

7.2.3.1.2 CYP11A1

In addition to using hand columns for the purification of CYP11A1, purification experiments using the ion exchange technique with a column packed with SP-Sepharose were performed. For purification, the ÄKTApurifier was used. After equilibrating the whole system with the used buffer, the column was washed with 5 CV equilibration buffer. Afterwards the protein was loaded onto the column and elution was accomplished by a linear gradient over 5 CV changing gradually from the equilibration buffer to the elution buffer.

7.2.3.1.3 Adx

For the purification of Adx, anion exchange chromatography using a column packed with DEAE-Sepharose were performed. For purification, the ÄKTApurifier was used. After equilibrating the whole system with the used buffer, the column was washed with 5 CV equilibration buffer. Afterwards the protein was loaded onto the column and elution was accomplished by a linear gradient over 10 CV changing gradually from the equilibration buffer to the elution buffer.

Additionally gelfiltration was accomplished using Superdex G200 material. For this approach, also the system was equilibrated with equilibration buffer and afterwards, the column was washed with equilibration buffer. The protein was loaded on the column and the protein eluted with the same buffer.

Furthermore, hydrophobic interaction chromatography with a column packer with Phenylsepharose was performed. The same method as for the affinity chromatography was applied.

7.2.3.1.4 AdR

For AdR anion exchange chromatography was performed using a column packed with Source Q material. For purification, the ÄKTApurifier was used. After washing the whole system with the used buffer, the column was also equilibrated with 5 CV equilibration buffer. After loading the protein solution on the column, elution was accomplished by a linear gradient over 10 CV changing gradually from the equilibration buffer to the elution buffer.

Additionally, affinity chromatography was performed using 2-5 ADP-Sepharose and anion exchange chromatography using a column packed with DEAE-Sepharose. Here, the same procedure was used as described for anion exchange chromatography.

7.2.3.2 Desalting

All obtained elution fraction from protein purification were desalted using PD-10 columns (GE Healthcare, Freiburg, Germany). Desalting was performed as suggested from the

manufacturer. Which buffer was used for elution from the column was different for all proteins. For most, the storage buffer was used.

7.2.3.3 Protein quantification

7.2.3.3.1 BCA assay

Protein concentrations of samples was determined using the Pierce™ BCA Assay Kit (Thermo Fisher Scientific, Waltham, USA). The assay was performed according to the manufacturer's instructions for the 96-well plate format. After incubation for at least 30 min at 37°C, the absorbance of all samples at λ=562 nm was determined. BSA standard solutions were always prepared fresh with the same buffer, the samples contained.

7.2.3.3.2 CO assay for P450 enzymes

The final P450 concentration obtained was determined using the CO assay as described by Omura et al. 1964.[32] The 2 mL sample was mixed with 2 µM safranin T as a redox indicator (Zitat: F.P. Guengerich et al., Measurement of cytochrome P450 and NADPH-cytochrome P450

reductase. Nat Protoc, 2009, **4**(9), followed by addition of one spatula tip of sodium dithionite. By slowly inverting the tube, the solution was mixed and 1 mL each was transferred in a new cuvette. In one cuvette approximately 1 bubble min^{-1} CO-gas is applied for 1 min. The other sample is measured as blank. Then, a spectrum is recorded between λ=400 nm and λ=500 nm (Table 49). With this difference spectrum, the concentration of Cytochrome P450 enzymes can be determined (Equation 2).

$$c = \frac{A_{450\ nm} - A_{490\ nm}}{1\ cm \cdot 91\ mM^{-1}cm^{-1}}$$

Equation 2: Equation for calculating concentration of correctly folded Cytochrome P450 enzyme, from values determined by the recorded difference spectrum.

Table 49: Settings used for the recording of CO difference spectra using the Jasco device.

Parameter	**Setting**
Wavelength	500 - 400 nm
Photometric mode	Abs
Response	medium
UV/Vis bandwidth	0.2 nm
Scan speed	200 nm/min
Delta interval	1 nm
Scan mode	Continuous
Number of cycles	1
Vertical scale	Auto 1 - 0

7.2.3.4 Substrate binding spectra of Cytochrome P450 enzymes

With the same general settings (Table 49), as described for the CO difference spectrum, substrate binding spectra can be recorded between 500 nm and 350 nm. Therefore, a Cytochrome P450 sample is measured as blank sample. After addition of substrate solution (10 mM cholesterol in 45% aqueous 2-hydroxypropyl-β-cyclodextrin diluted to final concentration of 0.2 mM for CYP11A1; 10 mM progesterone in pure ethanol, diluted to a final concentration of 0.2 mM for CYP17A1) the difference spectra were recorded, resembling the substrate binding spectra.

7.2.3.5 Investigation of the sensitivity of HyPer-3 towards hydrogen peroxide

With 5 µM of the purified HyPer-3 protein in storage buffer, were incubated with 20 mM, 10 mM, 5 mM, 2.5 mM, 1 mM and without hydrogen peroxide. The absorption was monitored at 420 nm and 500 nm over 10 min.

7.2.3.6 Ampliflu™ Red Assay

For the parallel detection of hydrogen peroxide production and NADPH consumption, the Ampliflu™ Red assay was performed in a microtiter plate-based format. In general, 100 µL sample were mixed with 100 µL of the Ampliflu™ Red assay solution. For all measurements standards were incubated with different hydrogen peroxide concentrations (100 µM, 50 µM, 25 µM, 10 µM, 5 µM, 2.5 µM and 1 µM), enabling a correct calculation of the exact hydrogen peroxide concentrations in the investigated samples. Absorption measurement was accomplished at λ=560 nm for resorufin and λ=340 nm for NADPH detection. If fluorescence measurement was performed for excitation $\lambda_{excitation}$=550 nm and for emission $\lambda_{emission}$=590 nm were used. If an enzymatic reaction was investigated, a 1.2 µM stock solution of Cytochrome P450 BM3 wild-type and variants was added and diluted in a ration of 1:4 in the final reaction. All samples were measured in triplicates.

7.2.3.6.1 Investigating the optimal enzyme concentration for the Ampliflu™ Red Assay

In order to investigate the optimal enzyme concentration used for the Ampliflu™ Red assay, purified 50 µL Cytochrome P450 BM3 solutions containing 5 µM, 2.5 µM, 1.2 µM and 0.6 µM enzyme were incubated with 50 µM NADPH and 100 µL of the Ampliflu™ Red solution. The reaction was monitored by absorption measurements over a reaction time of 8 min. All samples were measured in triplicates.

7.2.3.6.2 Investigation of the hydrogen peroxide formation and NADPH depletion of Cytochrome P450 BM3 wild-type and 5 mutants

For the investigation of the hydrogen peroxide formation and NADPH depletion in the reaction of Cytochrome P450 BM3 wild-type and 5 different mutants, 50 µL purified enzyme (1.2 µM in buffer A), 10 µL substrate solution (1 mM in ethanol: lauric acid, oleic acid, palmitic acid, pentadecanoic acid and 1-octanol or for measurements without substrate only ethanol), 10 µL NADPH (1 mM stock in buffer A) and 30 µL buffer A were incubated with 100 µL of the Ampliflu™ Red Assay solution. Both, the NADPH and resorufin concentration were detected

by absorption measurement in parallel over 10 min reaction time. As negative controls, the enzyme solutions were incubated without addition of NADPH or substrate with Ampliflu™ Red Assay solution. Additionally, all substrates solutions were incubated separately as well as NADPH and substrate with NADPH in combination, without enzyme present were incubated with the Ampliflu™ Red Assay solution. All samples were measured in triplicates.

7.2.3.6.3 Control reactions to investigate the Ampliflu™ Red Assay further

With Cytochrome P450 BM3 wild-type several control reactions were performed. The enzyme (1.2 µM stock, 1:4 diluted in final reaction; in 50 mM sodium phosphate buffer pH 7.4) was incubated with and without NADPH. Additionally, for one sample no HRP was added and one sample contained NADPH and 20 U mL^{-1} Catalase. A last sample contained NADPH and 2 U mL^{-1} superoxide dismutase (SOD). The concentrations of NADPH and resorufin were determined by absorption measurement over a reaction time of 30 min. All samples were measured in triplicates.

7.2.3.6.4 Investigating the uncoupling of CPR from *C. apicola*

In order to investigate the uncoupling of CPR from *C. apicola*, the protein was incubated with different NADPH concentrations. Therefore, 0.2 µM purified CPR in buffer A, were incubated with 22 µM, 12 µM and 6 µM NADPH (final concentration). 2 U mL^{-1} of SOD were added. For one sample additionally, 20 U mL^{-1} catalase were added. NADPH and resorufin concentrations were determined by absorption measurement over a reaction time of 30 min. All samples were measured in triplicates.

7.2.3.7 Biocatalysis

7.2.3.7.1 *In vitro* biocatalysis with the bovine CYP11A1

Biocatalysis with the purified bovine CYP11A1 enzyme was in general performed in 20mM HEPES buffer with a pH of 7.3 containing KCl and DTT. Each sample had a final volume of 1 mL containing 1.7mg DOPC and 1.75mM cholesterol. For biocatalysis, 0.4 µM CYP11A1 was used, Pdx was used in a concentration of 5 µM, Adx 0.5 µM, PdR 0.4 µM, BMR 5 µM and 1.5 mM NAD(P)H. For NAD(P)H recycling 0.1 mM glucose and GDH 105 was added in an unknown concentration to some samples. All samples were incubated at 37°C for 16 h and 300 rpm shaking velocity, if not indicated otherwise (t_0=sample immediately extracted after 0 h)

Table 50: Overview of the sample composition from the first biocatalytic approach. The concentration of the Glucose-Dehydrogenase (GDH 105 from Codexis) was unknown.

sample	CYP11A1	Pdx	Adx	PdR	CPR	Glucose	GDH	NADH	NADPH
1	+	+	-	+	-	+	+	+	-
2	+	-	-	-	+	+	+	-	+
3	+	-	+	+	-	+	+	+	-
4	+	-	-	-	-	+	+	+	-
5	-	+	-	+	-	+	+	+	-

6	-	-	-	-	+	+	+	-	+
7	-	-	+	+	-	+	+	+	-
8	+	+	-	+	-	-	-	+	-
9 (t_0)	+	-	-	-	+	-	-	-	+

Table 51: Overview of the sample compositions from the second biocatalysis approach.

sample	P450	BMR	Pdx	PdR	NADPH	NADH	timepoint	temperature
1	+	+	-	-	+	-	t_0	
2	+	+	-	-	+	-	10 min	20
3	+	+	-	-	+	-	1h	20
4	+	+	-	-	+	-	o.n.	20
5	+	+	-	-	-	-	o.n.	20
6	+	+	-	-	+	-	10 min	30
7	+	+	-	-	+	-	1h	30
8	+	+	-	-	+	-	o.n.	30
9	+	+	-	-	-	-	o.n.	30
10	+	-	+	+	-	+	t_0	
11	+	-	+	+	-	+	10 min	20
12	+	-	+	+	-	+	1h	20
13	+	-	+	+	-	+	o.n.	20
14	+	-	+	+	-	-	o.n.	20
15	+	-	+	+	-	+	10 min	30
16	+	-	+	+	-	+	1h	30
17	+	-	+	+	-	+	o.n.	30
18	+	-	+	+	-	-	o.n.	30
19	+	-	-	-	+	+	t_0	
20	+	-	-	-	+	+	o.n.	20
21	+	-	-	-	+	+	o.n.	30
22	-	+	-	-	+	+	t_0	
23	-	+	-	-	+	+	o.n.	20
24	-	+	-	-	+	+	o.n.	30
25	-	-	+	+	+	+	t_0	
26	-	-	+	+	+	+	o.n.	20
27	-	-	+	+	+	+	o.n.	30
28	+	+	+	+	+	+	o.n.	30
29	+	+	+	+	+	+	o.n.	30

7.2.3.7.2 Whole cell biocatalysis with the bovine CYP11A1

With *E. coli* TOP10 (DE3) cells harboring the pBar_Triple plasmid, coding for all three proteins of the CYP11A1 system, whole cell biocatalysis according to Makeeva *et al*. was performed.[89] A volume of 50 mL TB-Amp medium was inoculated with 1% overnight culture. After incubation at 37°C and 160 rpm shaking velocity for four hours, 1 mM IPTG, 0.5 mM δ-Ala and 50 µL of each microelement solution were added. The incubation temperature was lowered to 29°C and after another two hours of cell growth, 0.5 mM cholesterol (final concentration) were added. At 24°C and 180 rpm shaking velocity, whole cell biocatalysis was performed for 74 h. In the end 10 mL of the cultivation were extracted and analyzed by HPLC.

7.2.3.7.3 Human CYP17A1

In the *in vitro* biocatalysis approach, *E. coli* JM109 (DE3) cell lysate containing human CYP17A1 was used. For each sample 100 µM progesterone were incubated with 4 µM CYP17A1, 0.5 µM PdR & 2.5 µM Pdx or 2.5 µM CPR and 100 µM NAD(P)H. For the Pdx/PdR system NADH was used and for CPR NADPH. All samples were incubated at 30°C at 600 rpm shaking velocity for 24 h, if not stated otherwise.

Table 52: Sample composition for the investigation of the redox partner system for human CYP17A1.

sample	CYP17A1	Pdx/PdR	CPR	NADH	NADPH	substrate
1 (t_0)	+	+	+	+	+	+
2	+	+	-	+	-	+
3	+	+	-	-	-	+
4	+	-	+	-	+	+
5	+	-	+	-	-	+
6	+	-	-	+	+	+
7	-	+	+	+	+	+

Table 53: Sample composition for the biocatalytic comparison between CYP17A1 wild-type (wt) and T306A (T) (++ = double the original concentration).

sample	CYP17A1	Pdx/PdR	NADH	substrate
1 t_0	+ wt	+	+	+
2	-	+	+	+
3	+ wt	+	+	+
4	+ wt	+	++	+
5	+ wt	+	-	+
6	+ wt	-	+	+
7	+ wt	+	+	-
8	+ T306A	+	+	+
9	+ T306A	+	++	+
10	+ T306A	-	+	+
11	+ T306A	+	-	+

With CYP17A1 wild-type and the alanine variants, biocatalysis using crude lysate was performed using 0.5 µM PdR, 2.5 µM Pdx or 2.5 µM CPR and 25 µM NAD(P)H for the transformation of 100 µM progesterone. All samples were incubated at 30°C at 600 rpm shaking velocity for 24 h. For each variant, one sample contained CPR, one sample Pdx/PdR. As negative controls for each variant one sample contained no redox partner system, one sample was incubated without substrate present.

7.2.3.7.4 Bovine CYP17A1

7.2.3.7.4.1 Whole cell biocatalysis

Whole cell biocatalysis with the bovine CYP17A1 was performed according to Shkumatov *et al*. with slight modifications.[197] The bovine CYP17A1 was expressed in *S. cerevisiae*, harboring the YEp5117α plasmid. A volume of 20 mL YPD medium was inoculated with a single colony picked from an agar plate and grown over night at 30°C and 180 rpm. For the cultivation, 39.5 mL YPD in a 300 mL Erlenmeyer flask were inoculated with 5 mL overnight culture and grown at 30°C and 180 rpm. After 24 h, 5 mL D-galactose (20% Stock in ddH_2O) and 500 µL progesterone (10 mM Stock in ethanol) were added. After another 24 h of growth, cultivation was determined.

For the investigation of the time dependent conversion, at different timepoints (4, 6, 8, 10, 12, 14, 16, 24 h) 2 mL samples were taken, extracted and analyzed by HPLC. For whole cell biocatalysis with the alanine variants, only 2 samples were taken for each flask (0 h and 24 h).

7.2.3.7.4.2 Preparative whole cell biocatalysis with bovine CYP17A1 V483A

The afore mentioned whole cell biocatalysis approach was scaled up. In a total volume of 1 L split in two times 500 mL YPD in two 5 L Erlenmeyer flasks, 100 mg progesterone were converted (314.14 µM). The cultivation time was expanded to 72 h. At the end, 2 mL samples were taken for the usual HPLC analysis. The rest of the supernatant was stored at -20°C until further usage.

7.2.3.8 Investigation of the stability of human CYP17A1 wild-type and 12 alanine variants

In order to investigate, whether the stability of the human CYP17A1 wild-type enzyme and the different alanine variants showed higher percentage of correct folded enzyme in other buffers, the cell pellets were resuspended in different buffers and lysed. As buffers, sodium phosphate buffer (50 mM sodium phosphate buffer pH 7.4, 20 % (w/v) glycerol; buffer **1**), a Tris-HCl buffer (50 mM TRIS-HCl pH 8, 1 mM EDTA, 20% (w/v) glycerol; buffer **2**), the buffer best suitable for IMAC purification of CYP11A1 (50 mM potassium phosphate pH7.4, 20% (w/v) glycerol, 1.5% sodium cholate, 500 mM sodium acetate, 1.5% Tween-20, 0.1 mM EDTA, 0.1 mM DTT, 0.1 mM PMSF from Mosa *et al*. 2014[192], buffer **3**), another TRIS-HCl buffer, containing EDTA and sorbitol (50mM TRIS pH 8, 1 mM EDTA, 0.6 M sorbitol from Dhir et al. 2007[199]; buffer **4**), a potassium phosphate buffer (100mM potassium phosphate pH7.4, 50mM NaCl from Khatri *et al*. 2014[198]; buffer **5**) and a MOPS buffer (50mM MOPS pH7.4 from Barnes *et al*. 1991[200]; buffer **6**) were used.

Afterwards, CO difference spectra were recorded in order to investigate whether more correct folded protein was obtained. Additionally, substrate binding was investigated with progesterone as substrate in buffer 2. Furthermore, the melting temperatures were investigated using the NanoTemper device with the standard settings and a temperature range from 20°C to 90°C.

7.2.3.9 Dual screening

7.2.3.9.1 Investigating the substrate to NADPH ratio

To investigate the optimal substrate (11-(4-trifluoromethylcoumarin-7-yloxy)undecanoic acid) to NADPH ratio in the dual screening approach, purified Cytochrome P450 BM3 wild-type, A74G/F87V and F87Y were used (1.2 µM stock, diluted 1:4 in final reaction). And different substrate to NADPH ratios used, with constant substrate concentration (10 µM). NADPH consumption was monitored at λ=340 nm, product formation at $\lambda_{excitation}$=420 nm and $\lambda_{emission}$=500 nm (gain: 100%) and hydrogen peroxide formation at $\lambda_{excitation}$=550 nm and $\lambda_{emission}$=590 nm (gain: 50%). The reaction was performed in 50 mM sodium phosphate buffer adjusted to pH7.4. All samples were measured in triplicates.

7.2.3.9.2 Investigating the product formation and hydrogen peroxide formation of five Cytochrome P450 BM3 variants

For the investigation of the uncoupling and product formation in parallel of the five Cytochrome P450 BM3 variants (R47L, Y51F, A82L, T268A and I401P), 100 µM substrate (11-(4-trifluoromethylcoumarin-7-yloxy)undecanoic acid) and 25 µM NADPH were used. The enzyme concentration was not determined, but the OD_{600} of the final culture determined. Afterwards, the amount of cells in the pellet were calculated and the concentration set to 1 cell per 4 pL. With the obtained cell lysate (in 50 mM sodium phosphate buffer, pH7.4) biocatalysis was performed. Product formation was monitored at $\lambda_{excitation}$=420 nm and $\lambda_{emission}$=500 nm (gain: 100%) and hydrogen peroxide formation at $\lambda_{excitation}$=550 nm and $\lambda_{emission}$=590 nm (gain: 50%). The reaction was performed in 50 mM sodium phosphate buffer adjusted to pH7.4. All samples were measured in triplicates.

7.2.3.10 SDS-PAGE

Protein samples were analyzed under denaturizing conditions by SDS-PAGE analysis. The samples were prepared by mixing 20 µL sample with 10 µL loading buffer. The mixture was incubated at 95°C for 10 min and afterwards centrifuged briefly for 15 s at 10000*g*. All samples and the protein marker were loaded on the before poured gels and run with 25 mA per gel for approximately 45 min or until the running front reached the bottom of the gel. Afterwards the gels were stained by incubation in staining solution overnight (Coomassie staining). The next day the background of the gels was destained with destaining solution, which was exchanged at least twice. The gels were incubated in the destaining solution, until clear protein bands and only little to no background color could be observed.

7.2.4 Analytics

7.2.4.1 CYP11A1

7.2.4.1.1 Sample preparation for GC-MS analysis

The samples were prepared following the method described by Saraiva et al. in 2011 with slight modifications.[233] After extracting the samples three times with n-hexane (same volume as sample) and evaporation of the solvent under a nitrogen stream, the hydroxyl groups of e steroids were derivatized using a mixture of MSTFA (N-methyl-N-(trimethylsilyl)-trifluoroacetamide), DTT (1,4-dithioerythritol) and TMIS (trimethyliodosilane). Therefore, a volume of 50 µL of the derivatization mixture MSTFA:DTE:TMIS (5000:10:10) was added and the sample was incubated at 60°C for one hour.

7.2.4.1.2 GC-MS analysis of cholesterol and pregnenolone

The derivatized compounds were analyzed on a BPX5 column (length: 25 m, diameter: 0.25 µm). As temperature program, a method at temperatures between 240°C and 300°C was used (Table 54) using the standard settings of the GC-MS (

Table 55).

Table 54: Temperature program used for the analysis of cholesterol and pregnenolone.

Temperature [°C]	**Time**
240	Hold 3 min
Increase with 10°C min^{-1}	6 min
300	Hold 10 min

Table 55: General settings for GC-MS analysis of cholesterol and pregnenolone.

parameter	**setting**
pressure	101.3 kPa
Total flow	13.4 mL min^{-1}
Column flow	0.95 mL min^{-1}
Linear velocity	41.8 cm s^{-1}
Purch flow	3 mL min^{-1}
Split	10
Injector temperature	250°C
Ion source	240°C
Interface temperature	310°C

7.2.4.1.3 Sample preparation of whole cell biocatalysis with the CYP11A1 system

The 10 mL samples were extracted twice, once with 20 mL and once with 10 mL ethyl acetate. The organic solvent was separated and evaporated using a rotary evaporator. The remaining solids were resuspended in 1 mL 50% aqueous acetonitrile. After centrifugation at 5000 x g for 30 min, the supernatant of the sample was analyzed by HPLC.

7.2.4.1.4 HPLC analysis of whole cell biocatalysis samples

For HPLC analysis of the samples obtained from whole cell biocatalysis, an isocratic method with 52% acetonitrile, 48% water and 0.01% acetic acid were used as mobile phase, at a flow rate of 1 mL min^{-1}. As column, the LiChrospher®100 RP-18 (5 µm), a reversed phase C18 column was used.

7.2.4.2 CYP17A1

7.2.4.2.1 Extraction of Steroids

All 2 mL samples were extracted twice with 2 mL ethyl acetate. The solvent was evaporated at room temperature overnight and the sample was resolved in 200 µL methanol.

7.2.4.2.2 HPLC analysis of Steroids

A volume of 10 µL of the steroid samples was analyzed with a Kromasil C18 column at room temperature under isocratic conditions with acetonitrile:water (60:40) as solvent in a flow rate of 1 mL min^{-1}. Or on a LiChrospher® 100 RP-18e (5 µm) column, under the same conditions but using acetonitrile:water (40:60) as solvent in a flowrate of 0.8 mL min^{-1} for better separation of all compounds.

7.2.4.2.3 Extraction of the preparative biocatalysis

The supernatant of the preparative biocatalysis was extracted trice with 330 mL ethyl acetate. Using a rotary evaporator, all solvent was removed, and the residual oily, brown fluid was diluted with 500 µL DMSO and 5 mL methanol.

7.2.4.2.4 Preparative HPLC separation

For preparative HPLC, 2 mL sample volume were applied per run. As column, a 250x25 mm LiChrospher® 100 RP-18e (5 µm) column with acetonitrile:water (40:60) as solvent in a flowrate of 30 mL min^{-1} were used. The different peak fractions were collected manually into different flasks. The acetonitrile-water mixture was evaporated using a liquid nitrogen evaporator. Afterwards, the residual water was removed in a lyophilizer overnight.

7.2.4.3 NMR

NMR analysis was performed with a Bruker Avance II 300 equipped with 5 mm PABBO BB-1H/D T-GRD Z104275/0398 probehead. Tetramethylsilane was used for the calibration of all measurements. As solvent $CDCl_3$ was used to solve the samples. The ^{1}H NMR was recorded at 200 MHz and the ^{13}C NMR at 75 MHz.

7.2.5 Chemical methods

7.2.5.1 Ampliflu™ Red Assay

7.2.5.1.1 Comparison between the spectra of AmplifluTM Red, NADPH and ABTS

The spectra of Ampliflu™ Red, resorufin, ABTS, $ABTS^{\cdot}$ and NADPH in a range of wavelength from 275 nm to 700 nm was recorded in buffer A. Final concentrations of Ampliflu™ Red and ABTS were 10 µM and for NADPH a final concentration of 50 µM was used.

7.2.5.1.2 Hydrogen peroxide detection range of the Ampliflu™ Red Assay

For the investigation of the detection range of the Ampliflu™ Red Assay, 100 µL of buffer A containing different concentrations of hydrogen peroxide (100 µM, 50 µM, 25 µM, 10 µM, 5 µM, 2.5 µM, 1 µM, 0.5 µM, 250 nM, 100 nM, 50 nM, 25 nM and 10 nM) were incubated with 100 µL of the standard assay solution. The samples were investigated by both, absorption and fluorescence measurement. All samples were measured in triplicates.

7.2.5.1.3 pH range of the Ampliflu™ Red Assay

For the investigation of the pH range of the Ampliflu™ Red Assay the standard hydrogen peroxide solutions were produced in buffer A adjusted to pH6.0, 6.5, 7.0, 7.4, 8.0, 8.5 and 9.0. 100 µL of these samples were incubated with 100 µL of the Ampliflu™ Red assay solution adjusted to the same pH values. Absorption was monitored over 30 min. All samples were measured in triplicates.

7.2.5.1.4 Signal stability of the Ampliflu™ Red Assay

The signal stability of the Ampliflu™ Red Assay was investigated by monitoring the created absorption of resorufin upon incubation with the different standard hydrogen peroxide solution over 20 min of time. In an additional experiment, 50 µL of crude lysate of E. coli TOP10 (DE3) cells (5 mL buffer per 1 g wet cell mass) were incubated with 100 µL Ampliflu™ Red solution and with 50 µL of the standard hydrogen peroxide solutions with the double concentration, to yield the same final concentrations. These samples were incubated for 3 h. All samples were measured in triplicates.

7.2.5.2 Preparation of DOPC vesicles

40 mg DOPC were dissolved in 3 mL chloroform, afterwards 300 µL methanol were added. This mixture was poured into a round bottom flask and carefully overlayed with 20 mL buffer. Using a rotary evaporator with an oil bath temperature of 40°C, the solvent was slowely evaporated leading to the spontaneous formation of vesicles, visible through a change of color.

7.2.5.3 Dual screening approach

7.2.5.3.1 Synthesis of 11-(4-trifluoromethylcumarin-7-yloxy)undecanoate

According to Neufeld et al. 2014, undecanoic acid was chemically linked to the 7,4-HFC derivate 7-hydroxy-4-trifluoromethylcoumarin.[24]

First, 1.25 mmol 7-hydroxy-4-trifluoromethylcoumarin were incubated with 1.42 mmol anhydrous potassium carbonate (K_2CO_3) for 2 h at room temperature in 10 mL DMF. After addition of 1.32 mmol methyl 11-bromo undecanoate, the reaction mixture was heated in an oil bath to 90°C and incubated for 15 h. Next, the mixture was slowly cooled to room temperature under constant stirring. To the cooled reaction mixture, 100 mL ethyl acetate were added. With 30 mL of a saturated sodium bicarbonate solution, the reaction mixture was washed twice, followed by two washing steps with 30 mL of brine. After drying the organic phase with magnesium sulfate, the organic solvent was evaporated to complete dryness.

The residual powder was resuspended in 10 mL THF and cooled in an ice bath. Drop-wise 10 mL of a 0.62 M potassium hydroxide solution was added. After incubating the reaction mixture for 2 h on ice, the ice bath was removed and the flask was kept at room temperature for another 2 h. Full conversion was confirmed by TLC with different standard and a sample of the reaction mixture. A mixture of petrol ether:ethyl acetate in a ratio of 7:3 was used as mobile phase.

The reaction was stopped by addition of 40 mL ice-cold 1 M HCl and the product extracted four times with 30 mL dichloromethane. The pooled organic phase was dried with magnesium sulfate and the residual volume reduce to approximately 2 mL. The final product was purified on a silica column using petrol ether:ethyl acetate in a ratio of 7:3 as mobile phase. 10 mL fractions were collected and analyzed by TLC. The fractions containing the product were combined and the organic solvent was evaporated using a rotary evaporator.

10 mg of the product were analyzed by NMR, confirming that the correct product was obtained in high purity.

7.2.5.3.2 Investigating the detection range of HDCF-DA for hydrogen peroxide

In order to investigation the detection limit of HDCF-DA, the probe was solved in 50 mM sodium phosphate buffer adjusted to pH 7.4. A final concentration of 100 µM of HDCF-DA was imcubated with 100 µM, 50 µM, 25 µM, 12.5 µM, 5 µM, 2.5 µM, 1.25 µM and 0.5 µM hydrogen peroxide (final concentrations). Fluorescence was measured with an excitation wahelength of $\lambda_{excitation}$=490 nm and an emission wavelength of $\lambda_{emission}$=520 nm (gain: 50%) in 96-well plates

7.2.5.3.3 Signal stability of resorufin and 7-Hydroxy-4-trifluoromethylcoumarin in HFE-7500

In order to determine in which phase the two probes reside after incubation, 50 mM sodium phosphate buffers, adjusted to pH 6.0, 6.5, 7.0, 7.4, 8, 8.5 and 9.0 were used. 50 µM of each probe were separately solved in the different buffers (resorufin from a 10 mM stock in DMSO). 500 µL of the HFE-7500 oil were overlaid with 500 µL of the different buffers, containing the probes. Next, the vails containing the oil and buffer were incubated at 25°C and shaken at 1200 rpm. At timepoint 0 h, 2 h, 4 h, 8 h and 24 h, 20 µL samples were taken from the buffer. The 20 µL samples were diluted with 80 µL buffer and analyzed with an excitation wavelength of $\lambda_{excitation}$=560 nm and an emission of wavelength $\lambda_{emission}$=590 nm (gain: 84%) for resorufin, and an excitation wavelength of $\lambda_{excitation}$=400 nm and an emission wavelength of $\lambda_{emission}$=500 nm (gain: 100%) for 7-Hydroxy-4-trifluoromethylcoumarin in 96-well plates.

7.2.6 Bioinformatic methods

7.2.6.1 Used software

Table 56: List of used important software.

Software	Purpose	Developer
ACD/NMR Processor Academic Edition	Evaluation of NMR-spectra	Advanced Chemistry Development, Inc.
Chem Draw 12.0	Creation of chemical molecule structures and reaction schemes	Cambridge Soft
Geneious	Construction of primers and virtual cloning, DNA sequence analysis and management	Biomatters, Ltd.
i-control™	Software to control the Tecan device	Tecan Trading AG
PyMol	Protein structure visualization	Schrödinger, LLC.
YASARA[205]	Generation of homology models and docking experiments	E. Krieger

7.2.6.2 Homology Modeling with YASARA

The homology model of bovine CYP17A1 was constructed with the YASARA software.[205] The software, automatically starts by performing a BLAST search in order to find already crystallized sequences, that show high homologies to the submitted template protein. With each of these found protein crystals and alignment is performed, which leads in the end to the creation of several possible homology models. In addition, a chimera model, consisting of the best evaluated parts of all created homology models is created. After a refinement of the model with the lowest energy, the YASARA macro md_refine was run, which performs a refinement of the structure. This final construct was evaluated with MolProbity.[206]

8 Literature

[1] N. J. Turner, *Nat. Chem. Biol.* **2009**, *5*, 567–573.

[2] U. T. Bornscheuer, G. W. Huisman, R. J. Kazlauskas, S. Lutz, J. C. Moore, K. Robins, *Nature* **2012**, *485*, 185–194.

[3] L. Rosenthaler, *Biochem. Z.* **1908**, *14*, 238–253.

[4] L. Poppe, B. G. Vértessy, *ChemBioChem* **2018**, *19*, 284–287.

[5] A. Schmid, J. S. Dordick, B. Hauer, A. Kiener, M. Wubbolts, B. Witholt, *Nature* **2001**, *409*, 258–68.

[6] J. M. Woodley, *Trends Biotechnol.* **2008**, *26*, 321–327.

[7] U. T. Bornscheuer, M. Pohl, *Biocatal. Biotransformation* **2001**, *5*, 137–143.

[8] S. L. Flitsch, S. J. Aitken, C. S. Y. Chow, G. Grogan, A. Staines, *Bioorg. Chem.* **1999**, *27*, 81–90.

[9] L. Setti, G. Lanzarini, P. G. Pifferi, *Fuel Process. Technol.* **1997**, *52*, 145–153.

[10] S. G. Burton, D. A. Cowan, J. M. Woodley, *Nat. Biotechnol.* **2002**, *20*, 37–45.

[11] J. Wachtmeister, D. Rother, *Curr. Opin. Biotechnol.* **2016**, *42*, 169–177.

[12] S. Lutz, U. T. Bornscheuer, *Protein Engineering Handbook*, WILEY-VCH Verlag GmbH, **2012**.

[13] K. Balke, A. Beier, U. T. Bornscheuer, *Biotechnol. Adv.* **2018**, *36*, 247–263.

[14] L. G. Otten, W. J. Quax, *Biomol. Eng.* **2005**, *22*, 1–9.

[15] M. D. Lane, B. Seelig, *Curr. Opin. Chem. Biol.* **2014**, *22*, 129–136.

[16] H. Leemhuis, R. M. Kelly, L. Dijkhuizen, *IUBMB Life* **2009**, *61*, 222–228.

[17] A. E. Donnelly, G. S. Murphy, K. M. Digianantonio, M. H. Hecht, *Nat. Chem. Biol.* **2018**, *14*, 253–255.

[18] A. J. Ruff, A. Dennig, G. Wirtz, M. Blanusa, U. Schwaneberg, *ACS Catal.* **2012**, *2*, 2724–2728.

[19] J. Jose, *Appl. Microbiol. Biotechnol.* **2006**, *69*, 607–614.

[20] R. Ostafe, R. Prodanovic, W. L. Ung, D. A. Weitz, R. Fischer, R. Ostafe, R. Prodanovic, W. L. Ung, D. A. Weitz, *Biomicrofluidics* **2014**, *8*, 1–4.

[21] D. J. Sukovich, S. C. Kim, N. Ahmed, A. R. Abate, *Analyst* **2017**, *142*, 4618–4622.

[22] D. S. Tawfik, A. D. Griffiths, *Nat. Biotechnol.* **1998**, *16*, 652–656.

[23] U. Schwaneberg, C. Schmidt-Dannert, J. Schmitt, R. D. Schmid, *Anal. Biochem.* **1999**, *269*, 359–366.

[24] K. Neufeld, S. M. Zu Berstenhorst, J. Pietruszka, *Anal. Biochem.* **2014**, *456*, 70–81.

[25] C. Schmidt-Dannert, F. H. Arnold, *Tibtech* **1999**, *17*, 135–136.

[26] T. Omura, R. Sato, *J. Biol. Chem.* **1962**, *237*, 1375–1376.

[27] T. Omura, *Biochem. Biophys. Res. Commun.* **1999**, *266*, 690–698.

[28] S. T. Jung, R. Lauchli, F. H. Arnold, *Curr. Opin. Biotechnol.* **2011**, *22*, 809–817.

[29] M. K. Julsing, S. Cornelissen, B. Bühler, A. Schmid, *Curr. Opin. Chem. Biol.* **2008**, *12*, 177–186.

[30] D. Zehentgruber, F. Hannemann, S. Bleif, R. Bernhardt, S. Lütz, *ChemBioChem* **2010**, *11*, 713–721.
[31] D. Y. Cooper, R. W. Estabrook, O. Rosenthal, *J. Biol. Chem.* **1963**, *238*, 1320–1323.
[32] R. Omura, Tsuneo; Sato, *J. Biol. Chem.* **1964**, *239*, 2370–2378.
[33] "https://cyped.biocatnet.de/sequence-browser," **2018**.
[34] R. Bernhardt, *J. Biotechnol.* **2006**, *124*, 128–145.
[35] M. Sono, M. P. Roach, E. D. Coulter, J. H. Dawson, *Chem. Rev.* **1996**, *96*, 2841–2888.
[36] T. Hakki, R. Bernhardt, *J. Mol. Catal. B Enzym.* **2013**, *103*, 67–71.
[37] R. W. Estabrook, A. G. Hildebrandt, J. Baron, K. J. Netter, K. Leibman, *Biochem. Biophys. Res. Commun.* **1971**, *42*, 132–139.
[38] Y. Wang, Y. Li, B. Wang, *J. Phys. Chem. B* **2007**, *111*, 4251–60.
[39] H. Suzuki, K. Inabe, Y. Shirakawa, N. Umezawa, N. Kato, T. Higuchi, *Inorg. Chem.* **2017**, *56*, 4245–4248.
[40] R. C. Zangar, D. R. Davydov, S. Verma, *Toxicol. Appl. Pharmacol.* **2004**, *199*, 316–331.
[41] H. Yasui, S. Hayashi, H. Sakurai, *Drug Metab. Pharmacokinet.* **2005**, *20*, 1–13.
[42] I. Schlichting, J. Berendzen, K. Chu, A. M. Stock, S. A. Maves, D. E. Benson, R. M. Sweet, D. Ringe, G. A. Petsko, S. G. Sligar, *Science.* **2000**, *287*, 1615–1622.
[43] E. M. Isin, F. P. Guengerich, *Biochim. Biophys. Acta - Gen. Subj.* **2007**, *1770*, 314–329.
[44] C. H. Yun, K. H. Kim, M. W. Calcutt, F. P. Guengerich, *J. Biol. Chem.* **2005**, *280*, 12279–12291.
[45] F. P. Guengerich, J. W. W., *Biochemistry* **1997**, *36*, 14741–14750.
[46] A. Luthra, I. G. Denisov, S. G. Sligar, *Arch. Biochem. Biophys.* **2011**, *507*, 26–35.
[47] J. B. Schenkman, S. G. Sligar, D. L. Cinti, *Pharmacol. Ther.* **1981**, *12*, 43–71.
[48] C. W. Locuson, J. M. Hutzler, T. S. Tracy, *Drug Metab. Dispos.* **2007**, *35*, 614–622.
[49] D. Degregorio, S. J. Sadeghi, G. Di Nardo, G. Gilardi, S. P. Solinas, *J Biol Inorg Chem* **2011**, *16*, 109–116.
[50] M. J. Coon, *Annu. Rev. Pharmacol. Toxicol.* **2005**, *45*, 1–25.
[51] I. G. Denisov, T. M. Makris, S. G. Sligar, I. Schlichting, *Chem. Rev.* **2005**, *105*, 2253–2277.
[52] H. Joo, Z. Lin, F. H. Arnold, *Nature* **1999**, *399*, 670–673.
[53] P. C. Cirino, F. H. Arnold, *Adv. Synth. Catal.* **2002**, *344*, 932–937.
[54] I. G. Denisov, B. J. Baas, Y. V. Grinkova, S. . Sligar, *J. Biol. Chem.* **2007**, *282*, 7066–7076.
[55] P. J. Loida, S. G. Sligar, *Biochemistry* **1993**, *32*, 11530–11538.
[56] A. Perret, D. Pompon, *Biochemistry* **1998**, *37*, 11412–11424.
[57] O. Sibbesen, Z. Zhang, P. R. O. De Montellano, *Arch. Biochem. Biophys.* **1998**, *353*, 285–296.
[58] H. Yeom, S. G. Sligar, *Arch. Biochem. Biophys.* **1997**, *337*, 209–216.
[59] Y. Kimata, H. Shimada, T. Hirose, Y. Ishimura, *Biochem. Biophys. Res. Commun.* **1995**, *208*, 96–102.
[60] M. Fairhead, S. Giannini, E. M. J. Gillam, G. Gilardi, *J Biol Inorg Chem* **2005**, 842–853.
[61] V. Mishin, J. P. Gray, D. E. Heck, D. L. Laskin, J. D. Laskin, *Free Radic. Biol. Med.* **2010**, *48*,

1485–1491.

[62] H. Yeom, S. G. Sligar, A. J. Fulco, *Biochemistry* **1995**, *34*, 14733–14740.

[63] G. G. Guilbaul, D. N. Kramer, E. Hackley, *Anal. Chem.* **1967**, *39*, 271.

[64] D. D. Oprians, L. D. Gorskyb, M. J. Coon, *J. Biol. Chem.* **1982**, *258*, 8684–8691.

[65] I. Hanukoglu, R. Rapoport, L. Weiner, D. Sklan, *Arch. Biochem. Biophys.* **1993**, *305*, 489–498.

[66] J. J. De Voss, O. Sibbesen, Z. Zhang, P. R. Ortiz De Montellano, *J. Am. Chem. Soc.* **1997**, *119*, 5489–5498.

[67] D. S. Bilan, L. Pase, L. Joosen, A. Y. Gorokhovatsky, Y. G. Ermakova, T. W. J. Gadella, C. Grabher, C. Schultz, S. Lukyanov, V. V. Belousov, *ACS Chem. Biol.* **2013**, *8*, 535–542.

[68] S. G. Rhee, T.-S. Chang, W. Jeong, D. Kang, *Mol. Cells* **2010**, *29*, 539–549.

[69] F. Hannemann, A. Bichet, K. M. Ewen, R. Bernhardt, *Biochim. Biophys. Acta - Gen. Subj.* **2007**, *1770*, 330–344.

[70] I. Hanukoglu, *Adv. Mol. Cell Biol.* **1996**, *14*, 29–56.

[71] D. B. Hawkes, G. W. Adams, A. L. Burlingame, P. R. Ortiz de Montellano, J. J. De Voss, *J. Biol. Chem.* **2002**, *277*, 27725–27732.

[72] A. V. Puchkaev, P. R. Ortiz De Montellano, *Arch. Biochem. Biophys.* **2005**, *434*, 169–177.

[73] C. J. Jackson, D. C. Lamb, T. H. Marczylo, A. G. S. Warrilow, N. J. Manning, D. J. Lowe, D. E. Kelly, S. L. Kelly, *J. Biol. Chem.* **2002**, *277*, 46959–46965.

[74] E. L. Rylott, R. G. Jackson, J. Edwards, G. L. Womack, H. M. B. Seth-smith, D. A. Rathbone, S. E. Strand, N. C. Bruce, *Nat. Biotechnol.* **2006**, *24*, 216–219.

[75] G. A. Roberts, G. Grogan, A. Greter, S. L. Flitsch, N. J. Turner, *J. Bacteriol.* **2002**, *184*, 3898–3908.

[76] D. J. B. Hunter, G. A. Roberts, T. W. B. Ost, J. H. White, S. Mu, N. J. Turner, S. L. Flitsch, S. K. Chapman, *FEBS Lett.* **2005**, *579*, 2215–2220.

[77] J. Fulco, Y. Miura, *J. Biol. Chem.* **1974**, *249*, 1880–1888.

[78] H. Kizawas, D. Tomura, M. Odat, A. Fukamizu, T. Hoshino, O. Gotohll, T. Yasui, H. Shounij, *J. Biol. Chem.* **1991**, *266*, 10632–10637.

[79] K. Nakahara, T. Tanimoto, K. Hatano, K. Usuda, H. Shount, *J. Biol. Chem.* **1993**, *268*, 8350–8355.

[80] J. E. Froehlich, A. Itoh, G. A. Howe, *Plant Physiol.* **2001**, *125*, 306–317.

[81] A. H. Payne, D. B. Hales, *Endocr. Rev.* **2004**, *25*, 947–970.

[82] W. L. Miller, *Endocr Rev* **1988**, *9*, 295–318.

[83] M. Cutolo, B. Seriolo, B. Villagio, C. Pizzorino, C. Craviotto, A. Sulli, *Ann. N. Y. Acad. Sci.* **2002**, *966*, 131–142.

[84] F. Labrie, V. Luu-The, C. Labrie, J. Simard, *Front. Neuroendocrinol.* **2001**, *22*, 185–212.

[85] A. E. Schindler, C. Campagnoli, R. Druckmann, J. Huber, J. R. Pasqualini, K. W. Schweppe, J. H. H. Thijssen, *Maturitas* **2003**, *46*, 7–16.

[86] N. M. DeVore, E. E. Scott, *Nature* **2012**, *482*, 116–119.

[87] I. Hanukoglu, *Steroid Biochem. Molec. Biol* **1992**, *43*, 779–804.

[88] A. A. Gilep, T. A. Sushko, S. A. Usanov, *Biochim. Biophys. Acta - Proteins Proteomics* **2011**, *1814*, 200–209.
[89] D. Makeeva, D. Dovbnya, *Am. J. Mol. Biol.* **2013**, *2013*, 173–182.
[90] I. a. Pikuleva, N. Mast, W. L. Liao, I. V. Turko, *Lipids* **2008**, *43*, 1127–1132.
[91] I. A. Pikuleva, *Drug Metab. Dispos.* **2006**, *34*, 513–520.
[92] W. L. Miller, *J. Clin. Endocrinol. Metab.* **1998**, *83*, 1399–1400.
[93] M.-C. Hu, N. Hsu, N. EL Ben Hadj, C. Pai, H. Chu, C. Leo Wang, B. Chung, *Mol. Endocrinol.* **2002**, *16*, 1943–1950.
[94] A. T. Slominski, T. K. Kim, W. Li, A. K. Yi, A. Postlethwaite, R. C. Tuckey, *J. Steroid Biochem. Mol. Biol.* **2014**, *144*, 28–39.
[95] A. T. Slominski, T. K. Kim, W. Li, A. Postlethwaite, E. W. Tieu, E. K. Y. Tang, R. C. Tuckey, *Sci. Rep.* **2015**, *5*, 1–12.
[96] A. T. Slominski, W. Li, T. K. Kim, I. Semak, J. Wang, J. K. Zjawiony, R. C. Tuckey, *J. Steroid Biochem. Mol. Biol.* **2015**, *151*, 25–37.
[97] R. C. Tuckey, M. N. Nguyen, J. Chen, A. T. Slominski, D. M. Baldisseri, E. W. Tieu, J. K. Zjawiony, W. Li, *Drug Metab. Dispos.* **2012**, *40*, 436–444.
[98] N. Mast, A. J. Annalora, D. T. Lodowski, K. Palczewski, C. D. Stout, I. a. Pikuleva, *J. Biol. Chem.* **2011**, *286*, 5607–5613.
[99] F. Mackenzie, T. Cherkesova, I. Grabovec, N. Strushkevich, F. Mackenzie, T. Cherkesova, I. Grabovec, *Proc. Natl. Acad. Sci.* **2011**, *108*, 15535–15535.
[100] A. Wada, M. R. Waterman, *J. Biol. Chem.* **1992**, *267*, 22877–22882.
[101] T. B. Adamovich, I. A. Pikuleva, V. L. Chashchin, S. A. Usanov, *Biochim. Biophys. Acta* **1989**, *996*, 247–253.
[102] V. M. Coghlan, Vickery, *J. Biol. Chem.* **1992**, *267*, 8932–8935.
[103] V. M. Coghlan, L. E. Vickery, *J. Biol. Chem.* **1991**, *266*, 18606–18612.
[104] J. J. Müller, A. Lapko, G. Bourenkov, K. Ruckpaul, U. Heinemann, *J. Biol. Chem.* **2001**, *276*, 2786–2789.
[105] M. J. Headlam, M. C. J. Wilce, R. C. Tuckey, *Biochim. Biophys. Acta - Biomembr.* **2003**, *1617*, 96–108.
[106] D. Schwarz, P. Kisselev, R. Wessel, O. Jueptner, R. D. Schmid, *J. Biol. Chem.* **1996**, *271*, 12840–12846.
[107] P. Kisselev, R. Wessel, S. Pisch, U. Bornscheuer, R.-D. Schmid, D. Schwarz, *J. Biol. Chem.* **1998**, *273*, 1380–1386.
[108] A. C. Swart, K. H. Storbeck, P. Swart, *J. Steroid Biochem. Mol. Biol.* **2010**, *119*, 112–120.
[109] A. V. Pandey, W. L. Miller, *J. Biol. Chem.* **2005**, *280*, 13265–13271.
[110] E. M. Petrunak, N. M. Devore, P. R. Porubsky, E. E. Scott, *J. Biol. Chem.* **2014**, *289*, 32952–32964.
[111] P. S. Pallan, L. D. Nagy, L. Lei, E. Gonzalez, V. M. Kramlinger, C. M. Azumaya, Z. Wawrzak, M. R. Waterman, F. P. Guengerich, M. Egli, *J. Biol. Chem.* **2015**, *290*, 3248–3268.
[112] F. K. Yoshimoto, R. J. Auchus, *J. Steroid Biochem. Mol. Biol.* **2015**, *151*, 52–65.

[113] R. J. Auchus, T. C. Lee, W. L. Miller, *J. Biol. Chem.* **1998**, *273*, 3158–3165.
[114] S. Nakajin, M. Takahashi, M. Shinoda, P. F. Hall, *Biochem Biophys Res Commun* **1985**, *132*, 708–713.
[115] E. Missaghian, P. Kempná, B. Dick, A. Hirsch, R. Alikhani-Koupaei, B. Jégou, P. E. Mullis, B. M. Frey, C. E. Flück, *J. Endocrinol.* **2009**, *202*, 99–109.
[116] C. A. Marsh, R. J. Auchus, *Fertil. Steril.* **2014**, *101*, 317–322.
[117] C. M. Jenkins, M. R. Waterman, *J. Biol. Chem.* **1994**, *269*, 27401–27408.
[118] W. L. Miller, *Endocrinology* **2005**, *146*, 2544–2550.
[119] M. Onoda, P. Hall, *Biochem. Biophys. Res.* **1982**, *108*, 454–460.
[120] M. Katagiri, N. Kagawa, M. R. Waterman, *Arch. Biochem. Biophys.* **1995**, *317*, 343–347.
[121] P. Lee-Robichaud, M. E. Akhtar, M. Akhtar, *Biochem. J.* **1998**, *332 (Pt 2*, 293–296.
[122] E. M. Petrunak, S. A. Rogers, J. Aube, E. E. Scott, *Drug Metab. Dispos.* **2017**, *1*, 635–645.
[123] E. Gonzalez, K. K. Johnson, P. S. Pallan, T. T. N. Phan, W. Zhang, L. Lei, Z. Wawrzak, F. K. Yoshimoto, M. Egli, F. P. Guengerich, *J. Biol. Chem.* **2018**, *293*, 541–556.
[124] N. M. DeVore, K. M. Meneely, A. G. Bart, E. S. Stephens, K. P. Battaile, E. E. Scott, *FEBS J.* **2012**, *279*, 1621–1631.
[125] J. S. De Bono, C. J. Logothetis, A. Molina, K. Fizazi, S. North, L. Chu, K. N. Chi, R. J. Jones, O. B. Goodman, F. Saad, et al., *N. Engl. J. Med.* **2011**, *134*, 563–574.
[126] E. A. Mostaghel, B. T. Marck, S. R. Plymate, R. L. Vessella, S. Balk, A. M. Matsumoto, P. S. Nelson, R. B. Montgomery, *Clin. Cancer Res.* **2011**, *17*, 5913–5925.
[127] G. Attard, A. H. M. Reid, R. J. Auchus, B. A. Hughes, A. M. Cassidy, E. Thompson, N. B. Oommen, E. Folkerd, M. Dowsett, W. Arlt, et al., *J. Clin. Endocrinol. Metab.* **2012**, *97*, 507–516.
[128] V. Dhir, N. Reisch, C. M. Bleicken, J. Lebl, C. Kamrath, H. P. Schwarz, J. Grötzinger, W. G. Sippell, F. G. Riepe, W. Arlt, et al., *J. Clin. Endocrinol. Metab.* **2009**, *94*, 3058–3064.
[129] M.-J. Kim, H. S. Park, K. H. Seo, H.-J. Yang, S.-K. Kim, J.-H. Choi, *PLoS One* **2013**, *8*, e56168.
[130] C. J. C. Whitehouse, S. G. Bell, L.-L. Wong, *Chem. Soc. Rev.* **2012**, *41*, 1218–1260.
[131] L. O. Narhi, A. J. Fulco, *J. Biol. Chem.* **1987**, *262*, 6683–6690.
[132] L. O. Narhi, A. J. Fulco, *J. Biol. Chem.* **1986**, *261*, 7160–7169.
[133] M. J. Cryle, R. D. Espinoza, S. J. Smith, N. J. Matovic, J. J. De Voss, *Chem. Commun.* **2006**, 2353.
[134] M. Budde, M. Morr, R. D. Schmid, V. B. Urlacher, *ChemBioChem* **2006**, *7*, 789–794.
[135] M. A. Noble, C. S. Miles, S. K. Chapman, D. A. Lysek, A. C. Mackay, G. A. Reid, R. P. Hanzlik, A. W. Munro, *Biochem. J.* **1999**, *339*, 371–379.
[136] K. Ravichandran, S. Boddupalli, C. Hasermann, J. Peterson, J. Deisenhofer, *Science (80-.).* **1993**, *261*, 731–736.
[137] D. Roccatano, T. S. Wong, U. Schwaneberg, M. Zacharias, *Biopolymers* **2005**, *78*, 259–267.
[138] D. C. Haines, *Protein Pept. Lett.* **2006**, *13*, 977–980.
[139] D. C. Haines, D. R. Tomchick, M. Machius, J. A. Peterson, *Biochemistry* **2001**, *40*, 13456–

13465.
[140] H. Li, T. L. Poulos, *Nat. Struct. Biol.* **1997**, *4*, 140–146.
[141] S. Graham-Lorence, G. Truan, J. A. Peterson, J. R. Falck, S. Wei, C. Helvig, J. H. Capdevila, *J. Biol. Chem.* **1997**, *272*, 1127–1135.
[142] L. A. Cowart, J. R. Falck, J. H. Capdevila, *Arch. Biochem. Biophys.* **2001**, *387*, 117–124.
[143] E. Stjernschantz, B. M. A. Van Vugt-Lussenburg, A. Bonifacio, S. B. A. De Beer, G. Van Der Zwan, C. Gooijer, J. N. M. Commandeur, N. P. E. Vermeulen, C. Oostenbrink, *Proteins Struct. Funct. Genet.* **2008**, *71*, 336–352.
[144] G. Truan, J. A. Peterson, *Arch. Biochem. Biophys.* **1998**, *349*, 53–64.
[145] M. Girhard, F. Tieves, E. Weber, M. S. Smit, V. B. Urlacher, *Appl. Microbiol. Biotechnol.* **2013**, *97*, 1625–1635.
[146] C. A. Martinez, S. G. Rupashinghe, *Curr. Top. Med. Chem.* **2013**, *13*, 1470–1490.
[147] M. Katagiri, B. N. Ganguli, I. C. Gunsalus, *J. Biol. Chem.* **1968**, *243*, 3543–3546.
[148] J. H. Capdevila, S. Wei, C. Helvig, J. R. Falck, Y. Belosludtsev, G. Truan, S. E. Graham-Lorence, J. A. Peterson, *J. Biol. Chem.* **1996**, *271*, 22663–22671.
[149] S. J. Sadeghi, A. Fantuzzi, G. Gilardi, *Biochim. Biophys. Acta - Proteins Proteomics* **2011**, *1814*, 237–248.
[150] V. R. Dodhia, C. Sassone, A. Fantuzzi, G. Di Nardo, S. J. Sadeghi, G. Gilardi, *Electrochem. commun.* **2008**, *10*, 1744–1747.
[151] V. R. Dodhia, A. Fantuzzi, G. Gilardi, *J. Biol. Inorg. Chem.* **2006**, *11*, 903–916.
[152] D. Degregorio, S. D'Avino, S. Castrignano, G. di Nardo, S. J. Sadeghi, G. Catucci, G. Gilardi, *Front. Pharmacol.* **2017**, *8*, 1–13.
[153] V. B. Urlacher, S. Lutz-Wahl, R. D. Schmid, *Appl. Microbiol. Biotechnol.* **2004**, *64*, 317–325.
[154] V. Urlacher, R. D. Schmid, *Curr. Opin. Biotechnol.* **2002**, *13*, 557–564.
[155] T. C. Pochapsky, S. Kazanis, M. Dang, *Antioxid. Redox Signal.* **2010**, *13*, 1273–1296.
[156] T. W. B. Ost, C. S. Miles, J. Murdoch, Y. Cheung, G. a Reid, S. K. Chapman, A. W. Munro, *FEBS Lett.* **2000**, *486*, 4–8.
[157] S. Graham-Lorence, G. Truan, J. A. Peterson, J. R. Falck, S. Wei, C. Helvig, J. H. Capdevila, *J. Biol. Chem.* **1997**, *272*, 1127–1135.
[158] Q. S. Li, J. Ogawa, R. D. Schmid, S. Shimizu, *FEBS Lett.* **2001**, *508*, 249–252.
[159] C. J. C. Whitehouse, S. G. Bell, W. Yang, J. A. Yorke, C. F. Blanford, A. J. F. Strong, E. J. Morse, M. Bartlam, Z. Rao, L. L. Wong, *ChemBioChem* **2009**, *10*, 1654–1656.
[160] Q. Li, J. Ogawa, R. D. Schmid, S. Shimizu, *Appl. Environ. Microbiol.* **2001**, *67*, 5735–5739.
[161] P. C. Cirino, F. H. Arnold, *Angew. Chem. Int. Ed. Engl.* **2003**, *115*, 3421–3423.
[162] O. Salazar, P. C. Cirino, F. H. Arnold, *ChemBioChem* **2003**, *4*, 891–893.
[163] T. S. Wong, F. H. Arnold, U. Schwaneberg, *Biotechnol. Bioeng.* **2004**, *85*, 351–358.
[164] M. W. Peters, P. Meinhold, A. Glieder, F. H. Arnold, *J. Am. Chem. Soc.* **2003**, *125*, 13442–13450.
[165] R. Fasan, *ACS Catal.* **2012**, *2*, 647–666.

[166] Y. Miura, A. J. Fulco, *Biochim. Biophys. Acta (BBA)/Lipids Lipid Metab.* **1975**, *388*, 305–317.
[167] A. V. Klotz, J. J. Stegeman, C. Walsh, *Anal. Biochem.* **1984**, *140*, 138–145.
[168] A. Aitio, *Anal. Biochem.* **1978**, *85*, 488–491.
[169] J. G. Deluca, G. R. Dysart, D. Rasnick, M. O. Bradley, *Biochem. Pharmacol.* **1988**, *37*, 1731–1739.
[170] G. E. Tsotsou, A. Edward, G. Cass, G. Gilardi, *Biosens. Bioelectron.* **2002**, *17*, 119–131.
[171] A. J. Ruff, A. Dennig, G. Wirtz, M. Blanusa, U. Schwaneberg, *ACS Catal.* **2012**, *2*, 2724–2728.
[172] M. Opekarová, W. Tanner, *Biochim. Biophys. Acta - Biomembr.* **2003**, *1610*, 11–22.
[173] D. Schwarz, P. Kisselev, R. Wessel, S. Pisch, U. Bornscheuer, R. . Schmid, *Chem. Phys. Lipids* **1997**, *85*, 91–99.
[174] P. Kisselev, R. Wessel, S. Pisch, U. Bornscheuer, R. D. Schmid, D. Schwarz, *J. Biol. Chem.* **1998**, *273*, 1380–1386.
[175] P. Kisselev, R. C. Tuckey, S. T. Woods, T. Triantopoulos, D. Schwarz, *Eur. J. Biochem.* **1999**, *260*, 768–773.
[176] G. Gilardi, Y. T. Meharenna, G. E. Tsotsou, S. J. Sadeghi, M. Fairhead, S. Giannini, *Biosens. Bioelectron.* **2002**, *17*, 133–145.
[177] R. Rapoport, I. Hanukoglu, D. Sklan, *Anal. Biochem.* **1994**, *218*, 309–313.
[178] B. R. E. Childs, W. G. Bardsley, *Biochem. J.* **1975**, *145*, 93–103.
[179] L. K. Morlock, D. Böttcher, U. T. Bornscheuer, *Appl. Microbiol. Biotechnol.* **2018**, *102*, 985–994.
[180] A. B. Carmichael, L. L. Wong, *Eur. J. Biochem.* **2001**, *268*, 3117–3125.
[181] M. J. Cryle, J. J. De Voss, *ChemBioChem* **2008**, *9*, 261–266.
[182] H. Çelik, E. Arinç, *J. Pharm. Pharm. Sci.* **2008**, *11*, 68–82.
[183] B. Zhao, F. A. Summers, R. P. Mason, *Free Radic. Biol. Med.* **2013**, *53*, 1080–1087.
[184] K. Nishihara, M. Kanemori, H. Yanagi, T. Yura, *Appl. Environ. Microbiol.* **2000**, *66*, 884–889.
[185] K. Nishihara, M. Kanemori, M. Kitagawa, T. Yura, *Appl. Environ. Microbiol.* **1998**, *64*, 1694–1699.
[186] N. K. Nagradova, *Biochem.* **2004**, *69*, 830–843.
[187] S. Walter, J. Buchner, *Angew. Chem. Int. Ed. Engl.* **2002**, *41*, 1098–1113.
[188] S. Janocha, A. Bichet, A. Zöllner, R. Bernhardt, *Biochim. Biophys. Acta - Proteins Proteomics* **2011**, *1814*, 126–131.
[189] S. T. Woods, J. Sadleir, T. Downs, T. Triantopoulos, M. J. Headlam, R. C. Tuckey, *Arch. Biochem. Biophys.* **1998**, *353*, 109–115.
[190] G. I. Lepesheva, S. a Usanov, *Biochemistry. (Mosc).* **1998**, *63*, 224–234.
[191] R. A. Salomon, R. N. Farias, *J. Bacteriol.* **1995**, *177*, 3323–3325.
[192] A. Mosa, J. Neunzig, A. Gerber, J. Zapp, F. Hannemann, P. Pilak, R. Bernhardt, *J. Steroid Biochem. Mol. Biol.* **2015**, *150*, 1–10.

[193] J. Behlke, O. Ristau, E.-C. Müller, F. Hannemann, R. Bernhardt, *Biophys. Chem.* **2007**, *125*, 159–165.

[194] K. Suhara, T. Shigeki, M. Katagiri, *Biochim. Biophys. Acta* **1972**, *263*, 272–278.

[195] G. a Ziegler, C. Vonrhein, I. Hanukoglu, G. E. Schulz, *J. Mol. Biol.* **1999**, *289*, 981–990.

[196] C. Li, A. Wen, B. Shen, J. Lu, Y. Huang, Y. Chang, *BMC Biotechnol.* **2011**, *11*, DOI 10.1186/1472-6750-11-92.

[197] V. M. Shkumatov, E. V. Usova, Y. S. Poljakov, N. S. Frolova, V. G. Radyuk, S. Mauersberger, A. A. Chernogolov, H. Honeck, W.-H. Schunck, *Biochem.* **2002**, *67*, 457–467.

[198] Y. Khatri, M. C. Gregory, Y. V Grinkova, I. G. Denisov, S. G. Sligar, *Biochem. Biophys. Res. Commun.* **2014**, *443*, 179–184.

[199] V. Dhir, H. E. Ivison, N. Krone, C. H. L. Shackleton, A. J. Doherty, P. M. Stewart, W. Arlt, *Mol. Endocrinol.* **2007**, *21*, 1958–1968.

[200] H. J. Barnes, M. P. Arlotto, M. R. Waterman, **1991**, *88*, 5597–5601.

[201] V. M. Shkumatov, E. V. Usova, V. G. Radyuk, Z. N. Kashkan, N. V. Kovganko, T. Juretzek, S. Mauersberger, *Russ. J. Bioorganic Chem.* **2003**, *29*, 581–587.

[202] L. K. Morlock, S. Grobe, K. Balke, S. Mauersberger, D. Böttcher, U. T. Bornscheuer, *ChemBioChem* **2018**, *19*, 1954-1958.

[203] V. M. Shkumatov, N. S. Frolova, E. V. Rudaya, Y. V. Faletrov, S. Mauersberger, G. Barth, *Appl. Biochem. Microbiol.* **2006**, *42*, 472–478.

[204] V. M. Mauersberger, S. Novikova, L. A. Shkumatov, in *Yarrowia Lipolytica, Biotechnol. Appl. Microbiol. Monogr. 25* (Ed.: G. Barth), Springer-Verlag Berlin Heidelberg, **2013**, pp. 171–226.

[205] E. Krieger, G. Vriend, *Bioinformatics* **2014**, *30*, 2981–2982.

[206] V. B. Chen, W. B. Arendall, J. J. Headd, D. A. Keedy, R. M. Immormino, G. J. Kapral, L. W. Murray, J. S. Richardson, D. C. Richardson, *Acta Crystallogr. Sect. D Biol. Crystallogr.* **2010**, *66*, 12–21.

[207] J.-C. Baret, O. J. Miller, V. Taly, M. Ryckelynck, A. El-Harrak, L. Frenz, C. Rick, M. L. Samuels, J. B. Hutchison, J. J. Agresti, et al., *Lab Chip* **2009**, *9*, 1850–1858.

[208] H. H. Gorris, D. R. Walt, *J. Am. Chem. Soc.* **2009**, *131*, 6277–6282.

[209] W. M. Atkins, S. G. Sligar, *Biochemistry* **1988**, *27*, 1610–1616.

[210] P. B. Garland, P. J. Randle, *Nature* **1962**, *196*, 987–988.

[211] A. M. Seddon, P. Curnow, P. J. Booth, *Biochim. Biophys. Acta - Biomembr.* **2004**, *1666*, 105–117.

[212] A. Villaverde, M. M. Carrió, *Biotechnol. Lett.* **2003**, *25*, 1385–1395.

[213] K. Tsumoto, D. Ejima, I. Kumagai, T. Arakawa, *Protein Expr. Purif.* **2003**, *28*, 1–8.

[214] J. G. Thomas, a Ayling, F. Baneyx, *Appl. Biochem. Biotechnol.* **1997**, *66*, 197–238.

[215] K. Yu, C. Liu, B. G. Kim, D. Y. Lee, *Biotechnol. Adv.* **2015**, *33*, 155–164.

[216] D. E. Torres Pazmiño, A. Riebel, J. De Lange, F. Rudroff, M. D. Mihovilovic, M. W. Fraaije, *ChemBioChem* **2009**, *10*, 2595–2598.

[217] L. Iturrate, I. Sánchez-Moreno, I. Oroz-Guinea, J. Pérez-Gil, E. García-Junceda, *Chem. - A Eur. J.* **2010**, *16*, 4018–4030.

[218] Y. J. Zhou, W. Yang, L. Wang, Z. Zhu, S. Zhang, Z. K. Zhao, *Microb. Cell Fact.* **2013**, *12*, 1.

[219] J. N. Onuchic, P. G. Wolynes, *Curr. Opin. Struct. Biol.* **2004**, *14*, 70–75.

[220] A. R. Fersht, A. Matouschek, L. Serrano, *J. Mol. Biol.* **1991**, *224*, 771–782.

[221] W. T. Booth, C. R. Schlachter, S. Pote, N. Ussin, N. J. Mank, V. Klapper, L. R. Offermann, C. Tang, B. K. Hurlburt, M. Chruszcz, *ACS Omega* **2018**, *3*, 760–768.

[222] F. M. Szczebara, C. Chandelier, C. Villeret, A. Masurel, S. Bourot, C. Duport, S. Blanchard, A. Groisillier, E. Testet, P. Costaglioli, et al., *Nat. Biotechnol.* **2003**, *21*, 143–149.

[223] D. F. Estrada, J. S. Laurence, E. E. Scott, *J. Biol. Chem.* **2013**, *288*, 17008–17018.

[224] C. H. Chiang, R. Ramu, Y. J. Tu, C. L. Yang, K. Y. Ng, W. I. Luo, C. H. Chen, Y. Y. Lu, C. L. Liu, S. S. F. Yu, *Chem. - A Eur. J.* **2013**, *19*, 13680–13691.

[225] A. J. J. Straathof, S. Panke, A. Schmid, *Curr. Opin. Biotechnol.* **2002**, *13*, 548–556.

[226] H. Zhang, C. D. Davis, M. W. Sinz, A. D. Rodrigues, *Expert Opin. Drug Metab. Toxicol.* **2007**, *3*, 667–687.

[227] E. O'Reilly, V. Köhler, S. L. Flitsch, N. J. Turner, *Chem. Commun.* **2011**, *47*, 2490.

[228] G. Grogan, *Curr. Opin. Chem. Biol.* **2011**, *15*, 241–248.

[229] J. B. Van Beilen, W. A. Duetz, A. Schmid, B. Witholt, *Trends Biotechnol.* **2003**, *21*, 170–177.

[230] H. Uhlmann, V. Beckert, D. Schwarz, R. Bernhardt, *Biochem. Biophys. Res. Commun.* **1992**, *188*, 1131–1138.

[231] C. Vonrhein, U. Schmidt, G. a. Ziegler, S. Schweiger, I. Hanukoglu, G. E. Schulz, *FEBS Lett.* **1999**, *443*, 167–169.

[232] G. Hoffmann, K. Bönsch, T. Greiner-Stöffele, M. Ballschmiter, *Protein Eng. Des. Sel.* **2011**, *24*, 439–446.

[233] D. Saraiva, R. Semedo, M. D. C. Castilho, J. M. Silva, F. Ramos, *J. Chromatogr. B Anal. Technol. Biomed. Life Sci.* **2011**, *879*, 3806–3811.

9 Appendix

9.1 CYP17A1

```
CLUSTAL Omega (1.2.4) multiple sequence alignment


sp|P05185|CP17A_BOVIN       -------MWLLLAV-F-LLTLAYLFWP----KTKHSGAKYPRSLPSLPLVGSLPFLPRRG    47
sp|P05093|CP17A_HUMAN       -------MWELVAL-L-LLTLAYLFWP----KRRCPGAKYPKSLLSLPLVGSLPFLPRHG    47
tr|B3DH80|B3DH80_DANRE      MAEALILPWLLCLSLFSAVTLAALYLKQKMNGFVPAGNRSPPSLPSLPIIGSLLSLVSDS    60
tr|A7U483|A7U483_DANRE      -----MCSVSVCVC-FSALLLLLLLLVRRLLEGVGSSSVSFPCLPRLPLLGSLLHLRSNL    54
                                      :    :  : *  *            .     .*  **::***  *

sp|P05185|CP17A_BOVIN       QQHKNFFKLQEKYGPIYSFRLGSKTTVMIGHHQLAREVLLKKGKEFSGRPKVATLDILSD    107
sp|P05093|CP17A_HUMAN       HMHNNFFKLQKKYGPIYSVRMGTKTTVIVGHHQLAKEVLIKKGKDFSGRPQMATLDIASN    107
tr|B3DH80|B3DH80_DANRE      PPHIFFQDLQKKYGDLYSLMMGSHKLLIVNNHHHAKEILIKKGKIFAGRPRTVTTDLLTR    120
tr|A7U483|A7U483_DANRE      PPHLLFTQLSSQYGPLFGLYAGPHLTLVVSEIGLVREVLLQRGREFAGRPKMVTTDLLTQ    114
                              *  * .*..:** ::..  * :  :::..   .:*:*:::*: *:***: .* *: :

sp|P05185|CP17A_BOVIN       NQKGIAFADHGAHWQLHRKLALNAFALFKDGNLKLEKIINQEANVLCDFLATQHGEAIDL    167
sp|P05093|CP17A_HUMAN       NRKGIAFADSGAHWQLHRRLAMATFALFKDGDQKLEKIICQEISTLCDMLATHNGQSIDI    167
tr|B3DH80|B3DH80_DANRE      DGKDIAFADYSSTWKFHRKMVHGALCMFGEGSVSIEKIICREASSMCEVLTESQNSAVDL    180
tr|A7U483|A7U483_DANRE      GGKDIAFADYSPLWKNHRRLVHSSFTLFGEGSNKLQTIVQEAADSLCEELQACRGQSSDL    174
                            . *.***** .  *: **::.  :: :* :*. .::.*: .  . :*: *   ...: *:

sp|P05185|CP17A_BOVIN       SEPLSLAVTNIISFICFNFSFKNEDPALKAIQNVNDGILEVLSKEVLLDIFPVLKIFPSK    227
sp|P05093|CP17A_HUMAN       SFPVFVAVTNVISLICFNTSYKNGDPELNVIQNYNEGIIDNLSKDSLVDLVPWLKIFPNK    227
tr|B3DH80|B3DH80_DANRE      GPELTRAVTNVVCALCFNSSYKRGDAEFESMLQYSQGIVDTVAKDSLVDIFPWLQIFPNK    240
tr|A7U483|A7U483_DANRE      SVVLMRAVTNVICRLVFSSSYQPSDPELQTVIQYNDGIVQTIARGGLVDIFPWLRIFPNK    234
                            .  :  ****::. : *. *::  *  :: : : .:**:: :::  *:*:.* *:***.*

sp|P05185|CP17A_BOVIN       AMEKMKGCVQTRNELLNEILEKCQENFSSDSITNLLHILIQAKVNADNNNAGPDQDSKLL    287
sp|P05093|CP17A_HUMAN       TLEKLKSHVKIRNDLLNKILENYKEKFRSDSITNMLDTLMQAKMNSDNGNAGPDQDSELL    287
tr|B3DH80|B3DH80_DANRE      DLTILRQCISIRDKLLQKKYEEHKVTYSDNVQRDLLDALLRAKRSSENNNSSTR--DVGL    298
tr|A7U483|A7U483_DANRE      DLKRLKECVSIRDQLLYKKLLEHKKSLTPGEPRDLLDALLIGQQRGS-----GG--ADDI    287
                             :  ::  :. *:.** :   : : .   .   ::*. *: .:  ..           :

sp|P05185|CP17A_BOVIN       SNRHMLATIGDIFGAGVETTSVIKWIVAYLLHHPSLKKRIQDDIDQIIGFNRTPTISDR    347
sp|P05093|CP17A_HUMAN       SDNHILTTIGDIFGAGVETTSVVKWTLAFLLHNPQVKKKLYEEIDQNVGFSRTPTISDR    347
tr|B3DH80|B3DH80_DANRE      TEDHVLMTVGDIFGAGVETTTVLKWSIAYLVHNPQVQRKIQEELDSKIGKERHPQLSDR    358
tr|A7U483|A7U483_DANRE      TEDHVLMTAAEAFGAGVETTSTTLLWTIAFLLHHPQLQERVQAELDECVGVDRPPCLSDR    347
                            :: *:* * .: ********::.: * :*:*:*:*.::.::  ::*. :* .* * :***

sp|P05185|CP17A_BOVIN       NRLVLLEATIREVLRIRPVAPTLIPHKAVIDSSIGDLTIDKGTDVVVNLWALHHSEKEWQ    407
sp|P05093|CP17A_HUMAN       NRLLLLEATIREVLRLRPVAPMLIPHKANVDSSIGEFAVDKGTEVIINLWALHHNEKEWH    407
tr|B3DH80|B3DH80_DANRE      GNLPYLEATIREVLRIRPVSPLLIPHVALQDSSVGEYTVQKGTRVVINLWSLHHDKKEWK    418
tr|A7U483|A7U483_DANRE      PHLPLLDAVLCEVMRIRPVSPILIPHVAMQDTSLGGHSVPKGTRVLVNMWAIHHDPKHWD    407
                             .*  *:*.: **:*:***:* **** *  *:*:*  :: *** *::*:*::**. *.*.

sp|P05185|CP17A_BOVIN       HPDLFMPERFLDPTGTQLISPSLSYLPFGAGPRSCVGEMLARQELFLFMSRLLQRFNLEI    467
sp|P05093|CP17A_HUMAN       QPDQFMPERFLNPAGTQLISPSVSYLPFGAGPRSCIGEILARQELFLIMAWLLQRFDLEV    467
tr|B3DH80|B3DH80_DANRE      NPELFDPGRFLNEEGDGLCCPSGSYLPFGAGVRVCLGEALAKMELFLFLAWILQRFTLEM    478
tr|A7U483|A7U483_DANRE      QPEQFNPERFLEPSGKK--KTQSSFLPFGAGPRVCVGESLARIELFLFVSRPLQRFSFSC    465
                            :*: * * ***:  *      . *:****** * *:** **: ****:::  **** :.

sp|P05185|CP17A_BOVIN       PDDGKLPSLEGHASLVLQIKPFKVKIEVRQAWKEAQAEGSTP  509
sp|P05093|CP17A_HUMAN       PDDGQLPSLEGIPKVVFLIDSFKVKIKVRQAWREAQAEGST-  508
tr|B3DH80|B3DH80_DANRE      PTGQPLPDLQGKFGVVLQPKKFKVVAKVRADWEKSPLMQHC-  519
tr|A7U483|A7U483_DANRE      PSEASLPDLQGRFGVVLQPERYTVTVTPRH------------  495
                            *    **.*:*   :*:  . :.*    *
```

Figure A 1: Sequence alignement of bovine (CP17A_BOVIN) and human (CP17A_HUMAN) CYP17A1, CYP17A1 (B3DH80_DANRE) and CYP17A2 (A7U483_DANRE) from Zebra fish created with CLUSTAL Omega (version 1.2.4).

HPLC analysis of a 2 mL sample of the preparative biocatalysis approach with bovine CYP17A1 V483A:

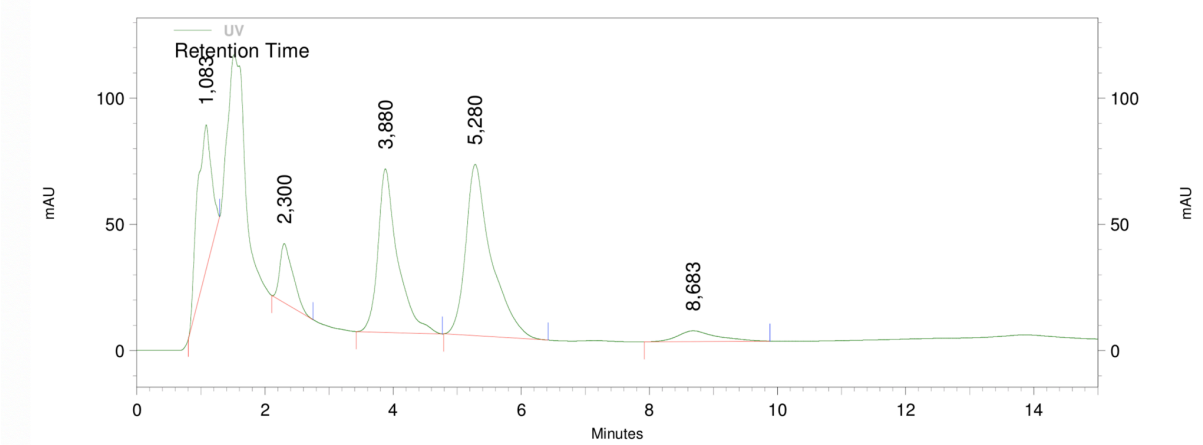

UV Results

Retention Time	Area	Area Percent
1,083	3600114	19,155
2,300	1353714	7,203
3,880	5565297	29,612
5,280	7554688	40,197
8,683	720368	3,833

Figure A 2: Chromatogram of the HPLC analysis of the preparative whole-cell biocatalysis of 100 mg progesterone with the bovine CYP17A1 V483A in a total cultivation volume of 1 L after 72 h. As column, a Kromasil C18 column was used with a flowrate of 0.8 mL min^{-1} of the mobile phase consisting of ACN:H_2O in a ratio of 40:60. The product 17α-hydroxyprogesterone can be found at a retention time of 8.683 min, 17α,20α-dihydroxyprogesterone can be found at a retention time of 5.280 min and 16α-hydroxyprogesterone can be found at a retention time of 3.880 min. The completely consumed substrate progesterone would have had a retention time of approximately 14 min. (Figure from second publication[202])

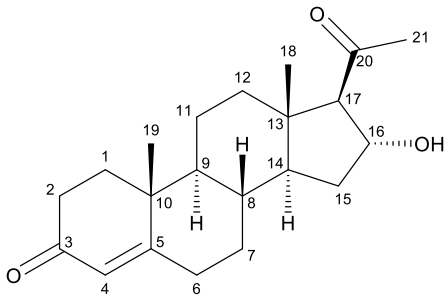

Figure A 3: Structure of 16α-hydroxyprogesterone ($C_{21}H_{30}O_3$) with C atom numbering according to IUPAC nomenclature.

^{1}H NMR (300 MHz, $CDCl_3$): *δ* 0.68 (s, 3H), 0.98-1.28 (m, 6H), 1.38-1.87 (m, 11H), 1.98-2.07 (m, 2H) ,2.18 (s, 3H) ,2.25-2.50 (m, 4H), 2.54 (d, *J*= 6.5 Hz, 1H), 4.83-4.88 (m, 1H), 5.74 (s, 1H).

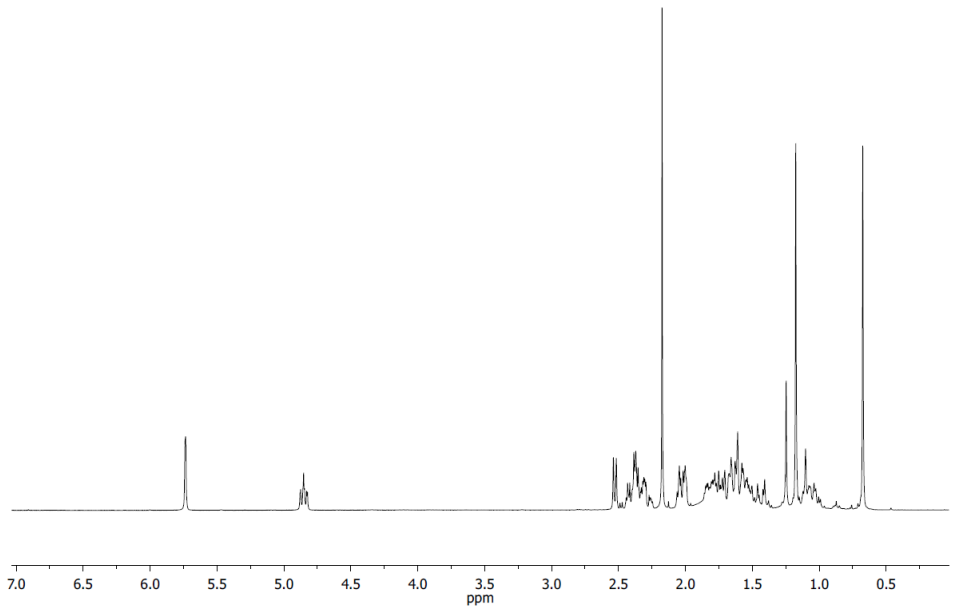

Figure A 4: ^{1}H-NMR of 16α-hydroxyprogesterone obtained from the preparative biocatalysis. (Figure from second publication[202])

^{13}C NMR (75 MHz, $CDCl_3$): *δ* 14.60 (C-18), 17.48 (C-19), 20.77 (C-11),31.82 (C-7), 31.83 (C-21), 32.81 (C-6), 34.05 (C-2), 35.26 (C-8), 35.31 (C-15), 35.76 (C-1), 38.69 (C-10), 38.74 (C-12), 44.92 (C-13), 53.63 (C-14), 53.84 (C-9), 72.19 (C-17), 73.68 (C-16), 124.24 (C-4), 170.65 (C-5), 199.47 (C-3), 208.40 (C-20).

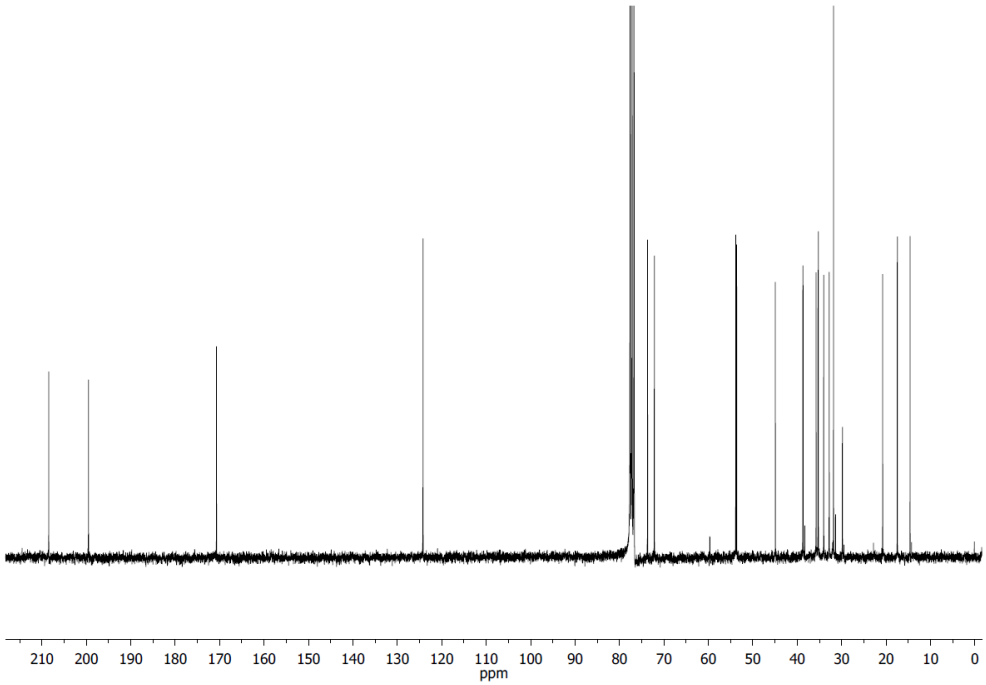

Figure A 5: ^{13}C-NMR of 16α-hydroxyprogesterone obtained from the preparative biocatalysis. (Figure from second publication[202])

2D NMR techniques were used to annotate the signals. The here observed signals are consistent for data faoun in literature for 16α-hydroxyprogesterone.*

* a) S. Kille, F. E. Zilly, J. P. Acevedo, M. T. Reetz, *Nature Chem.* **2011**, *3*, 738; b) D. Mizrachi, Z. Wang, K. K. Sharma, M. K. Gupta, K. Xu, C. R. Dwyer, R. J. Auchus, *Biochemistry* **2011**, *50*, 3968; c) D. N. Kirk, H. C. Toms, C. Douglas, K. A. White, K. E. Smith, S. Latif, R. W. P. Hubbard, *J. Chem. Soc., Perkin Trans. 2* **1990**, 1567.

9.2 Dual screening approach

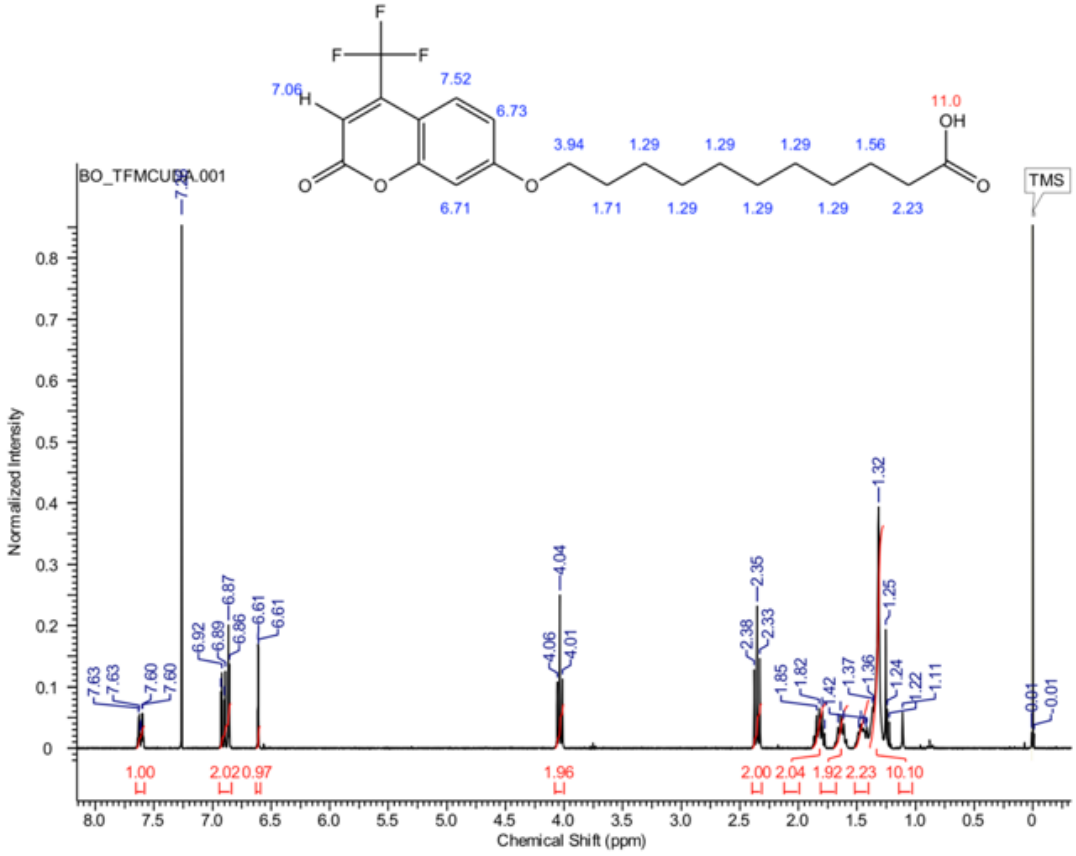

Figure A 6: ^{1}H-NMR of the synthetized 11-(4-trifluoromethylcoumarin-7-yloxy)undecanoic acid in $CDCl_3$.

^{1}H NMR result as published by Neufeld et al. in 2014: "($CDCl_3$): δ = 1.24–1.40 (m, 12 H, 4-H to 9-H), 1.47 (m_c, 2 H, 10-H), 1.63 (m_c, 2 H, 3-H), 1.82 (m_c, 2 H, 11-H), 2.35 (t, *J* = 7.5 Hz, 2 H, 2-H), 4.04 (t, *J* = 6.5 Hz, 2 H, 12-H), 6.61 (s, 1 H, 3-H_{Ar}), 6.86 (d, *J* = 2.5 Hz, 1 H, 8-H_{Ar}), 6.91 (dd, *J* = 9.0, 2.5 Hz, 1 H, 6-H_{Ar}), 7.61 (dd, *J* = 9.0, 1.7 Hz, 1 H, 5-H_{Ar}) ppm"

Eigenständigkeitserklärung

Hiermit erkläre ich, dass diese Arbeit bisher von mir weder an der Mathematisch-Naturwissenschaftlichen Fakultät der Ernst-Moritz-Arndt-Universität Greifswald noch einer anderen wissenschaftlichen Einrichtung zum Zwecke der Promotion eingereicht wurde.

Ferner erkläre ich, dass ich diese Arbeit selbstständig verfasst und keine anderen als die darin angegebenen Hilfsmittel und Hilfen benutzt und keine Textabschnitte eines Dritten ohne Kennzeichnung übernommen habe.

Unterschrift des Promovenden

List of publications

Published paper:

Morlock, L.K., Böttcher, D., Bornscheuer, U.T. (2018), Simultaneous detection of NADPH consumption and H_2O_2 production using the Ampliflu^{TM} Red assay for screening of P450 activities and uncoupling, *Appl. Microbiol. Biotechnol*., DOI: 10.1007/s00253-017-8636-3

Morlock, L. K., Grobe, S., Balke, K., Mauersberger, S., Böttcher, D., Bornscheuer, U. T. (2018), Protein engineering of the progesterone hydroxylating P450-monooxygenase CYP17A1 alters its regioselectivity, *ChemBioChem,* DOI: 10.1002/cbic.201800371

Contributions to conferences:

09/2015 Conference: „New Reactions with Enzymes and Microorganisms"; Stuttgart; presentation: "Influence of dioxygen on the selectivity and activity of membrane-bound P450 monooxygenase catalyzed oxidation reactions"

07/2017 Conference: „BioTrans 2017"; Budapest;
poster: „Determining the uncoupling rates of P450 enzymes with Ampliflu^{TM} Red" Morlock, L. K., Böttcher, D., Bornscheuer, U.T.

Danksagung

Zu aller erst möchte ich mich bei dir, Uwe bedanken. Auch wenn die Thematik sehr herausfordernd war, bin ich dennoch sehr froh meine Doktorarbeit in deiner Arbeitsgruppe angefertigt zu haben. Vielen Dank für deine Unterstützung und deinen wissenschaftlichen Input. Danke, dass du deine Emails in Lichtgeschwindigkeit beantwortest und auch auf deinen vielen Dienstreisen und sogar im Sabbatical stets deine Arbeitsgruppe und die vielen Projekte mit ihren Deadlines im Kopf behältst.

Ein großer Dank gilt der Deutschen Forschungsgemeinschaft, für die Finanzierung über das Graduiertenkolleg GRK 1947 BiOx. Danke auch an Dr. Lillig, Prof. Dr. Helm und Anett Stolte für alles Organisatorische.

Dominique, bei dir möchte ich mich für unsere vielen Meetings, deinen Input und dem Korrekturlesen der Publikationen bedanken. Besonders aber dafür, dass deine Tür immer offenstand und du stets ein offenes Ohr hattest.

Natürlich möchte ich mich auch bei dem gesamten Arbeitskreis für die wunderbare Arbeitsatmosphäre bedanken. Ich habe es stets genossen mit EUCH ALLEN zusammen arbeiten zu können. Ich finde es ist definitiv nicht selbstverständlich auf so viele hilfsbereite, aufgeschlossene und nette Menschen zu treffen. Besonders möchte ich mich auch bei Ina bedanken, für die Unterstützung an der GC-MS und HPLC, aber auch für die aufmunternden Worte und netten Gespräche. Auch Angelika gilt ein besonderer Dank, dafür, dass du alles am Laufen hältst, ebenso wie Frau Großmann.

Ayad, ich weiß gar nicht so genau für was alles ich mich bei dir bedanken will. Es war mir ein inneres Blumen pflücken, dass wir gemeinsam durch dick und dünn gegangen sind und alle Höhen und Tiefen gemeinsam gemeistert haben. Die kleinen Späße und Neckereien werde ich besonders vermissen, sowie dich als Tischnachbar im Büro. Danke, dass auch du immer Zeit hattest und mit mir so manches Problem diskutiert und gelöst hast. Danke, für alles!

Miriam, auch bei dir möchte ich mich bedanken. Dafür, dass du mich so manches Mal aufgemuntert hast. Dafür, dass wir zusammen Sport gemacht haben und nebenbei so vieles besprechen konnten, aber natürlich auch für die Kaffeepausen am Institut und die Unterstützung bei der Analytik. Danke für deine Freundschaft!

Auch bei dir, Katja, möchte ich mich bedanken. Für den wissenschaftlichen Austausch, sowie für die gemeinsamen Kaffee- und Mittagspausen.

Chris, I really want to thank you for the scientific input and discussions. I enjoyed them a lot. I am so thankful and want to express my appreciation for working together with you! Of course, I also want to thank Ingrid. Thank you two so much for all the help concerning the substrate synthesis and the NMR analysis. And somehow you three have to be named together: Isabelita! Thank you for being there for me, all the time. I am thankful for your wise and encouraging words whenever I needed them! Ay ay ay ay ay! Of course, I also loved our Wine and Cheese evenings! Thank you all for inventing them!

Thomas B. wo soll ich nur anfangen?! Ich habe selten einen Menschen getroffen der so viel Lebensfreude versprüht wie du. Auch wenn wir nur eine relativ kurze Zeit zusammen in Greifswald hatten, hast du wohl Recht mit der Aussage, dass Greifswald einfach zu klein für uns beide wäre. Danke für die lustige Zeit als Mitbewohner, es war mir eine riesige Freude!

Lukas, mein Lieblingskölner, auch bei dir möchte „isch misch“ bedanken! Für deine lustige Art und die Kaffeepausen, aber natürlich auch für unsere wissenschaftlichen Diskussionen. Es war wirklich schön für mich, dich im Team „P450“ zu haben und mich daher mit dir fachlich austauschen zu können. Auch bei der lieben Julia möchte ich mich bedanken. Es hat mir wahnsinnig viel Freude bereitet, dass wir uns jede Woche aufs Neue wieder für den Sport motiviert haben und dabei einfach Mal alles andere vergessen konnten. Dankeschön!

Auch bei dir, großer Florini möchte ich mich bedanken. Für die Hilfestellungen bezüglich PCR, aber auch für deine kleinen Zaubereinlagen im Labor, die gemeinsamen Mittagspausen und Abende in der Husche. Dafür möchte ich mich auch bei Euch, Thomas H. und Maika bedanken, sowie für das erste sportliche Jahr.

Judith, auch bei dir möchte ich mich bedanken. Es war eine wunderschöne Erfahrung, dich als Mitbewohnerin zu haben. Danke, für deine lustige und lebensfrohe Art.

Alberto, I want to thank you especially, for making me feel welcome in the new working group and for showing me around and introducing me to so many nice people. You made my start in Greifswald very easy and nice.

Vishnu, Claudia, Elia, Emil, Andy, Anders, Moritz & Sara, Eva, Askin, Hendrik, Sascha: I loved getting to know you all and I was very thankful for you, contributing to the nice working atmosphere and nice evenings in Greifswald.

Martina, I really miss our time together in Greifswald, I am more than thankful for having met you in Greifswald.

I also want to thank my Master student Christopher Grimm and Anna Kluza, who did an Erasmus Internship under my supervision. I appreciate your contributions to my work and liked working together with you.

Vielen Dank auch, an Sascha Grobe. Vor allem dafür, dass du die letzten Experimente durchgeführt hast.

Auch bei allen Studenten des Graduiertenkollegs GRK 1947 BiOx möchte ich mich bedanken. Hier im speziellen: Dana, Anna, Thomas P., Marina, Daniel und Nico. Es hat mir viel Freude bereitet, gemeinsam mit euch die vielen Workshops und Veranstaltungen erleben zu dürfen.

Meinen Freunden zu Hause möchte ich natürlich auch Danken! Danke, für die vielen Besuche während meiner Zeit in Greifswald, trotz der weiten Anreise. Ganz speziell vielen Danke an Süreyya, die wohl Beste Mitbewohnerin aus Stuttgart. Caro, vielen Dank für die gemeinsamen Stunden in der Bib in Stuttgart und für deine Freundschaft. Janina, schön dich schon seit der Schulzeit zu kennen. Es freut mich besonders, dass wir so viel zusammen machen. Nadja: meine Sandkastenfreundin, die ich nicht missen möchte. Meine Mädels Clique

aus Karlsruhe: Mira, Nadine und Anna, aber natürlich auch Marco, Domi, Christoph, Chris, Olli und Kerstin. Euch allen herzlichen Dank für eure Freundschaft über all die Jahre.

Natürlich möchte ich mich auch im speziellen bei meiner Familie bedanken. Besonderer Dank gilt meinen Eltern für die ständige Unterstützung während meines Studiums finanziell, sowie moralisch. Danke auch an die wohl Beste Schwiegermutter und Stiefschwester der Welt: Susanne und Annalena. Danke für die lustigen Spielpausen mit Euch während der Schreibphase.

Und zu allerletzt: Annabelle! Du bist die wohl Beste große Schwester der Welt. Vielen lieben Dank für deine Besuche, Karten, Blumen und Telefonate. Danke für deine Unterstützung.